UNIVERSITAT DE BARCELONA

Aminocyclitol and iminosugar derivatives related to Gauche disease

Ester Monlleó Mas

Aquesta tesi doctoral està subjecta a la llicència ***Reconeixement 3.0. Espanya de Creative Commons***.

Esta tesis doctoral está sujeta a la licencia ***Reconocimiento 3.0. España de Creative Commons***.

This doctoral thesis is licensed under the ***Creative Commons Attribution 3.0. Spain License***.

AMINOCYCLITOL AND IMINOSUGAR DERIVATIVES RELATED TO GAUCHER DISEASE

TESI DOCTORAL

Memòria presentada per Ester Monlleó Mas per optar al títol de doctora
per la Universitat de Barcelona

Aquesta tesi ha estat realitzada en el marc del Programa de Doctorat en Química Orgànica de la Universitat de Barcelona, a les instal·lacions de l'Institut de Química Avançada de Catalunya (IQAC- CSIC).

Doctoranda
Ester Monlleó Mas

Director
Dr. Amadeu Llebaria Soldevila
Investigador científic
Departament de Química Biomèdica
(IQAC-CSIC)

Codirectora
Dra. Mª Carmen Serra Comas
Directora tècnica de projectes industrials
Medicinal Chemistry and Synthesis group (MCS)
(IQAC-CSIC)

Tutor
Dr. Pedro Romea García
Professor Titular
Departament de Química Inorgànica i Orgànica
(Universitat de Barcelona)

La vida és un camí meravellós.

Quan el camí fa baixada, et pots deixar portar i gaudir de l'experiència... però quan fa pujada, amb una bona companyia s'avança millor.

Aquest treball està dedicat a totes i cadascuna de les persones que, d'una manera o altra, en algun moment de la seva vida han compartit un trosset del seu camí amb mi. Sense vosaltres, la meva vida no hagués estat igual i potser no hagués estat possible arribar fins aquí.

GRÀCIES. DE TOT COR.

Abbreviations

Ac	Acetate
ACN	Acetonitrile
AcOEt	Ethyl Acetate
aq.	Aqueous
BBB	Blood-Brain Barrier
Bn	Benzyl
BSA	Bovine Serum Albumine
Bu	Butyl
cat.	Catalytic
CBE	Conduritol β-epoxide
Cer	Ceramide
C_6-NBD	*N*-[6-[(7-nitro-2-1,3-benzoxadiazol-4-yl)amino]hexanoyl]
CNS	Central nervous system
DCM	Dichloromethane
DGJ	1-deoxygalactonijirimycin
DIPEA	*N,N*-diisopropylethylamine
DMAP	4-dimethylaminopyridine
DMEM	Dulbecco's modified Eagle's medium
DMF	*N,N*-dimethylformamide
DMSO	Dimethylsulfoxide
DNJ	Deoxynojirimycin
EDC	*N*-(3-Dimethylaminopropyl)-*N*'-ethylcarbodiimide hydrochloride
EDTA	Ethylenediaminetetraacetic acid
ee	Enantiomeric exces
ELS	Evaporative light scattering
Eq	Equivalent
ER	Endoplasmic Reticulum
ERT	Enzyme Replacement Theraphy
Et	Ethyl
EtOH	Ethanol
FBS/FCS	Fetal Bovine Serum/Fetal Calf Serum
Fig.	Figure
GBA	β-Glucocerebrosidase
GCase/GBA1	acid β-Glucocerebrosidase
GCS	Glucosyl Ceramide Synthase
GD	Gaucher Disease
COSY	Correlation spectroscopy
GluCer	Glucosylceramide
Graph.	Graphic
HEPES	4-(2-hydroxyethyl)-1-piperazineethanesulfonic acid
HPLC	High-performance liquid chromatography

HRMS	High-ressolution mass spectrometry
HOBT	1-Hydroxybenzotriazole hydrate
HSQC	Heteronuclear single quantum correlation
IC_{50}	Half maximal inhibitory concentration
IFG	Isofagomine
IMDM	Iscove's Modified Dubelco's Medium
IR	Infrared
K_a	Acidic dissociation constant
LAH	Lithium aluminum hydride
LIMP-2	lysosomal membrane protein 2
LSD	Lysosomal Storage Disease
Me	Methyl
MeOH	Methanol
MCPBA	*m*-chloroperbenzoic acid
m-PIC	Protease Inhibitor Cocktail for use with mammalian cell and tissue extracts
Ms	Mesyl
MTT	3-(4,5-dimethylthiazol-2-yl)-2,5-diphenyltetrazolium bromide
4-MU	4-Methylumbelliferone
4-MUG	4-Methylumbelliferyl β-D-glucopyranoside
MW	microwave irradiation
NAD	β-Nicotinamide adenine dinucleotide hydrate
NaOMe	Sodium methoxide
NB-DNJ	N-butyl-deoxynojirimycin
NMR	Nuclear magnetic resonance
NN-DNJ	*N*-nonyl-deoxynojirimycin
Non	Nonyl
PBS	Phosphates Buffer Solution
PC	Pharmacological Chaperone
PCT	Pharmacological Chaperone Therapy
P/S	Penicillin–streptomycin
rfu	Relative fluorescence units
SRT	Subtrate Reduction Therapy
TBAF	Tetrabutyl ammonium fluoride
Tf	Triflate
TFA	Trifluoroacetic acid
THF	Tetrahydrofurane
TLC	Thin Layer Cromathography
TMS	Tetramethylsilane
TRIS	Tris(hydroxymethyl)aminomethane
UDP	Uridine diphosphate

TABLE OF CONTENTS

A book is simply the container of an idea -like a bottle;
what is inside the book is what matters.

Angela Carter

1. INTRODUCTION 3

1.1 Gaucher disease 7

1.2 Glucosylceramide (GluCer) 8

1.2.1 Synthesis of GluCer.Glucosylceramide synthase (GCS) 9

1.2.2 Degradation of GluCer. Glucosylceramidases 10

1.3 Approaches to the treatment of Gaucher Disease 16

1.3.1 Enzyme Replacement Therapy (ERT) 17

1.3.2 Substrate Reduction Therapy (SRT) 18

1.3.3 Pharmacological Chaperone Therapy (PCT) 19

2. OBJECTIVES 23

3. RESULTS AND DISCUSSION 29

3.1 Study of the influence of the pK_a of the amino substitution in the side chain of DNJ derivatives 33

3.1.1 Introduction 33

3.1.2 Synthesis of DNJ aminoderivatives and compounds **16** 40

3.1.3 Synthesis of DNJ azido derivatives and compounds **31** 45

3.1.4 Imiglucerase inhibition assay 53

3.1.5 Analysis of pK_a 58

3.1.6 Synthesis of pyridine derivatives and analysis of their pK_a 60

3.1.7 Synthesis and evaluation of compounds **43** and **44** 63

3.1.8 Other biological assays 67

3.2 Study of the influence of the pK_a of the sugarmimethic core 74

3.2.1 Introduction 74

3.2.2 Synthesis of different cores and some *N*-butyl and *N*-nonyl derivatives 77

3.2.3 Synthesis of *N*-butyl inositol and DNJ derivatives with and without β-substitution 86

3.2.4 Imiglucerase inhibition assay and pK_a determination 96

3.2.5 Synthesis and evaluation of β-substituted *N*-nonyl derivatives 98

3.2.6 Global analysis of pK_a and Δ values 102

3.2.7 Other biological assays 108

3.2.7.1 Inhibition of commercial glycosidases 108

3.2.7.2 Inhibition of GCS 110

3.2.7.3 Cytotoxicity assay in WT human fibroblasts 111

3.3 Study of the GBA inhibition in detergent-free assays 113

3.3.1 Introduction 113

3.3.2 Detergent-free assays with cell homogenates 115

3.3.3 Intact cell assays 125

4. CONCLUSIONS 134

4.1 Study of the influence of the pK_a of the amino substitution in the side chain of DNJ derivatives 136

4.2 Study of the influence of the pK_a of the sugarmimethic core 137

4.3 GBA inhibition in detergent-free assays 138

5. EXPERIMENTAL SECTION 140

5.1 Synthesis and product characterization 144

5.1.1 General methods 144

5.1.2 Synthesis of DNJ derivatives with substitution at the end of the side chain 148

5.1.3 Synthesis of compounds with different pK_a in the sugarmimethic core 176

5.2 Biological assays 206

5.2.1 Assays with purified enzyme 206

5.2.2 Cell lines and culture 208

5.2.3 Assays with cell homogenates 208

5.2.4 Assays with intact cell 210

6. RESUM EN CATALÀ 212

6.1 Introducció 216

6.2 Objectius 219

6.3 Resultats i discussió 220

6.3.1 Estudi de la influència del pK_a de la cadena lateral 220

6.3.2 Estudi de la influència del pK_a del nucli central de l'inhibidor 231

6.3.3 Assajos sense detergents 241

6.4 Conclusions 245

BIBLIOGRAPHIC REFERENCES 250

INDEX OF COMPOUNDS 266

1. INTRODUCTION

千里之行，始于足下

The journey of a thousand miles begins with a single step.

Lao Tzu

Introduction contents

1.1 Gaucher disease

1.2 Glucosylceramide (GluCer)

1.2.1 Synthesis of GluCer. Glucosylceramide synthase (GCS)

1.2.2 Degradation of GluCer. Glucosylceramidases

1.2.2.1 Human lysosomal β-glucosidase, GBA1

1.2.2.2 Mechanism of hydrolisis of GluCer by GCase

1.2.2.3 Other substances involved in GluCer hydrolysis

1.3 Approaches to the treatment of Gaucher Disease

1.3.1 Enzyme Replacement Therapy (ERT)

1.3.2 Subtrate Reduction Therapy (SRT)

1.3.3 Pharmacological Chaperone Therapy (PCT)

1.1 Gaucher disease

Gaucher disease (GD) isan inherited autosomal recessive disorder, caused by the reduced activity of the enzyme β-glucocerebrosidase (GCase, GBA1) that result in a progressive accumulation of glucosylceramide (GluCer) within the lysosomes of cells, particularly macrophages and related.Thisaccumulation of undegradedGluCer leads to clinical manifestations that can include enlarged liver and spleen, bone complications, anemia, respiratory problems and, in more severe cases, CNS involvement or even death[1,2].

In a healthy person, GCase is transported from endoplasmic reticulum (ER) to the lysosome through the Golgi apparatus. Once in the lysosome, GCasehydrolizesGluCer giving glucose and ceramide. In the case of a GD patient, due to certain gene mutations, there is an incorrect folding of GCase. This misfolded GCase cannot be properly transported from endoplasmic reticulum (ER) to the Golgi apparatus and then to the lysosome. As a consequence, GluCer is not degraded in the lysosome and there is a subsequent accumulation of this glycolipid.

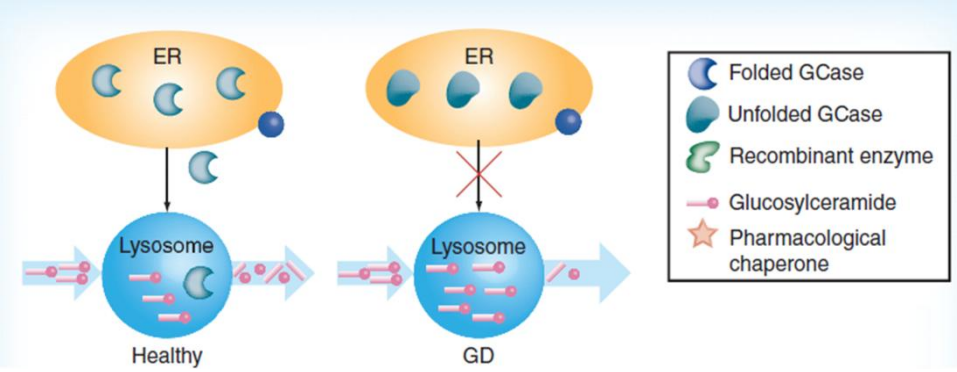

Figure 1 Metabolism of GluCer comparing a healthy person vs Gaucher patient**.**Figure adapted from Trapero *et al*[1].

GD was firstly described by Philippe Gaucher in his doctoral thesis in 1882[3]. However it was not until 1965 that Brady *et al* determined that the cause of the clinical manifestations was an accumulation of GluCer due to a reduced activity of GCase[4,5].

Although GD is considered a rare disease, it is the most prevalent lysosomal storage disorder (LSD),with an estimated incidence of one in 40,000-60,000 in the general population, and higher prevalence among the Ashkenazi Jewish population (one in 450)[6]

GD is traditionally classified into three different types or forms, based on the absence (type1) or presence and severity of neurological manifestations (types 2 and 3). Type 1 GD is the most common form, with more than 90% of cases in the USA and Europe[7]. Acute neuronopathic (type 2) GD is the rarest and most severe form of this disease. It shows rapidly progressing neurological deterioration, resulting in death within the earlyyears of life. GD type 3 is another neuronopathic form but its onset and progression of the neurological symptoms is at a later stage and slower than Type 2[8].

However, recent studies have described the presence of peripheral and central neurological symptoms in patients diagnosed with type 1 GD[7,9].Moreover, patients with the same gene mutation frequently showed different problems and grades of affectation[10], showing no direct correspondence between the mutations (genotype) and the clinical manifestations (phenotype). Due to the broad range of manifestations of the disease, it is often difficult to classify patients as a specific type of GD. This has led to the suggestion that GD may be more correctly described as a continuum of phenotypes, with neurological involvement in a proportion of patients ranging from mild-to-extreme severity[11,12].

1.2 Glucosylceramide (GluCer)

Glucosylceramide (Glucocerebroside, GluCer) is a glycosphingolipid whose accumulation in the lysosome causes the clinical manifestations in the case of GD. It is synthesized from UDP-glucose and ceramide by the transferase glucosylceramide synthase (GCS) in the cytosolic side of the Golgi apparatus, and it is hydrolyzed at lysosome by GCase in presence of saposin C.

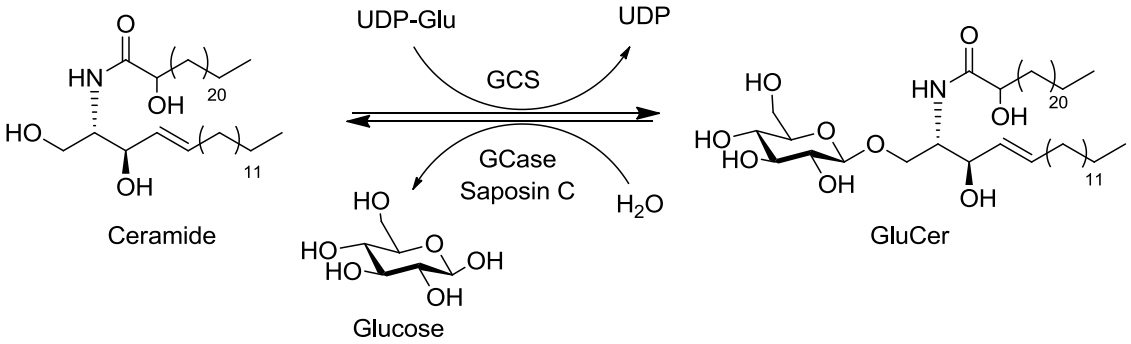

Scheme 1 Synthesis and hydrolysis of GluCer.

As shown in Fig. 2, GluCer is a fundamental precursor of a high amount of complex glycosphingolipids and gangliosides[13-15]. Although the specific function of most of these

compounds is not yet defined, it is known that, at least, they have an important role in the permeability barrier of the skin and seem to be required for intracellular membrane transport, cell proliferation and survival, as well as for various functions of the immune system. Thus, GluCer plays an essential role in human metabolism, and alterations in the level of GluCer can have influence in several disorders as cardiovascular disease, diabetes, skin disorders and cancer[16,17].

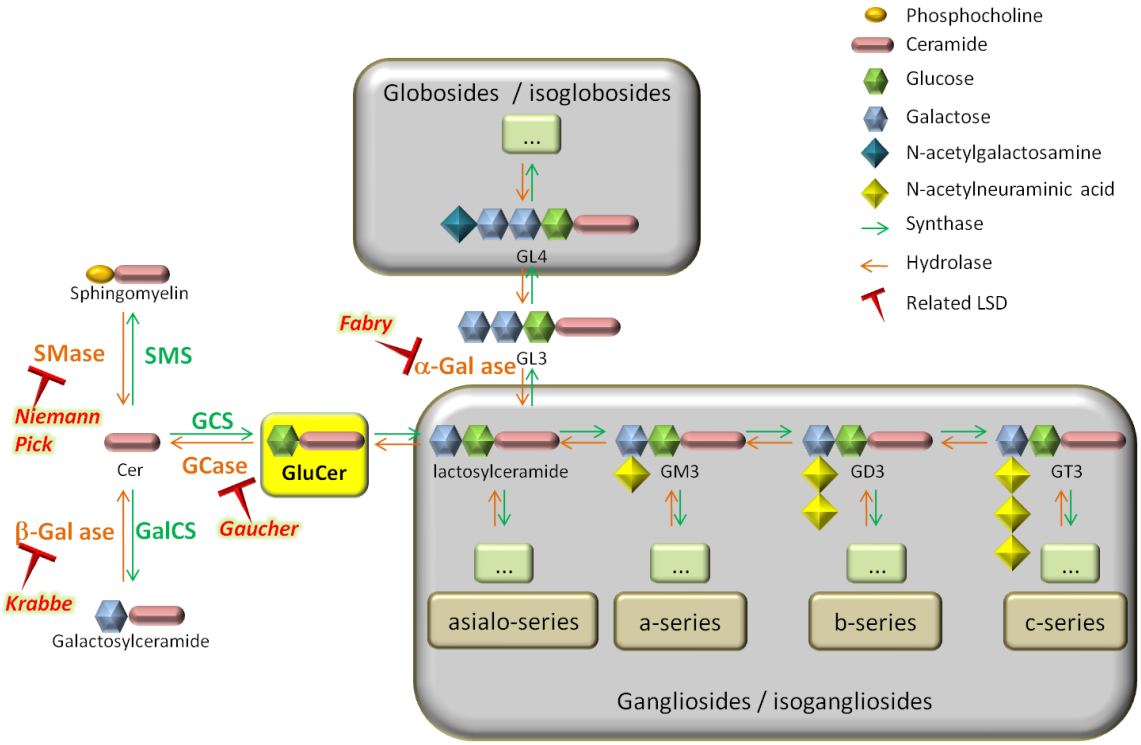

Figure 2 Metabolism and classification of some Glycosphingolipids, and related LSD.

1.2.1 Synthesis of GluCer.Glucosylceramide synthase (GCS)

GluCeris synthesized in the cytosolic side of the Golgi apparatus from UDP-glucose and ceramide by glucosylceramide synthase.

Human glucosylceramide synthase (GCS, ceramide glucosyltransferase, GlcT-1, EC:2.4.1.80) is a protein that catalyzes the transfer of glucose to ceramide[18] giving GluCer, the first step in biosynthesis of more complex glycosphingolipids that play important roles in a variety of cellular processes as cell recognition, growth, development and differentiation[15,19].

GCS is a transmembrane protein present on the Golgi apparatus with its catalytic site facing the cytosol[20]. It is encoded by gene UGCG, located in chromosome 9q31[21].

GCS and its activity were firstly described by Basu et al. in 1968[18]. Its cDNA encoding was isolated in 1996[22] and some of the active site residues have been characterized[23], but the complete 3D's structure of this enzyme has not been yet determined.

1.2.2 Degradation of GluCer. Glucosylceramidases

GluCer is degraded to glucose and ceramide by three different hydrolases: the lysosomal GBA1 and the non-lysosomal GBA2 and the cytosolic GBA3. The three GBA proteins are mainly located in different tissues and different parts of a cell and show no structural or sequence homology but interestingly share a similar enzymatic activity[24].

As shown in Fig. 3, most of the GluCer reaches the lysosomes with the help of lysosomal membrane protein 2 (LIMP-2) and is degraded in the lysosome lumen by GBA1.GD is caused by mutations in the *gba1* gene that causes a misfolding in GBA1 glucosidase, with a consequent diminution of the GBA1 transported to the lysosome and thus a reduction of GluCer cleavage and the accumulation of this glycolipid in lysosomes. Thus, the reduction of lysosomal GluCer hydrolysis in GD is due to a decrease of the amount of GCase that reaches the lysosome and not directly related to a reduction of its catalytic activity[25].

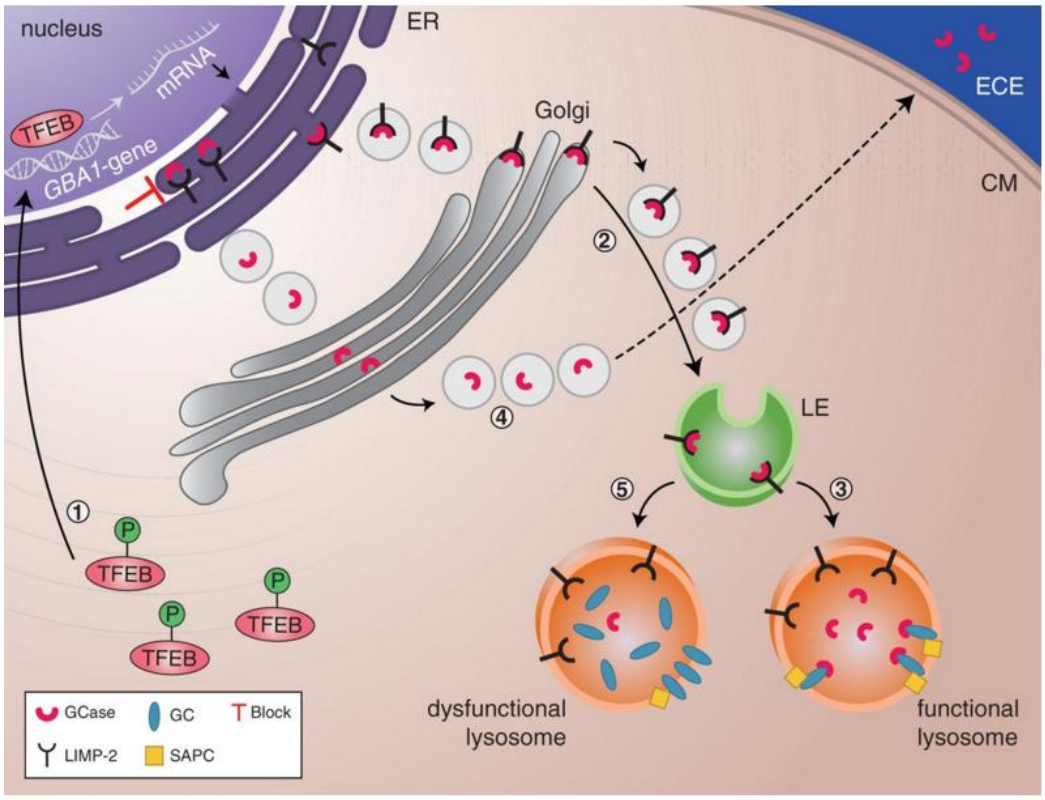

Figure 3 Regulators of *GBA1* expression and glucocerebrosidase activity and trafficking. (1) dephosphorylated transcription factor EB (TFEB)translocates to the nucleus where it regulates the transcription of genes, including *GBA1*. (2)*GBA1* messenger RNA is translated into glucocerebrosidase. The interaction with its receptor LIMP-2 facilitates translocation of glucocerebrosidase to the lysosomes via the endoplasmic reticulum (ER), Golgi and late endosomes (LE). (3) In the lysosomes, glucocerebrosidase dissociates from LIMP-2. The glucocerebrosidase activator, saposin C (SAPC), lifts glucocerebroside from the lysosomal membrane and/or membranes within the lysosome and makes it available for glucocerebrosidase-mediated breakdown. (4) When LIMP-2 is deficient or absent, the glucocerebrosidase enzyme cannot be correctly sorted to the lysosomes. As a consequence, glucocerebrosidase is secreted into the extracellular environment (ECE). (5) Saposin C deficiency leads to the impairment of glucocerebroside degradation sincethe substrate is not available to glucocerebrosidase and subsequently accumulates inside the lysosomes. CM = Cell Membrane[8].

The non-lysosomal GBA2 glucosidase is a non-integral membrane protein tightly associated with membranes. It is located at the cytosolic surface of the ER and Golgi (predominantly the cis-Golgi), with the N and C termini directly accessible from the cytosol and with the catalytic domain also located on the cytosolic side of membranes [24].

The cytosolic β-glucosidase (GBA3; EC 3.2.1.21) is a Klotho-related protein. It is able to hydrolyze a variety of substrates with a β-glucose, β-galactose, β-xylose, or α-arabinose moiety linked to a hydrophobic group. GBA3 is resistant to inhibition by conduritol-β-epoxide (CBE), but can be inhibited by β-D-glucosylsphingosine. The GBA3 gene is located in locus 4p15,31. The cDNA encodes a protein of 469 amino acid residues, possessing neither a signal peptide for secretion nor a transmembrane domain. GBA3 is particularly expressed in liver, kidney and intestine[26].

Although GBA2 and GBA3 also showed a glucosylceramidase activity, their expression in most of the tissues is lower than GBA1[27] and mutations in *gba2* and *gba3*genes do not seem to lead to GD clinical manifestations. Even so, GBA2-deficient mice accumulate GluCer in those tissues that expresses this protein most prominently (testis, liver and brain), causing an endoplasmic reticulum storage disease andmale infertility[28].

1.2.2.1 Human lysosomal β-glucosidase, GBA1

Human lysosomal β-glucosidase (acid β-glucosidase,Glucocerebrosidase, GCase, GBA1, EC 3.2.1.45) is a membrane associated enzyme that cleaves the β-glucosidic linkage of GluCer[29]. GCase is encoded by a gene located on chromosome 1q21 spanning 7.6kb and includes 11 exons[30,31].

The GCase 3D structure was solved in 2003 by 2.0-Å x-ray diffraction crystal analysis, revealing a typical $(\beta/\alpha)_8$ TIM barrel catalytic core[32]. This structure encompasses three non-contiguous domains stabilized by the formation of three disulfide bonds. Domain I consists of one major three-strand anti-parallel β sheet flanked by a loop and a perpendicular *N*-terminal strand. Domain II consists of two closely associated β sheets that form an independent domain resembling an immunoglobulin fold, and domain III is a $(\beta/\alpha)_8$ TIM barrel that contains the catalytic site. Domains I and II are packed against the same side of the larger TIM barrel domain.

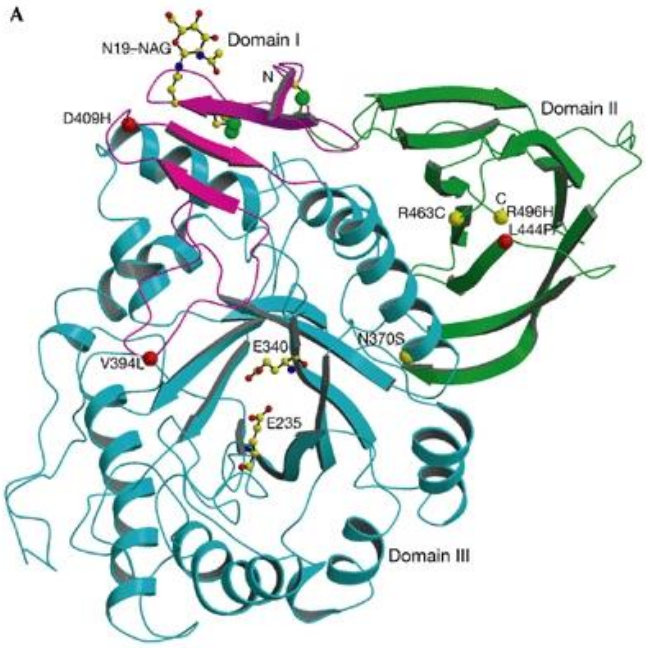

Figure 4 X-ray structure of acid-β-glucosidase. Domain I is shown in magenta and contains the two disulphide bridges, the sulphur atoms of which are shown as green balls. The glycosylation site at N19 is shown as a ball-and-stick model. Domain II, which is an immunoglobulin-like domain, is shown in green. The catalytic domain (domain III), which is a TIM barrel, is shown in blue, and the active-site residues E235 and E340 are shown as ball-and-stick models. The six most common GCase mutations are shown as balls, with those that cause predisposition to severe (types 2 and 3) and mild (type 1) disease in red and yellow, respectively[32].

To date, over 300 GCase pathogenic mutations and polymorphisms have been reported but correlations between the clinical phenotype and molecular genotype remain limited[10,33]. Although some mutations do not affect to the enzyme activity, some specific amino acid residues have a critical role for protein conformation. For example, the Asn370 is important for stabilization of the conformational change of one of the loops of the catalytic site. Substitution of this residue by a serine (mutation N370S) leads to destabilization of this loop, affecting to the enzymatic activity[34].

The most prevalent mutations reported in patients with GD are N370S and L444P[35].N370S missense mutation is the most prevalent mutation among type 1 GD patients, whereas patients homozygous for L444P (substitution of Pro444 for Leucine) usually display a more severe neuronopathic form[1,33].

1.2.2.2 Mechanism of hydrolisis of GluCer by GCase

GCase is a typical retaining β-glucosidase, whose catalytic cycle proceeds through a two-step reaction mechanism requiring glucosylation of the active site by substrate followed by deglucosylation with the release of D-glucose[36]. The nucleophile in this active site function is Glu340, and the acid/base is Glu235[37,38]. The *O*-glucosidic bond of substrates is protonated by the acid/base (Glu235)aminoacid and is then attacked by the active site nucleophile (Glu340). Glucose becomes then covalently attached, as aglycosidic ester with inversion of configuration at the glycosidic carbon, and the leaving group is removed. This is followed by deprotonation of water by the acid/base with attack of the enzyme-glucose complex by the liberated nucleophile in a second SN2 reaction and release of beta-D-glucose[39] with overallretention of configuration.

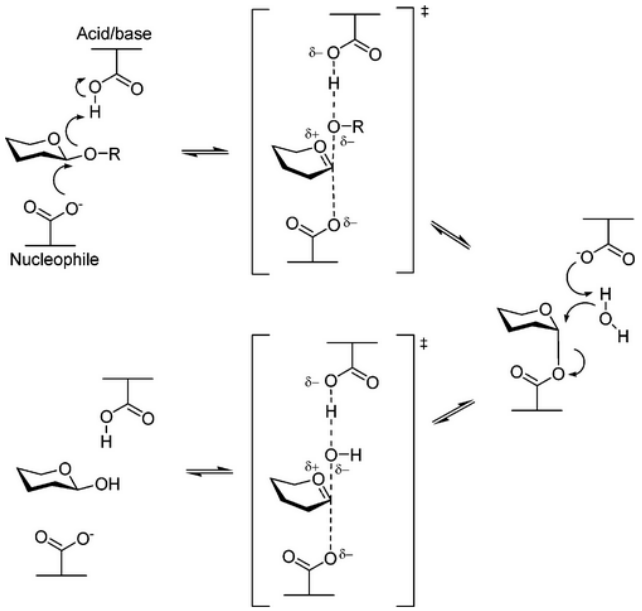

Figure 5 General mechanism of β-glycoside hydrolysis with retaining configuration[36].

1.2.2.3 Other substances involved in GluCer hydrolisis

It is necessary to point out that, to hydrolyze GluCer, GCase requires the coordinate action of saposinC and negatively charged lipids[40].Saposin C is a lysosomal membrane binding protein that acts as an activator for the hydrolysis of GluCer. This protein adopts different conformations according to the environment, changing its conformation and assembly depending on pH[41,42] and the presence or absence ofdetergents[43,44].Several studies demonstrated the crucial role of saposin C in *in vivo*GluCer hydrolysis[43-45]. In fact, a disfunction

ofsaposin C produce an accumulation of GluCer and lead to clinical manifestations similar to the GD that is due to mutant GCase[46,47].

However, the exact mechanism of saposinC's function has not been determined. Mechanistically, saposins appear to activate lipid hydrolysis by solubilizing the lipid substrates or possibly by destabilizing the membrane structure[48].According to solubilizer model, saposin C dissociates from the membrane in a soluble complex with GluCer, which is hydrolyzed by GCase in solution. In contrast, liftase model suggests thatsaposin C stably associates with the membrane and exposes GluCer for direct hydrolysis by GCase on the surface of thinned membrane domains[45,49].

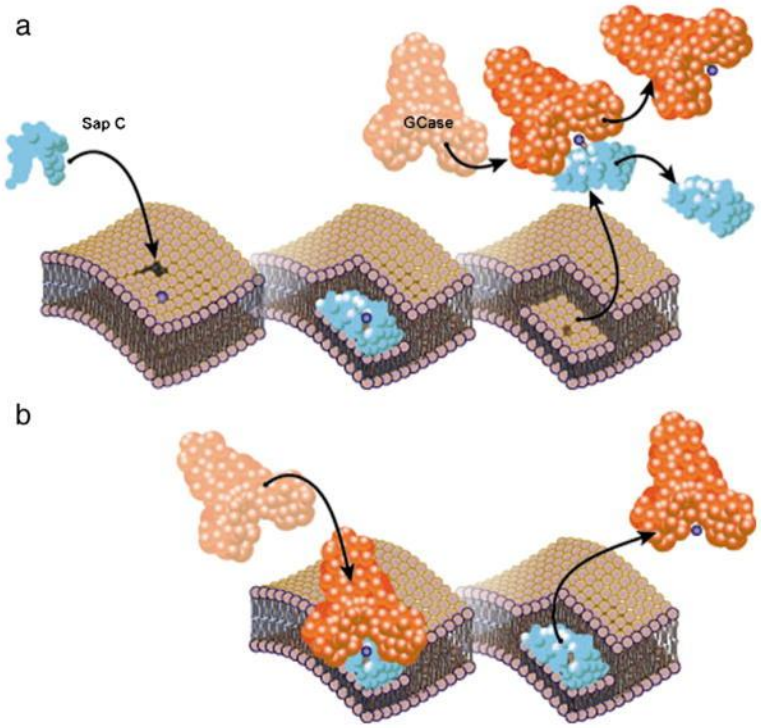

Figure 6 Proposed mechanisms of GCase (orange) activation by Saposin C (blue). Sap C embeds in preexisting defects in the bilayer membrane, resulting in a thinned membrane domain, and exposing the headgroup of glucocerebroside substrate (purple ball). Activated GCases is shown in red. **a)**Solubilizer model **b**) Liftase model[45].

1.3 Approaches to the treatment of Gaucher Disease

The first treatments for GD consisted in **supportive therapies** which may includedifferent cares as blood transfusions, pain reduction therapies, orthopedic surgery for bones and joints or splenectomy[50]. It must be noticed that the aim of those treatments was just managing or relieving the symptoms, without focusing on the origin of the problem. Nowadays this kind of therapies is still used as a complement to other treatment options for GD.

Another option for the treatment of GD is **bone marrow transplantation**[51]. Until now, it is the only treatment that solves the neuronophatic problems and for this reason it is mostly recommended for type 3 GD patients. Although it has the potential to cure GD, it has a significant morbidity and mortality associated[52]. Thus it is only applied when other treatment options are not applicable[53,54].

Moreover, different studies to introduce **gene therapy** as a treatmentfor GD have been performed. Most of those studies have been focused into transferring the gene coding forGCase via a retroviral vector into cultured bone marrow cells of GD patients to express the functional GCase[55-59]. Although it could seem an attractive option, no effective gene therapy has been developed yet[54].

On the other hand, two therapeutic approaches are currently approved for the treatment of GD[1].The first, and most common treatment, is **Enzyme Replacement Therapy** (ERT)[60,61], which involves the direct administration of recombinantly expressed human GCaseto supplement the patient's levels of GCase activity. The second therapeutic approach is **Substrate Reduction Therapy** (SRT)[62] which consists on the reduction of the biosynthesis of GluCer by inhibition of glucosylceramide synthase (GCS).

Alternatively, **Pharmacological Chaperone Theraphy** (PCT) is another interesting approach that could lead to a group of new drugs for LSD. This approach is based on the idea that a competitive reversible inhibitor binding to a mutant misfolding enzyme can lead to a correct protein folding, resulting in an improvement of its stability and trafficking and, as a consequence, producing an enhancement of the enzyme activity.

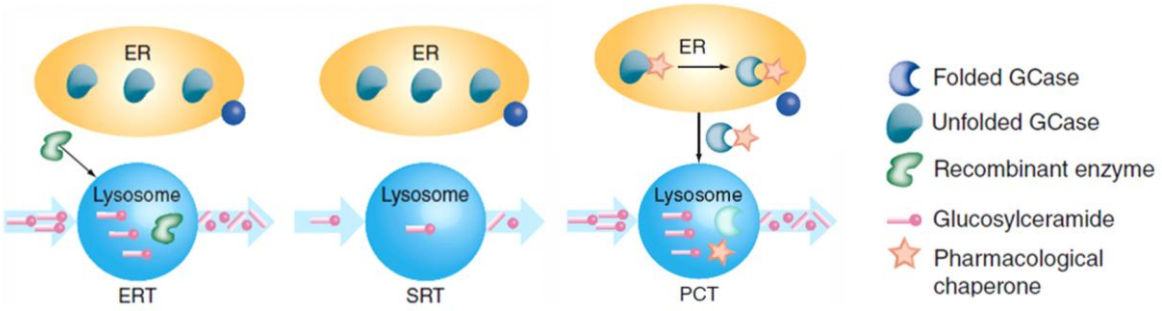

Figure 7 Some potential therapies for GD and other LSD. Figure adapted from Trapero *et al*[1].

1.3.1 Enzyme Replacement Therapy (ERT)

Brady et al demonstrated in 1966 the deficiency of glucocerebroside-cleaving enzyme in Gaucher disease[5]. It was not before the early 90s when he and collaborators proved the effectiveness of the ERT in GD[61,63,64]. Thus, from 1991 to nowadays several enzymes are approved for their use in ERT for GD:

Alglucerase (Ceredase®) was the first enzyme used for ERT for the treatment of GD. Alglucerase is a Gcase extracted from human placental tissue. Precisely this reliance on human placenta suggested the need of another ERT approach due to its cost and difficulty to harvest and transport the amount of placenta necessary for obtaining all the doses (50,000 individual placentas per patient per year). The use of Alglucerase as ERT was approved by the FDA in 1991 but this protein was finally discontinued and replaced by Imiglucerase in 1998[65].

Imiglucerase (Cerezyme®) is a recombinant enzyme currently used for more than 20 years in enzyme replacement therapy for Gaucher Disease. It is obtained from mutant Chinese hamster ovary cells, anddiffering from the sequence of the native human GCase, it contains a histidine at position 495 instead of an arginine. This substitution at 495 does not alter the protein structure neither enzymatic activity[66].

Velaglucerase alfa (VPRIV®) is a replacement enzyme produced by gene activation in human fibroblast cell line HT-1080. This technique leads to a GCase that has the same aminoacid sequence as that of wild-type Gcase. Velaglucerase alfa was approved in 2010 by the FDA and EMA for long term ERT of pediatric and adult patients with GD[67].

Taliglucerase alfa (Elelyso®) is a GCase obtained from carrot root cell cultures.It was approved by FDA as ERT for GD in 2012. In fact, Taliglucerasealfa is the first approved plant cell-expressed recombinant therapeutic protein[68,69].

Unfortunately, due to the difficulty for those enzymes to cross the BBB, ERT is not effective for the neuronopathic variant of GD.Moreover, some patients can experience hypersensitivity reactions or develop antibodies after ERT[69]. The approval of different enzymes for ERT opens the door to the treatment of more patients and prevents a possible lack of enzyme for ERT due to potential production problems.

In addition to the lack of effectiveness to treat the neuronopathic form of GD, ERT has other important disadvantages as the fact that those drugs are not orally available and periodic intravenous administration of recombinant enzyme is necessary, often in a hospital setting. Furthermore, this therapeutic approach is also very expensive (US$100,000–200,000/patient/year) and so it is likely that many patients do not have access to ERT[1].

1.3.2 Substrate Reduction Therapy (SRT)

The therapeutic strategy of Substrate Reduction Therapy (SRT) applied to lysosomal storage diseases was first proposed by Radin *et al* in 1972[70,71]. This concept, if applied in the case of Gaucherdisease, states that inhibition of glucosylceramide synthase (GCS) will be an effective approach to diminish the amount of GluCer accumulated in lysosome, especially if defective hydrolase GCase retains any residual activity[72].

Nowadays there are two drugs approved by the FDA as oral SRT for the treatment of GD. One of them is the iminosugar *N*-butyl-deoxinojirimicin (NB-DNJ, **Miglustat**, Zavesca®) approved by the FDA in 2003 and, due to its side effects (mainly diarrheaand weight loss, in addition to some reported cases of peripheral neuropathy), it is recommended only for the treatment of GD for adult patients for whom ERT is unsuitable[73-75]. The other drug is **Eliglustat tartrate** (Cerdelga®)[76], approved by the FDA in 2014, and it is the first non ERT that can be used as a first option instead of ERT. It has shown similar effects than ERT with a daily oral administration, which will suppose an important advantage for the quality of life of the patients. Furthermore, a simple blood test analyzing the CYP2D6 metabolizer status of the patient can determine if Cerdelga® will be a good treatment option for that GD patient[77].

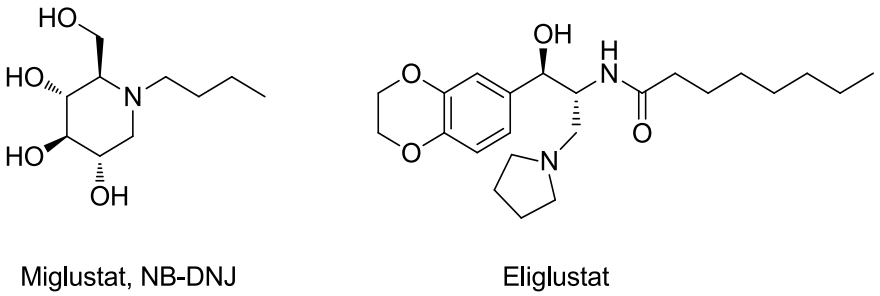

Figure 8 Chemical structures of Miglustat and Eliglustat.

It should be highlighted that Miglustat seemed to partially cross the BBB[78] but Eliglustat does not[77]. Although SRT drugs have the potential for oral bioavailability, broad tissue distribution and better CNS penetration than ERT, SRT has not succeeded in bringing up suitable candidates for the treatment of neuronopathic variants until now.Furthermore, due GluCer crucial role in different biological pathways[13-17], inhibiting its synthesis can arise to important side effects due to the lack of this essential glycosphingolipid.

Thus, although SRT can offer an oral available drug that avoids the annoying periodic intravenous administration of the recombinant enzyme, it still does not give a solution for the neuronopathic form of GD. Moreover, this kind of therapy potentially can produce important side effects related to cardiovascular problems, diabetes, skin disorders or cancer and others, due to the lack of GluCer.

1.3.3 Pharmacological Chaperone Therapy (PCT)

As shown in Fig. 9, lysosomal hydrolase folding commences in the endoplasmic reticulum (ER) at neutral pH. The folded enzyme is trafficked through increasingly acidic compartments to the lysosome. Deficient in folding enzymes in the ER aretargeted for degradation by the proteosome. A Pharmacological Chaperone (PC) for the treatment of GD should reversibly bind the misfolded GCase in the ER (neutral pH), stabilizing it with the correct folding and enhancing the transport of the protein to the lysosome through the Golgi apparatus. Once in the lysosome (pH 5.2), PC will compete with GluCer that will be hydrolyzed by this re-folded and catalytically active enzyme[79].

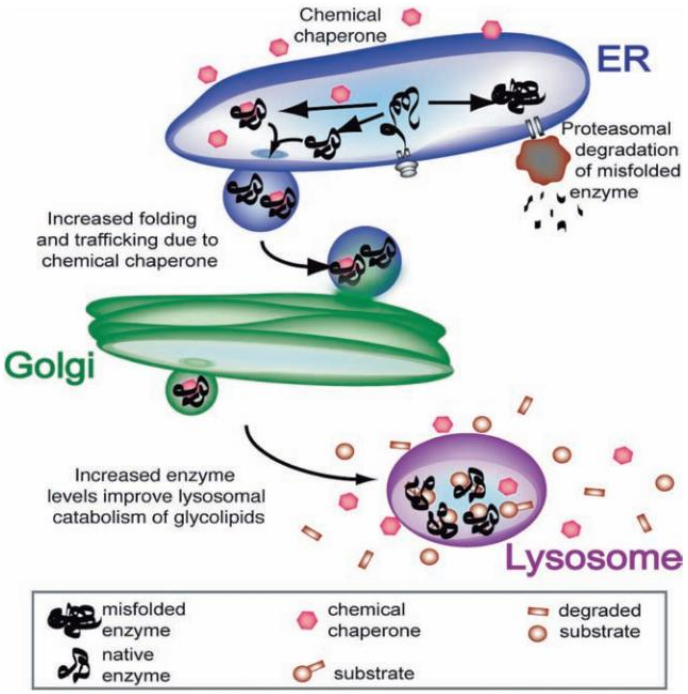

Figure 9 Proposed mechanism of chemical/pharmacological chaperoning.

The major advantages of PCT, compared to ERT, are the lower costs,presumedoral availability and the better biodistribution.PCs are small molecules and probably able to cross the BBB, thus PC have a potential for the treatment of diseases with CNS involvement[80]. Moreover, as a PC would promote the availability of functional GCase inlysosomes without involving the inhibition of GCS, this therapy would also solve the side effects of SRT due to the lack of GluCer.

A pioneering study by Fan et al[81] demonstrated for the first time in 1999 a chaperone effect of an imino sugar in lymphoblasts from patients with Fabry disease, caused by the deficiency of the lysosomal hydrolase α-galactosidase A (GLA). Subsequently, other studies provided the proof of principle for the use of PCT in a few other LSDs, including Gaucher disease[34,82,83].

On the other hand, some studies showed that PCs are also able to enhance physical stability and potentiate the therapeutic action of enzymes used for ERT[84-89]. In the case of GD, this fact could be particularly valuable since the half-life of Imiglucerasein the circulation is of the order of 10-15 min[90], and only small amounts of the injected enzyme are actually internalized by macrophagues. A stabilization of the recombinant exogenous enzyme by a PC could lead to an increased hydrolase activity. Thus, the combination of PC and ERT may convey to a reduction of the dose or frequency of the ERT infusionsand, as a consequence, potentially reduce the cost of treatment and improve the quality of life for GD patients[91,92].

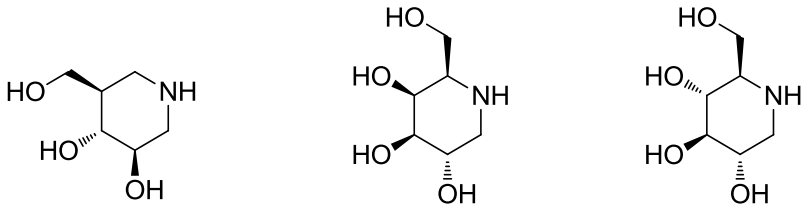

Afegostat
IFG
AT2101

Migalastat
DGJ
AT1001

Duvoglustat
DNJ
AT2220

Figure10 Chemical structures of IFG, DGJ and DNJ, PC for a potential treatment of Gaucher, Fabry and Pompe diseases respectively[93-96].

Until now, IFG has reached Phase II clinical trials as PCT for GD, and DGJ has several phase III clinical trials ongoing nowadays, as a PCT for Fabry disease treatment (see trials NCT00433147, NCT00813865 and NCT00446550 for IFG, and trials NCT00925301, NCT01458119 and NCT02194985 for DGJat http://clinicaltrials.gov). On the other hand, Phase II studies for combined ERT and PC therapy for Fabry and Pompe diseases have been performed too (trials NCT01196871 and NCT01380743).

2. OBJECTIVES

They did not know it was impossible, so they did it.

Mark Twain

PCT is a promising therapy approach with high interest thanks to its potential oral administration, lower side effects, cheaper cost and, above all, their potential to cross the BBB allowing the treatment of the neuropathic form of GD. On the other hand, some drugs has been approved as PCT for other diseases, but not yet for GD. Considering that, this thesis has been focused on the synthesis of compounds with potential PC profile.

Thus, an ideal PC for the treatment of GD should accomplish some "basic premises":

- To be a competitive inhibitor of GCase with high affinity for the enzyme in ER (neutral pH) to induce the correct folding of the protein and facilitate its transport.

- To have a smooth dissociation from the enzyme in lysosomic conditions, to facilitate the binding between the enzyme and GluCer.

- To be selective for GCase, to avoid potential side effects.

- To have a good biodistribution and cross the BBB, to be useful for the treatment of the neuropathic forms of GD.

-To have low toxicity.

Bioactive molecules that mimic the sugar structures, as aminocyclitols or iminosugars, are compounds of high interest in the field of glycolipid metabolism. Thanks to their structural similarities with the natural substrates, some of them display interesting biological and enzymatic activities, especially as glycosidase inhibitors[97,98].

Iminosugars (as DNJ, IFG or DGJ) are analogs of monosaccharides with endocyclic oxygen replaced by a nitrogen atom. Several iminosugar derivatives showed GCS and/or GCase inhibition, demonstrating its potential use as treatment for GD[73,93,99-103]. Iminosugars were the first type of compounds systematically investigated as PCT for GD and still are the main source of investigational drugs for the treatment of LSDs[1].

Aminocyclitols are amino polyhydroxylatedcycloalcanes that can be found in nature in several families of natural products. Among them, **inositol** derivatives have a particular relevance in cell function and regulation and for this reason they have been widely a subject of study. For example, and with reference to GD, several studies performed inour group have revealed

different series of inositol analogues as potent GCase inhibitors able to enhance the activity of this enzyme in Gaucher cells[104-111].

Furthermore, iminosugars as NB-DNJ and NN-DNJ showed higher GCase inhibition under neutral conditions than acidic. It seems that NB-DNJ binding to GCase is controlled by pH, whereas IFG-GCase binding is not so pH dependent[92]. That fact has special interest since an ideal PC for GD should have high affinity for the GCase in ER but not in the lysosome. The reason for this pH-dependence affinity could be the pK_a of NB-DNJ and NN-DNJ (7.1 and 6.7 respectively). Thus, these compounds would be neutralin the ER, favoring its binding to GCase but they would be charged under the acidic conditions of the lysosome, lowering their GCase affinity and thus competing less with GluCer[112].

Based on previous considerations, this thesis will be focused on the synthesis of novel DNJ derivatives trying to enhance their capacity of showing different activity according to the pH of the assay, but also studying if this property is extrapolated to inositol derivatives, a family of compounds in which our group has a long previous experience and that showed higher GCase affinity than DNJ derivatives.

Thus, the main goal of this thesis is to **design and synthesize potent GCase inhibitors with higher GCase affinity at neutral pH than acidic pH as potential PC for the treatment of GD.**

This objective includes the following specific objectives:

A) Study of the influence of the pK_a of the chain on the GCase hydrophobic pocket.

For this proposal, a small library of DNJ derivatives with different pK_as on its *N*-alkylated chain will be designed and synthesized.

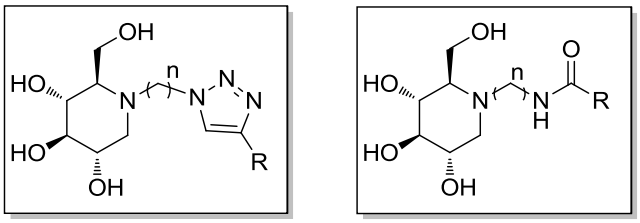

Figure 11 Families of compounds proposed for the study of the influence of the pK_a of the chain on the GCase hydrophobic pocket.

B) Study of the influence of the pK_a of the sugarmimetic core.

To afford this aim, different iminosugar and aminocyclitol derivatives with different substitutions on the chain or the core will be designed and synthesized, to provide a group of compounds with similar structure but a wide range of pK_as.

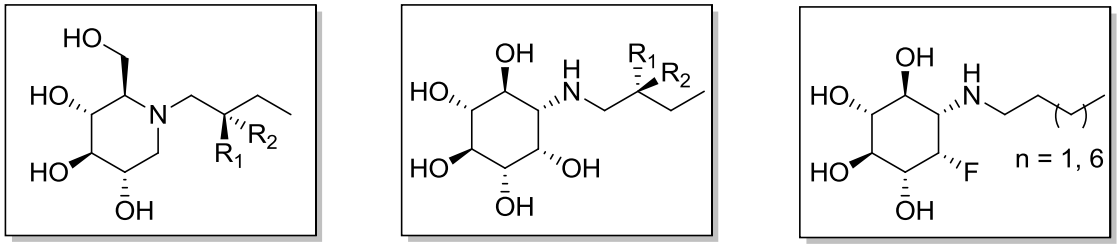

R_1, R_2 = H, OH, F

Figure 12 Families of compounds proposed for the study of the influence of the pK_a of the sugarmimetic core.

As some DNJ derivatives have shown to be GCS inhibitors, a secondary target will be to **obtain potent GCS inhibitors for their potential use as SRT or even dual compounds (GCS inhibitors and PC for GCase) for treatment of GD.**

3. RESULTS AND DISCUSSION

I'm a great believer in luck, and I find the harder I work the more I have of it.

Thomas Jefferson

Results and discussion contents

3.1 Study of the influence of the pK_a of the amino substitution in the side chain of DNJ derivatives

3.1.1 Introduction

3.1.1.1 DNJ derivatives binding to GCase

3.1.1.2 pK_a and equilibrium dissociation

3.1.2 Synthesis of DNJ aminoderivatives and compounds **16**

3.1.3 Synthesis of DNJ azidoderivatives and compounds **31**

3.1.4 Imiglucerase inhibition assay

3.1.5 Analysis of pK_a

3.1.6 Synthesis of pyridine derivatives and analysis of their pK_a

3.1.7 Synthesis and evaluation of compounds **43** and **44**

3.1.8 Other biological assays

3.1.7.1 Inhibition of commercial glycosidases

3.1.7.2 Inhibition of glucosylceramide synthase (GCS)

3.1.7.3 Cytotoxicity assay in WT human fibroblasts

3.2 Study of the influence of the pK_a of the sugarmimethic core

3.2.1 Introduction

3.2.1.1Customization of pK_a

3.2.1.2 Selection of the objective compounds

3.2.2 Synthesis of different cores and some *N*-butyl and *N*-nonyl derivatives

3.2.2.1 Synthesis of benzylated *myo*-inositol core (**63**).

3.2.2.2 Synthesis of F-inositol core and derivatives

3.2.3 Synthesis of *N*-butyl inositol and DNJ derivatives with and without β-substitution.

3.2.3.1 Synthesis of *N*-butyl and *N*-difluorobutyl inositol derivatives (compounds **47x** and **76**).

3.2.3.2 Synthesis of *N*-difluorobutyl DNJ derivative **82**

3.2.3.3 Synthesis of NB-DNJ derivatives with mono β-substitution (compounds **85x** and **87x**)

3.2.3.4 Synthesis of NB-inositol derivatives with mono β-substitution (compounds **89x** and **91x**)

3.2.4 Imiglucerase inhibition assay and pK_a determination

3.2.5 Synthesis and evaluation of β-substituted *N*-nonyl derivatives

3.2.6Global analysis of pK_a and Δ values

3.2.7 Other biological assays

3.2.7.1 Inhibition of commercial glycosidases

3.2.7.2 Inhibition of GCS

3.2.7.3 Cytotoxicity assay in WT human fibroblasts

3.1 Study of the GBA inhibition in detergent-free assays

3.3.1 Introduction

3.3.2 Detergent-free assays with cell homogenates

3.3.2.1 Determination of GBA1 inhibition

3.3.2.2 Determination of GBA2 inhibition

3.3.3 Intact cell assays

3.3.3.1 Tuning up of the assay and analysis of GBA2 inhibition in HAP1_001 (GBA1-KO) cells

3.3.3.2 Analysis of GBA1 inhibition and activity recovery in HAP1_001 (GBA2-KO) cells

3.1 Study of the influence of the pK_a of the amino substitution in the side chain of DNJ derivatives

3.1.1 Introduction

DNJ derivatives are a widely studied family of compounds that showed GCase inhibition. Particularly, NB-DNJ and NN-DNJ have demonstrated their potential as pharmacological chaperones stabilizing wild type GCase and increasing the proper trafficking from the reticulum of N730S mutated GCase[103,113].

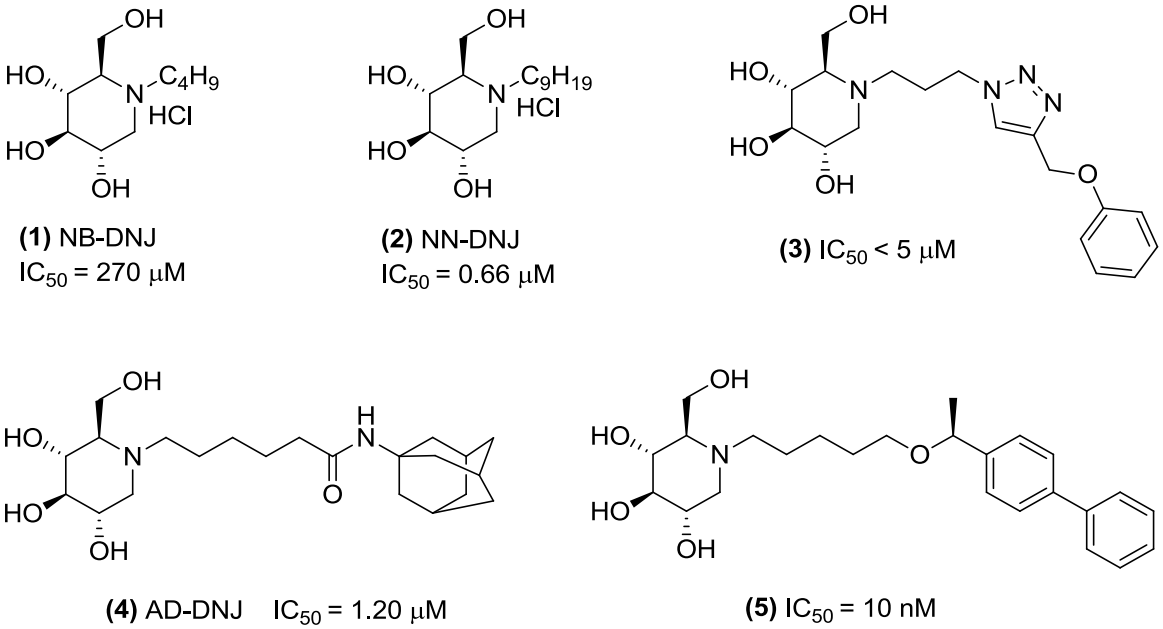

Figure 13 Examples of some DNJ-derivatives and their IC_{50} against GCase[1].

As a consequence of the interest of this family of compounds, the influence of several modifications performed to DNJ has been studied in order to obtain compounds with higher potency or improved pharmacological properties. For this purpose both modifications in the DNJ core as well as in the alkyl chain have been studied.

Thus, modifications of the DNJ ring could include changes or addition of substituents that sometimes could even lead to studies of different sugar mimetic cores. As an example, by introducing a long alkyl chain in the ring carbon in α position (compound **6**) it was possible to obtain a compound with similar activity against GCase that when the chain is in the nitrogen, but with potentially different metabolism. Going one step further, as shown in Fig. 14, another example of introducing diversity to the core was the attachment of an imidazole

moiety into the DNJ ring. In this case, glucoimidazole derivatives showed to be much potent GCase inhibitorsthan DNJ derivatives with similar chains[114].

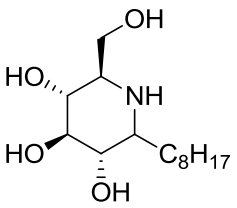

(6) α-1-C-octyl-DNJ IC_{50} = 0.50 μM

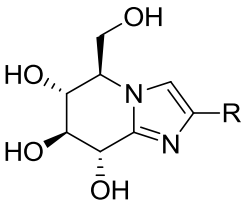

(7) R = 2-phenylethyl IC_{50} = 1.1 nM
(8) R = 2-octyl IC_{50} = 0.07 nM
(9) R = 2-dimethylbutyl IC_{50} = 0.03 nM

Figure 14 Examples of structural modifications from DNJ basis[1,115].

Regarding to the diversification of the chain, several studies have showed the advantages and versatility of using click chemistry[116,117,118] or amide synthesis[101] to introduce chemical diversity in the synthesis of DNJ derivatives as potential chaperones for GD.

The term "click chemistry" was firstly defined by Sharpless et al in 2001. It includes a wide range of different chemical reactions that are modular, wide in scope, give very high yields, generate only inoffensive byproducts that can be removed by non-chromatographic methods, and be stereospecific. The required process characteristics include simple reaction conditions, readily available starting materials and reagents, the use of no solvent or a solvent that is benign (such as water) or easily removed, and simple product isolation[119].

One of the click reactions most used nowadays in drug design is the Huisgen 1,3-dipolar cycloaddition between alkynes and azides to form 1,4-disubsituted-1,2,3-triazoles (Scheme 2). The copper (I)-catalyzed reaction is mild and very efficient, requiring no protecting groups, and requiring no purification in many cases. The azide and alkyne functional groups are largely inert towards biological molecules and aqueous environments, which allows the use of the Huisgen 1,3-dipolar cycloaddition in target guided synthesis and activity-based protein profiling. Moreover, the triazole has similarities to the ubiquitous amide moiety found in nature, but unlike amides, is not susceptible to cleavage.

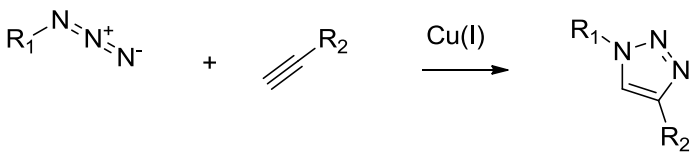

Scheme 2 Cu(I) catalyzed Huisgen 1,3-dipolar cycloaddition reaction.

Thus, by synthetic routes involving diversification by Huisgen 1,3-dipolar cycloaddition or amide formation, it has been possible the obtainment of small libraries of compounds that allowed the analysis of the influence of different substituents. For example, regarding to the influence of the length of the chain, previous studies suggested that the longer the chain, the best inhibition rates, but also the higher toxicity. Thus, it seems that the best balance between potency and toxicity is for those compounds whose chain between the DNJ group and the triazol linker has lengths between 4 and 6 carbons[118].

On the other hand, the prospect of in situ screening of compounds obtained by click reaction[107] or by amide formation[101], added another factor of interest in these kinds of reactions.

3.1.1.1 DNJ derivatives binding to GCase

The crystallographic structures of NB-DNJ and NN-DNJ binding GCase have been determined and, therefore, we could know how those compounds actually bind this enzyme.

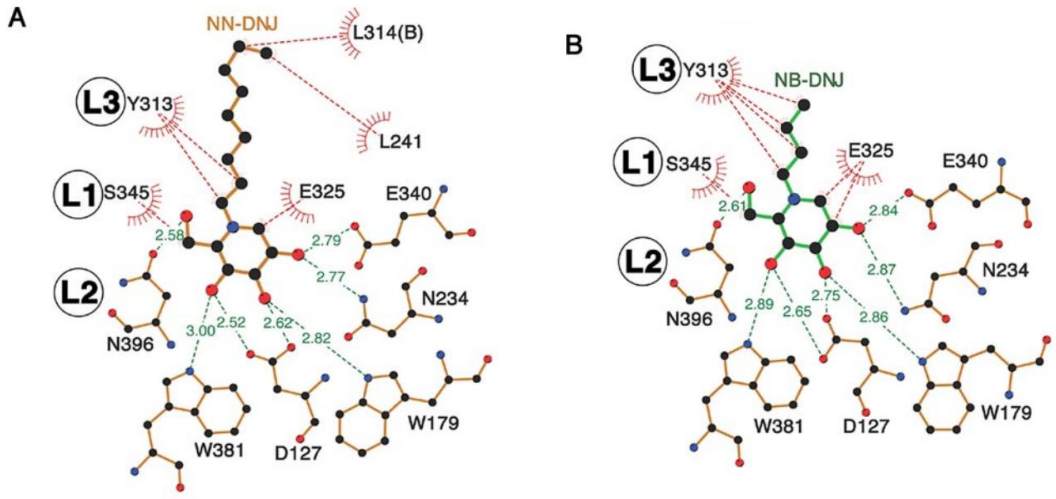

Figure 15 Comparison of binding of non-covalent inhibitors to GCase. **(A)**, NN-DNJ/pGCase (PDB ID: 2V3E). **(B)** NB-DNJ/pGCase (PDB ID: 2V3D). Green lines represent hydrogen bonds and red lines hydrophobic interactions. L1, loop 1 (residues 341–350); L2, loop 2 (residues 393–396); L3, loop 3 (residues312–319). 314 (B) in panel A corresponds to the side chain of a symmetrically related molecule. Figure adapted from Brumshtein *et al*[112].

As show in Fig. 15, both inhibitors bind to the active site of pGCase (recombinant human GCase, expressed in cultured plant cells)[120], with the iminosugar making hydrogen bonds with

side chains of active site residues. Hydrogen bond distances between the iminosugar and the active site residues are similar for NB-DNJ and NN-DNJ. The alkyl chains of NB-DNJ and NN-DNJ are oriented toward the entrance of the active site. The alkyl chains of both inhibitors are stabilized by interaction with Tyr313 near the active site, and the alkyl chain of NN-DNJ makes an additional contact with Leu314, near the entrance to the active site.Nevertheless, this additional interaction cannot explain the difference of affinity between both compounds, what seems to be due a reflection of the increased overall hydrophobicity of NN-DNJ compared with NB-DNJ, with the hydrophobic surface at the entrance to the active site favoring the more hydrophobic ligand[112].

This apparent higher affinity for the enzyme for compounds with more hydrophobic chains, together with the fact that ER (where the misfolded GCase is located) possess neutral pH while in the lysosome (where GluCer should be degraded) the pH is slightly acidic, could suggest that synthesizing a family of compounds with differenthydrophobicity on the chain depending on the pH of the environment, may lead to the achievement of compounds with different enzyme affinity and therefore different inhibitory capacity.

Thus, in order to obtain compounds with different hydrophobicities on the chain, it could be interesting to focus in the pK_a of the substituents in these chains.

3.1.1.2 pK_a and equilibrium dissociation[121]

The different chemical species (cationic, neutral, or anionic) often have vastly different properties with respect to water solubility, volatility, UV absorption, and reactivity. The ionized form is usually more water soluble, while the neutral form is more lipophilic and use to have higher membrane permeability. The ionization state of any compound is controlled both by solution pH and acidic dissociation constants (K_a).

An acid dissociation constant,K_a, is aquantitativemeasure of thestrength of an acid in solution. It is the equilibrium constant for a chemical reaction known as dissociation in the context of acid–base reactions. In aqueous solution, the equilibrium of acid dissociation can be written as:

$$\mathbf{HA + H_2O \rightleftharpoons A^- + H_3O^+}$$

In concentrated aqueous solutions of an acid the concentration of water can be taken as constant and can be ignored. Thus, K_a can be defined as:

$$K_a = \frac{[A^-][H^+]}{[HA]}$$

For many practical purposes it is more convenient to discuss the logarithmic constant, pK_a:

$$pK_a = -\log_{10} K_a$$

The pH of a solution of a weak acid may be calculated from the Henderson-Hasselbalch equation:

$$pH = pK_a + \log_{10} \frac{[basic\ species]}{[acidic\ species]}$$

Similarly, for basic compounds, it is possible to talk about basicity constant (pK_b) or the pK_a of the conjugated acid (pK_a). Thus, for a basic compound:

$$pK_a = pH - \log_{10} \frac{[no\ ionized\ species]}{[ionized\ species]}$$

From Henderson-Hasselbach equation, and as shown in the example of Fig. 16, it is possible to assume that for weak basic compounds, when pH is lower than pK_a-1, 90% of compound would be ionized, while when pH is higher than pK_a+1, around 90% of the compound would be no ionized.

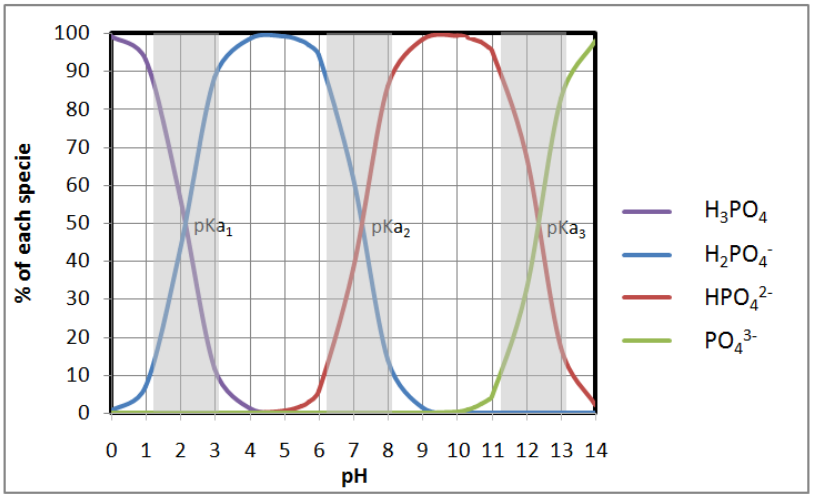

Figure 16 Species distribution diagram for phosphoric acid at different pH. In grey, intervals pK_a ± 1. In those intervals is possible to find amounts of the two species involved in the equilibrium related to that pK_a. For pH values lower than pK_a-1 the protonated specie is present in a proportion around 90%, while for pH values higher that pK_a+1 is the non-protonated specie what is present in this proportion.

Different ionized species of one compound would have different properties, and then it could be possible to take advantage of them to obtain different affinity for an enzyme at different pH. In cells, misfolded GCase can be found at ER (where the pH is neutral), while is not able to reach the lysosomes (pH 5.2) where the cleavage of GluCer takes place. Moreover, it is known that GCase has a hydrophobic pocket where the ceramide is located when the GluCer cleavage is performed. So, a compound that have the property of being neutral at pH 7 and ionizated at pH 5.2 could possess the desired affinity for GCase at both pHs.

Thus, at pH 7, the affinity of those compounds for GCase would be high. The binding of those compounds with the mutated enzyme would help it to acquire the correctfolding and thus, facilitate GCase transportation to the lysosome. Then, once in the lysosome, the compound would be protonated in the slightly acidic environment and, due to its ionization, the compound affinity for the GCase's binding side would be lower than in the endoplasmic reticulum. Hence, that compound with low GCase affinity would not effectively compete with GluCer in the lysosome. In this way, it would be possible to promote the lysosomal hydrolysis of GluCer by increasing the amount of correct folded GCase there, without having an extra inhibition in the function of this enzyme that could take place if the compound would have a high affinity for GCase in the lysosome.

Thereby, as pyridine has pK_a value of 5.3, it could be thought that compounds that contain a pyridine at the end of the N-chain would have this differential affinity by remaining mostly neutral at pH 7 while being partially or totally protonated (and thus having less affinity for the binding side) at pH 5.2.

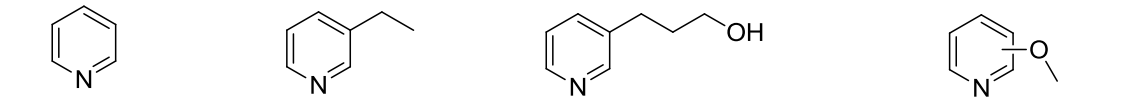

Figure 17 Examples of some pK_a of different pyridines[122,123].

To the best of our knowledge, the introduction of ionizable groups as pyridines in the chain of potential GCase inhibitors would be a new approach for modulating the GCase inhibition according the pH of the environment and, thereby, to achieve compounds with strong

chaperone function, binding the misfolded enzyme and increasing the amount of functional enzyme in the lysosome, without inhibiting its hydrolase activity.

As previously explained, the *N*-chain of a DNJ derivative is expected to be orientated towards the hydrophobic entrance of the GCase's active site. For this reason, the introduction of polar groups as pyridines at the end of this chain could result in a diminution of affinity. Nevertheless, although the introduction of pyridines could involve a loss of potency, their capacity of changing its protonation state at pH around 5-6 would turn quite interesting the study of the influence of this different ionized species in their potency as GCase inhibitors at different pHs.

Therefore, the aim of this section was to design and synthesize a small library of DNJ derivatives with different pyridine rings in their chains by introducing chemical diversity by Huisgen 1,3-dipolar cycloaddition or amide formation, in order to study the influence of the pK_a of those pyridines in the capacity of inhibition of GCase at different pH.

In particular, we intended the synthesis of compounds with amide or triazole linkers (compounds **16** and **31** respectively), with pyridine substituents and different chain lengths, as shown in Fig. 18.

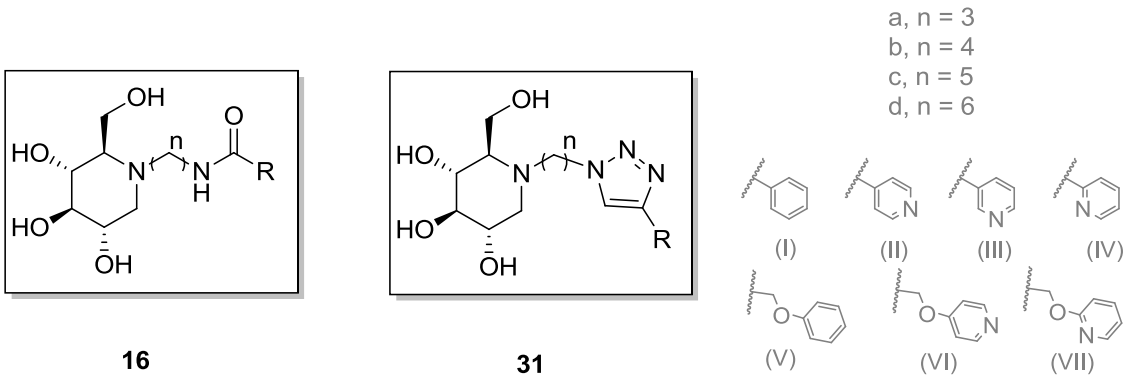

Figure 18 Representation of the aim compounds for this section.

3.1.2 Synthesis of DNJ aminoderivatives and compounds 16

As shown in Scheme 3, the synthesis of amido derivatives **16** was intended by acylation of the corresponding amino derivatives **15**. The synthesis of these amines**15(a-d)** was done, following previously described methodologies[124], via reduction of the azido derivatives **14(a-d)** that were obtained in turn from alkylation of **13** with the azidotosylates **12(a-d)**. Benzylated DNJ **13** was kindly provided by SIMChem (Service of Synthesis of High added value Molecules, IQAC-CSIC), and azidotosylates **12(a-d)** were obtained, following procedures previously described in the literature[125,126], starting from the corresponding bromoalcohols, as will be described below.

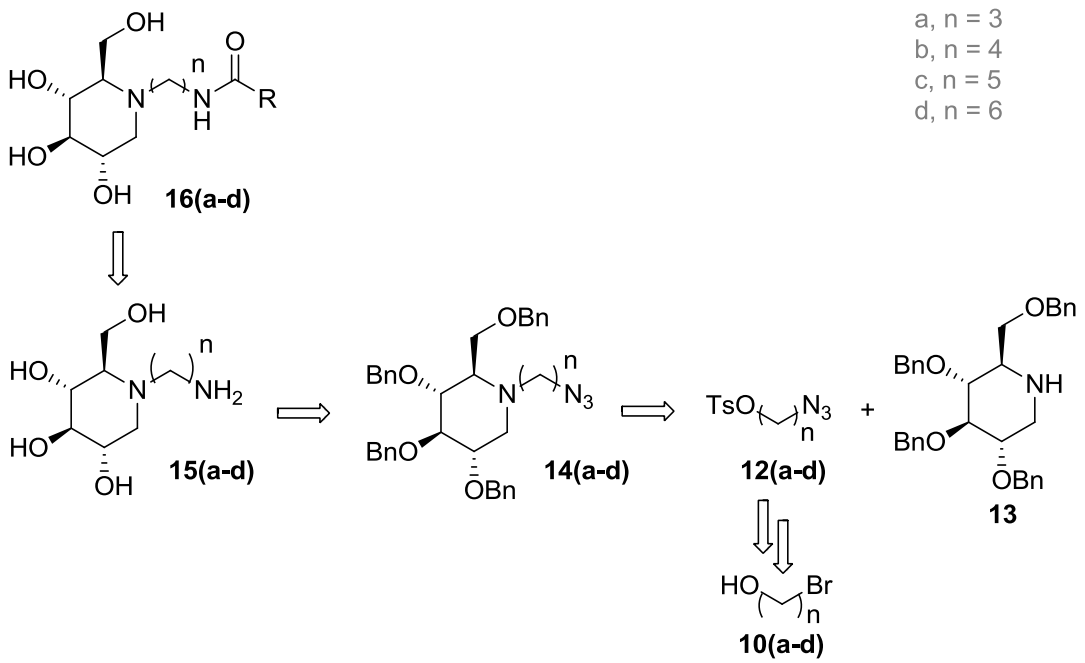

Scheme 3 Proposed retrosynthesis for **16d** derivatives

Thus, azidoalcohols **11** were obtained by substitution of the bromine atom by azide in the corresponding bromoalcohols **10**. This reaction was carried out following standard procedures in the presence of NaN_3 and DMF, at 70ºC. Once the azidoalcohols **11(a-d)** were synthesized, they were treated with TsCl in presence of Et_3N and DCM at 0ºC to obtain the desired azidotosylates **12(a-d)** with good yields (Scheme 4).

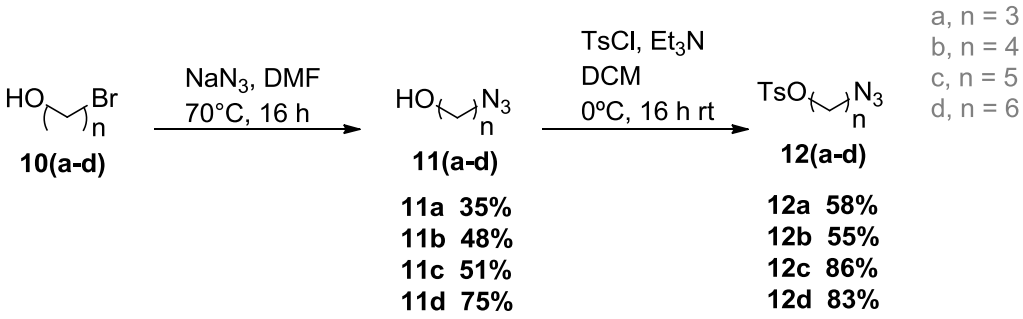

Scheme 4 Synthesis of azydotosylates **12(a-d).**

The synthesis of compounds **14** was firstly afforded following procedures previously described in the literature[118]. Thus, the alkylation of **13** with **12d** at 85ºC in ACN in presence of K_2CO_3 gave the desired compound **14d** but with only 15% yield (Table 1, *entry I*).

In an attempt to get the desired compounds **14** in higher yields, different conditions of reaction were analyzed using **14d** as a model to find the best conditions for the alkylation (different assay conditions showed in Table 1). The variation of conditions included: increasing the time of reaction (*entry II*), changing the temperature and solvent (*entry III*) or even irradiating the mixture of reaction with microwaves instead of performing the reaction under thermic conditions (*entries IV and V*). The higher yield (53%) was obtained using microwave irradiation, adding 1.7 mmol-equivalents of azidotosylate **12d** and a catalytic amount of KI (*entry V*).

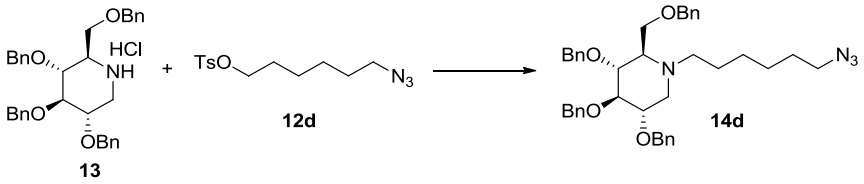

Entry	reaction	Eq **13d**	eq KI	solvent	conditions	yield
I	thermic	1.2	--	ACN	85ºC 12h	15%
II	thermic	1.2	--	ACN	85ºC **48h**	31%
III	thermic	1.2	--	**DMSO**	**120ºC 48h**	10%
IV	**MW**	1.2	--	**ACN**	Tmax=85ºC, 150w 2h	33%
V	MW	**1.7**	**0.1**	ACN	Tmax=85ºC, 150w 2h	53%

Table 1 Different conditions for synthesis of **14d**.

The best reaction conditions (Table 1**Table 1**, *entry V*) were extrapolated to the synthesis of the azide compounds **14** with other chain lengths, obtaining low to moderate yields, depending on the case (Scheme 5, compounds **14(a-c)**). When performing this reaction in the MW vessel, it was observed that most of the K_2CO_3 remained insoluble on the reaction mixture, and seemed to difficult the stirring of the reaction. We thought that this could be one of the cause for the low yield obtained. For this reason and in order to confirm this hypothesis, the synthesis of compounds **14b** and **14c** (the two compounds obtained with lower yield in the conditions of *entry V* in Table 1) were repeated using DIPEA (liquid at rt), instead of K_2CO_3 (solid and insoluble in reaction conditions) as base. In these new conditions, the yields of those reactions were increased from 9% to 16% yield for **14b** and from 23% to 59% yield for **14c**.

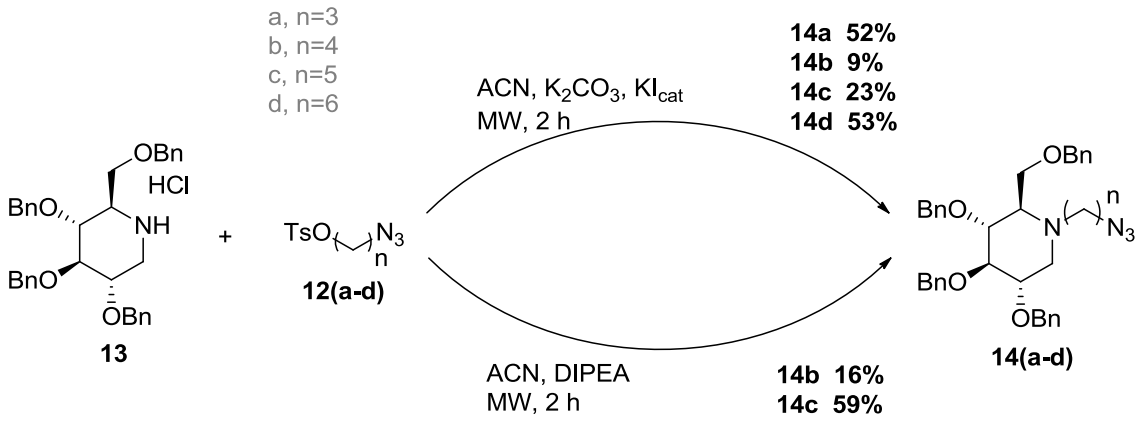

Scheme 5 Synthesis of compounds **14(a-d).**

After this, the debenzylation and reduction of the azido derivarives **14(a-d)** were carried out by catalyzed hydrogenation in presence of Pearlman's catalyst ($Pd(OH)_2$) and strongly acidic media. It should be highlighted the importance of this acidic conditions to avoid poisoning of the palladium catalyst[127].Thus, amino compounds **15(a-d)** were obtained with good yields.

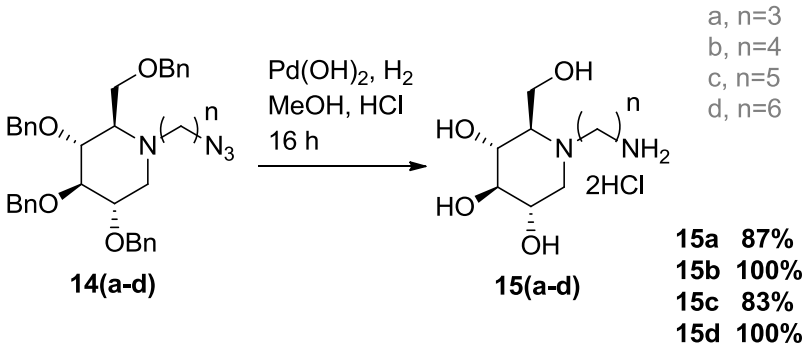

Scheme 6 Synthesis of compounds **15(a-d)**.

Solid phase synthesis has been successfully wide used for the preparation of peptides and for facilitating synthetic organic transformations. The main property of the solid support is that, thanks to its insolubility, permits purification by filtration, providing speed and simplicity in the sample processing during and after the reaction.

For this reason, once amino derivatives **15(a-d)** were obtained, the synthesis of amido derivatives **16** were afforded by acylation with the corresponding acids activated with HOBT supported in a polystyrene matrix and PyBrOP (Bromotripyrrolidinophosphonium hexafluorophosphate) as activating agent, in order to achieve the final compound avoiding chromatographic purification and expecting to be able to perform the biological *in vitro* assays directly from the crude of reaction.

To carry out reactions in solid support, it is important that the reactants are properly solubilized and the resin beads remain swelled in order to facilitate the diffusion of reagents and their accessibility to the binding sites[128]. At this point, the solubility of **14d** in different solvents and mixtures of solvents was studied, showing good solubility in water and MeOH, an acceptable solubility in DMSO but remaining almost insoluble in the solvents suggested for the correct swollen of the resin (DMF, THF orDCM). Similarly, the acceptance of those solvents by the polystyrene resin was also checked. As expected, the resin was swelled in presence of DMF, THF or DCM and shrunk in presence of polar protic solvents as water or MeOH. In DMSO, the resin remained only partially swelled. The use of mixtures of solvents, did not give better results. Although DMSO was not able to totally swell the resin, it was the solvent with what we achieved a better compromise between the solubility of the amine and the swelling of the solid support. Thus, the reactions were finally carried out in DMSO.

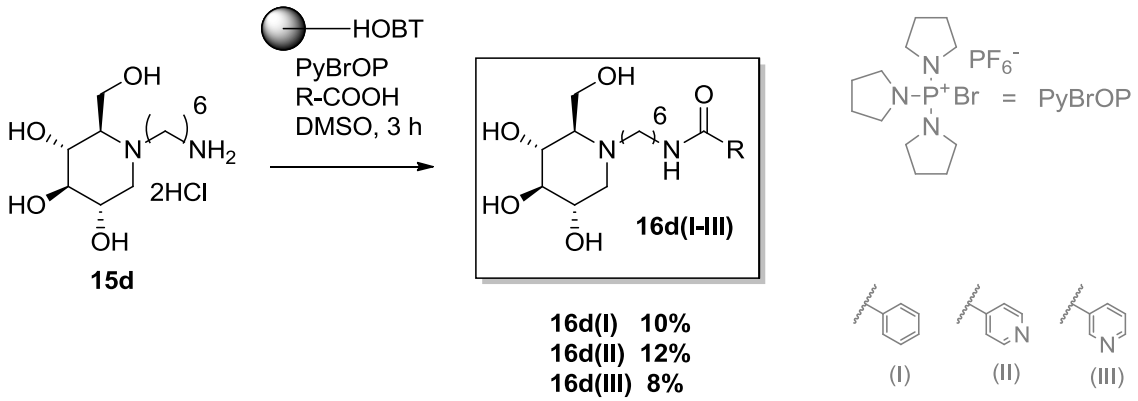

Scheme 7 Synthesis of compounds **16(I-III).**

Unfortunately, although one of the higher advantages of solid support synthesis is avoiding further purifications, the residues obtained from these reactions (Fig. 19A) were a mixture of compounds that included, among them, the corresponding starting acids and another impurity that seemed to be tripyrrolidinophoshorid acid triamide (TPPA, ^{1}H NMR (400MHz, MeOD) δ 3.19-3.15 (m, 12H), 1.92-1.80 (m, 12H)), derived from the activating agent PyBrOP[129,130]. For this reason, in order to purify them, the residues were first redissolved and treated with a strongly basic that retained the acids (Fig. 19B). Then, the residues were treated with $CHCl_3$ that solubilized the TPPA (Fig. 19C), obtaining in this way the amido derivatives **16d** with an acceptable purity(Fig. 19D). Thus, compounds **16d(I-III)** were finally obtained with yields between 8and 12%.

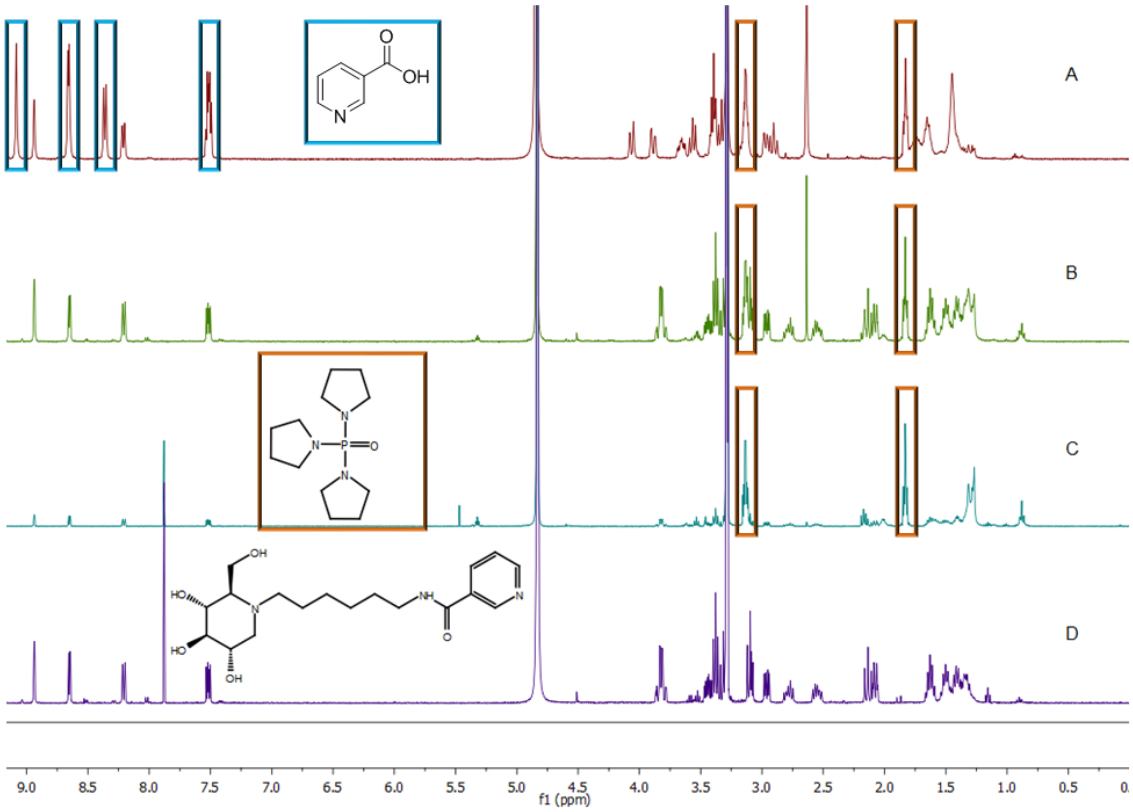

Figure 19 ^{1}H-NMR spectra (400MHz, MeOD) of the different residues obtained during the synthesis and successive purification of **16(III)**: **(A)** fraction obtainedafter reaction in HOBT-solid support, **(B)** fraction obtained after purification with strongly resin IRA-400 (OH^-), **(C)** soluble in $CHCl_3$, **(D)**precipitated in $CHCl_3$.

Both the impurities derived from PyBrOP and acids, as well as the low yield of the reactions could be consequence of the use of a solvent that was not able to promote the appropriate swelling of the resin. Furthermore, those impurities impeded the direct biological assays of the crudes of reaction as was initially expected by this synthesis on solid phase. For this reason, compounds **16(a-c)** were not synthesized at this point to wait for the biological data of compounds **16d(I-III)** in order to evaluate the interest of synthesizing more compounds of this family. In that case, other synthetic conditions on solid phase or, the more conventional alternative using synthesis in solution with posterior purification by column chromatography should be considered for the synthesis of other compounds of this series.

3.1.3 Synthesis of DNJ azido derivatives and compounds 31

The synthesis of compounds **31** was designed by Huisgen 1,3-cycloaddition between the debenzylated azido derivatives **24** and different alkynes with pyridine groups, or by cycloaddition with the benzylated azido derivatives **14** and posterior debenzylation, as shown in Scheme 8. We firstly decided to try the click reaction with the debenzylated azido derivative **24** for two main reasons: on one hand, to reduce the number of reactions by introducing the diversity on the last synthetic step, and on the other hand, to take advantage of the click reaction and the fact that the crudes of those reactions could be directly tested in *in vitro* biological assays. Thus, the first goal of this section was to synthesize compounds **24**.

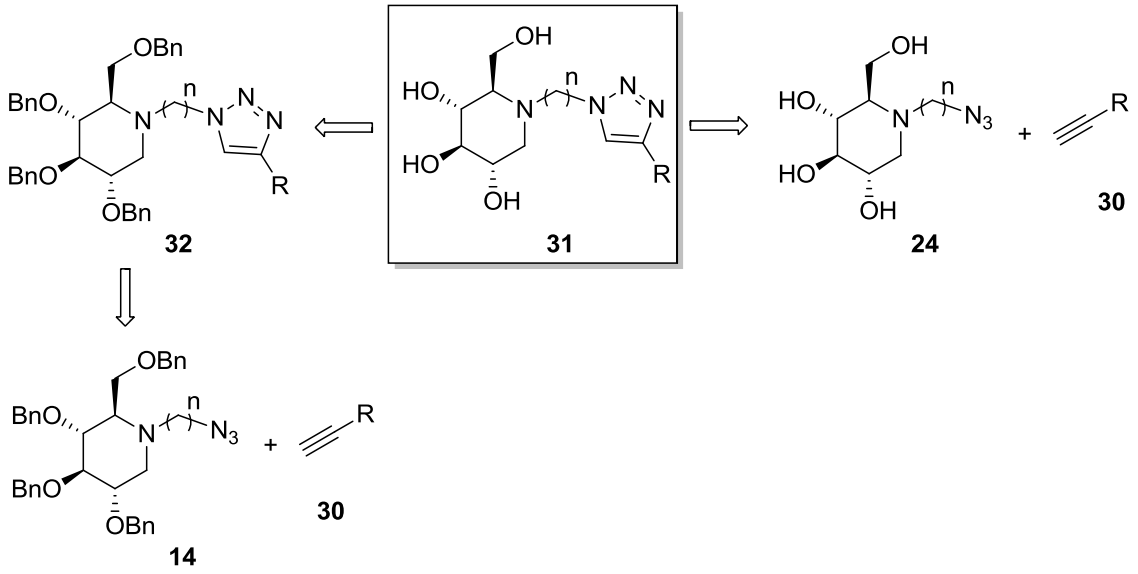

Scheme 8 Restrosynthetic approaches for compounds **31**.

A first attempt of synthesis of debenzylated azido derivatives **24** consisted on debenzylation of intermediate **14c** previously obtained for the synthesis of the amido derivatives **16c**. The reaction, as shown in Scheme 9, was carried out in presence of BCl_3 at -78ºC following a procedure similar to those described in the literature for debenzylation of alcohols in presence of other azido groups in the molecule[131,132]. Although it is possible to find examples were the deprotection is described to take place without reducing the azide, in our case the crude of reaction resulted in a mixture of compounds that could not be separated and whose main product was the debenzylated compound with reduction of the azide to amine (**15c**). Due to the observed difficulty of debenzylation and purification of **14c** without reduction of theazido group in these conditions, we decided to try the synthesis compound **24** by a different route.

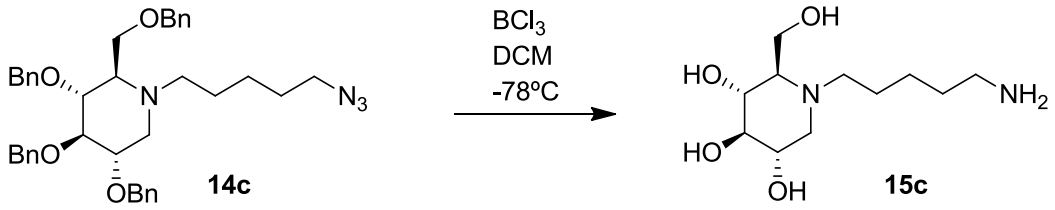

Scheme 9 Reduction of **14c.**

A second approach to compounds **24** consisted in introducing the azido group in the last step, once the DNJ tosyl derivative was debenzylated (compound **22**), as shown in Scheme 10. The debenzylated tosyl derivative **22** would be directly obtained from one-pot hydrogenation that includes a reductive amination between **13** and the corresponding tosyloxyaldehyde **20**, and a posterior debenzylation.

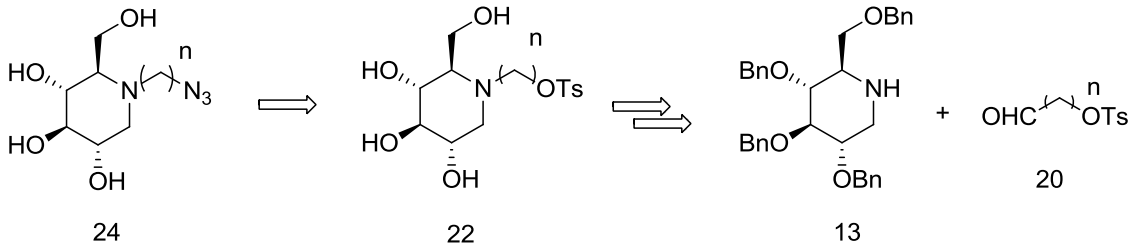

Scheme 10 Retrosynthetic approach for the obtaining of compounds **24**.

To this purpose, we started trying to synthesize **22c** following procedures similar to those described in the literature[133]. Thus, 1,5-pentanediol **17** was treatedwith 0.5 eq. of Ts-Cl to minimize the formation of ditosylate **18**, as shown in Scheme 11. Then, the monotosylated alcohol **19** (obtained with 70% yield) was oxidized to aldehyde by a TEMPO/bleach Anelli's oxidation, giving **20** with good yield (87%).

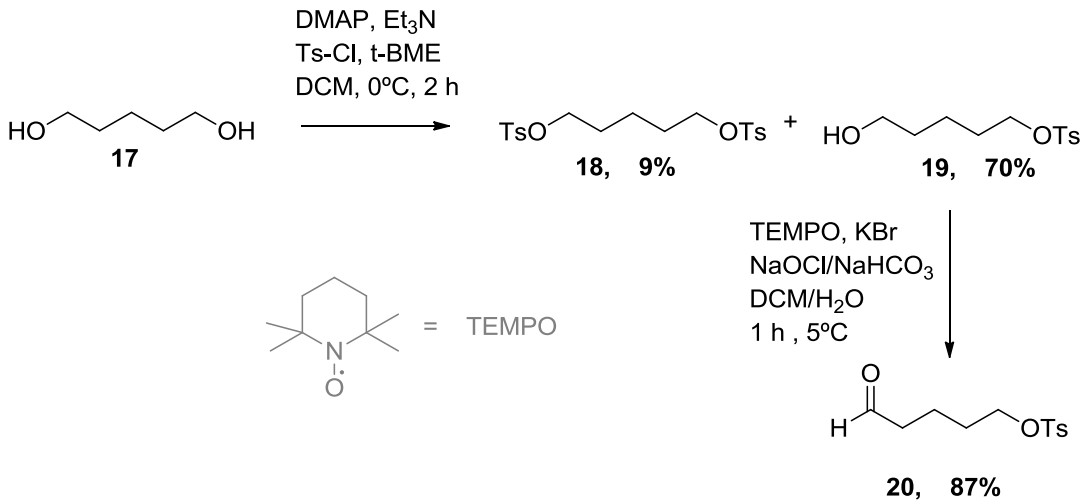

Scheme 11 Synthesis of azidotosylate **20.**

Following the retrosynthetic approach mentioned before, the synthesis of **22** was attempted by one-pot reductive amination between **13** and the aldehydotosylate **20** (Scheme 12) and posterior debenzylation. The first reaction was carried out by catalyzed hydrogenation in presence of Pd/C and acetic acid. Once the reductive amination was accomplished, aqueous HCl was added to the reaction mixture to give the strong acidic media that is necessary for the debenzylation step. Extra Pd/C was added too, in order to compensate for the expected catalyst inactivation. Then, the reaction was submitted again to hydrogenation until the deprotection of the alcohols was completed. After work-up the reaction by filtration over a pad of celite® the residue obtained was a mixture of compounds, that seemed to include the desired tosylate derivative **22** and the by-product of its cyclization (compound **23**). This mixture evolved to only the cyclic compound **23** when treated with strongly basic resin IRA-400.

Taking this into account, we decided to continue the synthesis with the substitution of the tosyl group by azide directly after the hydrogenation (without any purification of the mixture or treatment with basic resin) to see if compound **22** in its hydrochloride form was stable enough to allow the substitution of the tosyl by azide without cyclize. Unfortunatelly, when the mixture was treated directly with NaN_3 and DMF at 80ºC the DNJ derivative cyclized again, giving only compound **23**. For this reason we decided to try another approach to obtain azidoderivatives **24.**

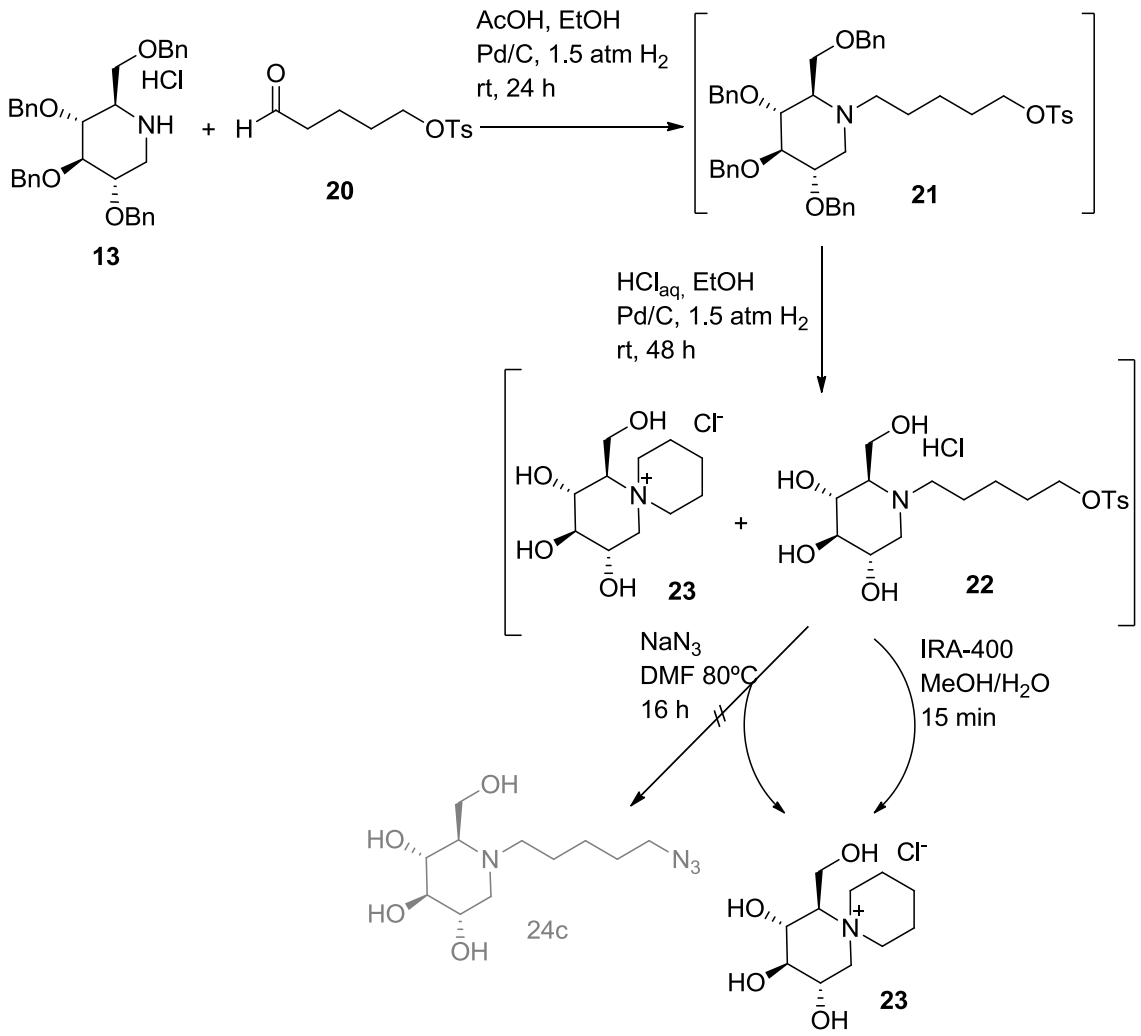

Scheme 12 Second attempt of synthesis of compounds **24**.

The synthesis of the azido derivatives **24** was then tried by reductive amination between the azidopentanal **25** and the debenzylated DNJ (**27**), as shown in Scheme 13. With this approach it should be noticed that it was necessary to find conditions for the reductive amination that do not reduce the azido group to amine. In this way, sodium triacetoxyborohydride was described as a reducing agent suitable for this kind of reactions, without producing a reduction of the azide[134]. On the other hand, azido pentanal **25** would be obtained from previously synthesized aldehydetosylate **20** by substitution of the tosyl group by azide.

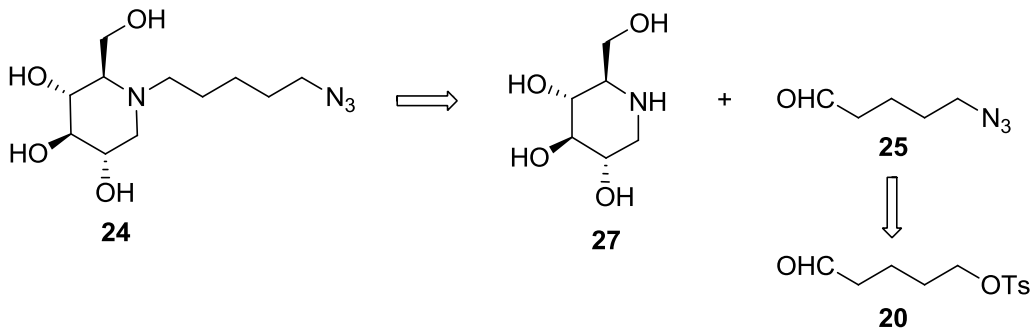

Scheme 13 Retrosynthetic approach for synthesis of compounds **24** by reductive amination.

Thus, in a first attempt for the synthesis of **25**, performing the reaction of substitution of the tosyl group by azida at 80ºC, after 16h of reaction compound **25** was not detected in the crude of reaction. Instead, the cyclic compound **26** was obtained with some impurities that were not further separated and characterized (Scheme 14). This potential cyclization was described to take place when heating similar compounds, with shorter chain lengths[135]. Although it was published that cyclization of **25** does not take place at temperatures under 110ºC, in our hands it was smoothly occurring at 80ºC. In the same article it was suggested that cyclization could be avoided by cooling the mixture of reaction. For this reason, a second attempt was carried out by cooling the reaction to 0ºC and, after 5h of reaction the desired azidopentanal **25** was obtained with 42% yield. In this case, compound **26** was not detected, but 10% of the starting tosylate **20** was recovered without react.

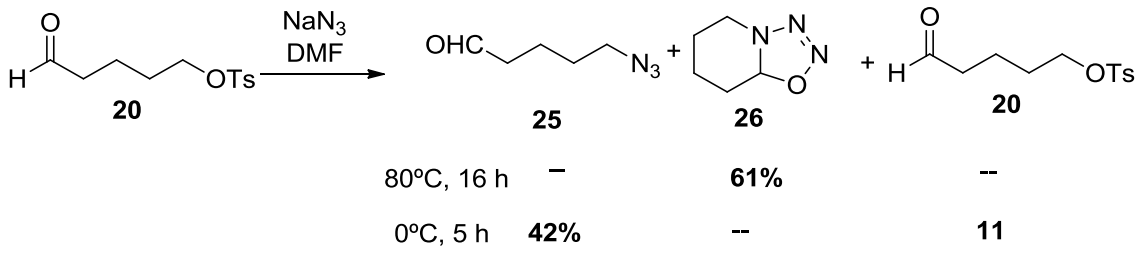

Scheme 14 Synthesis of azidopentanal **25**.

Simultaneously to the synthesis of **25**, benzylated compound **13** was submitted to a catalyzed hydrogenation in presence of ($Pd(OH)_2$) and strongly acidic media. DNJ (**27**) was obtained quantitatively.

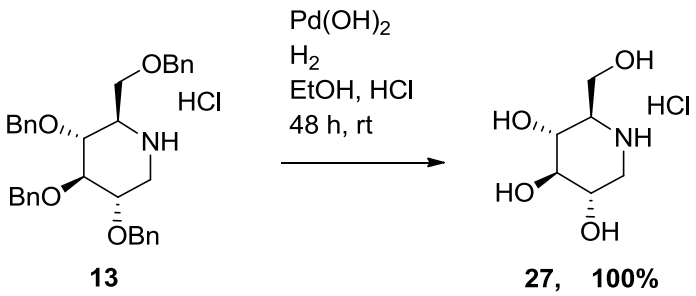

13 **27, 100%**

Scheme 15 Deprotection of DNJ (**27**).

Once the azidopentanal **25** and the debenzylated DNJ **27** were reached, the desired DNJ azidoderivative **24c** was tried to obtain by reductive amination with sodium triacetoxyborohydride. In order to try to avoid the intramolecular cyclation of the azidoaldehyde **25** to **26**, that is described to take place with heating[135], this reaction was carried out at rt. Unfortunately, after 16h of reaction we obtained most of the starting DNJ unaltered (Scheme 16).For this reason we decided to try another approach for the synthesis of **24c** that would not show those problems of intramolecular cyclation.

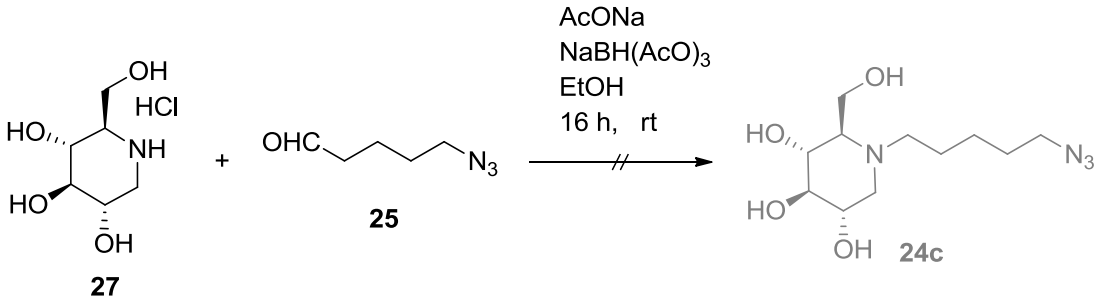

27 **25**

Scheme 16 Attempt of synthesis of **24c** by reductive amination.

Thus, the azido derivative **24** was designed by alkylation of **27** with the corresponding azidotosylate derivative **12**, following the procedure previously described for compound **14a,** but starting from the deprotected DNJ **27** (Scheme 17).

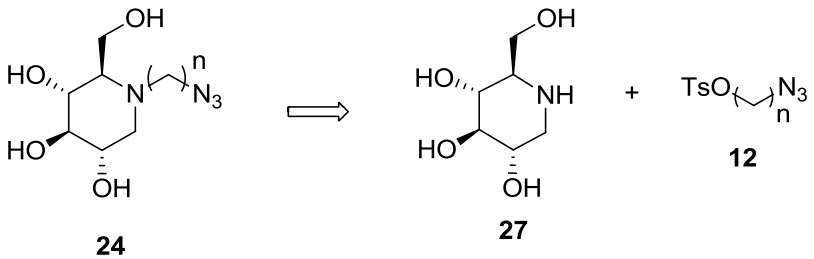

24 **27** **12**

Scheme 17 Retrosynthetic approach for synthesis of compounds **24** by alkylation.

Thus, azido derivative **24c** was synthetized by alkylation of **27** by azidotosylate **12d**, as shown in Scheme 18. In this case the reaction resulted in a mixture of compounds. After purification by preparative HPLC in reverse phase (water/ACN + 0.2% formic acid), we were finally able to obtain 7 mg of **24d** as a formate salt (17% yield).

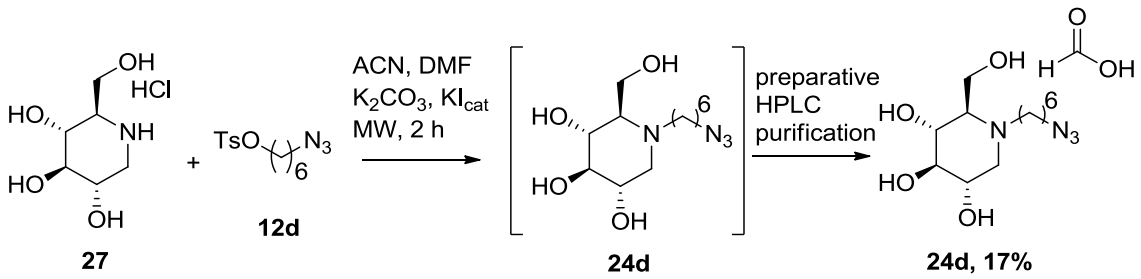

Scheme 18 Synthesis of debenzylated azidoderivative **24d**.

Although the yield for synthesis of azidoderivative **24d** was low, as click chemistry is supposed to take place with good yields and to be possible to test the compounds directly from the crude of reaction, we decided to try the synthesis of compounds **31d** (Scheme 19).

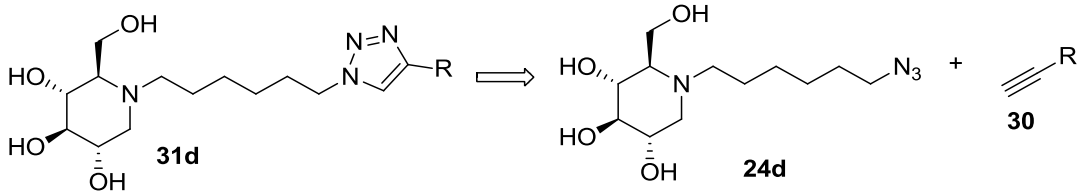

Scheme 19 Retrosynthetic approach for synthesis of compounds **31d.**

For this purpose, we used alkynes **30(I-V)** provided from commercial sources, and **30(VI-VII)** were synthesized from the corresponding pyridine alcohol **28** and bromoalkyne **29** (Scheme 20).

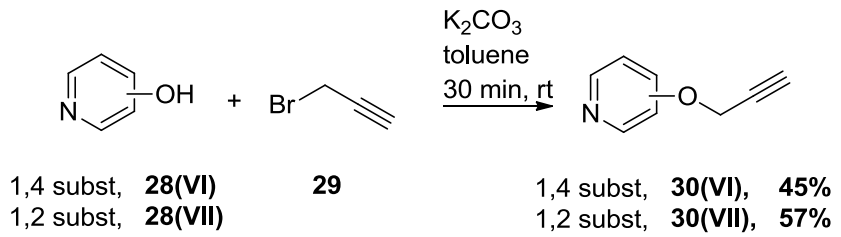

Scheme 20 Synthesis of alkyne **30(VI)**.

The synthesis of **31d(I-VI)** were finally afforded by using previously described procedures for Huisgen 1,3-cycloaddition[136,137], and detailed in Fig. 20A. The evolution of the reaction was

followed by HRMS, showing the necessity of different reaction times and temperatures, depending on the alkyne. Thus, for example, for synthesis of **31d(IV)**, the reaction was completed after 30 minutes at room temperature, while for synthesis of **31d(I)** it was necessary to heat the mixture to 60ºC overnight to achieve the completion of the reaction, after showing low evolution during 5 days at room temperature (Fig. 20B).

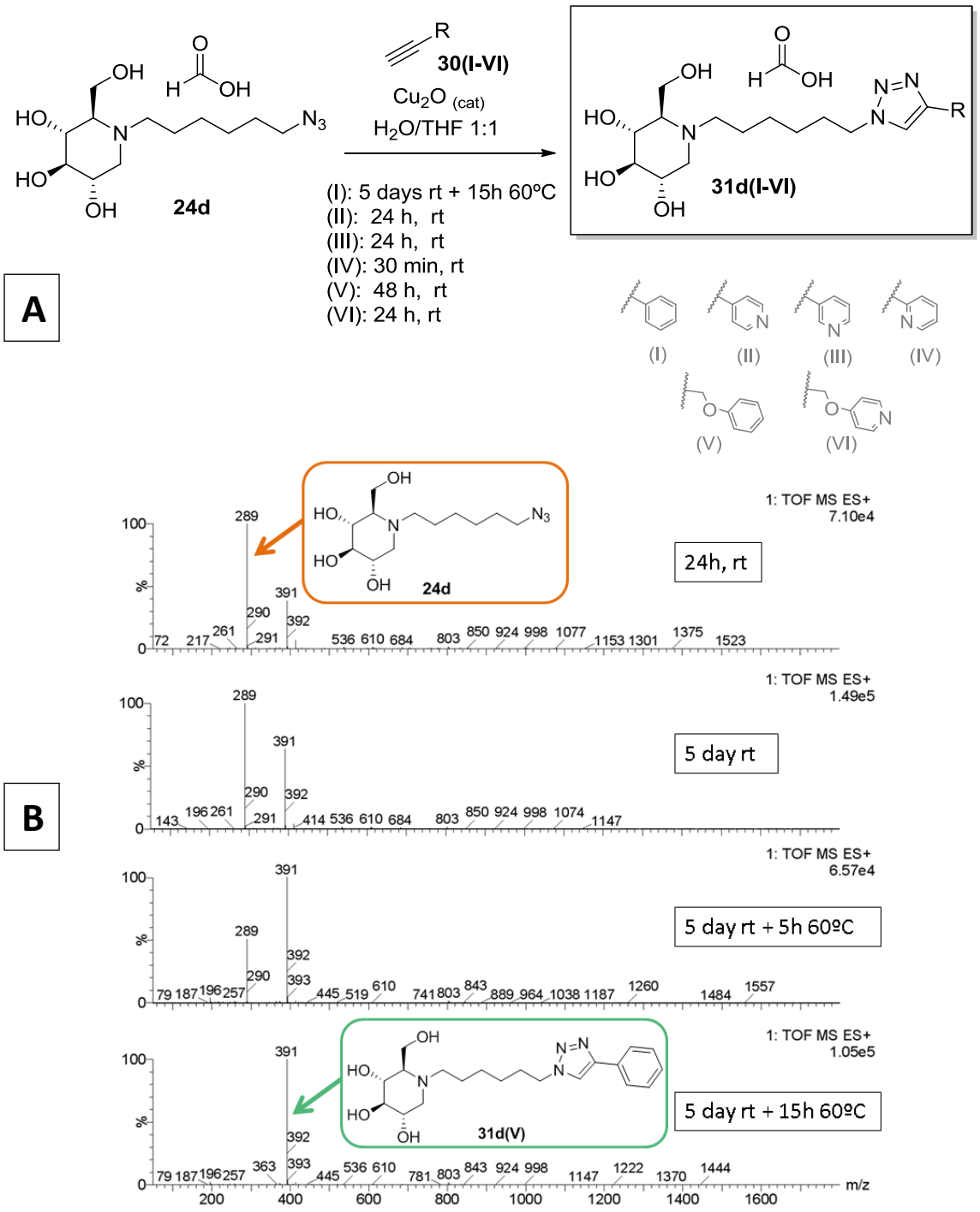

Figure 20 (A) Synthesis of compounds **31d (I-VI))** by Huisgen 1,3-cycloaddition. **(B)** Evolution of synthesis of **31d(V)**. Reaction followed by HRMS in acidic conditions.

Due to the difficulty of synthesis of the azido derivatives **24d** with good yield or in higher amounts, we decided not to synthesize other compounds of this family with other chain lengths following this synthetic route, before analyzing the data obtained from imiglucerase inhibition assays of compounds **31d(I-VI)**.

Moreover, although we were finally able to obtain the **31d(I-VI)** derivatives in enough amount for test them (without further purification) in *in vitro* assays, this quantity was not enough for a detailed compound characterization and pK_a determination. For this reason, in order to obtain some compounds with enough quantity to allow the determination of its experimental pK_a and their proper characterization, higher amounts of compounds **31b(VI-VII)** were synthesized by doing first the Huisgen 1,3-cycloaddition with intermediate **14b**, and performing the debenzylation with BCl_3 in the last step, as shown in Scheme 21.

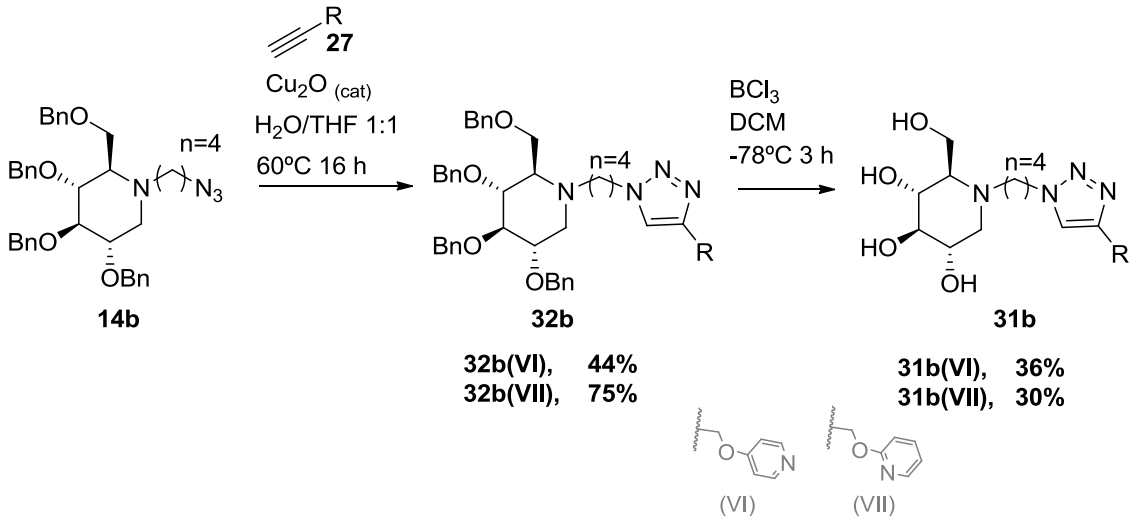

Scheme 21 Synthesis of compounds **31b (VI, VII)** by click reaction and posterior debenzylation.

Although the approach that includes the debenzylation after the Huisgen 1,3-cycloaddition may be less convergent, it bypass the problematic synthesis of debenzylated azidoderivatives **24**, allowing us to obtain higher amounts of the desired compounds.

3.1.4 Imiglucerase inhibition assay

To analyze if the synthesized compounds had actually more affinity for GCase at the endoplasmic reticulum (neutral environment) than in the lysosome (pH around 5.2), it was studied their capacity of inhibition of imiglucerase at both pHs, following previously described assays with the fluorogenic substrate 4-methylumbellyferyl β-D-glucopyranoside (4-MUG)[138].

β-glucosylceramidases (GBA1, GBA2 or GBA3) naturally hydrolyze GluCer in cells, but are also able to process other substrates. Taking advantage of this property, it is possible to analyze the activity of this kind of enzymes by using substrates that present different absorbance or fluorescence when cleaved.

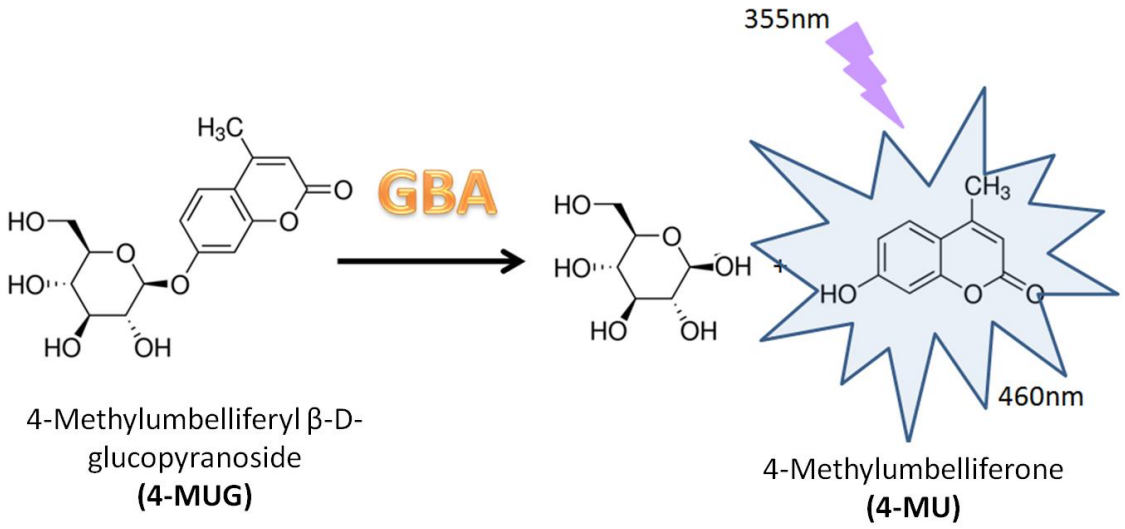

Figure 21 Representation of cleavage of 4-MUG by GBA. The not inhibited enzyme hydrolyzes 4-MUG, giving 4-MU and glucose. The cleaved product 4-MU shows fluorescence at 460nm when irradiated at 355nm. This fluorescence can be measured and is proportional to the concentration of 4-MU and, thus, to the activity of the enzyme.

In this assay, in order to analyze GCase activity at different pH's, we used the purified enzyme imiglucerase (Cerezyme®). This enzyme, as mentioned before, is a recombinant enzyme obtained from Chinese hamster ovary cells that has been used for more than 20 years in enzyme replacement therapy for GD. The fact of using purified enzyme instead of Wild type cell homogenates assure that we were able to measure only the enzyme loss of activity due to imiglucerase-inhibitor interaction without any GBA2 or GBA3 interferences.

Thus, the purified enzyme imiglucerase was preincubated with or without the compound (control) in the presence of sodium taurocholate and Triton X-100® to try to emulate the lipids and detergents naturally present in the cells and that are necessary for the activity of the enzyme. After 30 minutes incubation, the substrate was added. The capacity of cleaving of the enzyme can be measured by fluorescence (λ_{exc} 355 nm, λ_{em}460 nm) as 4-MUG is not fluorescent under these conditions but so is the product of hydrolysis. Thus, the fluorescence measured will correlate with the GCase activity, and when compared with the untreated

control, will give a measurement of the extent of the imiglucerase inhibition by the tested compound.

In addition to amido and triazole derivatives (**16d** and **31(b,d)**respectively), the debenzylated intermediate compounds with final amino(**15(a,b,d)**)or azido groups (**24d**) were also tested as imiglucerase inhibitors. NB-DNJ and NN-DNJ were provided by SIMChem (Service of Synthesis of High added value Molecules, IQAC-CSIC) and they were analyzed similarly to the other compounds synthesized in this chapter, for comparison purposes. The obtained IC_{50} values are showed in Table 2, and data will be analyzed in more detail below.

	pH 5.2 IC_{50} (μM)	pH 7.0 IC_{50} (μM)	Δ
NB-DNJ	430	145	3.0
NN-DNJ	1.03	0.25	4.2
15a	>50	>50	-
15b	>50	>50	-
15d	>50	>50	-
16d(I)	22.8	5.6	4.1
16d(II)	35.4	18.7	1.9
16d(III)	42.6	24.2	1.8
24d	15.7	5.5	2.8
31b(VI)	>50	>50	-
31b(VII)	>50	>50	-
31d(I)	8.5	1.6	5.2
31d(II)	22.6	7.1	3.2
31d(III)	27.2	6.3	4.4
31d(IV)	6.4	1.6	4.0
31d(V)	2.4	0.8	2.8
31d(VI)	>50	>50	-

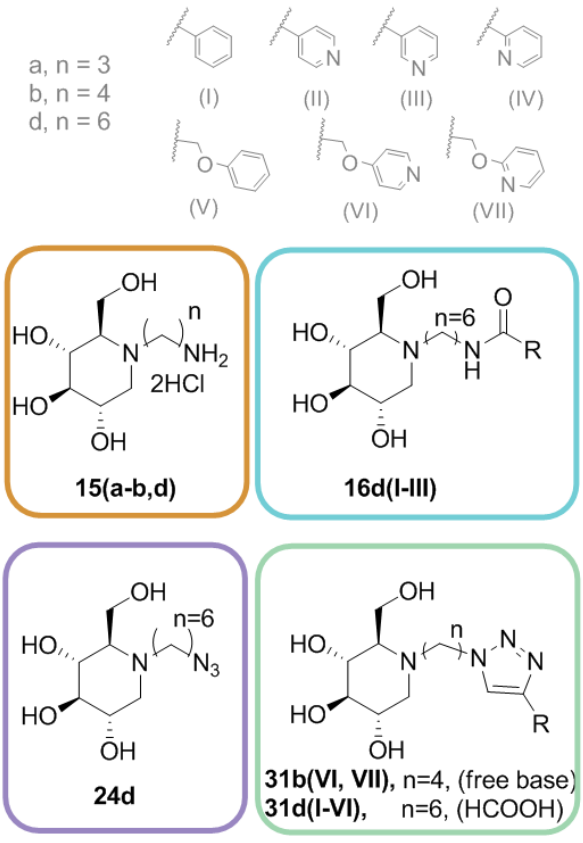

Table 2 Inhibition of imiglucerase. IC_{50} (μM) values for tested compounds, at pH 5.2 and pH 7, and relationship of the difference of the values obtained at both pH (Δ= IC_{50} (pH 5.2, μM) / IC_{50} (pH 7, μM)).

As shown in Table 2, compounds **15(a,b,d)** (with primary amine at the end of the chain) have IC_{50} values higher than 50 μM, while **24d** (with a terminal azide instead of amine) have more affinity for the enzyme showing IC_{50} values of 15.7 and 5.5 μM for pH 5.2 and 7 respectively. The low GCase affinity of compounds with terminal amine (**15(a,b,d)**) is in concordance with the fact that the groups at the end of the chainwould be accommodated into the hydrophobic

GCase pocket, and thus, compounds with polar groups at the end of the chain would have less affinity for this enzyme.

In addition, still in concordance with the potential loss of affinity due to the introduction of a polar group at the end of the chain, most of compounds with pyridine groups showed considerably higher IC_{50} values than their homologous with benzyl group (comparing compounds **16d(II-(III)** with **16d(I)**, compounds **31d(II-IV)** with **31d(I)** and compounds **31b/d(VI-VII)** with **31b/d(V)**). Unexpectedly, **31d(IV)**showed potency similar to **31d(I)** (see Table 2 and Graph. 1).

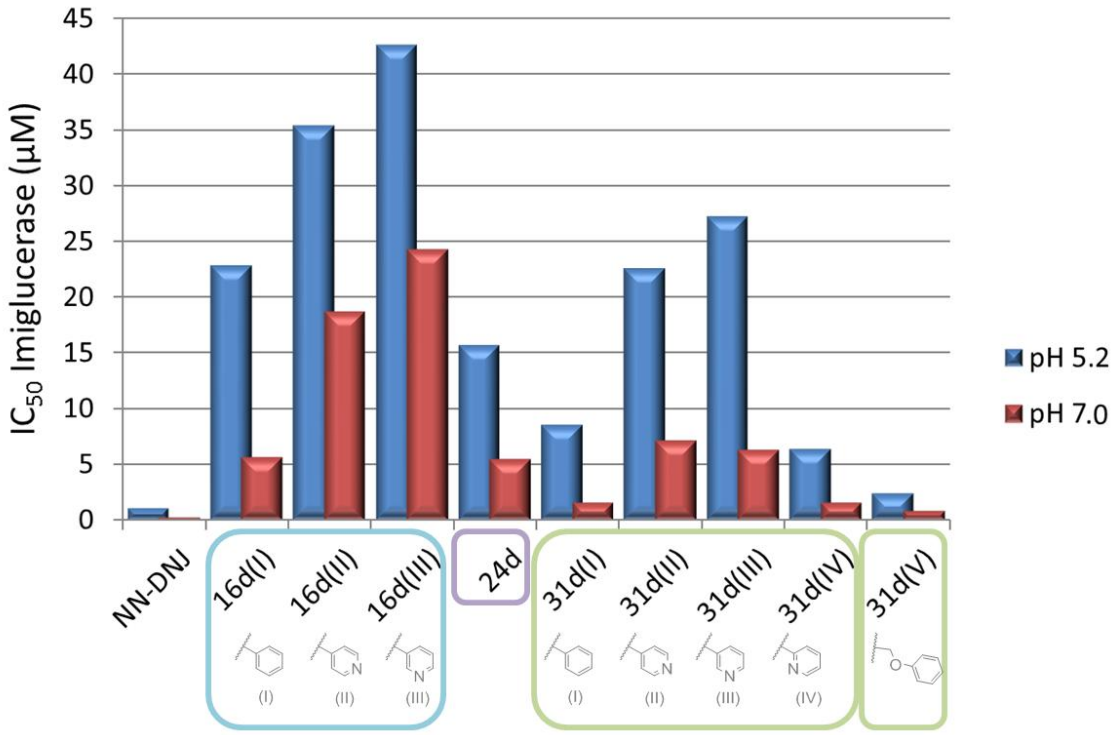

Graphic 1 Imiglucerase inhibition.IC_{50} (µM) values for the most potent GCase inhibitors of this section.

Moreover, when comparing the data obtained for compounds with amido linkers (**16d(I-III)**) and those with triazole linkers (**31d(I-IV)**), the second ones seemed to be more potent inhibitors of imiglucerase (Graph. 1).

Regarding to the difference of GCase affinity according to the pH of the assay, it must be highlighted that all the compounds whose IC_{50} were determined, showed higher affinity for the enzyme at pH 7.0 than at pH 5.2 under this assay conditions. However,contrary to what we expected, all compounds with pyridine groups presented lower differences of activity

according to the pH of the assay than their homologous bearing a phenyl group. The increase of affinity for the enzyme when the assay was performed at pH 7.0 with respect to the assay at pH 5.2 (Δ) was calculated as quotient between the IC_{50} value at pH 5.2 and the IC value obtained from the assays at pH 7.0 (data showed in Table 2, and graphically represented in Graph. 2). For example, in the case of compounds **16d**, **16d(I)** has IC_{50} four times lower at pH 7.0 than at pH 5.2, while for **16d(II-III)** this difference is less than two times. In the case of compounds **31d**, the IC_{50} difference between **31d(I)** and **31d(II-IV)** is not as high, but still compound **31d(I)**, with a benzyl substituent instead of a pyridine group, has the highest difference of activity between the two assays, showing more than 5 times lower IC_{50} value at pH 7.0.

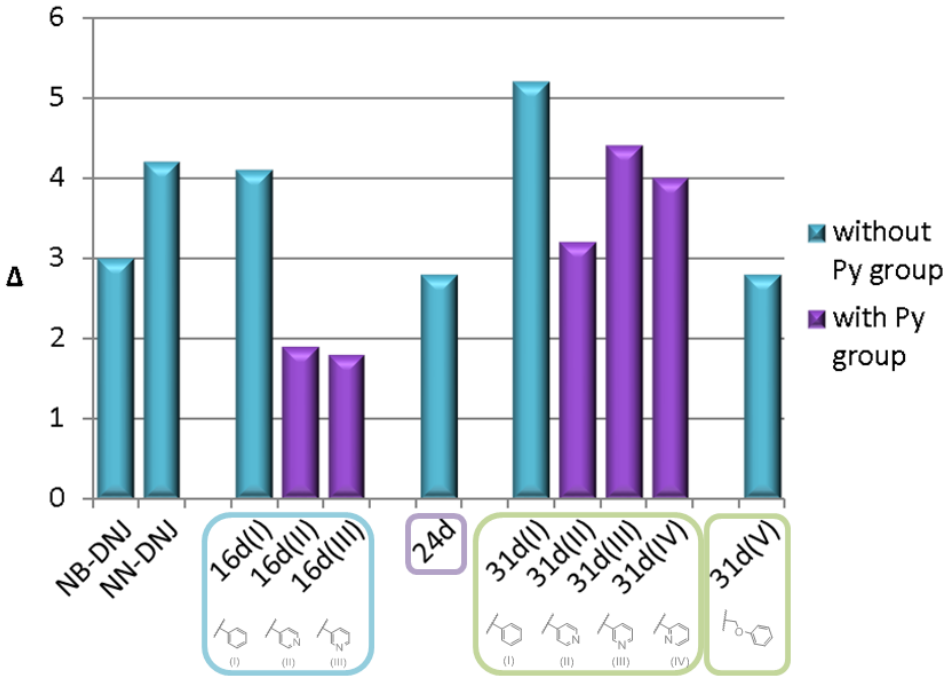

Graphic 2 Representation of the difference of IC_{50} at pH 5.2 vs pH 7.0 (Δ) for compounds with (purple) and without (blue) pyridine group at the end of the chain. (Δ= IC_{50} (pH 5.2, μM) / IC_{50} (pH 7, μM)).

Nevertheless, when comparing the data obtained for compounds with amido linkers (**16d(I-III)**) and those with triazole linkers (**31d(I-IV)**), it seems that the last ones possess higher difference of affinity for the enzyme according to the pH of the assay, than the compounds with amide linker.

One possible explanation for these unexpected results could be that our starting hypothesis that pyridine groups would be protonated when performing the assay at pH 5.2 and deprotonated at pH 7.0 could not be correct. For this reason, we decided to determine

experimentally the pK_a of the pyridine of those tested compounds that were synthesized with enough amounts (compounds **31b(VI)** and **31b(VII)**), in order to know if they experimentally posses the range of pK_a that we initially expected.

3.1.5 Analysis of pK_a

In order to evaluate the pK_a of their amines, the hydrochlorides of compounds **31b(VI)** and **31(VII)** were submitted to a titrationwith NaOH 0.01M while the pH -variation was measured as detailed in Fig. 22.

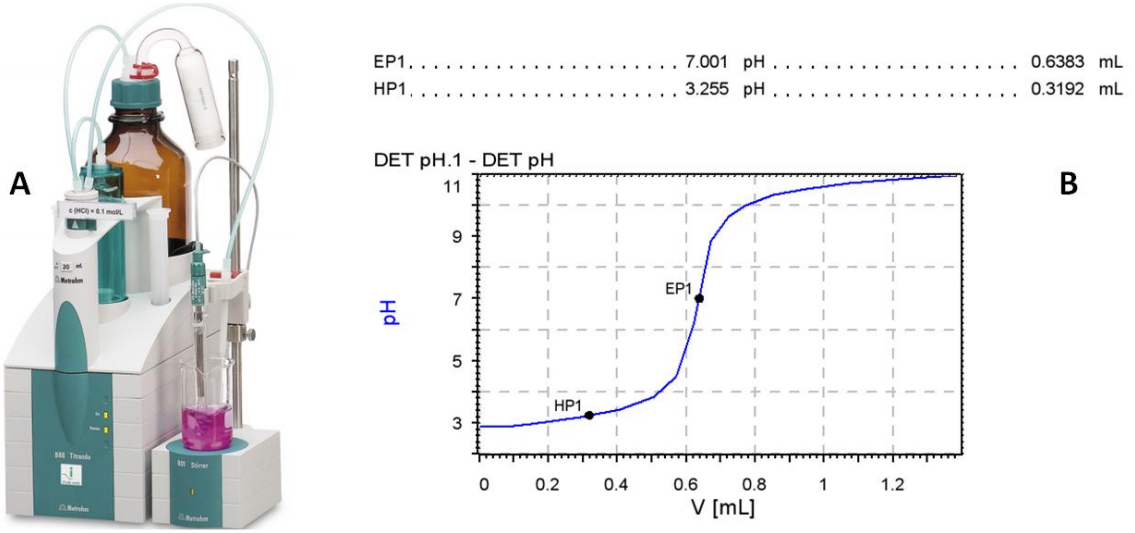

Figure 22 (A) 888-Titrando® (image from Methrom 888-Titrando® users manual). The titrant is stored in the bottle and automatically added, via a microburette, to the wessel that contains the sample with magnetic stirring. The pH is measured by the microelectrode and is continuously monitorized in a computer. **(B)** Example of a titration curve analized with Tiamo®. The ending point (EP1) is defined as the inflexion point. pK_a is determined as the pH of the sample when half of the volume added at the ending point was added (HP1). Thus, in this example pK_a = 3.255.

It must be noticed that compounds **31b(VI-VII)** possess two protonable nitrogen: the one in the DNJ core and the one in the terminal pyridine. For this reason, if the pK_a values of those amines are different enough, we should be able to detect two inflexion points (EP) during the titration. On the contrary, other methods for analysis of pK_a would be necessary.

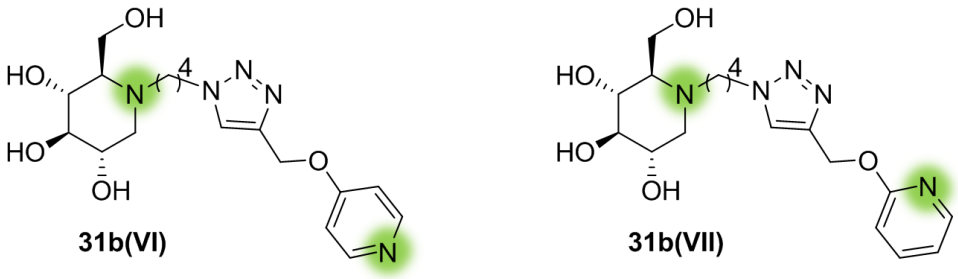

Figure 23 Structures of **31b(VI)** and **31b(VII)**. Highlighted in green, their amines potentially protonable during titration with NaOH 0.01M.

NB-DNJ and NN-DNJ are described to have pK_a values of 7.1 and 6.7, respectively[112]. Due to the distance between the triazole moiety and the DNJ core, it could be expected that this group do not have a strong influence in the pK_a of the amine of the core in both compounds. On the other hand, having an triazole group near the methoxypyridine moiety could increase a bit its acidity, thus the pK_a values of the amine in the pyridine groups of our compound are expected to be slightly lower than the ones for a methoxypyridine (pK_a 3.28 for 2-methoxypyridine and 6.62 for 4-methoxypyridine)[123].

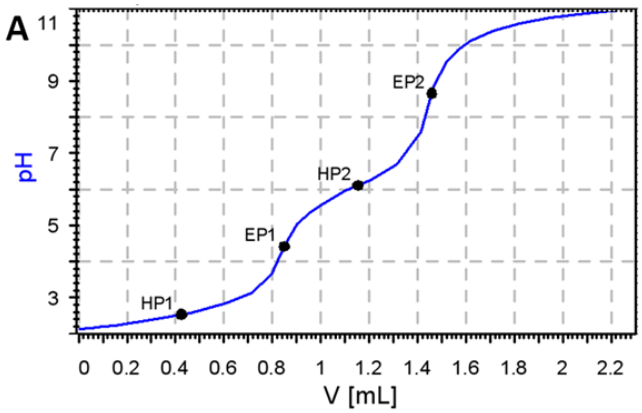

compound (BH⁺)	pK_a
31b(VI)	2.62 ± 0.06 (pK_{a1}) 6.03 ± 0.05 (pK_{a2})
31b(VII)	2.66 ± 0.19 (pK_{a1}) 6.21 ± 0.09 (pK_{a2})

B

Figure 24 (A) Titration curve obtained for compound **31b (VII)**.In this graph it is possible to observe two ending points (EP) and, thus, two pK_a values (HP), corresponding to the two protonable amines of this molecule. **(B)** Experimental pK_a values (mean ± standard deviation; n=3).

As shown in the example of Fig. 24A, the titration curves for compounds **31b(VI)** and **31b(VII)** showed two clearly differentiated inflexion points, allowing us the determination of the pK_a values for both amines. Thus, both compounds presented the experimental pK_a of one of their

amines in the range of pK_a that we expected (around 6.0-6.2), but the other amine was more acidic than what we expected (pK_a around 2.6, Fig. 24B). This low pK_a value would mean that the pyridine would be deprotonated at pH 7.0 as well as at pH 5.2. This could be one reason why we did not see higher differences of activity according to the pH of the assay than compounds without a protonable group.

Therefore, we decided to analyze the pK_a of the pyridine groups of the other synthesized compounds. As mentioned before, compounds **16(I-III)** and **31(I-VI)** were not synthesized in enough amounts to determine experimentally their pK_a. For this reason, and due to the difficulty of their synthesis, we decided to synthesize and determine the p$K_a$of homologous derivatives without the DNJ core (see Fig. 25) to have an idea of the pK_a of different pyridine groups next to a triazole ring or to an amide moiety.

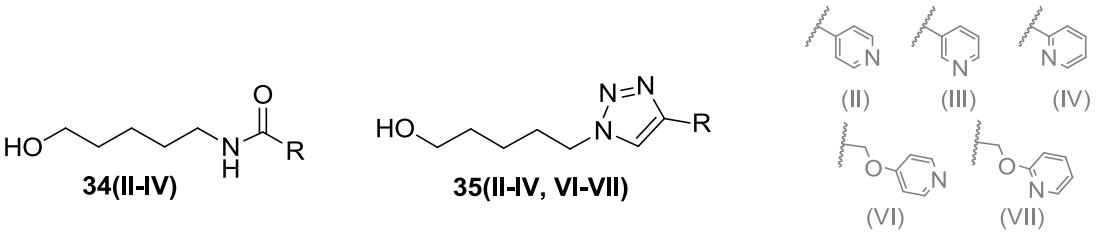

Figure 25 Proposed compounds to synthesize and analyze their pK_a.

3.1.6 Synthesis of pyridine derivatives and analysis of their pK_a

In order to evaluate the range of pK_a of the previously synthesized pyridine derivatives **16(II-IV) and 31(II-IV, VI-VII)**, the homologous derivatives without the sugar mimetic part (compounds **34(II-IV)** and **35(VI-VII)** respectively) were synthesized, purified and their pK_a analyzed.

Thus, the synthesis of amidoderivatives **34(II-IV)** were carried out in solution by acilation of 5-aminopentanol with the corresponding acid, activated using EDC and HOBT as coupling agent. It must be highlighted that, although that kind of reactions are usually expected to have good yields, compounds **34(II)** and **34(III)** were obtained in low yields (Scheme 22). In the case of compound **34(IV)**, the work-up was slightly modified by distilling off the solvent of the reaction and performing the purification by flash chromatography of the obtained residue without a previousaqueous extraction. In this case, **34(IV)** was obtained with excellent yield, suggesting that a high proportion of compounds **34(II)** and **34(III)** remained in the aqueous phase when we did the partition during the reaction work-up.

On the other hand, triazole derivatives **35(II-IV, VI-VII)** were synthesized by Huisgen 1,3-cycloaddition catalyzed by Cu_2O(I), following a procedure similar to the synthesis of compounds **31**. In this case, the reaction was performed between the azidoalcohol **11c** (previously obtained as intermediate compound for the synthesis of DNJ aminoderivative **15c**) and the corresponding alkynes. The time and temperature of reaction were standardized and all the reactions were carried out at 60ºC overnight. In this way, compounds **35(II-IV, VI-VII)** were obtained with variable yields, depending on the alkyne used.

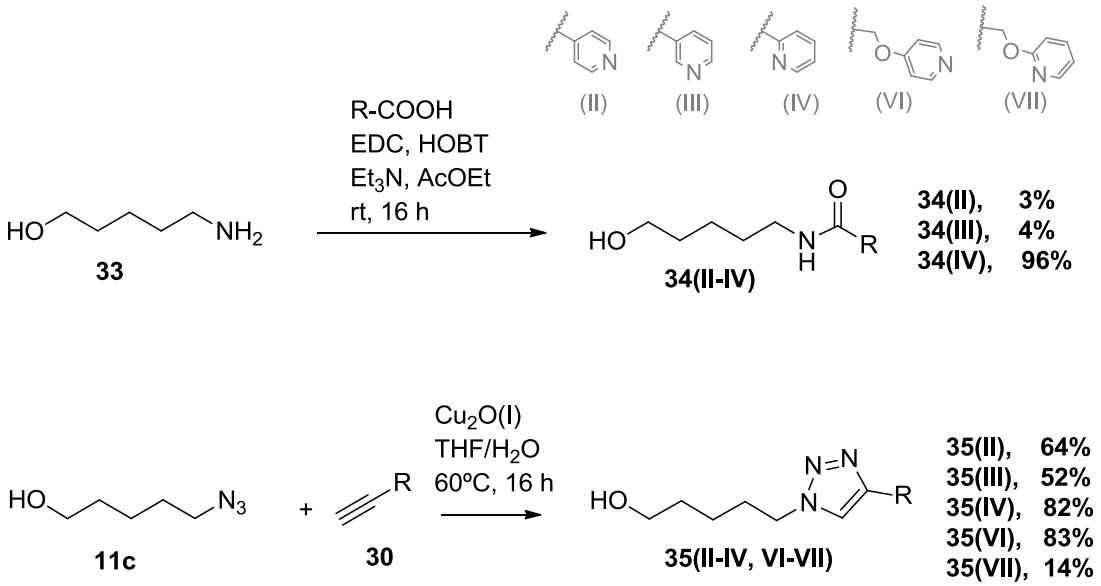

Scheme 22 Synthesis of compounds **34(II-IV)** and **35(II-IV, VI-VII).**

Once the desired compounds **34(II-IV)** and **35(II-IV, VI-VII)** were synthesized, their hydrochlorides were submitted to a titration with NaOH 0.01M, for the determination of their pK_a, as explained in *Section 3.1.5.*

As shown in Table 3, the experimental pK_a values are between 3 and 4 for the amide derivatives (compounds **34(II-IV)**), around 3 for compounds **35(VI-VII)** (triazole-methoxypyridine derivatives), and between 4 and 5 for the triazole-pyridine derivatives (compounds **35(II-IV)**).

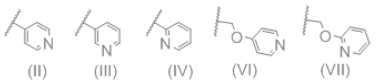

compound (BH^+)	pK_a
34(II)	3.95 ± 0.30
34(III)	3.89 ± 0.34
34(IV)	3.04 ± 0.07
35(II)	4.86 ± 0.21
35(III)	4.22 ± 0.04
35(IV)	4.21 ± 0.61
35(VI)	3.12 ± 0.13
35(VII)	3.04 ± 0.26

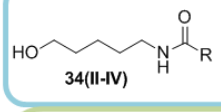

34(II-IV)

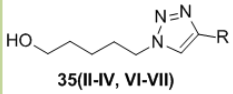

35(II-IV, VI-VII)

Table 3 Experimental pK_a values (mean ± standard deviation; n=3).

Thus, when comparing the alcohol intermediates **35(VI)** and **35(VII)** (pK_a=3.1 and 3.0 respectively) with its corresponding DNJ derivatives **31b(VI)** and **31b(VIII)** (pK_a1 = 2.6 and 2.7 respectively), we can see a slight decrease of the pK_a value. Then, by extrapolation, we would expect the compounds **31d** to have a similar range of pK_a, with probably lower values than the alcohol intermediates synthesized in this section.

These low pK_a values could explain why compounds **16d(II, III)** do not have higher differences in the affinity for GCase at pH 7.0 or at pH 5 in comparison with compound **16d(I)**, and the same with compounds **31d(II-IV, VI)** and **31b(VI-VII)** in comparison with **31d(I, V).** If the pK_a of the pyridine rings of our compounds would have been around 5, we would expect these compounds to be partially protonated at pH 5.2, while at pH 7.0 would be totally deprotonated. This would have allowed us to test the hypothesis of the different affinity for the hydrophobic side of the GCase. Instead, as the pyridine pK_a is around 3-4, this group will be almost quantitatively deprotonated both at pH 5.2 and 7.0, showing no essential differences regarding the pH of the assay,with other compounds containing non protonable groups in their chain such as **16d(I)** or **31d (I, V)**.

For this reason, we decided to analyze the pK_a of other compounds with pyridine, to see if we could achieve compounds with higher pK_a values. Thus, as shown in Scheme 23A, compound **38** was synthesized following methodology similar to compounds **34(II-IV)**, to see if a longer distance between the amido group and the pyridine has lower influence in the basicity of this moiety giving pK_a values around 5. In the same way, the pK_a of 3-(pyridin-4-yl)propan-1-ol

hydrochloride (compound **39**, provided by a commercial source) was also analyzed. As shown in Scheme 23B, in this case both compounds showed pK_a values higher than 5.

A

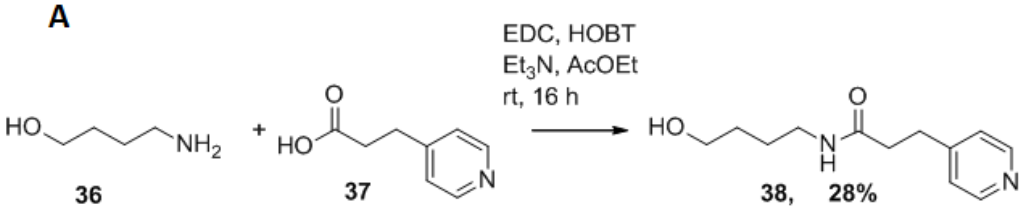

B

compound (BH^+)	pK_a
38	5,37 ± 0,09
39	5,94 ± 0,15

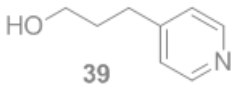

Scheme 23 (A) Synthesis of **38**. **(B)** Experimental pK_a values (mean ± standard deviation; n=3).

Based on these values, we decided to synthesize a DNJ derivative with 4-pyridylpropyl substitution (compound **44**) to verify if we could obtain a compound with higher affinity to GCase at pH7.0 and lower affinity at pH 5.2, based in its different protonation state.

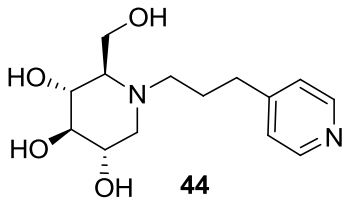

44

Figure 26 Structure of compound **44**.

3.1.7 Synthesis and evaluation of compounds 43 and 44

As shown in Scheme 24, the synthesis of compound **44** was attempted by debenzylation of **41** that would be in turn obtained by alkylation of benzylated DNJ **13** with the tosylate **42** or by reductive amination between **13** and the aldehyde **40**. Both the aldehyde or tosylate derivatives would be obtained by transformation of alcohol **39**.

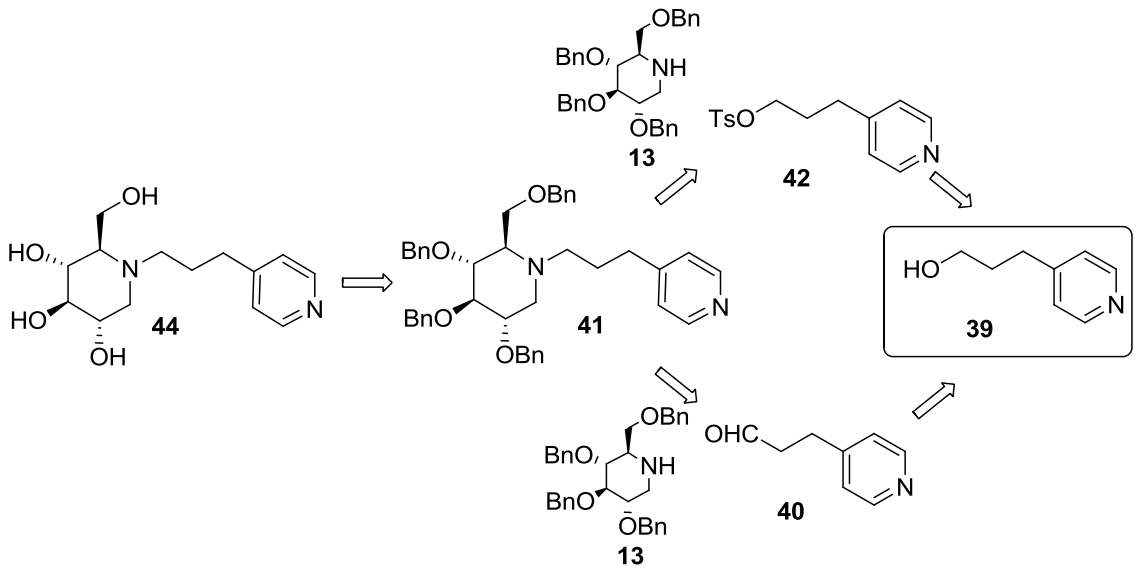

Scheme 24 Proposed retrosynthesis for compound **44**.

Therefore, as shown in Scheme 25, the synthesis of **41** was carried out following these two different approaches. On one hand via alkylation of **13** with the corresponding tosylate using microwave irradiation and, in the other hand, via reductive amination of **13** with the aldehyde **40**, obtained after submitting 3-(pyridine-4-yl)propan-1-ol to a Swern oxidation. In both cases the yield was low but we were able to obtain the desired compound.

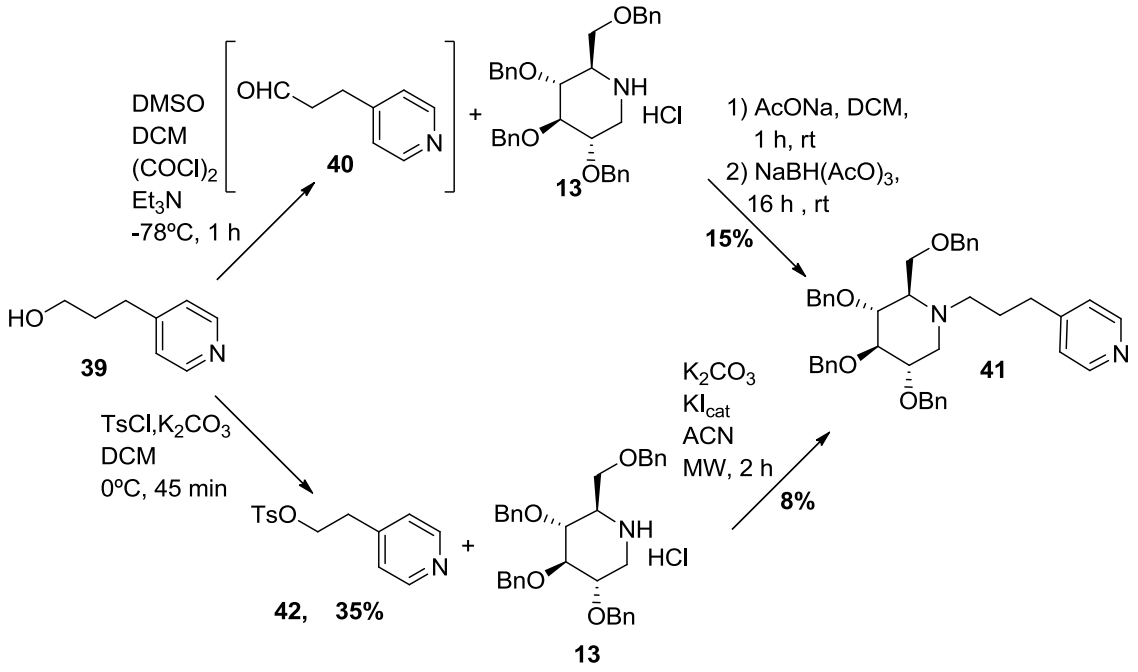

Scheme 25 Synthesis of compound **41**.

Once **41** was obtained, we next tried to obtain compound **44** by debenzylation of **41** by hydrogenation in presence of $Pd(OH)_2$ in acidic solution but, unfortunately, the pyridine was also hydrogenated under these conditions, giving **43** quantitatively. The debenzylation was then performed with BCl_3, finally giving the desired compound **44** with 42% of yield.

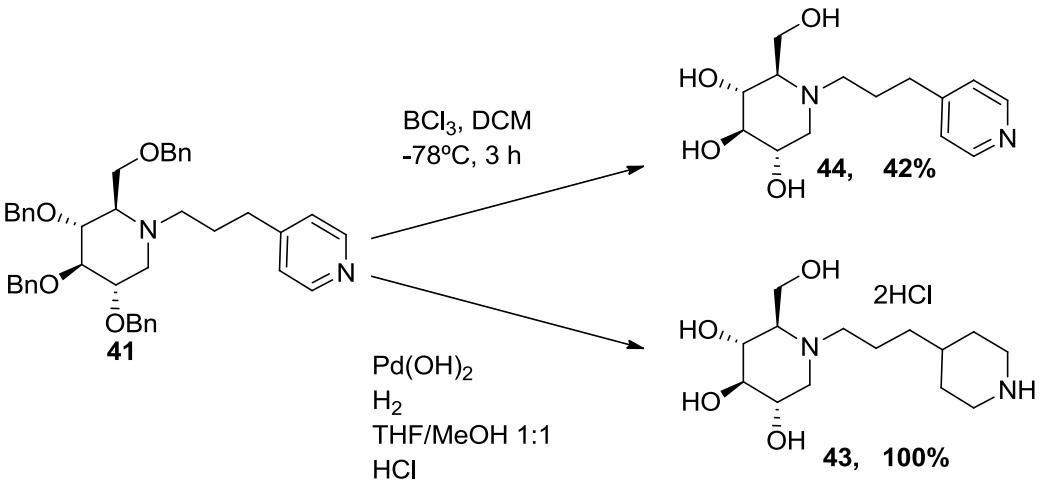

Scheme 26 Synthesis of compounds **43** and **44**.

Finally we were in a position to determine the pK_a of compound **44**. Unfortunately, in this case, we could not determine the pK_a's of the two amines in the same way that we did for compounds **31b** because the two pK_a values of **44** where closer and we could not distinguish the two inflexion points during the titration, in order to determine the ending points. For this reason, the pK_a determination was performed in a more controlled environment: the compound, as free base, was dissolved in aquesous NaCl 150mM (instead of water) to try to maintain constant the ionic strength during the determination. The hydrochloride of **44** was generated in situ by addition of a known excess of hydrochloric acid. The titration with NaOH 0.1M was then performed in a thermostatized vessel (25ºC) with magnetic stirring and under inert atmosphere. The evolution of pH was monitored and recorded with Tiamo® software. Finally, data analysis was performed by Dr. Ignacio Alfonso from Supramolecular Chemistry Group, at IQAC-CSIC, using the computer program HYPERQUAD®. As shown in Fig. 27, this program interpolates the pK_a values that could fit with the titration curve. Thus, according to this determination, the pK_a values for **44** would be 4.850 ±0.023 and 6.178 ± 0.023.

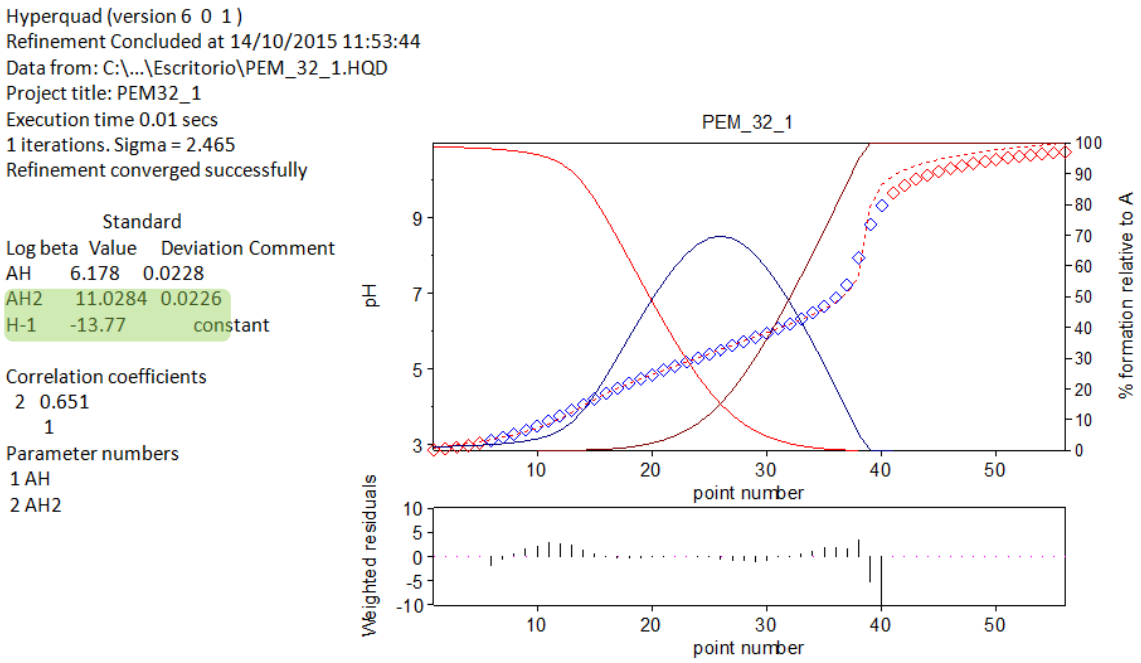

Figure 27 Analysis of pK_a values for **44**. Blue squares represent the experimental titration points. Discontinuous red line represents the adjustment for the theoretical titration curve of a compound with the determined pK_a values.

Observing an species distribution diagram of a diprotonable compound with pK_as 4.85 and 6.18 (Fig. 28, we could notice that this compound would be deprotonated at pH 7.0, but at pH 5.2 it would be around 65% monoprotonated and 30% diprotonated. This means that as we expected, **44** would be neutral at pH 7.0 but ionizated at pH 5.2 and for this reason we would expect it to have less affinity for GCase at this pH.

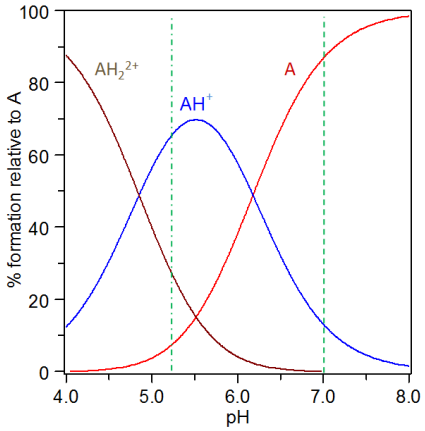

Figure 28 Species distribution diagram (brown= diprotonated, blue= monoprotonated, red = deprotonated) for diprotonable compound with p$K_a$values of 4.85 and 6.18. In green, pH 5.2 (- · -) and pH 7.0 (- - -)

At this point, we decided to test not only compound **44** but also **43** as imiglucerase inhibitors under the assay conditions previously described, obtaining the IC_{50} values showed in Table 4. Although the pK_a of **44** seemed to be adequate to have much more affinity for GCase at pH 7.0 than at pH 5.2, this difference of affinity was translated into just two times more potency at pH 7.0 than pH 5.2. Instead, in the case of **43**, were we would expect a similar activity at both pH, this difference is higher. This result seems to suggest that this approach for obtaining compounds with higher affinity for GCase at pH 7.0 than at pH 5.2 is not working as we initially expected,probably due to the fact that the affinity of the compound and an enzyme are determined by a combination of factors and in our approach we are taking into account a preponderant one, that perhaps is not playing the essential role that we hypothesized.

Compound	IC_{50} (pH 5.2, μM)	IC_{50} (pH 7, μM)	Δ
43	105	33	3.2
44	414	203	2.0

Table 4 Inhibition of imiglucerase. IC_{50} (μM) values for tested compounds, at pH 5.2 and pH 7, and relationship of the difference of the values obtained at both pH.

As we mentioned in the introduction of this chapter, the interactions of GCase with the alkyl chains are via hydrophobic interactions and are, therefore, less specific than the hydrogen bond interactions formed with the DNJ ring. This fact is consistent with the ability of iminosugars with alkyl chains of varying lengths to bind to GCase[139], and could explain why we do not see the expected difference of activity of the compounds assayed in this section, according to the pH of the assay.

3.1.8 Other biological assays

3.1.8.1 Inhibition of commercial glycosidases

In order to evaluate the selectivity of the synthesized compounds, they were also tested in front of other commercial glycosidases: α-glucosidase from *Saccharomyces cerevisiae*, β-glucosidase from almond, α-galactosidase from green coffee beans, β-galactosidase from bovine liver. Those assays are based on approaches similar to the one used for imiglucerase

assay but, in this case following previously reported protocols[138], the substrate used was a 4-nitrophenyl-glycopyranoside instead of 4-MUG. Each 4-nitrophenyl-glycopyranoside substrate is selective for each enzyme (α-glucosidase, β-glucosidase, α-galactosidase or β-galactosidase) and its cleavage is measured as absorbance at 405nm.

When tested at 100 µM, compounds **15(a-b,d)**, **31b(VI-VII)**, **44** and NB-DNJ showed low inhibition (<30% of all tested commercial glycosidases except **31b(VII)** that presented 38 % of inhibition of β-glucosidase from almond). Data obtained for the rest of compounds are represented in Graph. 3.

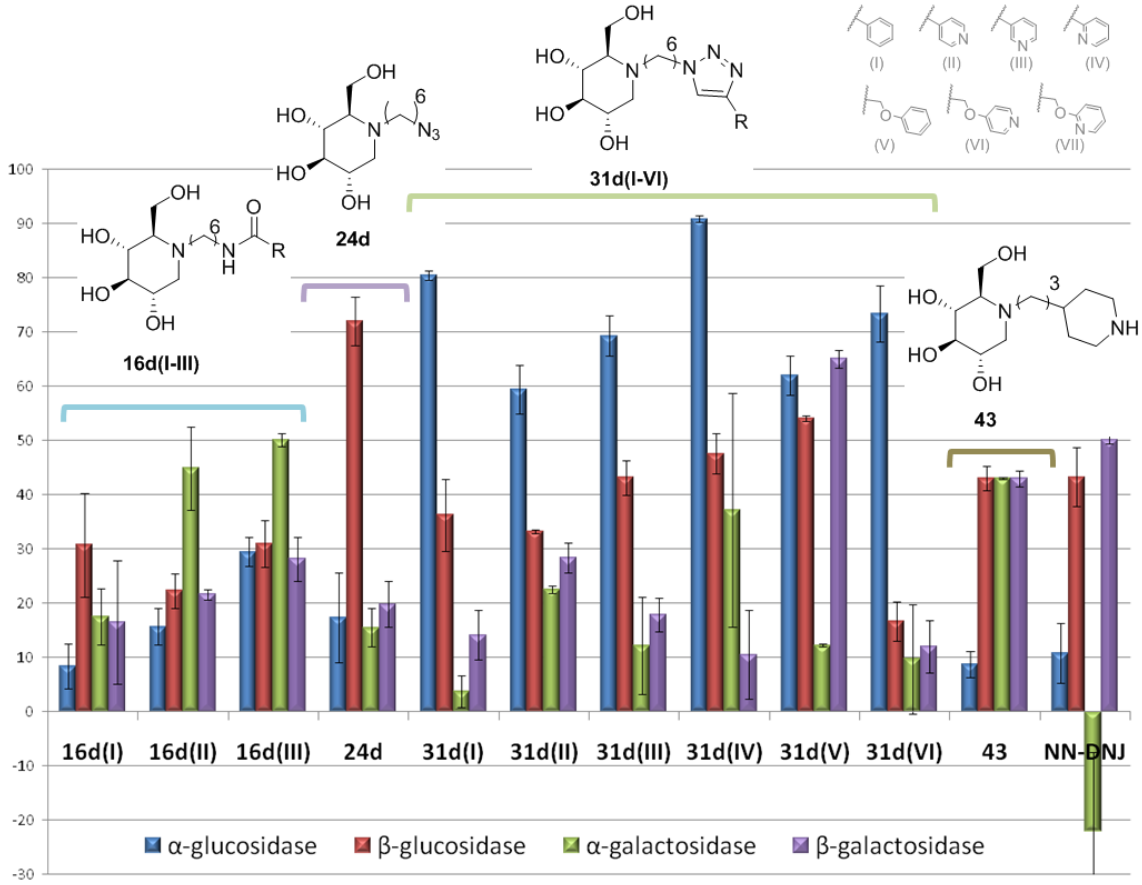

Graphic 3 Inhibition of commercial glucosidases (% inhibition of the enzyme when tested at inhibitor concentration = 100 µM. Mean and standard deviation of at least two independent assays with triplicates.

As can be observed in Graph. 3, only compounds **31d** presented percentatge of α-glucosidaseinhibition higher than 50% when tested at 100 µM, meaning than their IC_{50} against that enzyme would be lower than 100 µM. The most potent inhibitor of this enzyme seemed

to be **31d(IV)**, with IC_{50} 20 μM (its IC_{50} values against imiglucerase were 6.4 μM and 1.6 μM when tested at pH 5.2 or pH 7.0 respectively).

Regarding to almond β-glucosidase, all tested compounds showed IC_{50} lower than 100 μM, except **31d(V)** that presented IC_{50}s around at 100 μM (50 or 100 times the value of its IC_{50} for imiglucerase, depending on the pH of the assay), and **24d** that showed 72% in inhibition of this enzyme at 100 μM (while its IC_{50} for imiglucerase was 15.7 and 5.5 μM at pH 5.2 and 7 respectively).

All tested compounds exhibitedvalues of inhibition of α-galactosidase lower than 50%, and interestingly NN-DNJ even seemed to activate this enzyme.

With reference to the assay of inhibition of β-galactosidase, all assayed compounds showed low inhibition of this enzyme (<30% inhibition) when tested at 100 μM, except compounds **31d(V)**, **43** and NN-DNJ, that presented 63%, 43% and 50% of inhibition respectively.

In conclusion, all the tested compounds with interest as imiglucerase inhibitors showed good selectivity for imiglucerase in front β-glucosidase from almond, α-galactosidase from green coffee beans, β-galactosidase from bovine liver. Moreover, most of the assayed compounds seemed to have good selectivity for imiglucerase against α-glucosidase from *Saccharomyces cerevisiae*, except family of compounds **31d**, which also showed some affinity for this enzyme.

3.1.8.2 Inhibition of glucosylceramide synthase (GCS):

The inhibition of GCS is an interesting approach for the treatment of GD. In fact, NB-DNJ is actually used as GCS inhibitor for the treatment of this disease in humans. As compounds synthesized in this section are DNJ derivatives, they were also evaluated as GCS inhibitors in cell homogenates to determine its capacity as inhibitors for this enzyme.

In this case, following previously described methodologies[140], we used the fluorescent substrate Cer-C6-NBD to measure the activity of the enzyme GCS, as explained in Fig. 29.

Thus, this assay was performed *in vitro* with A459 cell homogenates in eppendorf tubes. After a preincubation of the cell homogenate in presence or absence (control 0% inhibition) of the compound to test, NAD and UDP-Glucose solutions were added, followed by addition of a Cer-C6-NBD/BSA complex. After incubate this mixture for 15 min, the reaction was quenched by

MeOH addition. The supernatants were separated by centrifugation and analyzed by HPLC with fluorescence detector (λ_{exc} 470 nm, λ_{em} 530 nm). The percentage of the newly synthesized GluCer-C6-NBD in front of theadministered Cer-C6-NBD was calculated from the chromatograms. The percentages of GCS inhibition were calculated as the percentage of reduction in the synthesis of GluCer-C6-NBD in comparison with the control without inhibitor.

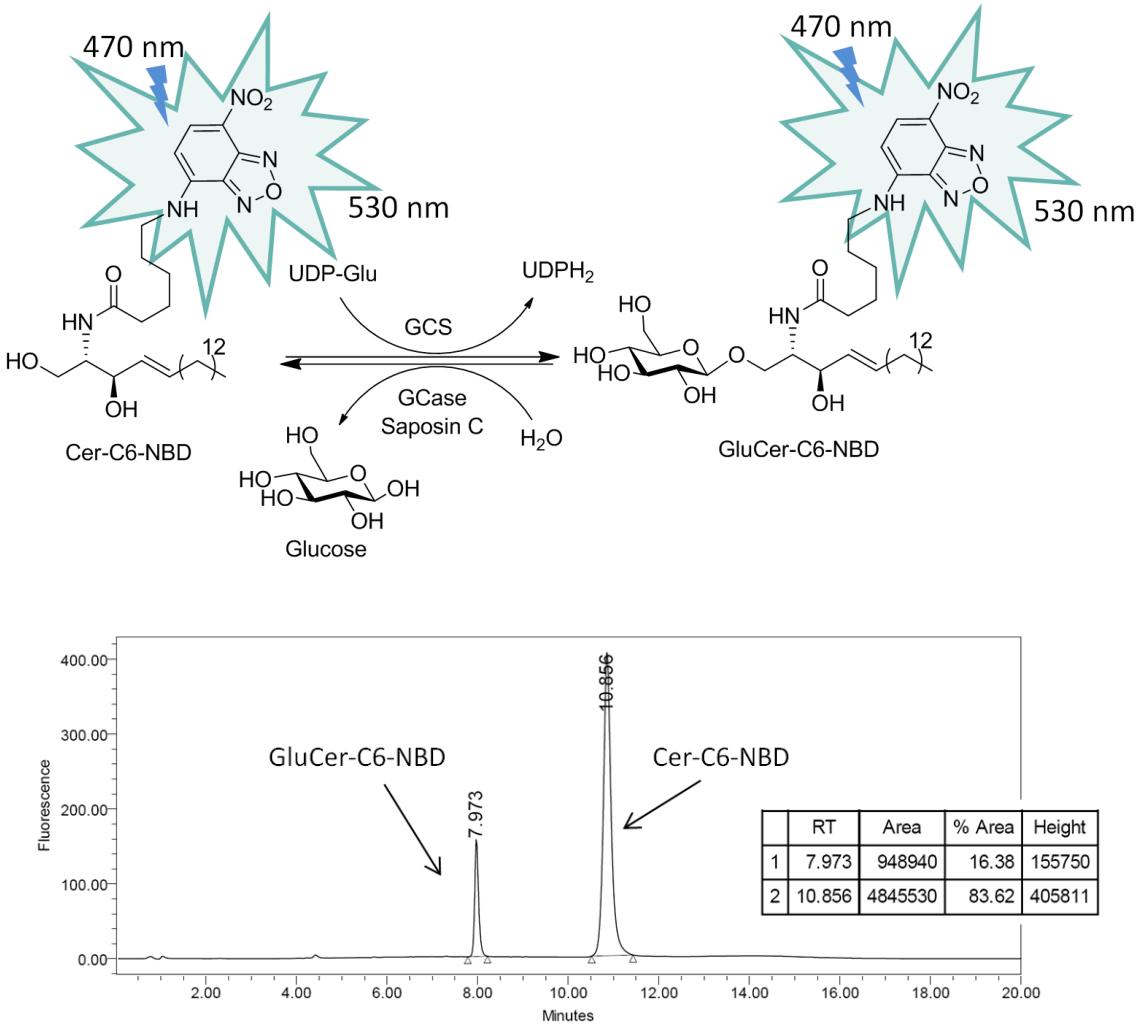

Figure 29 (A) Representation of the GCS inhibition assay with Cer-C6-NBD. GluCer-C6-NBD is synthesized from Cer-C6-NBD by non inhibited GCS, in presence of UDP-Glu. both compounds with NBD moitety are fluorescent and their relative proportions can be determined by HPLC attached to fluorescence detector. **(B)** Example of HPLC chromatogram of the injected supernatant to analyze GCS inhibition. In this chromatogram GluCer-C6-NBD and Ceramide-C6-NBD are detected (rt: 7.973 and 10.856 minutes respectively). Column Zorbax Eclipse Plus C18 , 3.5 µm, 4.6 x 75 mm. Flow: 1 ml/min ; eluent; A:H2O + 0.1% TFA; B: ACN+0.1%TFA ; eluent conditions: 2 minutes 70/30. After, 4 minutes gradient to 25/75. Then, maintain this proportion for 8 minutes. λ_{exc} 47 0 nm, λ_{em} 530 nm.

As shown in Table 5, DNJ derivatives with a terminal primary amine (compounds **15(a,b,d)**, 4-alcoxypyridine derivatives (compounds **31b(VI-VII) and 31d(VI)**) and compounds **43** and **44** showed less than 50% of GCS inhibition when tested at 100 µM. On the contrary, DNJ derivatives with triazole or azide linkers and a terminal pyridine or phenyl group (compounds **16d(I-III)** and **31d(I-V)**), compound **24d** (a DNJ derivative with a terminal azide), as well as NB-DNJ and NN-DNJ showed a percentage of inhibition of GCS higher than 50% and were tested at 10 µM. Data obtained for those compounds in both assays are shown in Table 5 and Graph. 4.

	GCS (A459 homogenates)	
	%inh at 100 µM[a]	%inh at 10 µM (IC_{50})[b]
15a	18	n.d.
15b	14	n.d.
15d	37	n.d.
16d(I)	79	34 ± 9.1
16d(II)	85	37 ± 11.3
16d(III)	71	24 ± 7
24d	80	25 ± 12.8
31b(VI)	39	n.d.
31b(VII)	30	n.d.
31d(I)	91	55 ± 8.2
31d(II)	93	55 ± 8
31d(III)	89	45 ± 11
31d(IV)	96	53 ± 15.8
31d(V)	99	80 ± 3.8 (2.0 µM)
31d(VI)	37	n.d.
43	26	n.d.
44	12	n.d.
NB-DNJ	64	26 ± 7.1
NN-DNJ	95	69 ± 2.8 (4.0 µM)

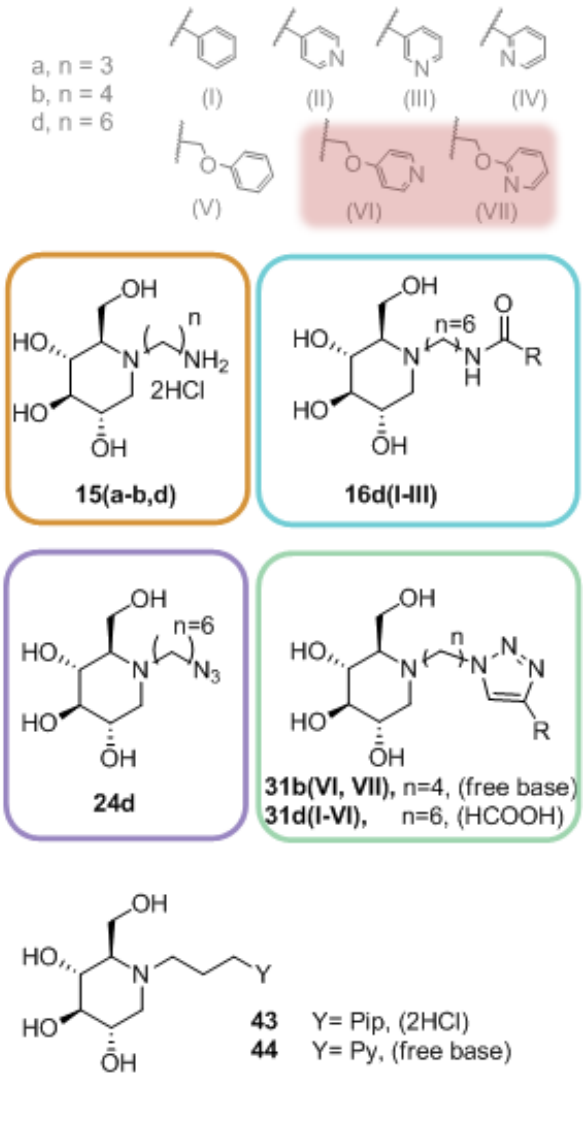

Table 5 Determination of the inhibition of GCS and cell viability in MTT assay, experimental values.
[a] mean of three independent assays, standard deviation <10
[b] mean of three independent assays ± standard deviation, IC50 (µM) in brackets
n.d. = not determined

Interestingly, both families of compounds (**16d(I-III)** and **31d(I-IV)**) resulted to be similar or better GCS inhibitors than NB-DNJ, a compound that is actually used in clinic as a GCS inhibitor for treatment of GD. When comparing compounds with amido or triazole linkers, triazole compounds **31d(I-IV)** are better GCS inhibitors, with IC_{50} aroung 10 µM, in front of the IC_{50} values between 10 and 100 µM of **16d(I-III)** amido-derivatives.

Moreover, although compounds with a alcoxypyridine terminal substituents (compounds **31d(VI) and 31b(VI, VII)**) showed no significant inhibition of GCS at 100 µM, their equivalent with phenyl instead of a pyridine group (compound **31d(V)**), resulted in the more potent GCS inhibitor among all the compounds tested in this section (IC_{50} 2 µM), even better than NN-DNJ (IC_{50} 4 µM).

On the other hand, it should be highlighted that compounds **16d(I-III)** and **31d(I-V)** showed IC_{50} values in the same range for GCS and imiglucerase (Graph. 4). This property is interesting as those compounds could be used as dual compounds inhibiting simultaneously the synthesis of GluCer while could work as chaperone for GCase..

A

	Imiglucerase	
	pH 5.2 IC_{50} (µM)	pH 7.0 IC_{50} (µM)
NB-DNJ	430	145
NN-DNJ	1.03	0.25
16d(I)	22.8	5.6
16d(II)	35.4	18.7
16d(III)	42.6	24.2
24d	15.7	5.5
31d(I)	8.5	1.6
31d(II)	22.6	7.1
31d(III)	27.2	6.3
31d(IV)	6.4	1.6
31d(V)	2.4	0.8

B

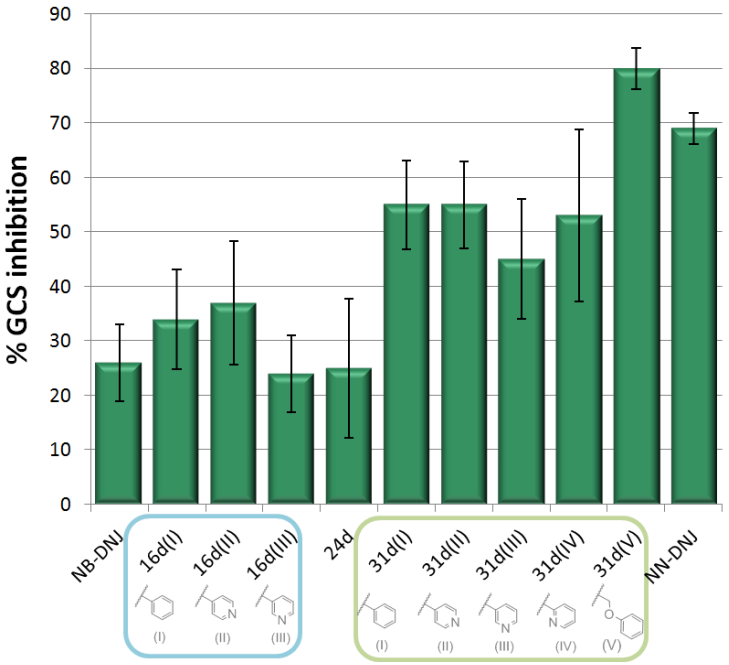

Graphic 4 (A) IC_{50} against imiglucerase. **(B)**%GCS inhibition at 10 µM in A459 cell homogenates (assay performed by independent triplicates with one point each time. Representation of mean values and standard deviation).

In contrast to the clinical dogma of compound selectivity, dual compounds able to inhibit the synthesis of the enzyme substrate GluCer and increase the enzyme hydrolytic activity acting as GCase's Pharmacological Chaperones could represent a better therapeutic agent having a synergic activity[141]. Further studies would be necessary, however, but these findings can open the door to new families of dual compounds with potential for the treatment of GD.

3.1.8.3 Cytotoxicity assay in WT human fibroblasts.

In order to evaluate the toxicity of those compounds, they were submitted to MTT assay. This assay, described firstly by Mosmann in 1983[142], became one of the most used methods of cell proliferation to study the effect produced by addition of substances in the culture medium. The MTT assay is a colorimetric assay based on the addition of yellowish dye 3-(4,5-dimethylthiazol-2-yl)-2,5-diphenyltetrazolium bromide (MTT) that is reduced by mitochondrial enzymes to formazan, a water insoluble purple crystalline material that can be solubilized by DMSO and whose formation can be quantified by measurement of the absorbance at 570 nm. Thus, a higher absorbance value is related with a higher mitochondrial activity and this is correlated with the amount of living cells. In this assay, the viability of cells in presence of our inhibitors is referred as percentage of viability, compared with a control without inhibitor.

As shown in Graph. 5, none of the compounds assayed in this section displayed high toxicity at 200 µM. Compounds **16d(I)** and **16d(III)** showed the higher toxicity, having 62 and 78% of viability at that concentration. Thus, when comparing the concentrations from which the compounds start showing cytotoxicity and the concentrations from which they presented inhibition of the desired enzymes, compounds **43**, **44**, and **16d(I-III**), presented a good safety window, but compounds **16d(I-III)** showed a moderate safety range. In the case of compounds **43** and **44**, as they resulted less potent inhibitors of the enzymes of interest, it would be necessary toevaluate their cytotoxicity at higher concentrations in order to properly evaluate its safety window. Interestingly, the best imiglucerase and GCS inhibitors from this section (compound **24d** and the family of compounds **31d**) showed a high safety range.

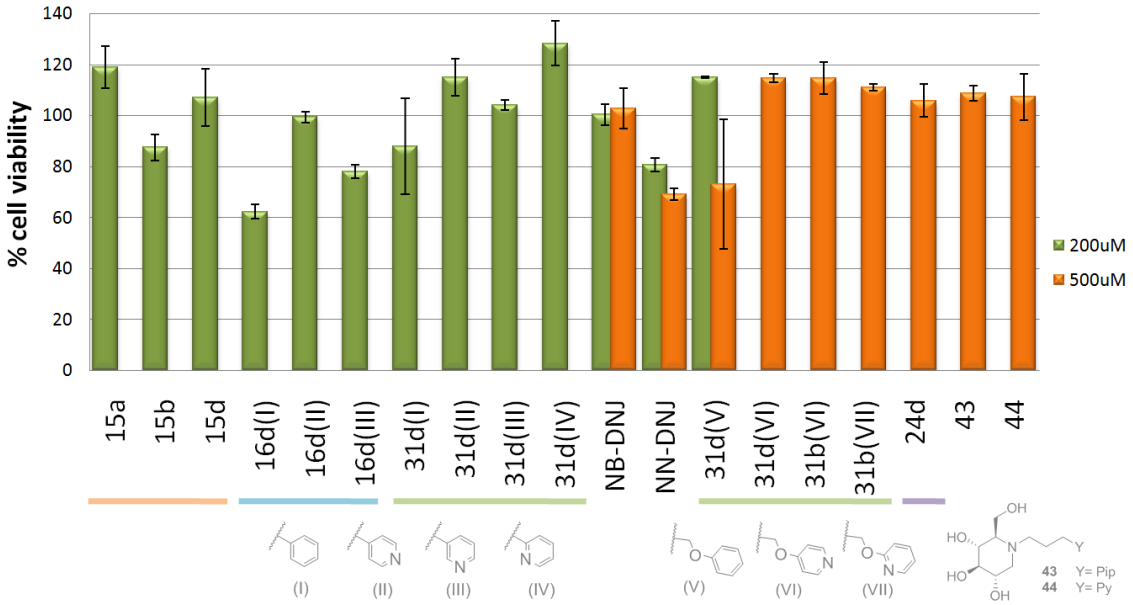

Graphic 5 Cell viability after 24h MTT assay in WT human fibroblasts in presence of inhibitors (assay performed by CID Cell culture Service. In the graph, mean with standard deviation of a single assay with triplicates).

3.2 Study of the influence of the pK_a of the sugarmimethic core

3.2.1 Introduction

In the previous section we tried to modulate the affinity of different GCase inhibitors according to the pH of the assay, by introducing chemical groups at the end of the chain of those inhibitors that were expected to be in different states of protonation depending on the pH of the assay, and thus would interact differently with the hydrophobic pocket on GCase binding site. Alternatively, in the present chapter we will analyze the influence of the pK_a of the amine of the sugar mimetic core in the affinity of different inhibitors for GCase at different pHs.

It is known that glycosidases usually have two carboxylic acid groups in the active site, and only display catalytic activity in sugar hydrolysis when one of these is protonated in acidic neutral form and the other deprotonated in the carboxylate anionic form. As explained in chapter one, in the case of GCase, the residue Glu340 acts as anucleophile and would be initially in the carboxylate form, while Glu235 would initially be protonated acting as acid in the enzymatic reaction. This necessity of a specific state of protonation of those glutamate residues implies a pH dependency of the activity of the enzyme, resulting on a lack of activity at those pHs where

both carboxylates are either protonated or unprotonated. Moreover, the position of amines in DNJ derivatives mimics the endocyclic oxygen of the glucose head group of GluCer[143]. Thus, changes in the protonation state of the nitrogen in the DNJ moiety are expected to modify the interaction of those inhibitors with GCase.

3.2.1.1 Customization of pK_a

The pK_a of an *N*-alkyl amine can be modulated by introduction of different substituents in its *N*-alkylic chain. For example, as shown in Fig. 30A, it is possible to decrease the basicity of *N,N*-dimethylethylamine (pK_a 10.2) by introducing an hydroxyl or fluorine group in the β-position from the amine (pK_a 9.0 and 8.5 respectively). Besides, it is known that the influence of these electrowithdrawing substituents in the basicity of an amine decreases with its distance to the amino group. Moreover, the effect of each fluorine group seems to be accumulative, decreasing the pK_a of the amine in between 1.6 and 1.9 pK_a units for each fluorine substituted in the β-position both in open chain molecules as in cyclic aliphatic amines (Fig. 30B)[144].

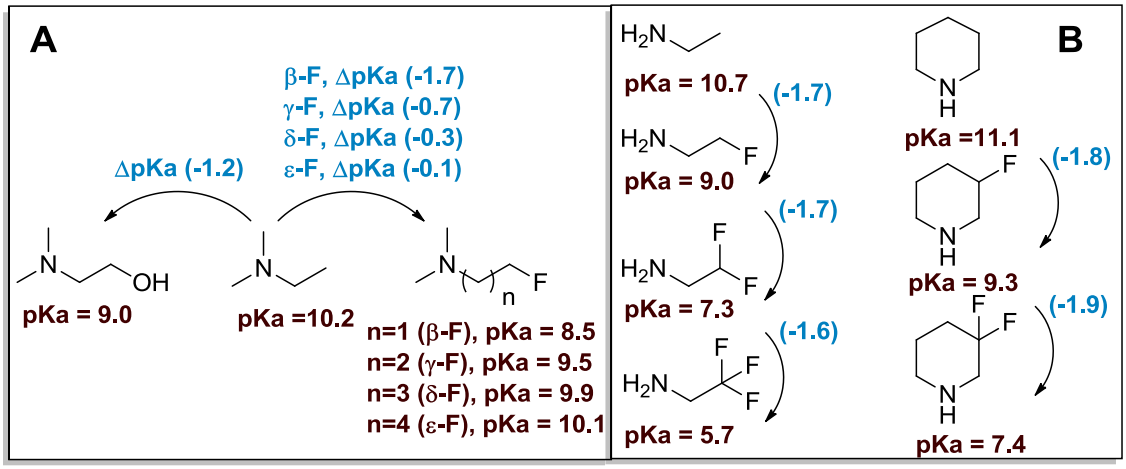

Figure 30 (A) Variation of pK_a by addition of hydroxyl or fluoroβ-susbtituent, and influence of the distance of the fluorine subtitution. **(B)** Variation of pK_a according to the number of fluorine atoms substituted in the β-position in open chain molecules and in cyclic aliphatic amines[144].

As explained before, NB-DNJ and NN-DNJ pK_as are 7.1 and 6.7 respectively[112]. Thus, they are expected to be protonated in the acidic lysosomal media and partially protonated in the neutral environment of the endoplasmic reticulum. Moreover, an ideal pharmacological

chaperone would have higher affinity for GCase at pH 7.0 than at pH 5.2 in order to facilitate the correct folding of GCase in the reticulum without blocking the GluCer hydrolysis in the lysosome. In this way, we expect that compounds with pK_a around 6 would show the desired differential GCase affinity according to the pH of the assay.

Thus, the synthesis of DNJ derivatives with hydroxyl or fluorine substitution in the β-position may be interesting as it could provide DNJ derivatives with different ranges of pK_a and would allow the analysis of both the influence of those substituents in a sugarmimetic core and the influence of the pK_a of the nitrogen in the DNJ moiety in the affinity against GCase.

3.2.1.2 Selection of the objective compounds

Besides DNJ derivatives, inositol derivatives have also been found to be potent inhibitors of GCase. Between the different inositol stereoisomers, 1-amino-myo-inositol derivatives (for example compound **47y**) seemed to be the most potent[145,146].

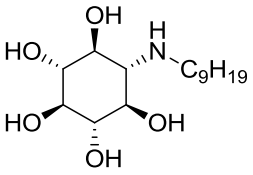

45

IC_{50} (pH 5.2) = 3.9 μM
IC_{50} (pH 7.0) = 0.78 μM

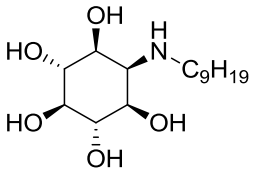

46

IC_{50} (pH 5.2) = 52.6 μM
IC_{50} (pH 7.0) = 24.9 μM

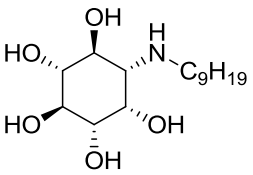

47y

IC_{50} (pH 5.2) = 0.08 μM
IC_{50} (pH 7.0) = 0.025 μM

Figure 31 Examples of three different stereoisomers of nonyl inositol and their IC_{50} values against Imiglucerase[145].

In order to study the influence of the pK_a of the amine in the sugarmimethic core the aim of this section would be to synthesize and analyze a small library of compounds with potential affinity for GCase that possess relatively structural similarities but different pK_a values. Thus, it will be intended to synthetize a range of DNJ and myo-inositol derivatives with or without hydroxyl or fluorine substitution in the β-position with regard to the amine of the core. For the same purpose, *N*-butyl and *N*-nonyl derivatives with a new core similar to *myo*-inositol but with the hydroxyl in position 2 substituted by fluorine will also be synthesized, evaluated and the data will be compared with the *myo*-inositol butyl and nonyl derivatives.

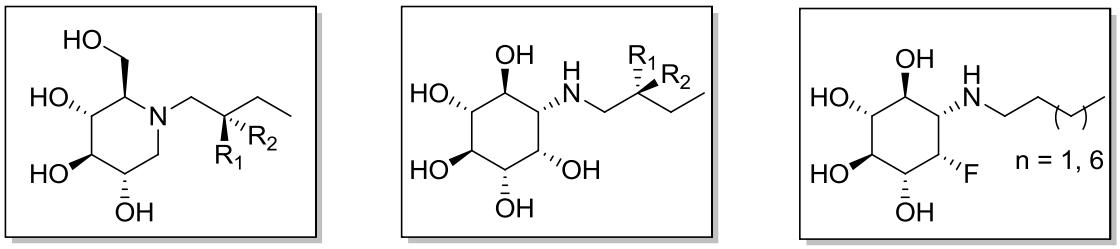

Figure 32 Representation of the aim compounds for this section.

3.2.2 Synthesis of different cores and some *N*-butyl and *N*-nonyl derivatives

N-nonyl inositol (**47y**) was previously synthesized by Dra. Ana Trapero during her doctoral thesis[111]. The synthesis of the other compounds of interest was carried out from the corresponding benzylated derivatives (Fig. 33). DNJ benzylated core **13** was provided by SIMChem (Service of Synthesis of High added value Molecules, IQAC-CSIC) and synthesis of the other derivatives will be described below.

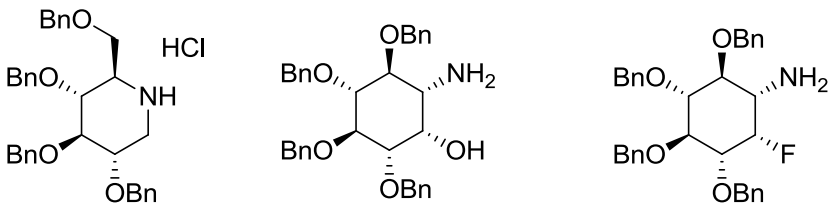

Figure 33 Protected structures of the cores that will be derivated in this chapter.

3.2.2.1 Synthesis of benzylated *myo*-inositol core (63).

Synthesis of **63** was previously described in the literature from *p*-benzoquinone. As the starting material is an achiral and symmetric precursor, one of the synthetic steps should include a resolution to separate the two enantiomers, in order to obtain **63** enantiomerically pure.

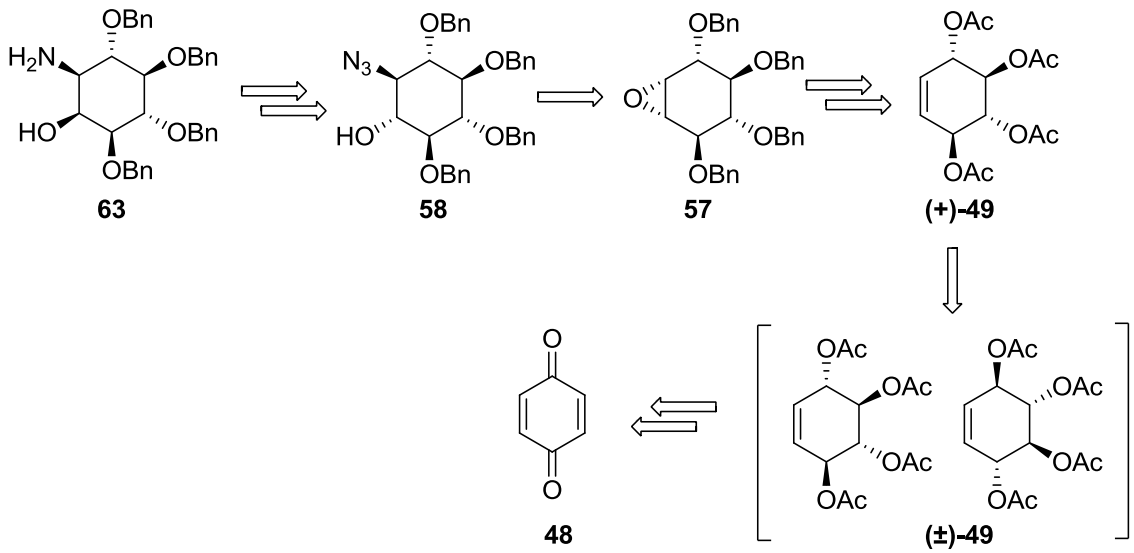

Scheme 27 Retrosynthetic approach for the synthesis of **63.**

In this way, Gonzalez-Bulnes *et al* [147]reported the synthesis of **63**, via resolution of racemic conduritol B tetracetate **(±)-49** using the palladium-catalyzed kinetic resolution previously developed by Trost and Hembre[148] (Scheme 28). It should be highlighted that this reaction it is very sensitive and the catalyst is quite unstable. This could cause that sometimes this reaction does not evolve as well as expected.

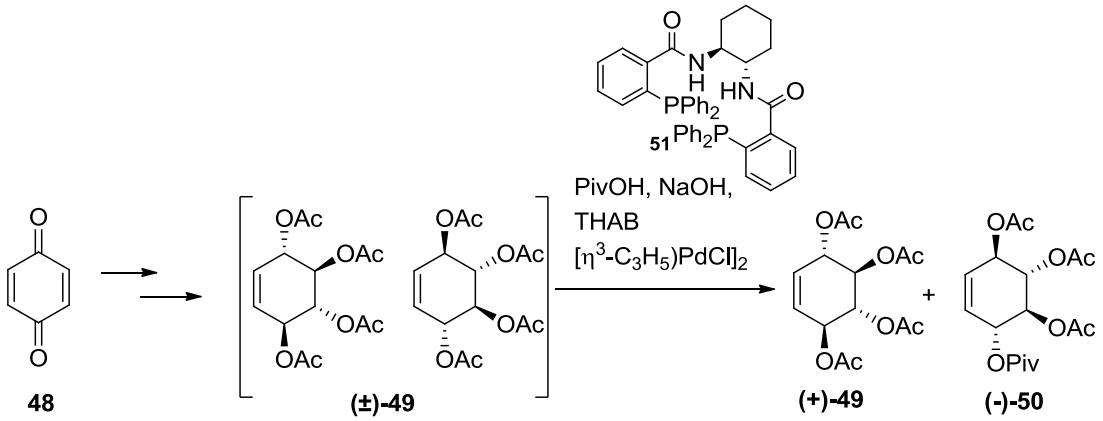

Scheme 28 Kinetic resolution of conduritol B tetraacetate**(±)-49.**

Aside from Trost resolution, other authors describe the differentiation of both enantiomers by enzymatic resolution. Thus, Sanfilippo *et al*[149]compared different lipases and conditions for biocatalysed alcoholysis of conduritol-B tetraacetate **(±)-49**, obtaining the best results for Lypozyme® (lipase from *Mucormiehei* absorved on support), in considerably robust conditions. For this reason, we chose this procedure to separate the two enantiomers.

Therefore, as shown in Scheme 27, the proposed retrosynthetic analysis of **63** involved the regioselective nucleophilic attack of azide on benzylated epoxide **57** to give azidoalcohol **58** that could be transformed into aminoalcohol **63** after inversion of the free hydroxyl group and reduction of the azide group. Epoxide **57** would be obtained after hydrolysis of the acetate esters in **(+)-49** and posterior epoxidation of the double bond and benzylation of the hydroxyl groups. As mentioned before, the enantiomerically pure of conduritol-B tetraacetate **(+)-49** would be obtained after enzymatic resolution of its racemic mixture **(±)-49.** Conduritol-B tetraacetate **(±)-49** would be obtained from achiral *p*-benzoquinone after successive reactions of bromation, reduction and acetylation.

Thus, conduritol-B tetraacetate (**(±)-49**) was synthesized following previously reported methodologies[150]. A racemic mixture of bromoalcohols **(±)-53** was obtained with moderate yield (46%) after a bromation of *p*-benzoquinone and posterior reduction of the cetone groups, as shown in Scheme 29. Then, the racemic **(±)-53** was acetylated in presence of AcOK in a mixture of AcOH/Ac_2O giving a racemic mixture of conduritol-B tetraacetate (**(±)-49**) with 31% yield, and recovering some by-products only partially acetylated that were separated by flash chromatography.

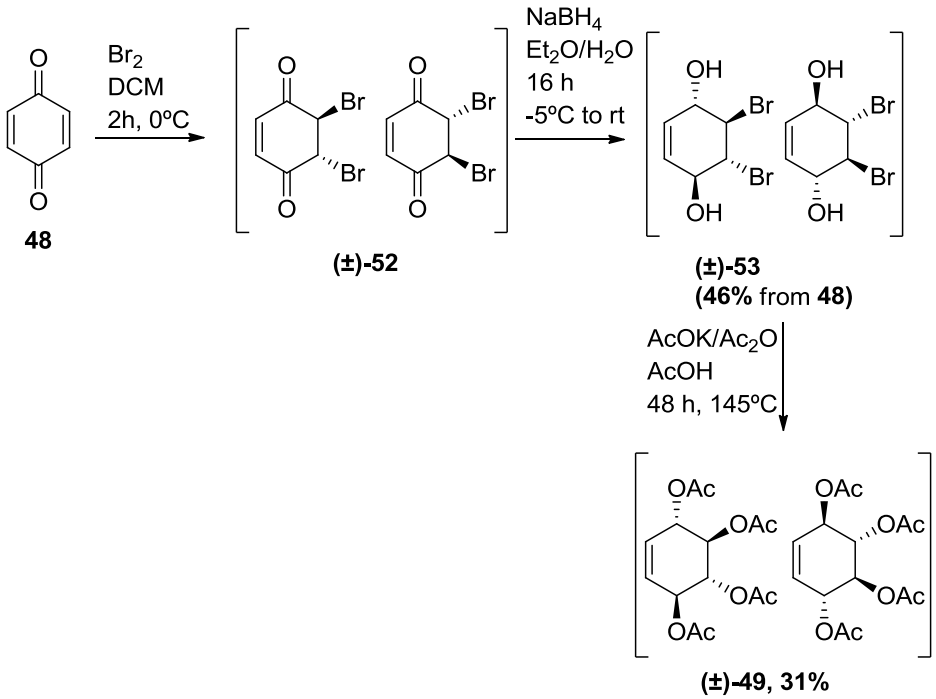

Scheme 29 Synthesis of conduritol-B tetraacetate **(±)-49** from *p*-benzoquinone.

Once the racemic tetraester **(±)-49** was obtained, it was submited to an enzymatic resolution with Lipozyme®, a lipase obtained from *Mucormiehei immobilized* on solid support, in order to continue the synthesis only with the enantiomers of interest, instead of racemic mixtures. Lipozyme® possess *R* stereopreference and, in this way, the desired enantiomerically pure tetracetate **(+)-49** and diol **(-)-54** were obtained with excellent yields after separation by flash chromatography (Scheme 30).

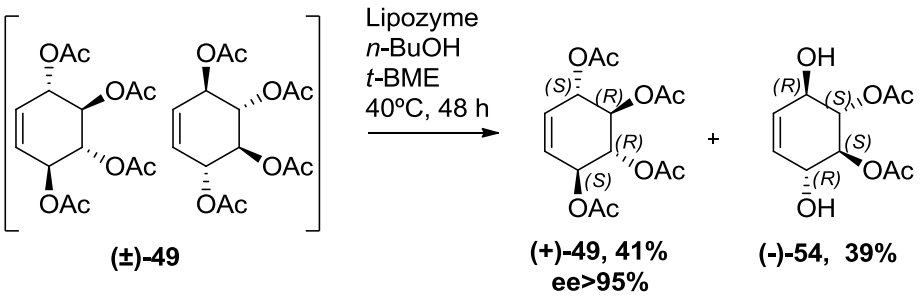

Scheme 30 Enzymatic resolution of **(±)-49**.

It is noteworthy that ester groups located on C-2 and C-3 in the enantiomer **(+)-49**, although having the suitable configuration for being hydrolyzed by Lipozyme®, do not undergo any alcoholysis. This unreactivity can be explained in terms of steric hindrance exercised by the vicinal allylic ester groups[149].

Moreover, we were not able to detect any signal of the enantiomer **(-)-49** when analyzing the enantiomeric purity of **(+)-49** by chiral HPLC, indicating ee>95%, as shown in Fig. 34.

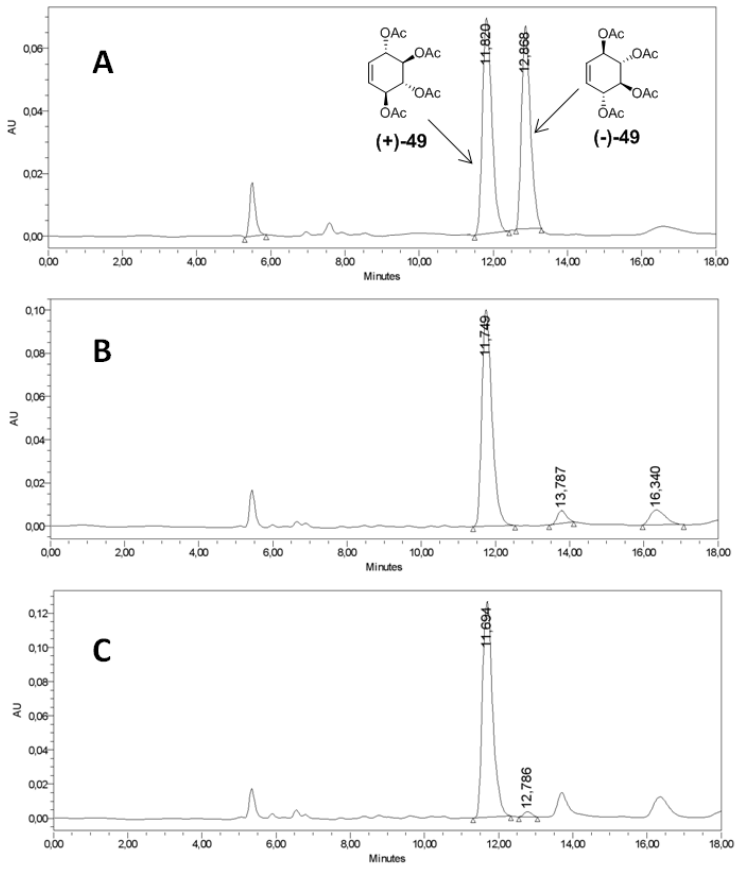

Figure 34 Chiral HPLC chromatograms of **49**. **(A)**racemic mixture **(±)-49**. **(B) (+)-49** obtained after treatment of the racemic mixture with Lipozyme®. **(C)(+)-49**with the addition of 5% of racemic mixture (ee=95%).

Once the enantiomerically pure tetraacetate **(+)-49** was obtained, we continued the synthesis of **63** by following a procedure previously developed in our group[147], as described before in Scheme 27. Thus, the acetyl esters of **(+)-49** were hydrolyzed in presence de Na and MeOH, giving the free tetraol **55** with good yield (87%). Then, **56** was obtained, also with good yield (88%), after epoxidation of the double bound by treating with *m*-CPBA a solution of **55** in MeOH.

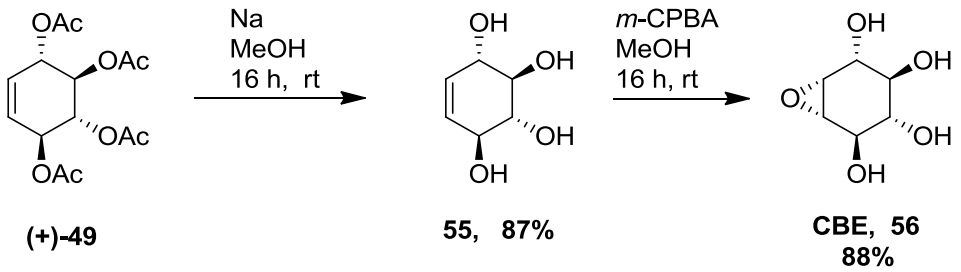

(+)-49 **55, 87%** **CBE, 56 88%**

Scheme 31 Synthesis of **(+)**-CBE **(56)** by hydrolysis of enantiomerically pure tetraacetate **(+)-49** and posterior epoxidation.

It should be noticed that Conduritol β-epoxide (CBE, **56**) has been shown to be a selective and irreversible inactivator of human GCase while not affecting the activity of other known mammalian β-glucosidases. This property has been widely used in biological research to mimic Gaucher's cells, for example to analyze the consequences of a blockage of GCase activity and GluCer accumulation[151]. As shown in Fig. 35, CBE covalently binds GCase by ester formation with Glu340. The reaction mechanism proposed by Premkumar *et al*[152], involves protonation of the epoxide oxygen of CBE by the catalytic acid/base Glu235, followed by nucleophilic attack of Glu340 at C1 of the CBE ring, causing diaxial opening of the epoxide and formation of a nucleophile-CBE ester bond.

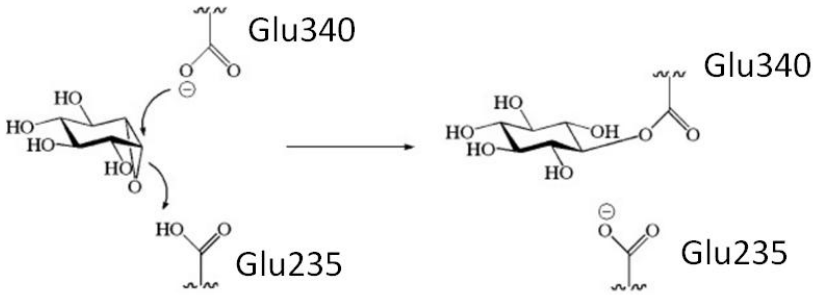

Figure 35 Mechanism of inactivation of a retaining β-glucosidase by CBE (**56**). Figure adapted from[151].

After synthesis of CBE (**56**) was reached, following the procedure previously developed in our group[147], the free hydroxyl groups were protected as benzyl ethers furnishing compound **57** with 85% yield. Then, epoxide opening of **57** with NaN_3 and $LiClO_4$ at 80ºC in ACN gave the desired regioisomer **58** with moderate yield (54%)and minor amounts of the byproduct of inverse epoxide opening (compound **59,** 16% yield), which were separated by column chromatography (Scheme 32).

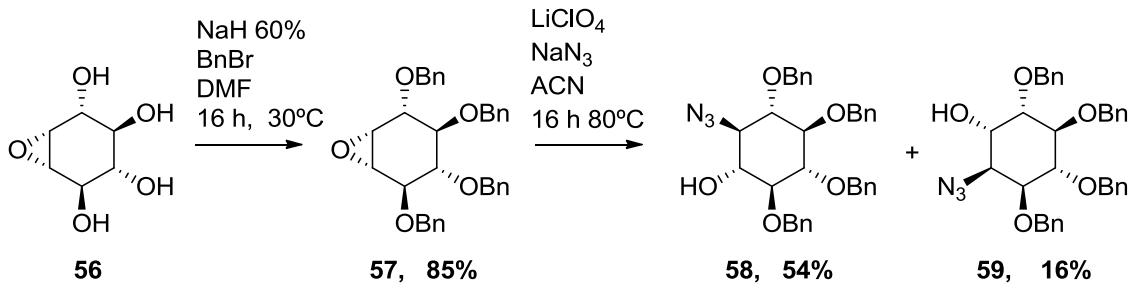

Scheme 32 Synthesis of azidodetivatives **58** and **59**.

Then, the free hydroxyl group in cyclitolazide **58** was transformed into its mesylate **60** in 99% yield and this compound was used to perform the stereo chemical inversion to azidocylitol **61** (Scheme 33). This reaction was attempted by heating in a sealed tube a solution of **58** in DMF with 2% of water at 140ºC, as described in the literature[147], but no transformation was observed after 11 days of reaction, even increasing the heating until 150ºC, recovering the unreacted starting mesylate.

The reaction was next tried under microwave irradiation. Unfortunately, the inositol derivative was degraded and we obtained a mixture of compounds that we were not able to separate or identify. Further trials with different reaction times, temperatures and power of microwave irradiation did not afford better results.

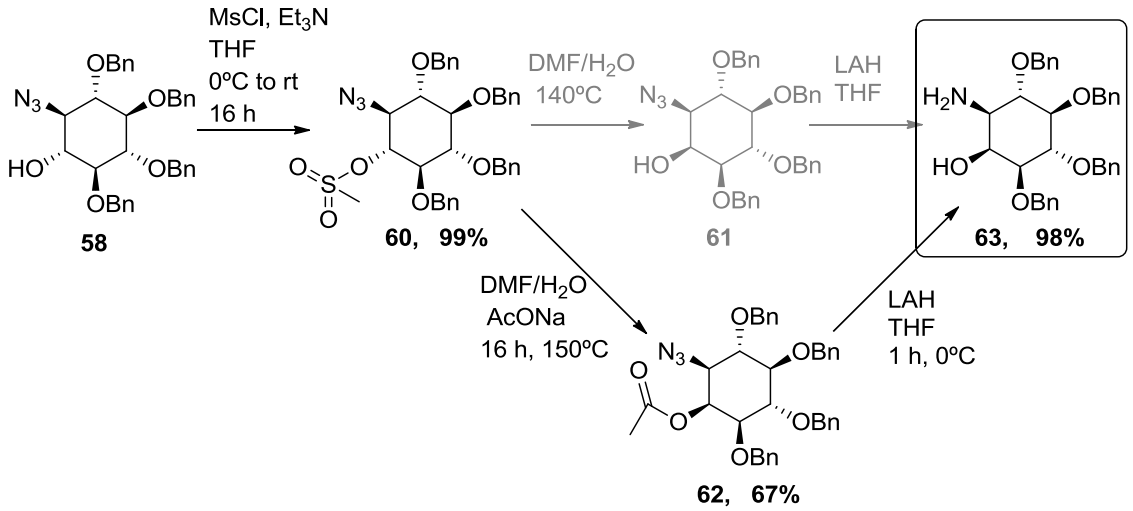

Scheme 33 Synthesis of aminoalcohol **63** from **58**.

Finally, following the idea of facilitating an hydroxyl inversion by substitution of a mesylate by an ester[153,154], the inversion was achieved by the synthesis of the acetate ester **62.** Thus, after 16h of reaction at 150ºC in DMF with 2% of water and adding 10 equivalent-mol of AcONa, the azido-acetate **62**, was achieved in good yield (67%). Then, treating with LAH a solution of **62** in THF for 1h, simultaneously reduced the azido group and the ester to give the desired aminoalcohol **63** with excellent yield (98%).

Compound **63** will be used as starting material for the synthesis of *myo*-inositol derivatives that will be described in the next sections. Moreover, we thought that it could be interesting

to evaluate the inhibitory capacity of the deprotected cores without *N*-substitution, in order to analyze potential differences of activity between different GCase inhibitors that could intrinsic to the core and not specifically related to the *N*-substituent. For this reason, **63** was debenzylated by hydrogenation catalyzed by $Pd(OH)_2/C$ in acidic conditions. Thus, as shown in Scheme 34, (−)-1-amino-1-deoxy-*myo*-inositol (**64**) was obtained with good yield (77%).

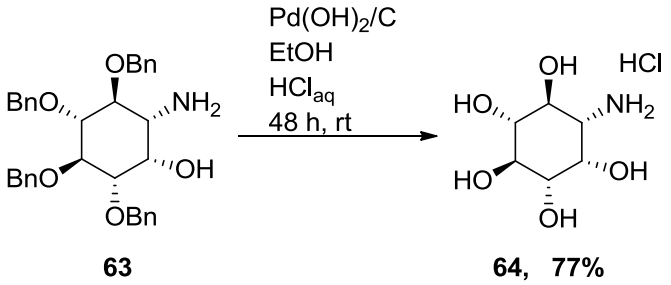

Scheme 34 Debenzylation of **63**.Synthesis of (-)-1-amino-1-deoxy-*myo*-inositol (**64**).

3.2.2.2 Synthesis of F-inositol core and derivatives

The synthesis of protected F-inositol core **66** was firstly tried by direct fluorination of compound **58**, an intermediate compound obtained for the synthesis of inositol core **63** with Deoxofluor®, but although the starting material disappeared during the reaction the compound of interest could not be obtained.

Then, the synthesis of **66** was afforded by introduction of a triflate group in the free hydroxyl group of compound **58** (Scheme 35). After formation of **65**, the triflate group was substituted by a fluorine atom with inversion of the configuration of this substituent. Thus, the fluorination was achieved treating **65** with TBAF for 16 h at rt using THF as a solvent, and compound **66** was obtained with good yield (77%).

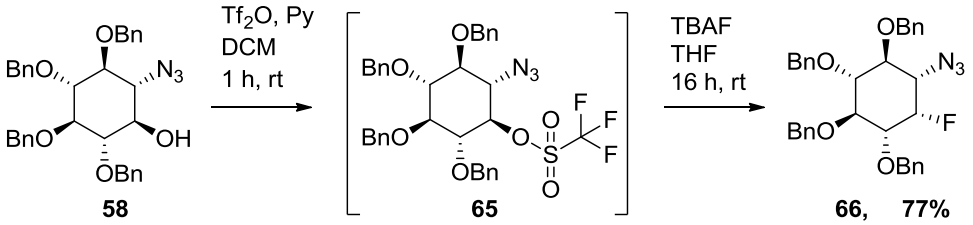

Scheme 35 Synthesis of **66**.

Once compound **66** was achieved, the butyl derivative **67x** was tried to obtain in a one-pot reaction that included a reduction of the azide group to amine in a first term, followed by a reductive amination and finally a posterior debenzylation in strong acidic environment (Scheme 36). Thus, a solution of **66** in EtOH was submitted to hydrogenation catalyzed with Pd/C to reduce the azide group. After 1 h of reaction, 2 equivalent-mol of butyraldehyde were added and the reductive amination was carriedout overnight under soft acidic conditions (AcOH). There was added an excess of aldehyde in order to minimize the proportion of unreacted F-inositol core, and taking into account that the disubstituted by-product **68x** would also be interesting to test as GCase inhibitor. Continuing with the one-pot reaction described before, we proceeded to the debenzylation step. Therefore, next day an extra portion of Pd/C was added to supply the potentially poisoned catalyst. It should be noticed that this kind of debenzylations need a strong acidic media under the experience acquired. For this reason, a mixture of aqueous HCl and EtOH was also added at this point. When the debenzylation was completed, the mixture of reaction was filtered over a pad of Celite®. Unfortunately, under these conditions, only the dialkylated compound **68x** was obtained, although with acceptable yield (62%).

Thus, compound **67x** was then tried to obtain with a similar synthesis, but adding only 1.05 equivalents-mol of butyraldehyde to minimize the disubstitution of the amine. In this case, it was obtained a mixture of compounds that included **67x** and a small proportion of **68x** (the proportion **67x**/**68x** was approximately 10:1 by ^{1}H-NMR). After purification by preparative HPLC, only **67x** was obtained (28% yield).

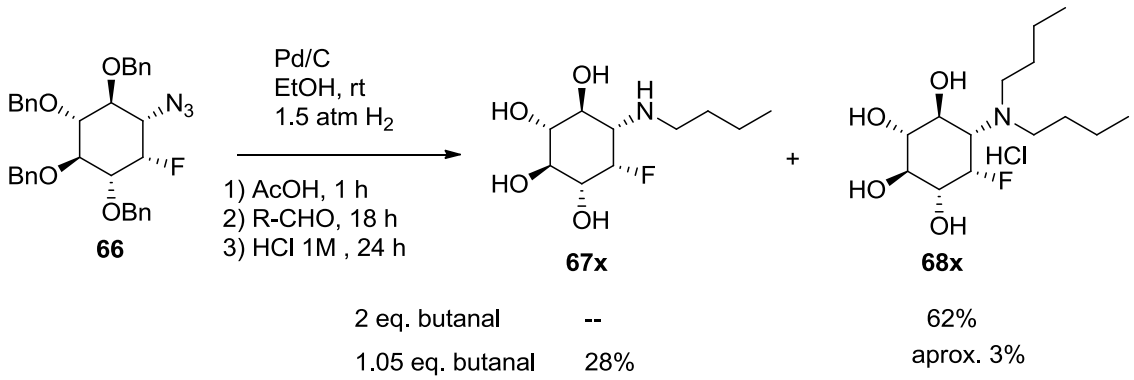

Scheme 36 Attempt of synthesis of **67x**. Synthesis of **68x**.

Taking into account the experience obtained with the butyl derivatives, the synthesis of nonyl derivatives was performed similarly, but adding 1.3 equivalent-mol of nonanal to try to obtain a mixture of mono- and di-substituted derivatives that would be separated by column chromatography in reverse phase. The hydrochloride salt of the disubstituted derivative was formed by treatment with HCl 1M/dioxane (Scheme 37). Thus, **67y** and **68y** were obtained with low yields (19 and 13% respectively).

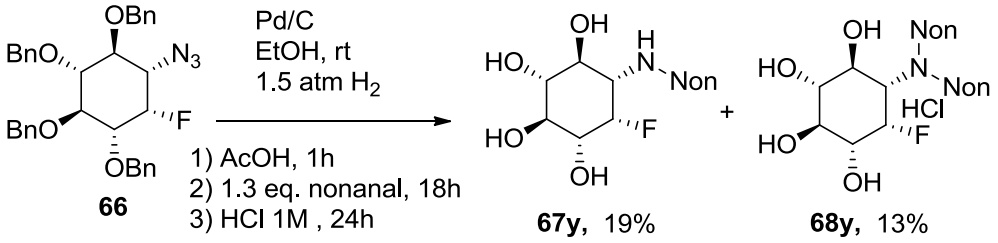

Scheme 37 Synthesis of compounds **67y** and**68y**.

On the other hand, similarly to compound **63**, compound **66** was also debenzylated giving **69** with good yield (80%, Scheme 38).

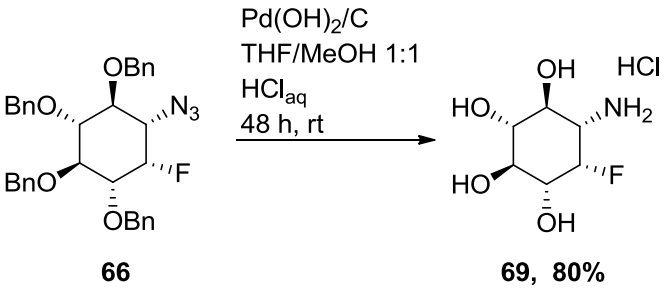

Scheme 38 Synthesis of compound **69.**

3.2.3 Synthesis of *N*-butyl inositol and DNJ derivatives with and without β-substitution

3.2.3.1 Synthesis of *N*-butyl and *N*-difluorobutyl inositol derivatives (compounds 47x and 76)

The synthesis of derivatives **47x** and **76** was first proposed from acylation of **63** with the acids **70** and **71**, provided from commercial sources, and followingreduction of the amide group and deprotection of the benzylated hydroxyl groups, as shown in Scheme 39.

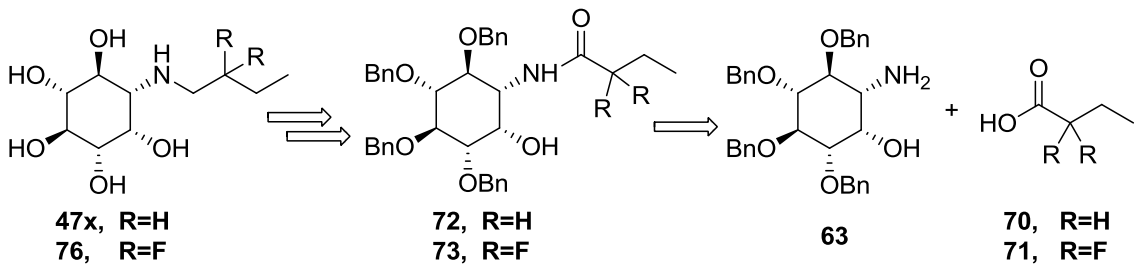

Scheme 39 Retrosynthetic approach for synthesis of compounds **47x** and **76**.

Thus, as shown in Scheme 40, after acylation of **63** with the carboxylic acids **70** and **71** in the presence of EDC, HOBT and Et_3N, the amido derivatives **72** and **73** were obtained in moderate yield (55% and 51% respectively).

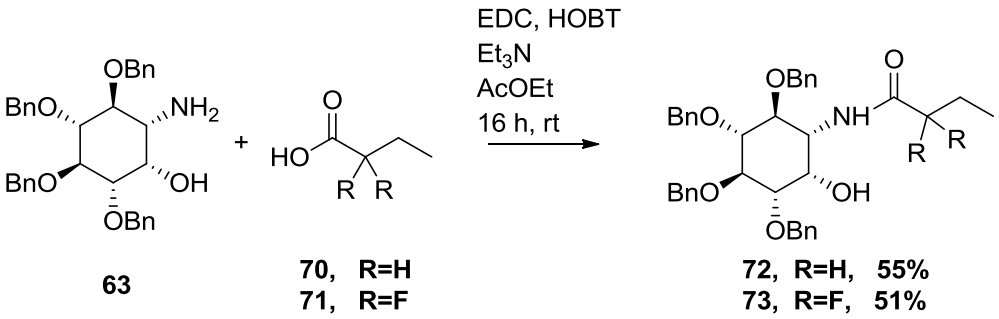

Scheme 40 Synthesis of compounds **72** and **73**.

Then, we tried to reduce the amido groups to amines in compounds **72** and **73** by using LAH as reductive agent (Scheme 41), but this reaction did not take place, recovering the starting compounds without any modification. At that point we tried to perform the reduction with borane, and this time the reduction took place, giving the amino derivatives **74** and **75** with moderate yields (51% for both compounds).

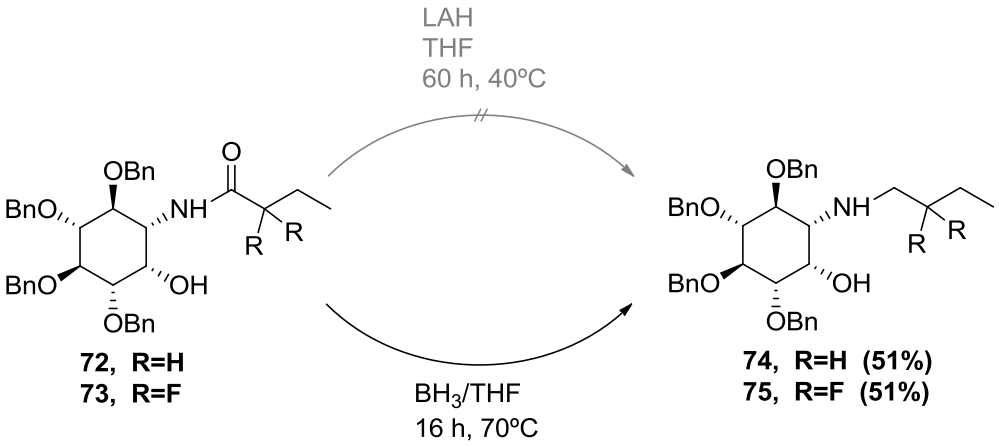

Scheme 41 Synthesis of compounds **74** and **75**.

Finally, as shown in Scheme 42, the desired compounds **47x** and **76** were obtained with excellent yields (83% and 100% respectively) after a catalyzed hydrogenation in acidic media of benzylated compounds **74** and **75**, under conditions similar to synthesis of compound **69**.

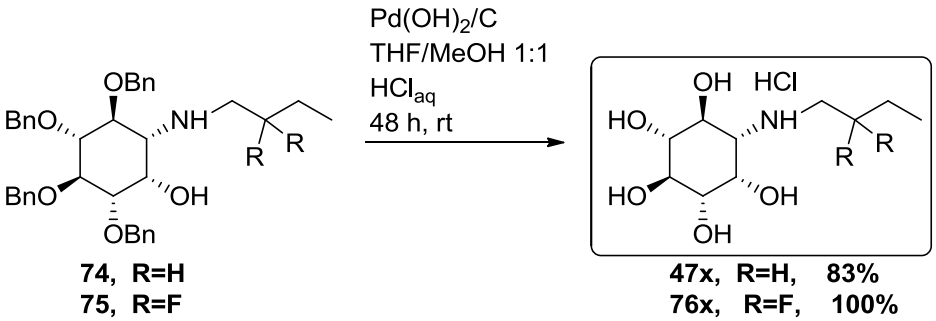

Scheme 42 Synthesis of compounds **47x** and **76x**.

3.2.3.2 Synthesis of *N*-difluorobutyl DNJ derivative 82.

Synthesis of difluorinated DNJ derivative **82** was firstly tried following a retrosynthetic approach similar to the one used for inositol derivatives in the previous section, that would include an acylation of DNJ derivative **13**, reduction of the amide group and a final deprotection of the benzylated hydroxyl groups, as shown in Scheme 43.

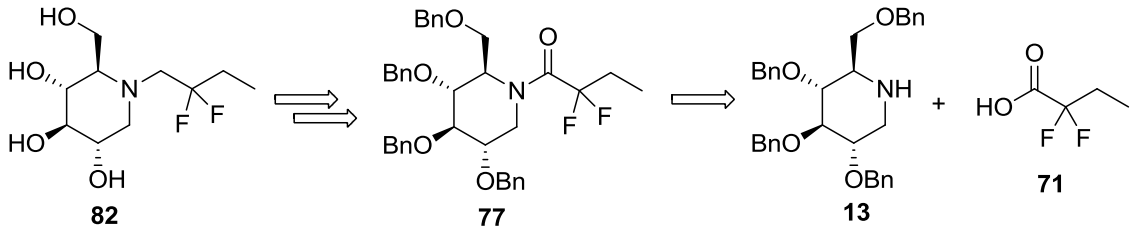

Scheme 43 Retrosynthetic approach for synthesis of compound **85** by acylation.

As shown in Scheme 44, acylation of **13** was first attempted under the previously described conditions, but the expected compound **77** was not detected when the reaction was performed at rt or heated overnight at 40ºC, and the starting amine **13** was recovered. For this reason, we decided to try the synthesis of **77** by using the acyl chloride **78**, generated *in situ* by treating **71** with $SOCl_2$. Unfortunately, this approach does not lead us to obtain **77** and again the starting benzylated DNJ (**13**) was recovered.

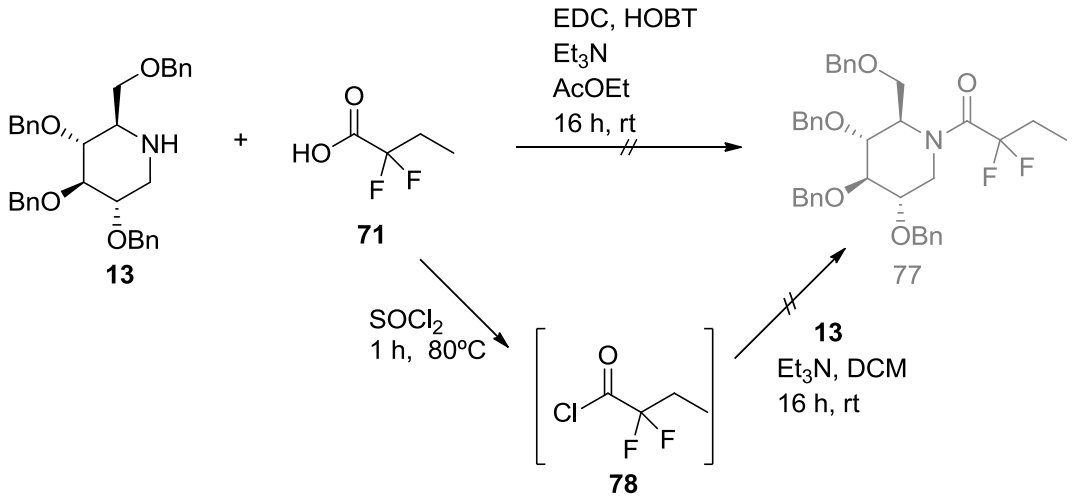

Scheme 44 Attemps of synthesis of compound **77**.

At this point, we decided to try a different approach to obtain compound **82**. Thus, as shown in Scheme 45, **82** would be obtained after a fluorination of the carbonyl group in **80** and final deprotection of the benzylated hydroxyl groups. Compound **80** would be obtained by alkylation of **13** with 1-bromobutan-2-one (**79**).

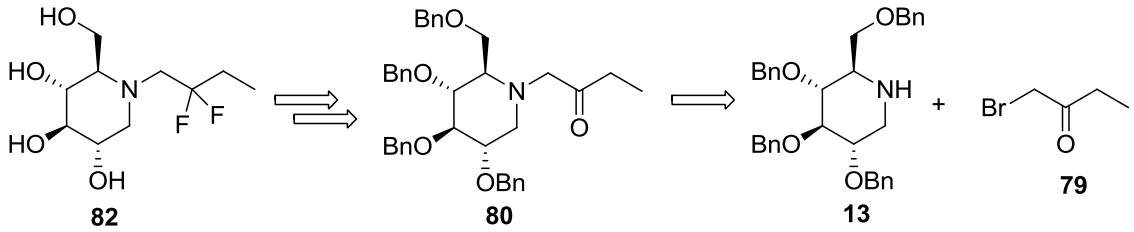

Scheme 45 Retrosynthetic approach for synthesis of compound **85** by alkylation.

Thus, the alkylation of **13** with bromoketone **79** was carried out in DMF solution after 60 minutes of microwave irradiation, in presence of DIPEA as a base. In this way, compound **80** was obtained quantitatively, as shown in Scheme 46.

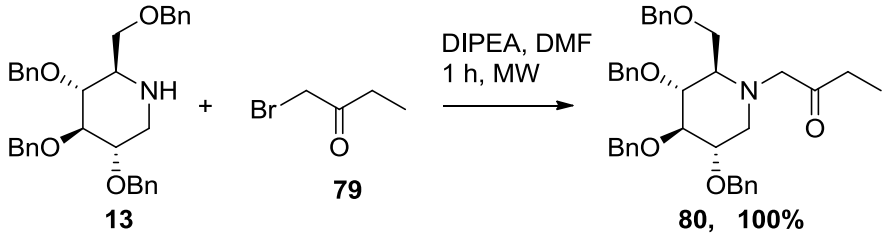

Scheme 46 Synthesis of compound **80**.

Next, following the proposed retrosynthetic approach, we proceeded to the fluorination of the carboxyl group of compound **80** (Scheme 47). Thus, a solution of this compound in 1,2-dicloroethane was treated overnight with the fluorinating agent Deoxofluor® in presence of EtOH as a catalyst[155]. Under these conditions we obtained a mixture of compounds and, after purification by flash chromatography, we were able to obtain the difluorinated derivative **81** with low yield (15%). A posterior hydrogenation catalyzed with $Pd(OH)_2/C$ under strong acidic conditions finally gave the desired difluorinated compound **82** (92% yield).

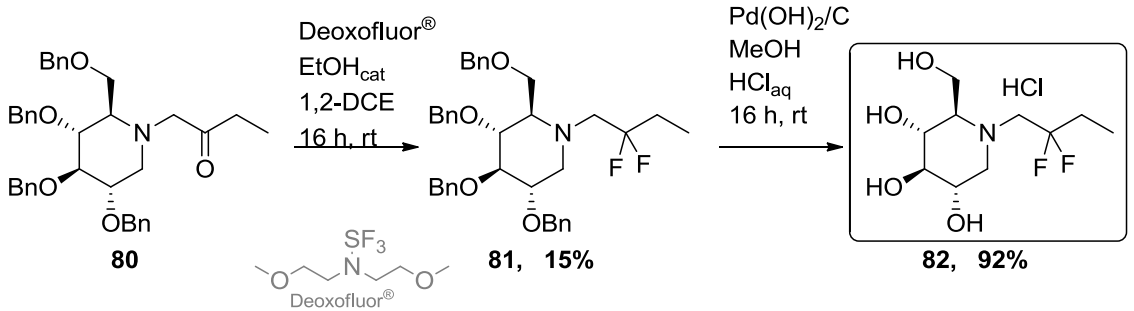

Scheme 47S ynthesisof compound **82**.

3.2.3.3 Synthesis of NB-DNJ derivatives with mono β-substitution (compounds 85x and 87x)

According to the retrosynthetic approach proposed in Scheme 48, compounds **85x** would be obtained from debenzylation of compounds **84x**. For the synthesis of compounds **(*R*)-84x** and **(*S*)-84x**, we proposed two different approaches: on one hand by reduction of the carbonyl group in **80**, a compound obtained for the synthesis of difluorinated derivative **82**; and in the other hand by regioselective opening of the desired enantiomer of 2-ethyloxyrane (**83x**) in presence of **13**. Moreover, compounds **86x** would be obtained by fluorination on the position of the free hydroxyl groups of compounds **84x**, and posterior debenzylation of the protected ones.

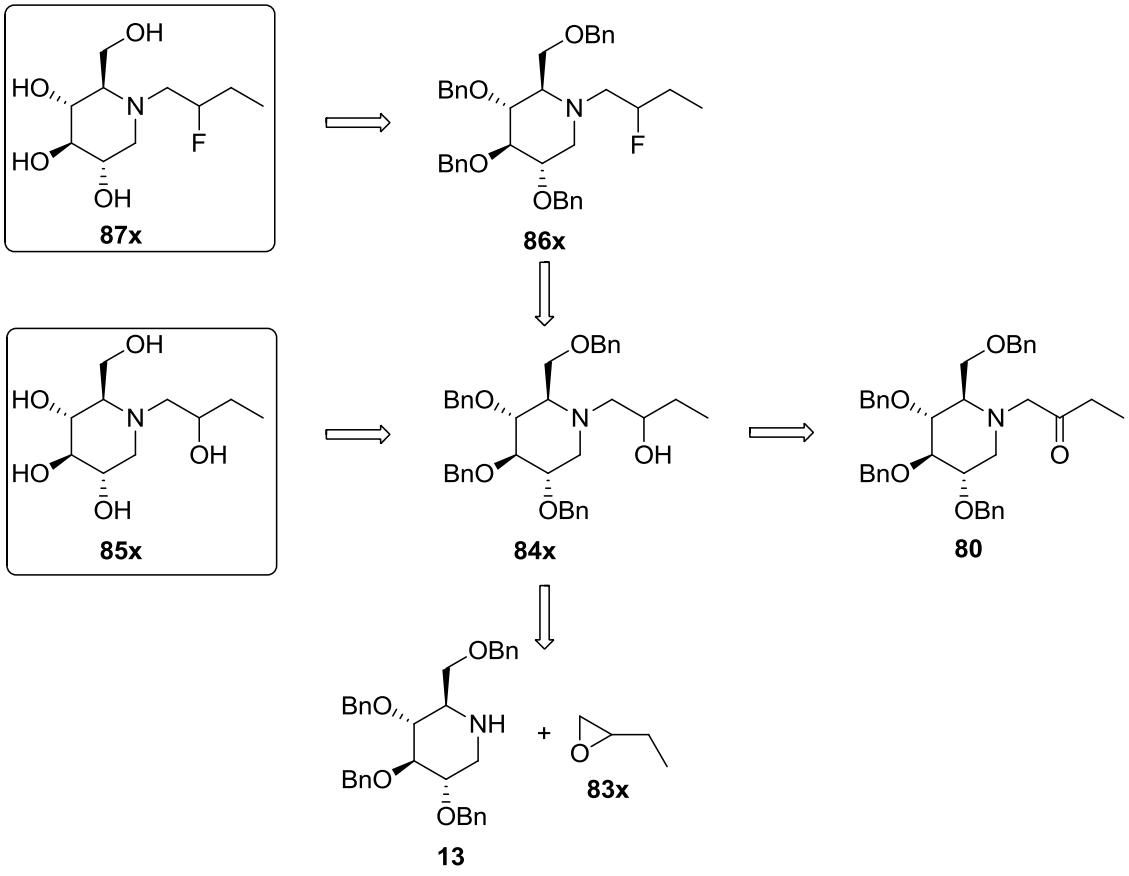

Scheme 48 Proposed retrosynthesis for compounds **85x** and **87x**.

All interactions between a potential inhibitor of an enzyme and this enzyme can contribute to their affinity and thus to the inhibitory capacity of those compounds. Although we did not expect strong differences in the pK_a of the amine depending on the configuration of the hydroxyl or fluorine group introduced in the chain of the DNJ derivatives, the configuration *R*

or *S* of those substituents can confer different affinities for enzyme binding site due to possible different interactions. For this reason, in this section we describe the work done for the synthesis of the diastereomeric derivatives with opposite configurations in the substituents of the alkyl chain.

Thus, as shown in Scheme 49, reduction of ketocompound **80** with $NaBH_4$ gave a mixture of diastereomeric hydroxylated compounds that were separated by flash chromatography, giving **(*R*)-84x** (32% yield) and **(*S*)-84x** (26% yield).

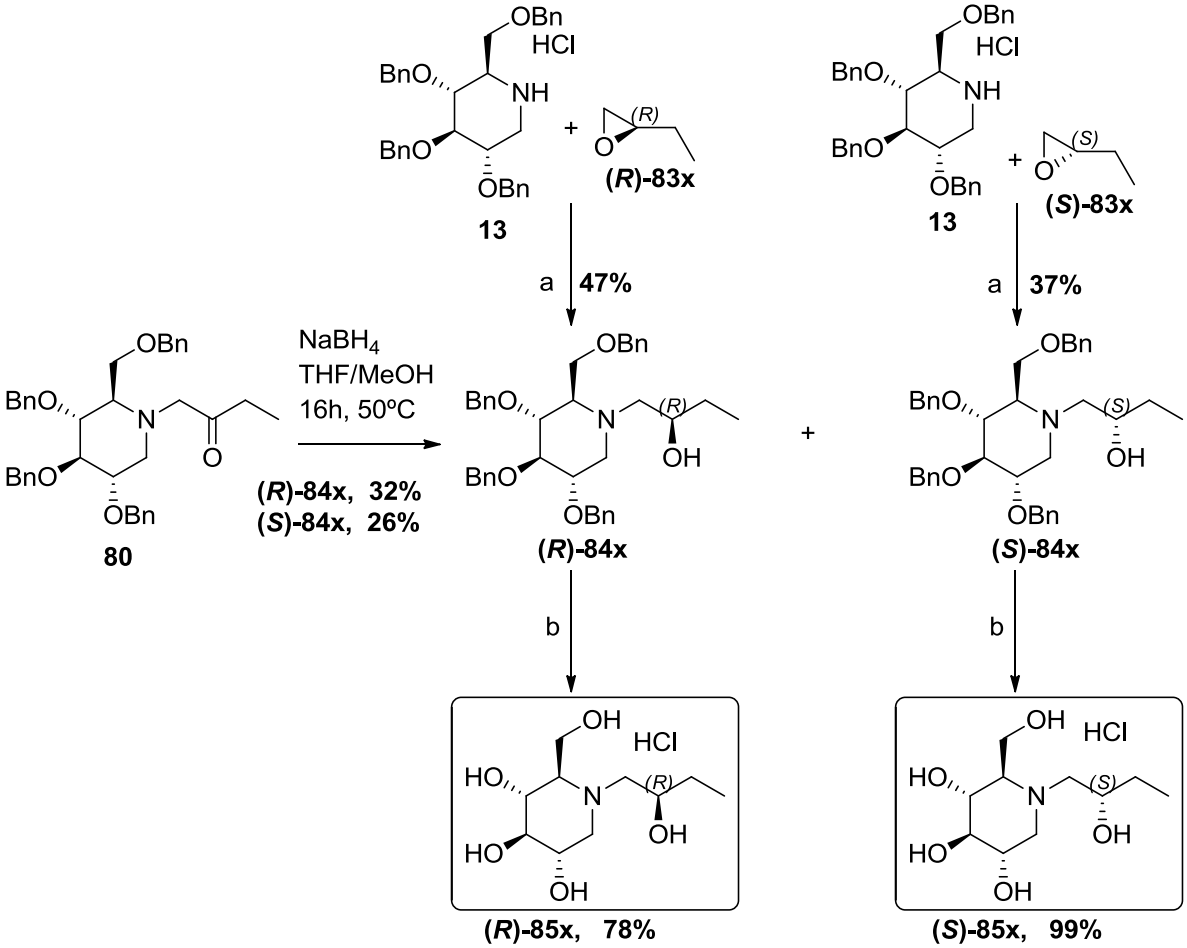

Scheme 49 Synthesis of compounds **84x** and **85x**.[a] $LiClO_4$, ACN, 16h, 80ºC; [b] $Pd(OH)_2/C$, THF/MeOH 1:1, HCl_{aq}, 16h, rt.

Furthermore, synthesis of **(*R*)-84x** and **(*S*)-84x** was also tried by regioselective epoxide aperture of the corresponding 2-ethyloxyranes (**(*R*)-83x** or **(*S*)-83x**) with amine **13** in presence of $LiClO_4$. In this case, **(*R*)-84x** and **(*S*)-84x** were obtained with moderate yield (47% and 37%

respectively). Moreover, the use of the enantiomeric epoxides allowed to unambiguously assigning the stereochemistry of the compounds obtained in the reduction of **80**.

Then, compounds **(*R*)-84x** and **(*S*)-84x** were submitted to hydrogenation catalyzed with $Pd(OH)_2/C$ under strong acidic conditions, to give the desired debenzylated compounds **(*R*)-85x** and **(*S*)-85x** with good yields (78% and 99% respectively).

On the other hand, following the previously described retrosynthetic approach for synthesis of fluoroderivatives **87x**, compounds **84x** were submited to a fluorination with Deoxofluor®. In this case, fluorination takes place with inversion of the configutation and the diastereomeric fluorides were obtained in moderate yields. Thus, fluoroderivative **(*S*)-86x** was produced in 52% yield starting from alcohol **(*R*)-84x** (Scheme 50). Similarly, **(*R*)-86x** was obtained (41% yield), starting from **(*S*)-84x**. Further deprotection of the benzylated hydroxyl groups by catalyzed hydrogenation in acidic conditions gave the desired compounds **(*S*)-87x** and **(*R*)-87x** with good yields (100% and 78% respectively).

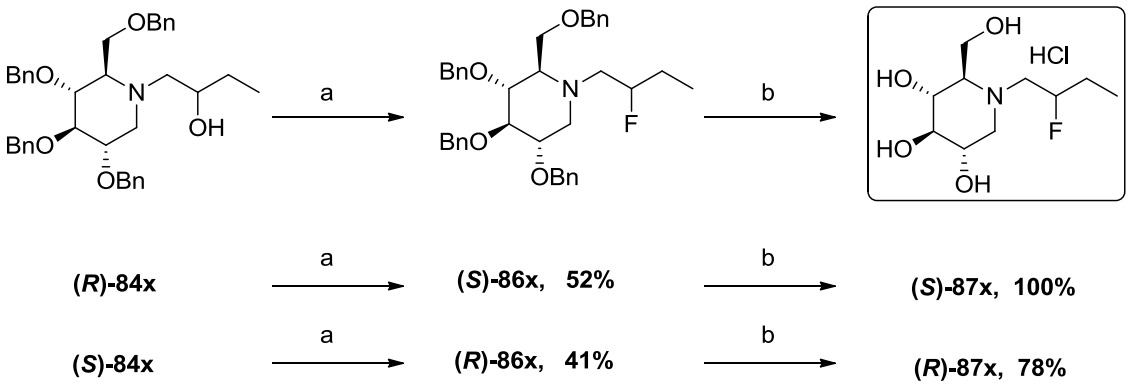

Scheme 50 Synthesis of compounds **86x** and **87x**. [a] Deoxofluor®, DCM, 16h, rt. [b] $Pd(OH)_2/C$, THF/MeOH 1:1, HCl_{aq}, 16h, rt.

3.2.3.4 Synthesis of NB-inositol derivatives with mono β-substitution (compounds 89x and 91x)

As shown in Scheme 51, for the synthesis of compounds **89x** and **92x**, we proposed a retrosynthetic approach similar to the one that we followed for synthesis of the DNJ derivatives. Thus, compounds **89x** and **92x** would be obtained after debenzylation of the alcohol and fluorinated derivatives (**88x** and **90x** respectively). The derivative **90x** is expected to be obtained by fluorination of compound **88x**. It should be noticed that, unlike DNJ

derivatives, compound **88x** possess two free hydroxyls susceptible to be substituted by a fluorine group. We expect that only the hydroxyl group located in the chain would be substituted, due to the steric hindrance present in the inositol cyclohexane core. Even so, if part of **88x** suffers the double fluorination, the difluorinated by-product **91x** would also be interesting to test as GCase inhibitor. For this reason we decided not to protect the free hydroxyl group in the inositol core at this point.

On the other hand, the derivatives with hydroxyl substitution in the chain (compounds **88x**) would be obtained by epoxide aperture of enantiomerically pure ethyloxyranes in order to obtain the derivatives with *R* and *S* configuration of the substituted carbon, in a similar way used for synthesis of compounds **84x**.

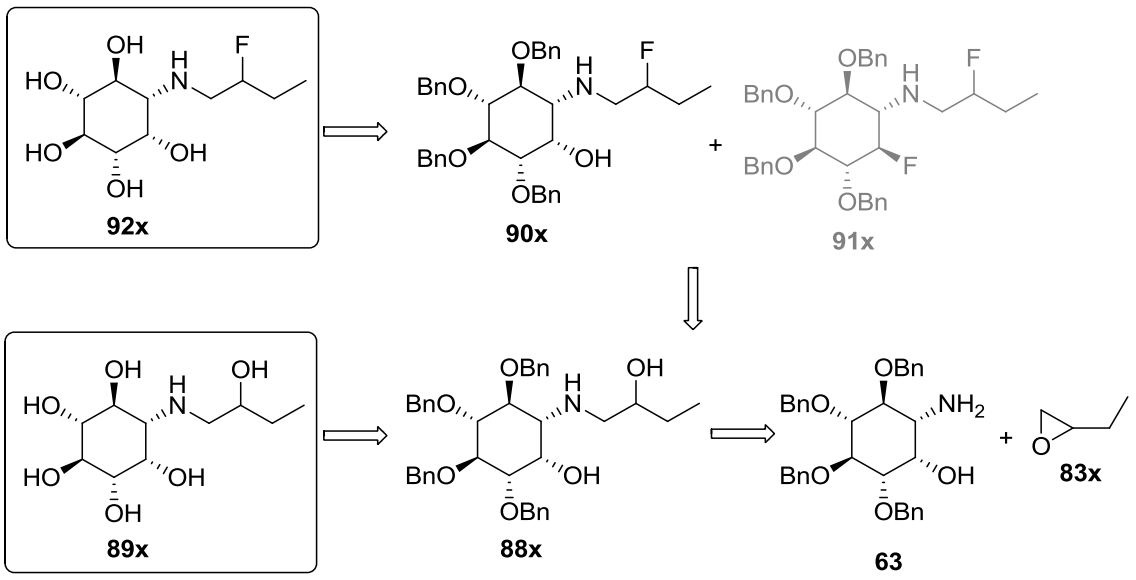

Scheme 51 Retrosynthetic approach for synthesis of compounds **89x** and **92x**.

Thus, as shown in Scheme 52, compound **(*R*)-88x** was obtained with low yield (20%) by (*R*)-2-ethyloxyrane (**(*R*)-83x**) with **63**, in presence of $LiClO_4$. A posterior catalyzed hydrogenation under acidic conditions provided the deprotected compound **(*R*)-89x** with good yield (75%). In the same way, compounds **(*S*)-88x** (26% yield) and **(*S*)-89x** (quantitatively) were obtained starting from (*S*)-2-ethyloxyrane **(*S*)-83x.**

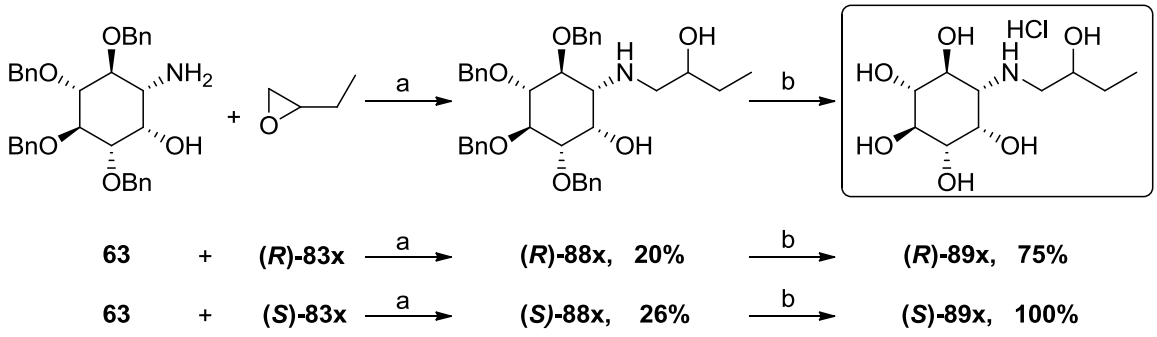

Scheme 52 Synthesis of compounds **88x** and **89x**.[a] $LiClO_4$, ACN, 16h, 80ºC; [b] $Pd(OH)_2/C$, THF/MeOH 1:1, HCl_{aq}, 16h, rt.

Unfortunately, when the fluorination with Deoxofluor® was tried in the same conditions that were previously used for DNJ derivatives, it seemed that it was obtained a complex derived from inositol core and deoxofluor derivative that remained soluble in the aqueous phase and was not further characterized. Neither compounds **88x**, **90x** or **91x** were detected (Scheme 53). Further modifications of the reaction conditions (proportions of reactants, temperature, time of reaction...) did not give better results.

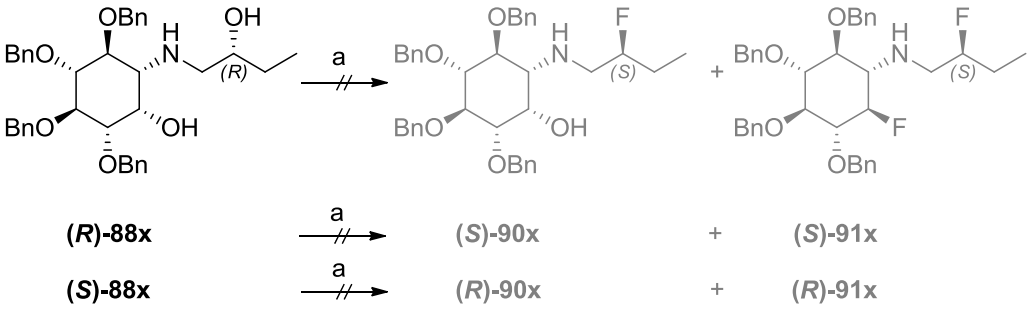

Scheme 53 Attempt of synthesis of compounds **91** and **91**.[a] Deoxofluor®, DCM.

At this point, we decided not to synthesize compounds **92x** before analyzing the GCase inhibition of the compounds already obtained in this section. Should these inhibitors be tested and the data analyzed, we will decide to try again to synthesize derivatives **92x** under different conditions or, alternatively, define if other derivatives are expected to be more interesting.

3.2.4 Imiglucerase inhibition assay and pK_a determination

In order to evaluate the potential chaperone activity of the compounds obtained in this section, they were tested as imiglucerase inhibitors at pH 5.2 and pH 7 as explained in the previous part (data shown in Table 6).

Moreover, in order to study a potential relationship between the pK_a of the inhibitors and the difference of their inhibitory capacity depending on the pH of the assay, we also tried to determine experimentally the pK_as of these compounds. In some cases (compounds **67x**, **68x**, **68y** and **(*R*)-89x**) pK_a values could not be determined because the amount of sample was not enough to carry out the titration and properly evaluate the end point. Even though, in the case of **67x** and **(*R*)-89x** we expect thatis reasonable their pK_a values would be similar to the respective nonyl derivative **67y** and *S*-hydroxybutyl inositol derivative **(*S*)-89x**.

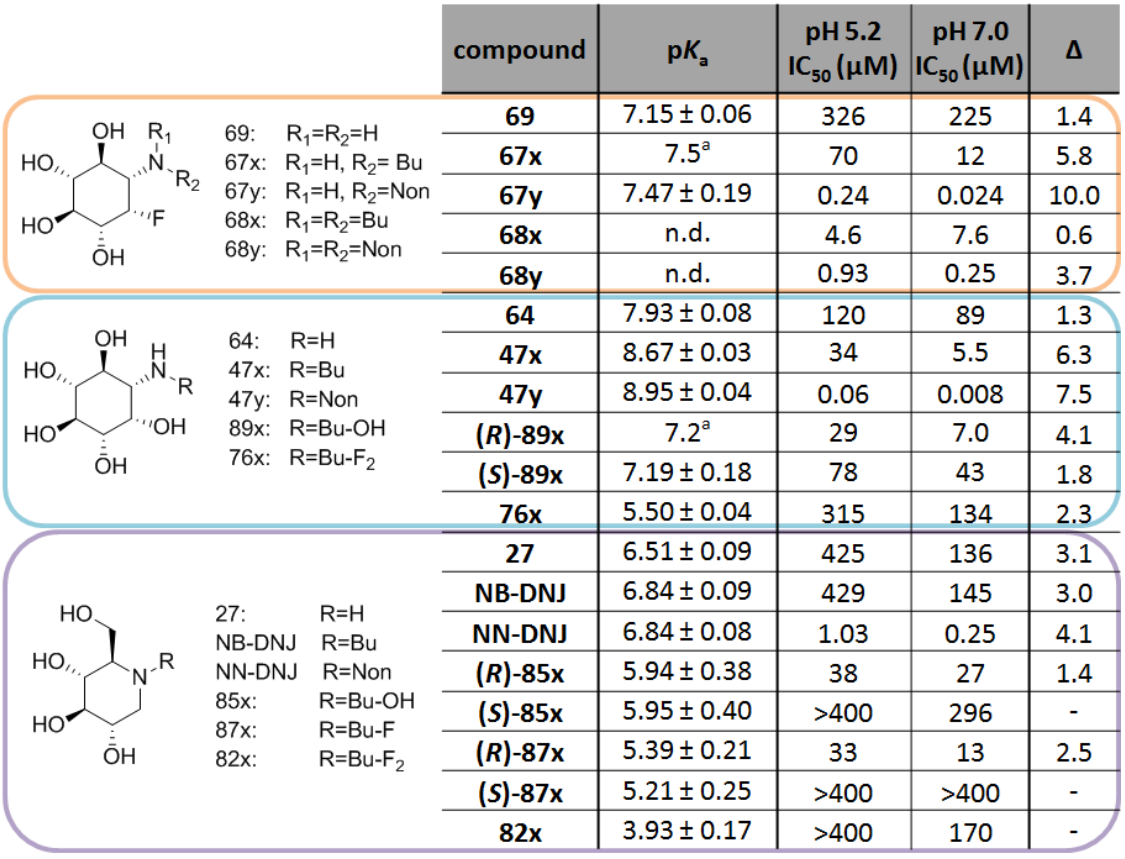

compound	pK_a	pH 5.2 IC_{50} (µM)	pH 7.0 IC_{50} (µM)	Δ
69	7.15 ± 0.06	326	225	1.4
67x	7.5[a]	70	12	5.8
67y	7.47 ± 0.19	0.24	0.024	10.0
68x	n.d.	4.6	7.6	0.6
68y	n.d.	0.93	0.25	3.7
64	7.93 ± 0.08	120	89	1.3
47x	8.67 ± 0.03	34	5.5	6.3
47y	8.95 ± 0.04	0.06	0.008	7.5
(*R*)-89x	7.2[a]	29	7.0	4.1
(*S*)-89x	7.19 ± 0.18	78	43	1.8
76x	5.50 ± 0.04	315	134	2.3
27	6.51 ± 0.09	425	136	3.1
NB-DNJ	6.84 ± 0.09	429	145	3.0
NN-DNJ	6.84 ± 0.08	1.03	0.25	4.1
(*R*)-85x	5.94 ± 0.38	38	27	1.4
(*S*)-85x	5.95 ± 0.40	>400	296	-
(*R*)-87x	5.39 ± 0.21	33	13	2.5
(*S*)-87x	5.21 ± 0.25	>400	>400	-
82x	3.93 ± 0.17	>400	170	-

Table 6 Experimental pK_a (mean ± standard deviation of three determinations) and inhibition of imiglucerase. IC_{50} (µM) values for tested compounds, at pH 5.2 and pH 7, and relationship of the difference of the values obtained at both pH (Δ= IC_{50} (pH 5.2, µM) / IC_{50} (pH 7, µM)). [a]predicted pK_a values.

After analyzing the pK_a and Δ values from Table 6, we could not establish a direct correlation between these two parameters. In some cases, compounds that were expected to have similar pK_a (for example when comparing **(*R*)-89x** and **(*S*)-89x** or comparing **67x** and **67y**), the Δ value of those compounds were quite different.

Moreover, compounds **(*S*)-85x** and **(*S*)-87x** and **82x** presented low GCase affinity and we could not determine the IC_{50} values and therefore the parameter Δ could not be established to analyze the difference of affinity for the enzyme at pH 5.2 and pH 7.0.

Interestingly, compound **67y** showed highest difference of inhibitory capacity according to the pH of the assay among the tested compounds, showing an IC_{50} value 10 times lower when the assay was performed at pH 7.0 than when it was carried out at pH5.2.

Regarding to the potency, when comparing the different cores, in the case of inositol and F-inositol cores, the introduction of a butyl chain (compounds **47x** and **67x**) increased considerably the potency as GCase inhibitor with respect to compounds without this alkylation (compounds **64** and **69** respectively). Instead, NB-DNJ has IC_{50} values similar to **27**, showing no differences in this core between the compound with or without N-butyl substitution in terms of potency of inhibition.

It must be highlighted that, in concordance with previous studies[124], the nonyl derivatives were more potent inhibitors than the corresponding butyl derivatives for the three cores. For this reason, it could be interesting to synthesize the NN-DNJ derivatives with β-substitution in the chain (homologues to compounds **85x** and **87x**), in order to analyze if compounds with similar pK_a would show the same difference of activity according to the pH of the assay.

It must be noticed that the introduction of a β-subtituent with *R* configuration in the chain of NB-DNJ (both in the case on a hydroxyl group or a fluorine substitution) conferred to the new compound an increase of its capacity of inhibit GCase. Thus, compounds **(*R*)-85x** and **(*R*)-87x** showed IC_{50} values around ten times lower than the IC_{50} values for NB-DNJ at both pH. On the contrary, the GCase inhibitory capacity of compounds with β-subtituent with *S* configuration (compounds **(*S*)-85x** and **(*S*)-87x**) is similar or even lower than NB-DNJ. In addition, in the case of compound **82x**, with fluorine disubstitution, it showed similar inhibition than NB-DNJ.

On the other hand, inositol derivatives with β-subtitution also presented different inhibitory potencies depending on the configuration of this substitution. In this case, **(*R*)-89x** showed

similar activity its homologous without β-subtitution (**47x**) while the derivative with *S* configuration (**(*S*)-89x**) seemed to have lower affinity for GCase enzyme.

The fact that subtituents in *R* configuration could confer extra inhibitory capacity to the compounds, together with the fact that nonyl derivatives are better GCaseinhibitors than the butyl ones, made even more interesting the synthesis and study of nonyl derivatives with β-subtitution. Thus, we decided to try to synthesize the nonyl derivatives **85y**, **87y** and **89y** (Fig. 36) with both configurations in order to**,** on one hand, to obtain a more complete set of data for the analysis of the potential relationship between the pK_a of the inhibitor and the difference of activity according to the pH of the assay and, in the other hand, to see if this increase of inhibitory capacity with the introduction of a β-subtituent with *R*configuration that we saw for butyl derivatives is translated to the nonyl derivatives, providing some of the most potent DNJ-based GCase inhibitors.

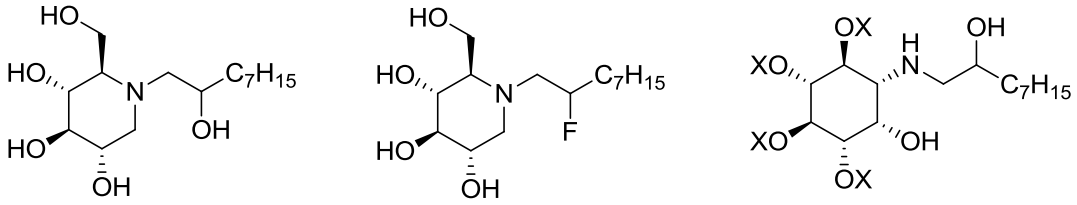

Figure 36 Proposed *N*-nonyl derivatives with β-substitution in the alkyl chain.

3.2.5 Synthesis and evaluation of β-substituted *N*-nonyl derivatives

Synthesis of β-substituted N-nonyl derivatives was afforded similarly to the butyl ones, via epoxide ring aperture, substitution of the hydroxyl group by a fluorine atom, and posterior debenzylation of all the β-substituted compounds (Scheme 54).

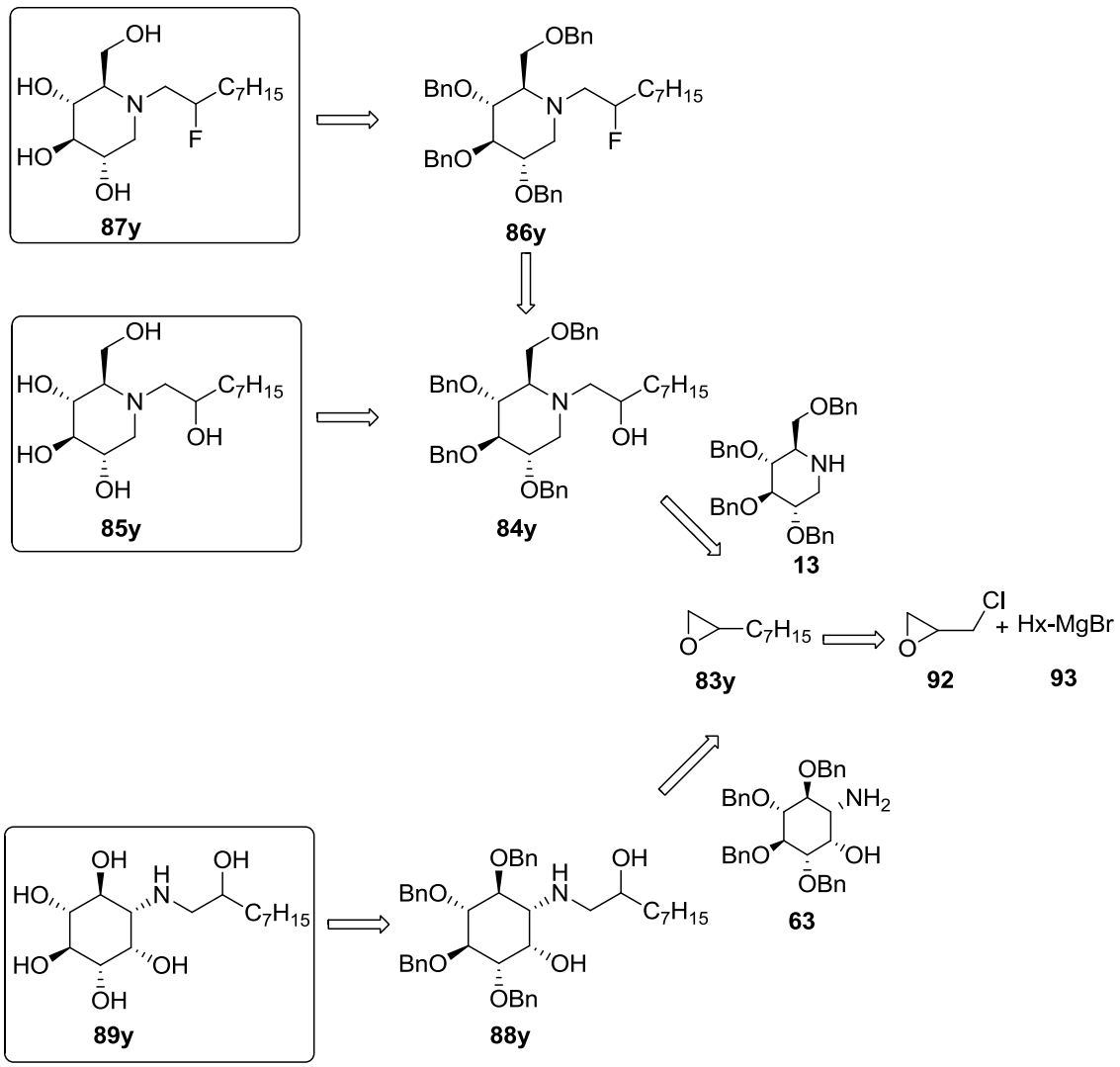

Scheme 54 Retrosynthetic approach for synthesis of nonyl derivatives **85y**, **87y** and **89y**.

In this ocasion, the corresponding epoxides (**(*S*)-83y** and **(*R*)-83y**) were not commercially available and were synthesized by copper-catalyzed epoxide ring-opening with Grignard reagent and posterior formation of a new epoxide by elimination of the chlorine moiety in strong basic media.

Thus, as shown in Scheme 55, the corresponding epichlorohydrin (**(*S*)-92** or **(*R*)-92**) was treated with hexylmagnesium bromide in presence of CuI(I) that act as a catalyst and compounds **94** were obtained with moderate yields (32% for **(*S*)-94** and 29% for **(*R*)-94**). Then, the chloroalcohol derivatives **94** were treated overnight with finely powdered NaOH to form the desired heptyloxiranes **(*S*)-83y** (49% yield) and (***R*)-83y** (47% yield).

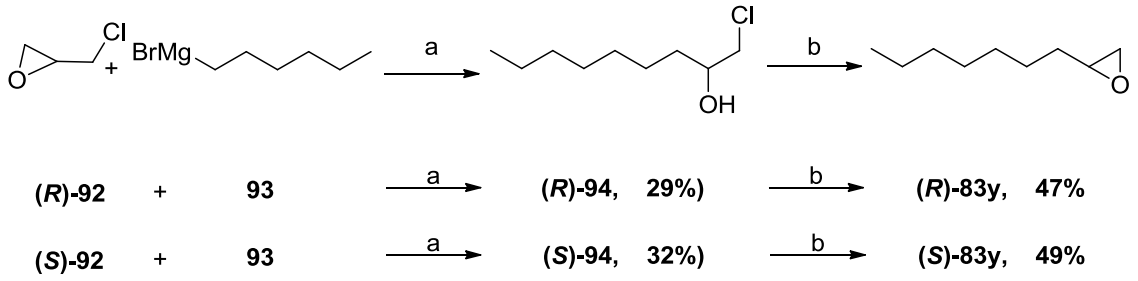

Scheme 55 Synthesis of compounds**83y**.[a] Et_2O/THF, CuI(I), -78ºC to 0ºC, 4h. [b] NaOH, Et_2O, 16h, rt.

Thus, following the methodology described for the DNJ butyl derivatives, the compounds with hydroxyl substitution in the chain (**(*R*)-84y** and **(*S*)-84y**) were obtained with moderate yield by ring opening aperture of the heptyloxiranes with **13**, in presence of $LiClO_4$. Then, part of those compounds was treated with Deoxofluor® to give the fluorinated derivative with inversion of configuration with moderate yield. Both compounds with hydroxyl and fluorine substitution in the chain were submitted to catalyzed hydrogenation to obtain the deprotected compounds **85y** and **87y** with excellent yield (Scheme 56).

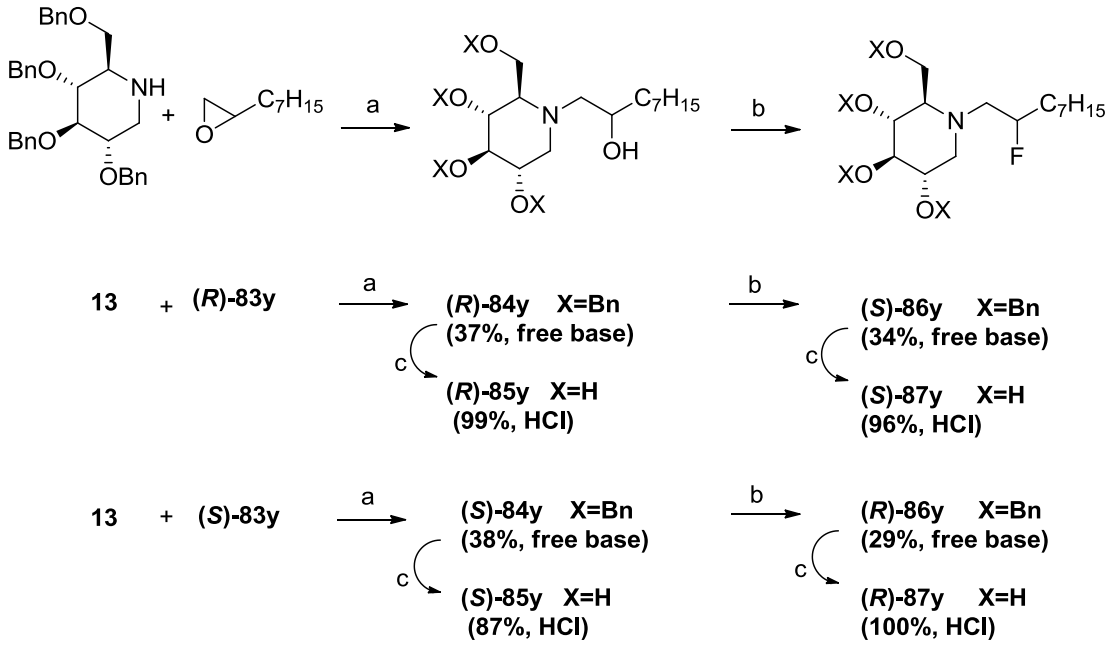

Scheme 56 Synthesis of compounds**85y** and **87y**.[a]ACN, $LiClO_4$, 50ºC, 16h. [b]Deoxofluor®, DCM, 2h, rt.[c] 1.5atm H_2, $Pd(OH)_2$/C, HCl_{aq}, THF/MeOH 1:1.

Similarly, inositol derivatives **(*R*)-88y** and **(*S*)-88y** were obtained with good yield from epoxide ring opening of the corresponding heptyloxirane with **63** (Scheme 57). The deprotection of the

hydroxyl groups by catalyzed hydrogenation in acidic conditions gave the desired compounds **(*R*)-89y** and **(*S*)-89y** with excellent yields (87% and 91% respectively).

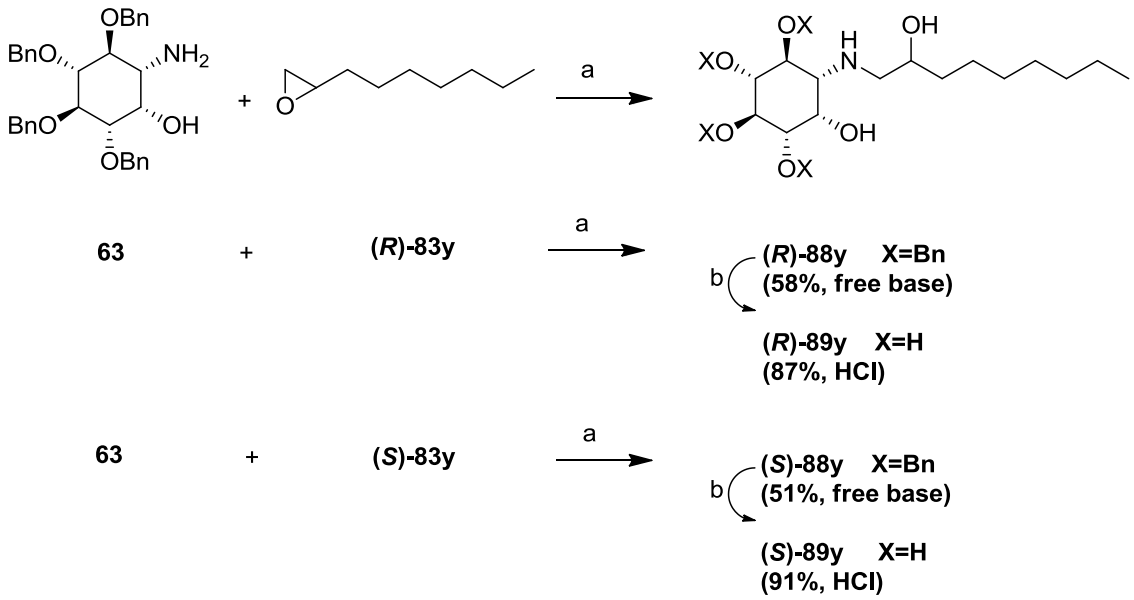

Scheme 57 Synthesis of compounds **89y**. [a]ACN, $LiClO_4$, 50ºC, 16h. [b] H_2, $Pd(OH)_2/C$, HCl_{aq}, THF/MeOH 1:1.

Then, the compounds synthesized in this section were tested as imiglucerase inhibitors, both at pH 5.2 and 7.0, with the assay previously explained, in presence on sodium taurocholate and Triton X-100. Moreover, their pK_a values were also experimentally determined by titration with NaOH (data shown in Table 7).

	compound	pK_a	pH 5.2 IC_{50} (μM)	pH 7.0 IC_{50} (μM)	Δ
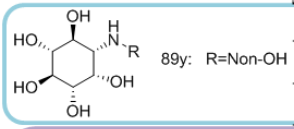 89y: R=Non-OH	**47y**	8.95 ± 0.04	0.065 ± 0.004	0.0075 ± 0.0003	7.5
	(*R*)-89y	7,22[a]	0.11 ± 0.01[a]	0.017 ± 0.001[a]	6.5
	(*S*)-89y	7,17[a]	2.12 ± 0.26[a]	0.244 ± 0.006[a]	8.8
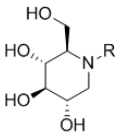 85y: R=Non-OH 87y: R=Non-F	**NN-DNJ**	6.84 ± 0.08	1.03 ± 0.12	0.25 ± 0.02	4.1
	(*R*)-85y	5.98 ± 0.11	0.078 ± 0.004	0.045 ± 0.003	1.7
	(*S*)-85y	5.94 ± 0.04	2.10 ± 0.15	1.23 ± 0.13	1.5
	(*R*)-87y	5,2[b]	5.90 ± 0.25	6.7 ± 0.60[a]	0.9
	(*S*)-87y	5.16 ± 0.10	2.94 ± 0.14	4.94 ± 0.45	0.6

Table 7 Experimental pK_a (mean ± standard deviation of three determinations) and inhibition of imiglucerase. IC_{50} (μM) values for tested compounds, at pH 5.2 and pH 7.0, and relationship of the difference of the values obtained at both pH (Δ= IC_{50} (pH 5.2, μM) / IC_{50} (pH 7.0, μM)). Three independent assays with triplicates. [a]single determination with triplicates. [b] predicted value.

Regarding to pKa, similarly to the previously analyzed butyl derivatives, no clear correlation between the pKa and Δ values was appreciated.

On the other hand, with reference to the potency, in the case of DNJ derivatives **(*R*)-85y**, **(*S*)-85y**, and **(*S*)-87y**, the first one showed an increase of inhibitory capacity showing IC_{50} values approximately one log lower than the corresponding DNJ derivative without β-substitution, while the two derivatives with *S* configuration (both with hydroxyl or fluorine β-substitution) possess less GCase affinity than NN-DNJ, similarly to what was previously observed for the DNJ-butyl derivatives. Surprisingly, the fluoro-derivative with *R* configuration (**(*R*)-87y**) presented higher IC_{50} values higher than NN-DNJ and **(*S*)-87y**, on the contrary of what was observed when comparing the corresponding butyl derivatives **(*R*)-87x** and NB-DNJ.

For the inositol derivatives, **(*R*)-89y** showed similar activity than the corresponding derivative without β-substitution (**47y**) while the derivative with β-hydroxyl substitution with *S* configuration **(*S*)-89y** showed lower GCase affinity, as was observed with the corresponding butyl derivatives.

It must be highlighted that compound **(*R*)-85y** is one of the most potent GCase inhibitor described so far from the family of DNJ. This increase of potency when a hydroxyl group with *R* configuration was introduced in this position was also observed for the butyl derivative **(*R*)-85x** but not in the case of inositol derivatives **(*R*)-89x** or **(*R*)-89y**, suggesting that this β-hydroxyl substitution with *R* configuration can play an important role in the affinity of DNJ derivatives for imiglucerase binding site, but not in the case of inositol derivatives.

3.2.6 Global analysis of pK_a and Δ values

In this chapter we were able to synthesize a small library of compounds with similar structure and a wide range of pK_as, as it was one of the aims of this thesis. The pK_a of the amine in the sugarmimethic core was modulated by introduction of different substituents in the β-position in the alkylic chain.

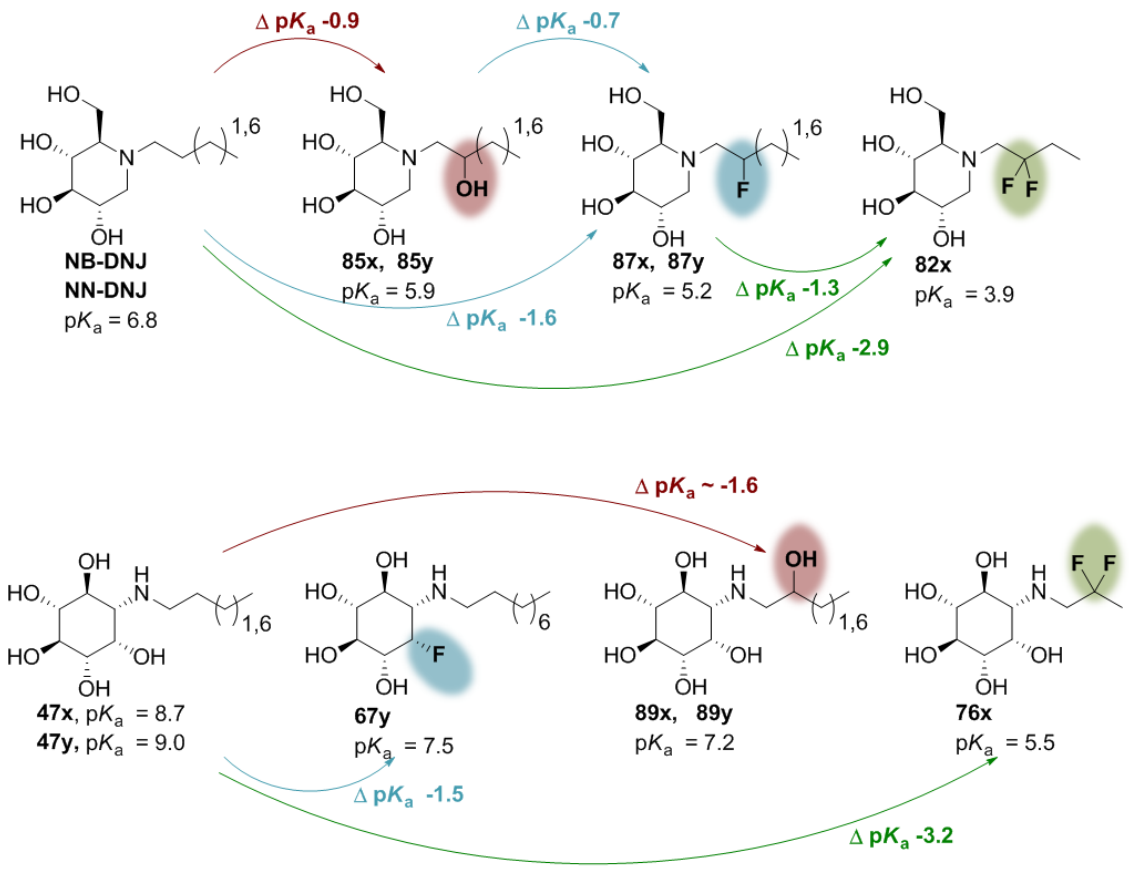

Figure 37 Influence of different β-substituents on the pK_a.

Thus, as shown in Fig. 37, the introduction on a hydroxyl group in the β-position for DNJ derivatives (compounds **(*R*)-85x**, **(*S*)-85x**, **(*R*)-85y** and **(*S*)-85y**), decreased in less of one unit the pK_a value of both *N*-butyl and *N*-nonyl DNJ compounds. When the unity introduced was a fluorine atom (compounds **(*R*)-87x**, **(*S*)-87x** and **(*S*)-87y**), the pK_a was reduced in 1.6 units with respect to the derivatives without β-substitution. The introduction of a second β-fluorine atom (compound **82x**) showed an effect a bit lower than two times the effect of adding one fluorine (pK_a of compound **82x** was 2.9 units lower than NB-DNJ pK_a). It must be highlighted than the assayed DNJ derivatives with the same β-substitution showed similar pK_a values, independently of the configuration of the stereocenter (*R* or *S*) and the length of the chain (butyl or nonyl). In this way, a group of DNJ derivatives with similar structure and different pK_a values (range of pK_a between 3.9 and 6.8) was obtained by introduction of a β-substitution in the side chain.

Although in the case of inositol derivatives the compounds with a β-hydroxyl substitution (compounds **(*S*)-89x**, **(*R*)-89y** and **(*S*)-89y**) showed similar pK_a values (7.2), it should be noticed that the pK_a of the β-substituted inositol derivatives was approximately 1.6 units lower than the corresponding compounds without the β-substitution, while as explained before, in the case of DNJ derivatives the pK_a value was diminished in 0.9 units (Fig. 37). Thus, the influence of introducing this hydroxyl group in inositol derivatives was stronger than in the case of the DNJ derivatives. In contrast, the influence of the introduction of two fluorine atoms has a similar influence for both cores decreasing the pK_a values in 3.2 units for inositol derivatives and 2.9 units for DNJ derivatives.

Taking into account these results, it seems feasible to assume that the pK_a values for compounds **(*R*)-89x** and **(*R*)-87y** would be similar to other compounds with similar structure. Thus, pK_a for **(*R*)-89x** would be around 7.2 and for **(*R*)-87y** around 5.2.

Interestingly, as shown in Fig. 37, the substitution of the hydroxyl group in the C-2 position in the ring by a fluorine atom (compound **67y**) showed similar influence in the pK_a of the amine than the introduction of a hydroxyl substitution in the side chain of the inositol derivative (compounds **(*R*)-89y** and **(*S*)-89y**). In this way, we obtained compounds with different cores (inositol and fluoro inositol), chain lengths (butyl and nonyl) and chain substitution (with or without hydroxyl substitution in the side chain) and similar pK_a values (between 7.2 and 7.5).

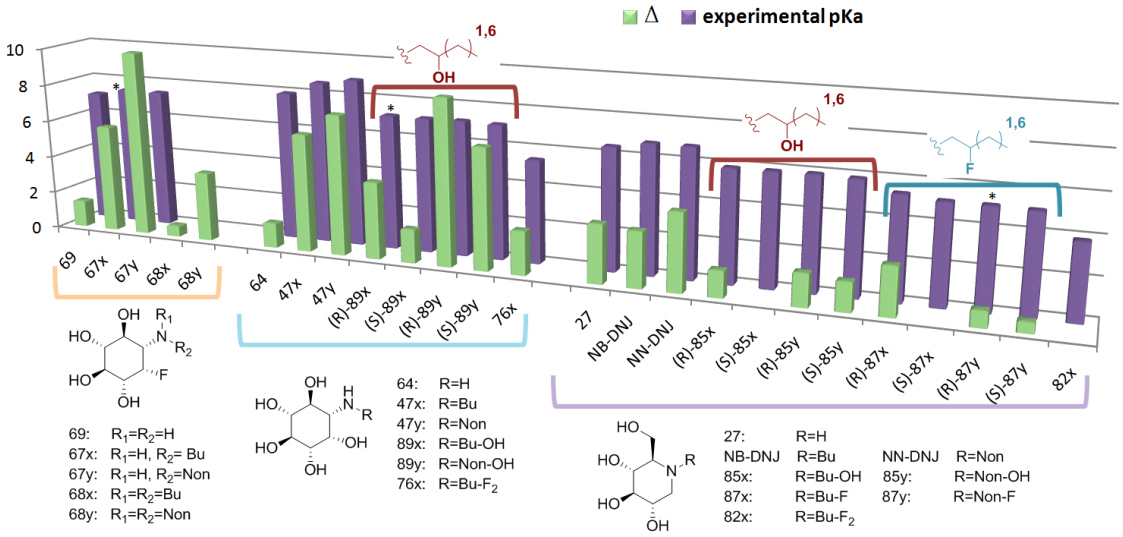

Graphic 6 Comparative of experimental pK_a values (purple) and Δ (green) as the difference of IC_{50} values against imiglucerase at pH 5.2 and 7.0 (Δ= IC_{50} (pH 5.2, μM) / IC_{50} (pH 7.0, μM)).(* predicted p$K_a$values.)

Regarding the difference of GCase affinity depending on the pH of the assay (Δ), it must be noticed that most of the assayed compounds showed higher GCase affinity at pH 7.0 than 5.2 under this assay conditions; the exceptions were the *N*-butyl fluoroinositol **68x** and the fluorononyl DNJ derivatives **(*R*)-87y** and **(*S*)-87y**.

A global analysis of data presented in Table 6 and Table 7 (Graph. 6), showed that the higher differences on GCase affinity between when the assay was performed at pH 5.2 or 7.0 (Δ) were observed in the case of inositol (blue) and F-inositol (orange) derivatives, while DNJ derivatives (purple) showed, in general, lower values. Moreover, it should be noticed that the nonyl derivatives that could be compared, presented higher Δ values than the corresponding derivatives with shorter chain, except **(*R*)-87y**.

Unfortunately, it seems that those differences in activity according to the pH are not directly governed by the pK_a of the inhibitor, as compounds with similar structure and pK_a (for example comparing compounds **(*R*)-89x**, **(*S*)-89x**, **(*R*)-89y**, **(*S*)-89y**) showed very diverse Δ values.

Susprisingly, when analyzing the compounds with higher Δ values (compounds **(*R*)-89y**, **(*S*)-89y**, **67y**, **47y** and **47x**), all of them have pK_a between 7.2 and 8.9, pK_a values much higher than the ones that we would expect to be optimal to confer the maximal difference of potency to the inhibitors, according to the pH of the assay (pK_as between 5.2 and 7.0).

However, data obtained in this chapter are in concordance with the study realized by López *et al*. in 2013[156], analyzing the binding of different inhibitors with almond and *Thermotoga maritima* (TmGH1) β-glucosidases. López *et al*. described that in most cases the binding between the enzyme and the inhibitor takes place as Enzyme-Inhibitor-H (EHI) complex, meaning that only one proton is shared between the two catalytic glutamates and the basic amine in the core of the iminosugar while the unprotonated or diprotonated complex (EI and EH_2I respectively) are not usual.

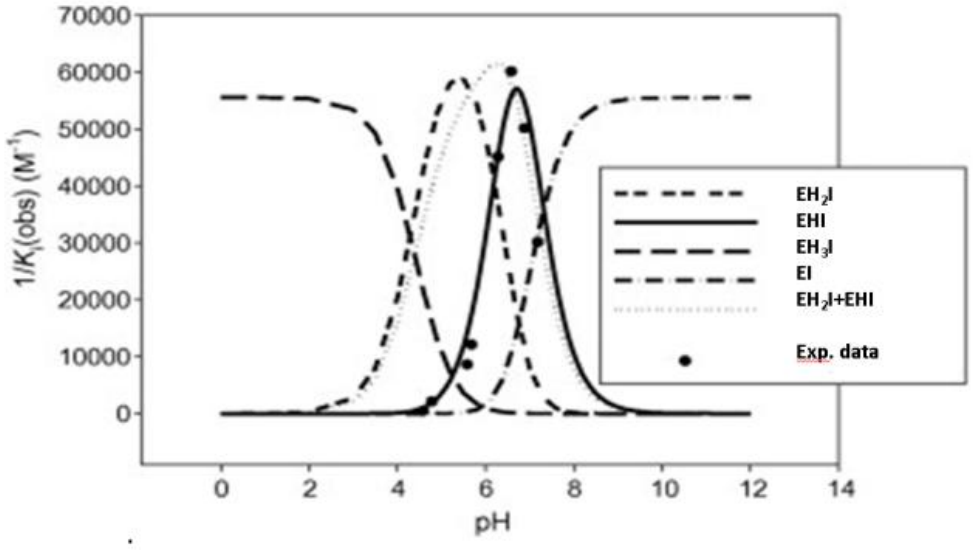

Figure 38 Predicted curves for binding of DNJ (**27**) to almond β-glucosidase with either EH_3I (– –), EH_2I (--), EHI (—), EI (-·-) or a mixture of EH_2I and EHI (···) being the predominant complex. The experimental data fit a EHI complex curve. Figure adapted from Lopez *et al*[156].

This EHI complex could potentially be formed by at least two routes: either the unprotonated inhibitor I binding to the monoprotonated enzyme EH, or by protonated inhibitor IH binding to unprotonated enzyme E. Thus, the ionization state of the amine of the sugar mimetic core (and therefore its pK_a) seemed to have a high influence on the affinity for GCase. López *et al*. proposed that the optimal inhibitor for a glycosidase at enzyme's optimum pH is a neutral inhibitor, while optimum inhibitor at pH values above this pH has a pK_a that approaches 2 x pH-pK_{aE2} (where pK_{aE2} is the pK_a of the catalytic carboxylate group with higher pK_a). This formula, together with the pK_a values for the catalytic glutamate residues that they determined, allowed us to calculate the optimal pK_a of an inhibitor to have the maximal inhibition at specific pH for our enzyme. As one of the aims of this thesis was to obtain compounds with higher inhibitory activity at pH 7.0 than at pH 5.2, it could be interesting to calculate which would be the optimal pK_a for a human GCase inhibitor at pH 7. As shown in Table 8, the optimal pK_a of an GCase inhibitor at pH 7 was calculated from the pK_a values of the glutamate residues described by Liou *et al*[39]**.** According to obtained data, it seems that a good GCase inhibitor at pH7 would have a pK_a between 7.1 and 7.7, depending on the GCase of study. Thus, it could be expected that compounds with pK_a around 7.2 would show higher affinity for GCase at pH 7 than at other pHs when tested in human-WT GCase or with N370S mutation, while the pK_a would be slightly higher (7.7) for assays performed with the recombinant enzyme imiglucerase. It should be noticed that Liou *et al.* were not able to determine the optimal pH

and the estimated pK_a of the catalytic glutamates for human-L444P GCase due to its instability. Thus, the optimal pK_a for a potential inhibitor at pH7 for this GCase could not be estimated by using this approach.

GCase	pH opt (enzyme) [b]	p$K_{a\ E1}$ [c]	p$K_{a\ E2}$ [c]	p$K_{a\ optinh}$ [d]
human-WT	5,6	4,7	6,7	**7,3**
human-N370S	5,6	4,6	6,9	**7,1**
human-L444P[a]	n.d.	n.d.	n.d.	n.d.
imiglucerase	5,6	4,7	6,3	**7,7**

Table 8 Optimal pH for different GCases, p$K_a$of their catalytic glutamate[39] and calculated optimal pK_a for an inhibitor for inhibition at pH 7.

[a]unstable; n.d.= not determined.

[b]determined by assay with citrate/phosphate buffers in presence of 0.25% sodium taurocholate and Triton X-100.

[c]estimated from enzyme optimal pH determination using a diprotic model approach.

[d]optimalpK_a for an inhibitor at pH 7, calculated as p$K_{aoptinh}$ = 2 x pH- pK_{aE2} =14-pK_{aE2}.

Thus, the fact that the optimal pK_a for a imiglucerase inhibitor at pH 7 calculated according Lopez et *al*.[156] and Liou *et al*[39] determinations was 7.7 could explain that the synthesized compounds with pK_a values around 6.0 did not show the expected difference of GCase affinity with regard to the pH of the assay. Thereby, this optimal pK_a value, higher than what we initially expected, could be related with the fact that in general, the higher differences of activity according to the pH of the assay have been showed in compounds with higher pK_as. Even though, these articles did not fully explain the experimental data obtained in this thesis, as it seems that there is no direct correlation between the pK_a or the compounds and the difference of GCase inhibition at pH 5.2 or 7.0.

3.2.7 Other biological assays

3.2.7.1 Inhibition of commercial glycosidases

In order to evaluate the selectivity of the synthesized compounds, they were also tested in front of other commercial glycosidases: α-glucosidase from S*accharomyces cerevisiae*, β-glucosidase from almond, α-galactosidase from green coffee beans, β-galactosidase from bovine liver, following the procedures described in *Chapter 3.1.* The obtained percentages of inhibition are shown in Table 9.

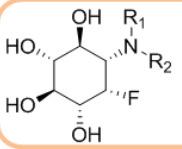

69: R_1=R_2=H
67x: R_1=H, R_2= Bu
67y: R_1=H, R_2=Non
68x: R_1=R_2=Bu
68y: R_1=R_2=Non

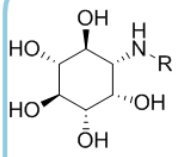

64: R=H
47x: R=Bu
47y: R=Non
89x: R=Bu-OH
89y: R=Non-OH
76x: R=Bu-F_2

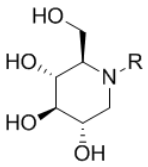

27: R=H
NB-DNJ R=Bu
NN-DNJ R=Non
85x: R=Bu-OH
85y: R=Non-OH
87x: R=Bu-F
87y: R=Non-F
82x: R=Bu-F_2

	% inh a 100 μM (IC_{50})			
	α-glucosidase	**β-glucosidase**	**α-galactosidase**	**β-galactosidase**
69	7 ± 10	-6 ± 7	5 ± 9	16 ± 1
67x	7 ± 9	27 ± 4	6 ± 3	19 ± 2
67y	2 ± 3	15 ± 1	-6 ± 5	63 ± 3
68x	34 ± 7	25 ± 4	75 ± 8	19 ± 3
68y	4 ± 3	-6 ± 8	-23 ± 29	35 ± 3
64	11 ± 16	-7 ± 8	12 ± 3	7 ± 5
47x	3 ± 4	0	1 ± 5	16 ± 4
47y	2 ± 6	0	-25 ± 27	6 ± 1
(*R*)-89x	-1 ± 4	2 ± 2	13 ± 6	12 ± 7
(*S*)-89x	7 ± 6	4 ± 4	10 ± 2	17 ± 4
(*S*)-89y	n.d.	n.d.	n.d.	n.d.
(*R*)-89y	n.d.	n.d.	n.d.	n.d.
76x	-4 ± 2	-4 ± 4	-4 ± 1	19 ± 13
27	40 ± 5	26 ± 2	35 ± 13	26 ± 4
NB-DNJ	7 ± 2	6 ± 5	6 ± 3	17 ± 3
NN-DNJ	11 ± 6	43 ± 5	-22 ± 15	50 ± 1
(*R*)-85x	18 ± 4	98 ± 1 (0.76 μM)	12 ± 16	43 ± 3
(*S*)-85x	19 ± 5	81 ± 1 (19.1 μM)	13 ± 2	26 ± 11
(*R*)-85y	13 ± 7	99 ± 1 (0.45 μM)	-19 ± 14	96 ± 1 (1.30 μM)
(*S*)-85y	1 ± 6	98 ± 1 (0.99 μM)	-9 ± 15	55 ± 5
(*R*)-87x	17 ± 4	17 ± 6	45 ± 19	23 ± 6
(*S*)-87x	4 ± 3	17 ± 5	4 ± 6	5 ± 5
(*R*)-87y	36 ± 3	39 ± 2	11 ± 6	30 ± 9
(*S*)-87y	5 ± 6	61 ± 5	-14 ± 21	45 ± 9
82x	4 ± 3	-1 ± 7	9 ± 10	24 ± 15

Table 9 Inhibiton of comercial glycosidases. Percentage of inhibition at 100 μM (mean ± standard deviation of at least two independent assays with triplicates). In brackets, IC_{50} values of the most potent inhibitors (single determination).

All the tested inositol derivatives (**64**, **47x**, **47y**, **(*R*)-89x**, **(*S*)-89x** and **76x**) as well as NB-DNJ presented percentages of inhibition of commercial glycosidases lower than 20% at 100 μM. Similarly, compounds without N-substitution **69** and **27** also showed low inhibition of commercial glycosidases, with values lower than 20% for the fluoro inositol core (**69**) and

between 30 and 40% for the DNJ core (**27**). The percentages of inhibition of the other compounds are represented in Graph. 7.

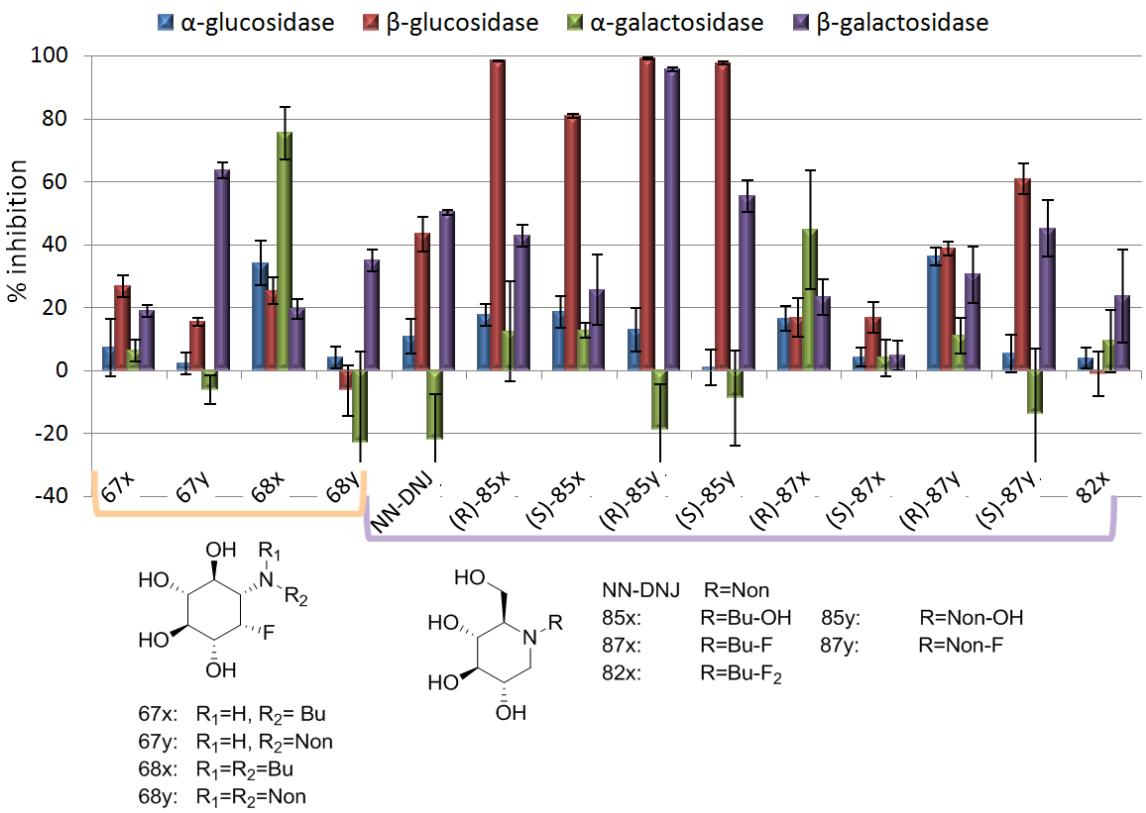

Graphic 7 Inhibition of commercial glucosidases (% inhibition of the enzyme when tested at inhibitor concentration = 100 µM. Mean and standard deviation of at least two independent assays with triplicates.

All compounds tested in this chapter also presented less than 40% of α-glucosidase inhibition at 100 µM. With regard to almond β-glucosidase, most of the compounds also presented low inhibition of this enzyme, except the fluorononyl DNJ derivative **(*R*)-87y** (61% if inhibition), and the DNJ derivatives with hydroxyl β-substitution in the side chain (compounds **(*R*)-85x**, **(*S*)-85x**, **(*R*)-85y** and **(*S*)-85y)**), whose percentages of inhibition were higher than 80%. The IC_{50} values against almond β-glucosidase were determined for these hydroxyl derivatives (Table 9). Only derivative **(*R*)-85y** showed moderate selectivity for imiglucerase in front of β-glucosidase from almond with IC_{50} against almond β-glucosidase of 0.45 µM, in front of IC_{50} values of 0.078 and 0.045 µM against imiglucerase at pH 5.2 and 7.0 respectively (Table 10). On the contrary, compounds **(*R*)-85x**, **(*S*)-85x** and **(*S*)-85y**), presented higher affinity for almond β-glucosidase

than for imiglucerase. Thus, these compounds did not show selectivity for imiglucerase in front of some other β-glucosidases.

	imiglucerase		almond β-glucosidase
compound	**pH 5.2 IC_{50} (μM)**	**pH 7.0 IC_{50} (μM)**	**IC_{50} (μM)**
(*R*)-85x	38	27	0.76
(*S*)-85x	>400	296	19.1
(*R*)-85y	0.078	0.045	0.45
(*S*)-85y	2.10	1.23	0.99

Table 10 Imiglucerase and β-glucosidase from almond inhibition.

In general, the compounds tested in this chapter exhibited low α-galactosidase inhibition rates. The exceptions were the dibutylfluoroinositol derivative **68x** (75% of inhibition at 100 μM) and the fluorobutyl DNJ derivative **(*R*)-87x** (45% of inhibition at 100 μM). Interestingly, all the nonyl derivatives except **(*R*)-87y** seemed to activate α-galactosidase from green coffee beans with percentages of activation up to 25%, as shown in Graph. 7 (represented with negative values).

The hydroxynonyl DNJ derivative **(*R*)-85y** showed the highest β-galactosidase inhibition (96% at 100 μM, IC_{50} 1.3 μM). Other compounds that presented high percentages of β-galactosidase inhibition were the *N*-nonyl fluoroinositol derivative (**67y**) and hydroxynonyl DNJ derivative **(*S*)-85y**, with 63 and 55% of β-galactosidase inhibition respectively at 100 μM. Even though, taking into account their highest affinity for imiglucerase, we would consider that there is an acceptable selectivity range for imiglucerase.

3.2.7.2 Inhibition of GCS

GCS inhibition in A459 cell homogenates was determined following the procedure described in *Chapter 3.1*. As can be observed in Graph. 8, most of the tested compounds presented moderate or low GCS inhibition at 100 μM. The only compounds that showed percentages of inhibition higher than 50% at that concentration were NB-DNJ, NN-DNJ and hydroxynonyl DNJ

derivative **(*R*)-85y**. These compounds were also tested at 10 µM giving percentages of GCS inhibition of 26, 69 and 33% respectively.

Thus, **(*R*)-85y** percentage of GCS inhibition is similar to the values obtained in the *Chapter 3.1* for amido and azido derivatives (**31d(I-III)** and **24d**) but lower than the values showed by triazole derivatives **31d(I-V)**. Even though, given the high affinity for imiglucerase of compound **(*R*)-85y** (IC_{50} values of 0.078 µM at pH 5.2 and 0.045 µM at pH 7.0), in this case we consider not suitable to talk about a dual compound GCS inhibitor and chaperone for GCase.

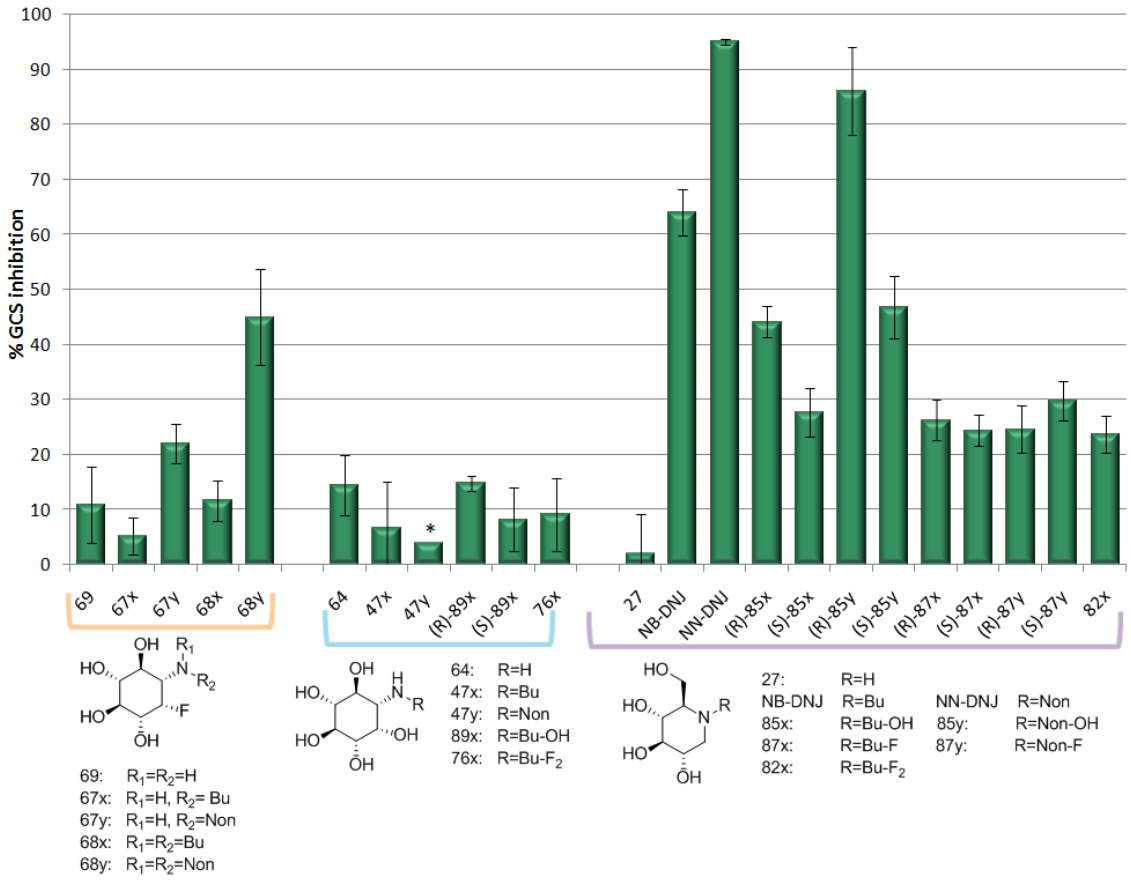

Graphic 8 Percentage of GCS inhibition in cell homogenates at 100 µM. Mean and standard deviation of three independent assays. *data extracted from Ana Trapero Doctoral Thesis[111], %GCS at 250 µM.

3.2.7.3 Cytotoxicity assay in WT human fibroblasts

Compounds synthesized in this chapter were submitted to MTT assay, following the procedure described in *Chapter 3.1*, in order to evaluate their potential cytotoxicity.The obtained percentages of cell viability after 24h of incubation of WT human fibroblasts in presence of the inhibitors are represented in Graph. 9.

Most of the tested compounds showed low cytotoxicity when the assay was performed at 500 µM. It can be noticed the relative cytoxicity of dinonyl fluoro inositol derivative **68y** (4.6% of cell viability at 200 µM) and N-Nonyl inositol **47y** (4.6% of cell viability at 500 µM). Although in light of these percentages of cell viability it could seem that these compounds were cytotoxic, it should be noticed that the IC_{50} against imiglucerase for both compounds were around 1 µM at pH 5.2 and 0.25 µM at pH 7.0. For this reason, the MTT assay should be performed at lower concentrations before getting other conclusions about their relative toxicity. In fact, inositol derivative **47y** did not present high cytotoxicity when tested at 300 µM[111], meaning that it has a good safety range.

On the other hand, it should be noticed that although nonyl derivatives **67y**, **68y**, **47y** and NN-DNJ presented good safety ranges, with slight cytotoxicity detected at 500 µM, while their correspondent butyl derivatives showed excellent percentages of cell viability at that concentration. This is consistent with the fact that compounds with longer chains present higher toxicity than compounds with shorter chains[111]. Surprisingly, hydroxybutyl DNJ derivative **(*R*)-85x** showed 68% of cell viability when tested at 500 µM, while the correspondent nonyl derivative **(*R*)-85y** showed 100% of cell viability at that concentration.

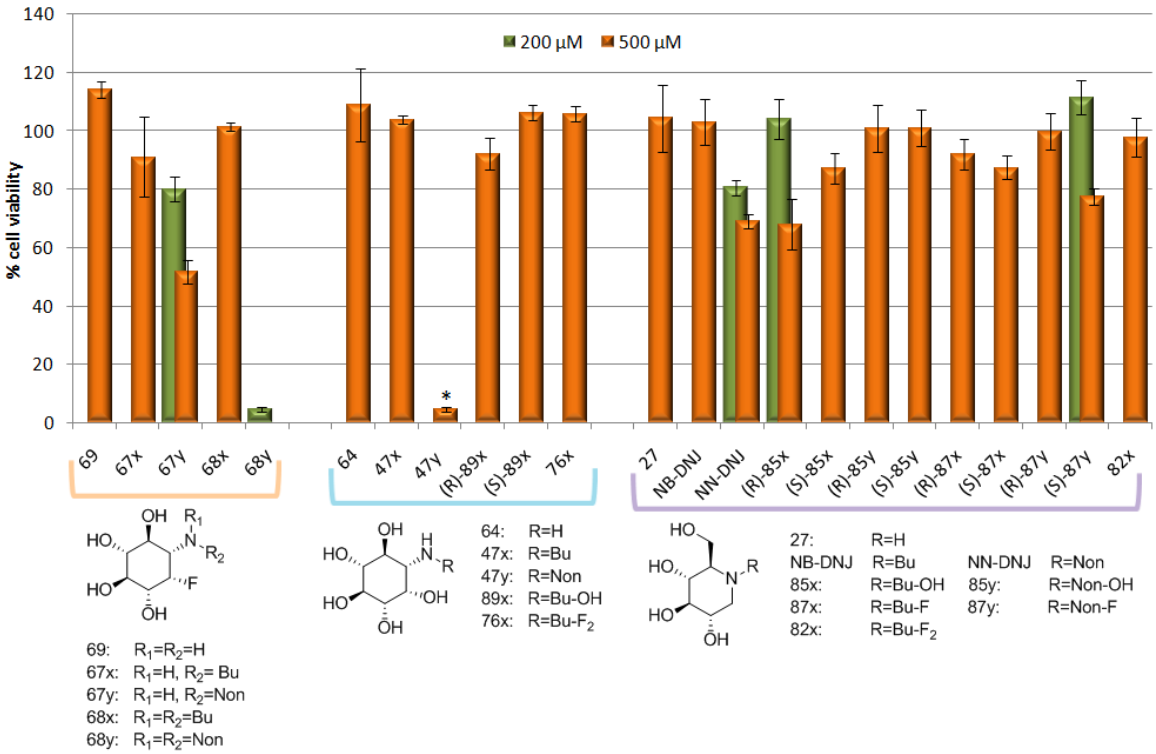

Graphic 9 Percentage of cell viability. Mean and standard deviation of an independent assay with triplicates. ***47y** did not show cytoxoxicity at 300 µM[111].

In summary, the compounds with good imiglucerase inhibition presented, in general, acceptable selectivity rates in front of other commercial glycosidases, except the chain hydroxylated DNJ derivatives **(*R*)-85x** and **(*S*)-85y**, which displayed no selectivity for imiglucerase in front of almond β-glucosidase.

The compounds were also tested as GCS inhibitors, showing in general moderate to low percentages of inhibition of this enzyme at 100 μM. The only compounds that showed better percentages of inhibition than the reference compound NB-DNJ (26% at 10 μM) were NN-DNJ and hydroxynonyl DNJ derivative **(*R*)-85y** (69% and 33% respectively at 10 μM). These compounds would not be considered as dual GCS and GCase inhibitors as their affinity for GCase in much higher than for GCS.

Although it has been noticed a tendency of showing higher toxicity for compounds with longer chains, all the tested compounds except dinonyl fluoroinositol derivative **68y** presented good safety profiles.

3.3 Study of the GBA inhibition in detergent-free assays

3.3.1 Introduction

As explained in the general introduction, GluCer is degraded to glucose and ceramide by three different hydrolases: the lysosomal GBA1, the non-lysosomal GBA2 and the cytosolic GBA3.

Körschen *et al.*[24], in 2013, demonstrated the important influence of detergents in the assays to determine GBA activities in different cell and tissue lysates. Wild type cell or tissue homogenates contain a mixture of GBA1, GBA2 and GBA3 enzymes and the necessary lipids and cofactor proteins (saposins) for the efficient GluCer hydrolysis. The proportion of GBA1, GBA2 and GBA3 expression can vary depending on the kind of cells and tissues. For example, HeLa cells present the three β-glucosidase activities while fibroblasts show little or no expression of GBA3[157,158].

In order to properly analyze the activity or inhibition of each of these β-glucosidases, it would be interesting to either minimize or block the proportion of activity of the other two in front of the glucosidase of interest. In this way, inhibitors like CBE, NB-DNJ andβ-D-glucosylsphingosine[24,26,159] have been used to selectively block GBA1, GBA2 and GBA3 activities

respectively. Alternatively to the addition of some inhibitors, the activity of some glycosidases could be modulated by genetic techniques as gene overexpression, missexpression or knockout[160].

Thus, Körschen *et al.* studied GBA1 activity by blockage of GBA2 activity with 10 µM NB-DNJ and GBA2 activity by blocking GBA1 activity with 30 µM CBE. Both activities were measured at different pHs in the presence or absence of detergents. As shown in Fig. 39A, in absence the detergents they found that in liver lysates of wild-type mice the maximal GBA1 hydrolytic activity (not blocked by 10 µM NB-DNJ) was found in the range of pH between 4 and 4.5, while this maximum was shifted to pHs around 5 and 5.5 in the case of assay with detergents (Fig. 39B). The GBA2 activity was studied similarly.

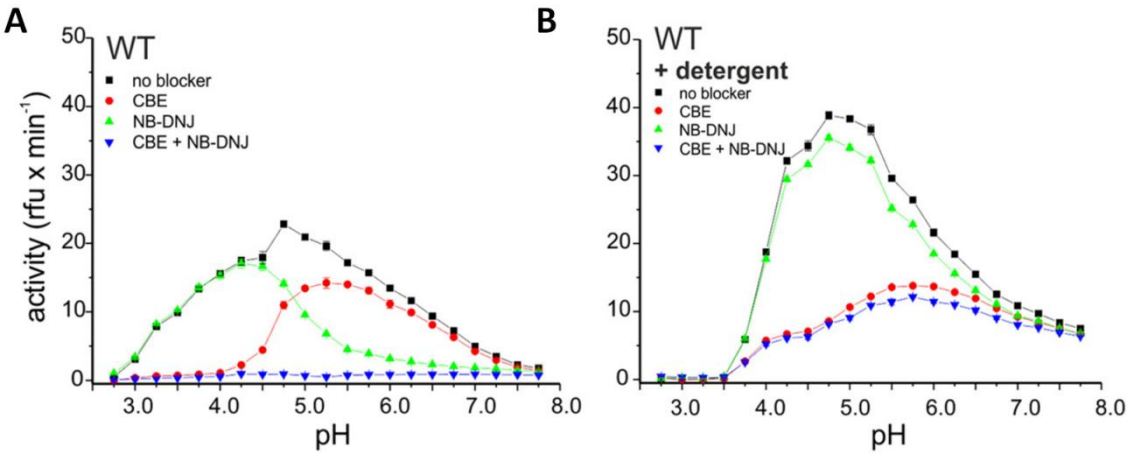

Figure 39 β-glucosidase activity in liver lysates from wild-type mice at different pH, in presence or absence of different blockers (30 µM CBE, 10µM NB-DNJ or both). **(A)** In the absence of detergents. **(B)** Containing 4mM mercaptoethanol, 0.25% of Triton X-100 and sodium taurocholate. Figure adapted from Körschen *et al*[24]**.**

Since now, all the assays performed to analyze the GCase inhibition in this thesis were performed with imiglucerase, a recombinant GBA1 enzyme extracted from CHO cells and that is actually administered to GD patients as a treatment for the disease. Thus, GBA2 and GBA3 activity could not be seen in those assays.Moreover, sodium taurocholate and Triton X-100 were added to assays in order to supply the need of other lipids for GCase activity, which are found in the natural cell environment.

In view of the foregoing, we decided to test some of the synthesized compounds in our assay conditions but without using exogenous detergents, in order to compare the imiglucerase inhibition at pH 5.2 and pH 7.0 in an assay with or without detergents. Unfortunately, we only could detect low GCase activity at pH 5.2, and no GCase activity was detected at pH 7.0 when the assay was performed with imiglucerase in the absence of detergents, even without adding any inhibitor.

This fact is in concordance with the fact that GCase needs the presence of other proteins and lipids to proceed to GluCer hydrolysis, as explained in the introduction of this Thesis. This could account for the low activity was detected when the assays were performed with recombinant enzyme without the addition of other detergents. Instead, in the case of the experiments performed by Körschen *et al,* they probably could detect GBA activity in their assay without addition of detergents because they were working with tissue or cell lysates and thus, the natural lipids present in the cells would facilitate the glycosidase activity.

For this reason we decided to test our compounds in collaboration with Dr. Wachten and Dr. Körschen at CAESAR institute in Bonn, and perform some assays in their detergent-free conditions, in order to analyze if the data obtained in the assay with recombinant GCase and detergents correlate with those obtained in detergent free conditions, and to see if under these new conditions it was possible to establish a relationship between the pK_as of the inhibitors and the GCase inhibition potency according the pH of the assay.

3.3.2 Detergent-free assays with cell homogenates

The detergent-free assays were also performed using 4-MUG as a fluorescent substrate and the pH of the assays were adjusted with McIlvaine buffer, as we previously did for the assays with pure recombinant imiglucerase. Differently, in this case, the assay was carried out with freshly prepared cell lysates as a source of enzyme, and the cleavage of 4-MUG was monitored in real time mode in a Fluostar Omega reader (MBG Labtech) at 30ºC using the filter pair 355 nm / 460 nm for excitation and emission, respectively and the activity was measured as change in relative fluorescence units (rfu) / min.

In order to determine the activity of GBA enzymes in the presence of inhibitors, first of all it was necessary to find the appropriate assay conditions. In general, the inhibition of enzymatic activity is studied under pH conditions where the activity without blockers is maximal, for a

best appreciation of the differences of activity. In the case of GBA1 inhibition, we would like to perform the assay at pH 5.2 and pH 7.0 for a better comparison of the data obtained in this assay with the data previously obtained in the assay with imiglucerase and detergents. Although the pHs for GBA1 inhibition studies were previously decided, it was necessary to verify that under the assay conditions we were able to properly detect the activity differences when the enzyme was active or fully blocked. For this reason, GBA1 and GBA2 activities where assayed at different pHs.

As shown in Graph. 10A, GBA2 activity was maximal at pH 6, and the inhibition of this enzyme could be properly tested at this pH using CHO cell homogenates with GBA2 overexpressed.

On the other hand, GBA1 activity could be tested at pHs between 4 and 5.5 in CHO cell homogenates with GBA1 overexpressed (Graph. 10B), as there is enough difference between the 100% of activity and the full blockage at those pHs. On the contrary, this assay conditions were not the most appropriate to determine GBA1 activity at pH 7, as the difference between the maximal (buffer) and minimal (CBE+NB-DNJ) activity was too small.

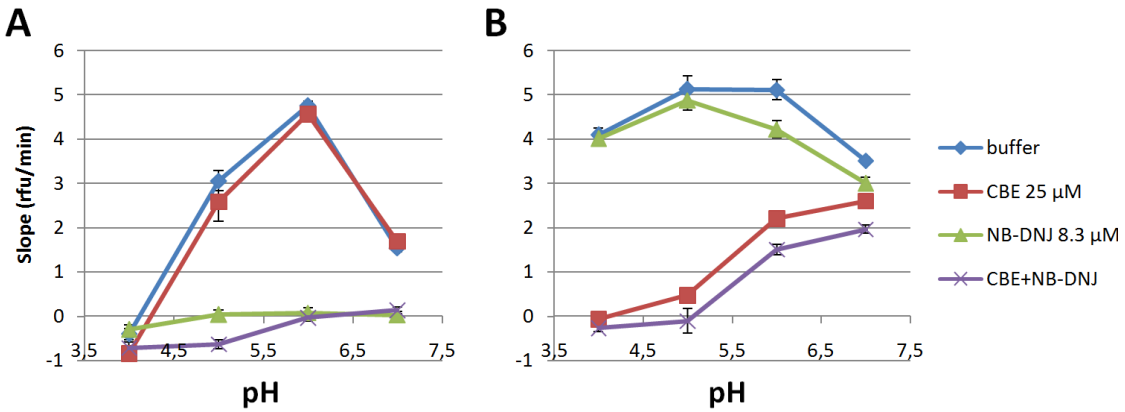

Graphic 10 GBA activity at pH 4, 5, 6 and 7; with and without blockers. Assay carried out with cell homogenates without addition of detergents (mean and standard deviation of one assay with quadruplicates). **(A)** CHO (GBA2 overexpressed) cell homogenates. **(B)** CHO (GBA1 overexpressed) cell homogenates.

As we were interested in determining GBA1 activity both at pH 5.2 and pH 7.0 in order to compare the data obtained in this assay with the previous ones, it was necessary to find different assay conditions allowing the accurate determination of GBA1 activity at pH 7, if it would be feasible.

In this way, the use of higher concentrations of CBE increased a bit the difference of the maximal and minimal activity at pH 7, suggesting that this inhibitor was not fully blocking the enzyme under these conditions. This is rather surprising result since CBE is considered a well established covalent inhibitor of GBA1. The use of other CHO cell lines also with GBA1 overexpression gave a similar outcome.

Finally, as shown in Graph. 11A we were able to properly analyze GBA1 activity at pH 5.2 and 7.0 by using HAP1 GBA2-Knock out cell homogenates and blocking the activity with 100 µM NN-DNJ (negative control). It must be highlighted that the maximal GBA1 activity was obtained when the assay was performed at pH between 4 and 5, and decreased drastically with the increase of the pH, resulting in a reduction of more of 50% of the activity when the assay was performed at pH 7.0. Moreover, in this assay we could also compare the blockage of 50 µM CBE (blocking less than 50% of the glucosidase activity observed at pH 7) and 100 µM NN-DNJ (fully blocking the activity).Taking into account that the cells used in this assay contain no GBA2 enzyme, and the increase amount of CBE from 25 to 50 µM resulted in a higher but still not full inhibition of GBA activity in those cell homogenates, it seems that CBE is not fully blocking GBA1 activity at neutral pH's.

On the other hand, we did a similar assay with imiglucerase without detergents (Graph. 11B), as expected we were able to detect some activity at pH 5.2, but not at pH 7.0. Surprisingly, with this enzyme no any activity was detected at pH 4.0, on the contrary of what happened with the cell homogenates previously analyzed.

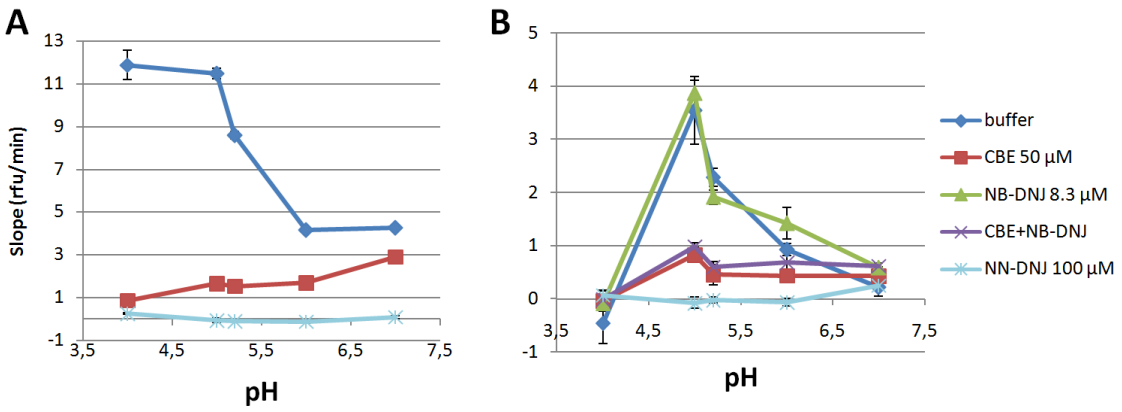

Graphic 11 GBA activity at pH 4, 5, 5.2, 6 and 7; with and without bloquers. Assay carried out without addition of detergents (mean and standard deviation of one assay with quadruplicates). **(A)** HAP1 (GBA2-KO) cell homogenates. **(B)** Imiglucerase.

3.3.2.1 Determination of GBA1 inhibition

Some representative compounds were selected to be tested as GBA1 inhibitors in a detergent-free assay with HAP1 (GBA2-KO) cell homogenates. Those compounds were added to a solution of cell lysates in McIlvaine buffer at pH 5.2 or 7.0. Then, 4-MUG was added and the variation of fluorescence was monitored during 2 h, without any preincubation. The GCase activity was measured as change in relative fluorescence units (rfu) / min. The obtained IC_{50} values are shown in Table 11.

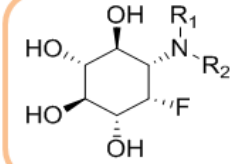

67x: R_1=H, R_2= Bu
67y: R_1=H, R_2=Non
68x: R_1=R_2=Bu
68y: R_1=R_2=Non

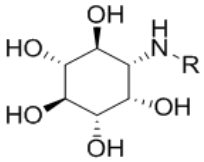

64: R=H
47x: R=Bu
47y: R=Non
89x: R=Bu-OH
89y: R=Non-OH
76x: R=Bu-F_2

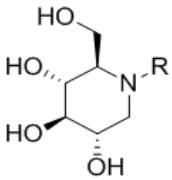

NN-DNJ R=Non
85x: R=Bu-OH
85y: R=Non-OH
87x: R=Bu-F
87y: R=Non-F

compound	pH 5.2 IC_{50} (µM)	pH 7.0 IC_{50} (µM)	Δ
67x	308	318	1.0
67y	0.66	0.76	0.9
68x	71	166	0.4
68y	6.6	9.5	0.7
64	>400	>400	-
47x	78	16	4.7
47y	0.29	0.14	2.0
(*R*)-89x	117	33	3.5
(*S*)-89x	622	236	2.6
(*R*)-89y	0.25	0.19	1.3
(*S*)-89y	1.4	0.67	2.1
76x	106	264	0.4
NN-DNJ	0.57	1.5	0.4
(*R*)-85x	24	49	0.5
(*R*)-85y	0.025	0.096	0.3
(*S*)-85y	0.54	1.9	0.3
(*R*)-87x	618	1007	0.6
(*R*)-87y	4.9	67	0.1
(*S*)-87y	1.3	14	0.1

Table 11 GBA1 inhibition in HAP1 (GBA2-KO) cell homogenates. Δ = IC_{50} (pH 5.2, µM) / IC_{50} (pH 7.0, µM).

The first interesting conclusion that can be deduced from the results in Table 11 and Graph. 12 is that, in this assay conditions, the inositol derivatives (blue box), except compound **76x** are the only compounds displaying a clear better inhibition at pH 7.0 than pH 5.2. In contrast, in the assay employing imiglucerase and detergents (Tables 6 and 7), most of the tested

compounds seemed to be better inhibitors at pH 7.0, irrespective of the chemical scaffold. This fact highlights the important influence of the different assay conditions and the enzyme source in the analysis of activity of an enzyme.

Moreover, a comparison between Δ values obtained in the assay with imiglucerase and detergents and the ones obtained with the detergent-free assay with cell homogenates (Graph. 12) reveals that, in general, the Δ values obtained in the detergent-free assay are lower than in the assay with detergents.

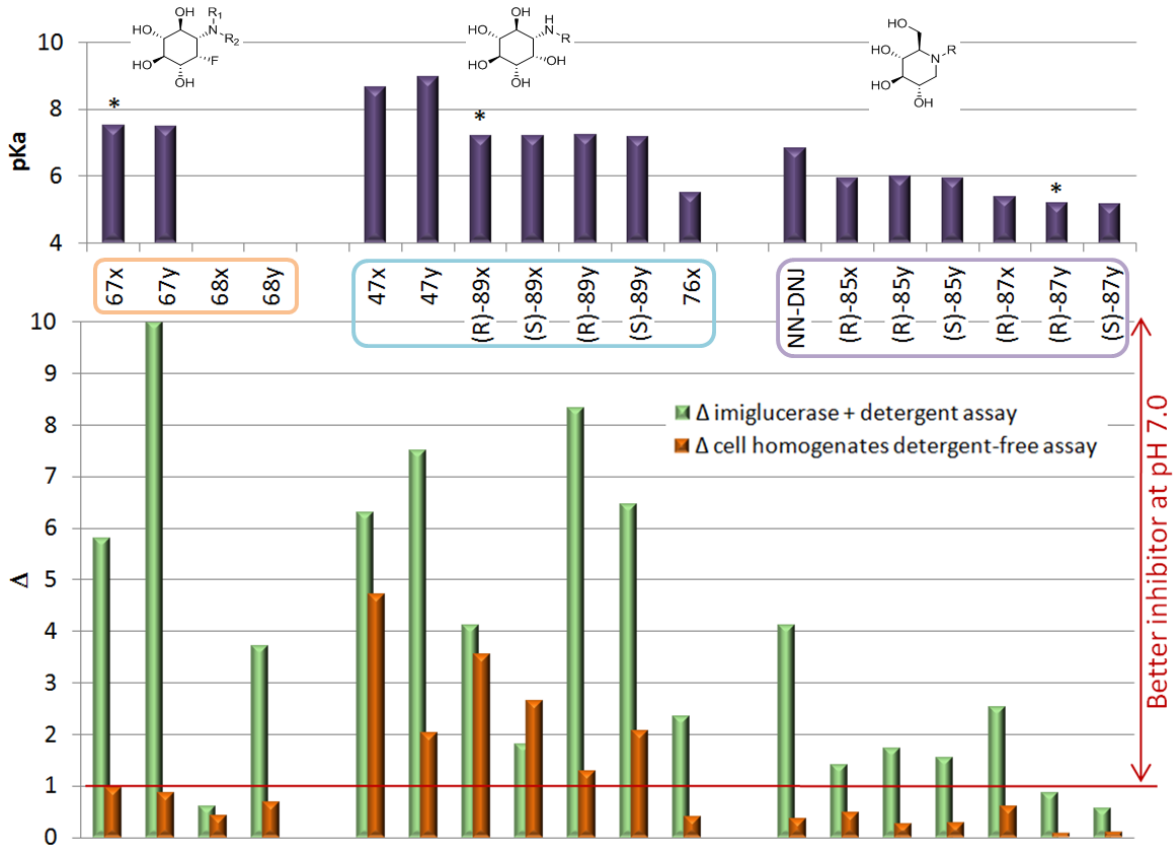

Graphic 12 Difference of IC_{50} values against GBA1 in cell homogenates at pH 5.2 and 7.0 (Δ= IC_{50} (pH 5.2, μM) / IC_{50} (pH 7.0, μM)). Values lower than 1 indicate compounds with better inhibition when the assay was performed at pH 5.2 than at pH 7.0. In the upper graph, experimental pK_a values for each compound (* extrapolated pK_a values).

In contrast with the results previously found in the imiglucerase assay, where *N*-nonyl fluoroinositol (**67y**) showed the higher difference of activity according to the pH of the assay (Δ = 10), in detergent-free conditions this compound showed almost no difference of activity (Δ = 0.9).

In fact, under the detergent-free assay with cell homogenates, although fluoro inositol derivatives resulted slightly better inhibitors a pH 5.2 than at pH 7.0, this family of compounds showed small difference of activity according to the pH of the assay.

Under detergent-free conditions, the DNJ derivatives showed high difference of activity according to the pH of the assay but, in the opposite sense of what we expected, they resulted better inhibitors at pH 5.2 than at pH 7.0 (Δ < 1), as shown in Graph. 12. Instead, as mentioned before, inositol derivatives except the difluorobutyl **76x** showed the desired better GCase inhibition at neutral pH than at pH 5.2. Thus, the inositols that showed higher Δ in the detergent-free assay were *N*-butyl (**47x**), and *N*-hydroxybutyl (**(*R*)-89x** and **(*S*)-89x**) derivatives, with Δ values of 4.7, 3.5 and 2.6 respectively.

Interestingly, as shown in Table 12, DNJ nonyl derivatives with hydroxyl (**85y**) or fluorine (**87y**) β-substitution in the chain showed the same Δ value for the *R* and *S* structures (0.3 for the hydroxyl derivatives, and 0.1 for the fluorine ones) in the assay with cell homogenates. This fact could be somewhat surprising in light of the different inhibition potency of the derivatives with different configuration. For example, **(*R*)-85y**is around 20 times more potent than **(*S*)-85y** at both pH's but, the Δ value for both compounds is 0.3. It should be noticed that, although the butyl derivatives **(*R*)-85x** and **(*R*)-87x** displayed similar pk_a values to the corresponding nonyl derivatives, their Δ values did not correlate with the ones obtained for the nonyl derivatives. Thus, although some kind of relationship between the structures and the Δ values for the DNJ derivatives could be intuited in the detergent-free assay, further studies would be necessary before establishing a possible correlation.

		imiglucerase + detergents			cell homogenates, detergent-free		
compound	pKa	pH 5.2 IC50 (μM)	pH 7 IC_{50} (μM)	Δ	pH 5.2 IC50 (μM)	pH 7 IC_{50} (μM)	Δ
NN-DNJ	6.84	1.03	0.25	4.1	0.57	1.5	0.4
(R)-85x	5.94	38	27	1.4	24	49	0.5
(R)-85y	5.98	0.078	0.045	1.7	0.025	0.096	0.3
(S)-85y	5.94	2.0	1.3	1.5	0.54	1.9	0.3
(R)-87x	5.39	33	13	2.5	618	1007	0.6
(R)-87y	5.2[a]	6.2	7.2	0.9	4.9	67	0.1
(S)-87y	5.16	3.0	5.3	0.6	1.3	14	0.1

Table 12 Comparative of IC_{50} and Δ values obtained with the imiglucerase and detergents assay and the detergent-free assay with cell homogenates.[a] extrapolated pK_a value.

We next decided to compare the IC_{50} values obtained in the imiglucerase + detergents assay with those obtained in the assay with cell homogenates without added detergent. For this purpose, we calculated the percentage of variation in the IC_{50} values when the assay was carried out in one or other conditions. The obtained data is presented in Graph. 13.

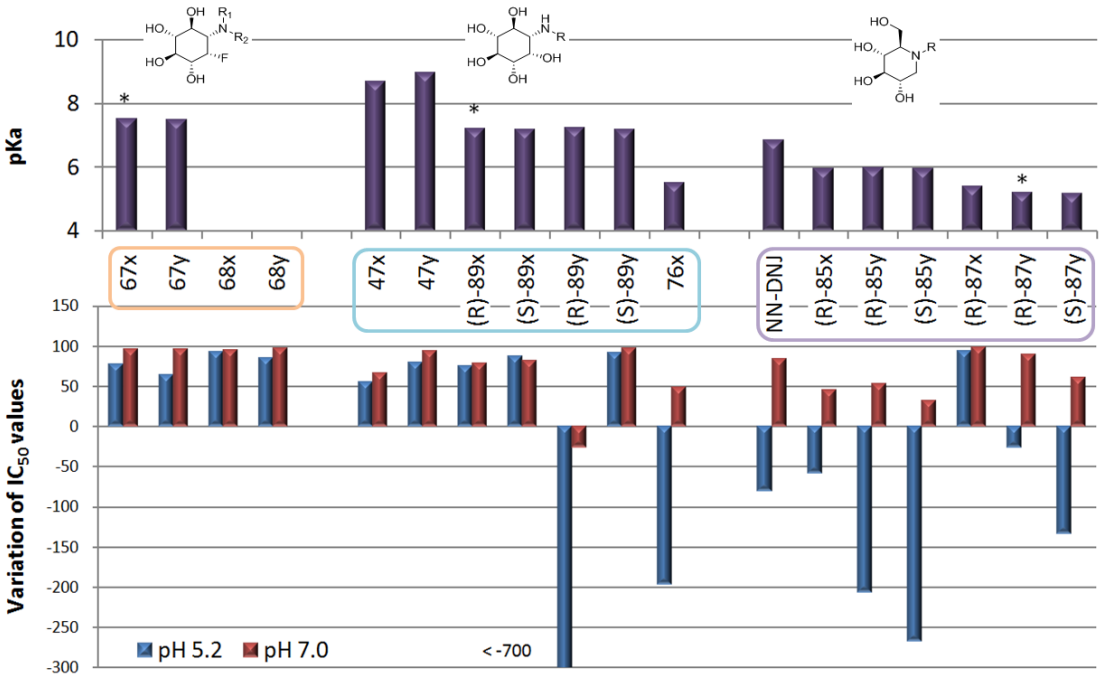

Graphic 13 Variation of the GCase inhibition according to the assay conditions, calculated as (a-b)/a x 100 where "a" is the IC_{50} value (µM) determined in the assay with cell homogenates and without detergents and "b"is the IC_{50}value (µM) determined in the assay with imiglucerase and detergents. In the upper graph, experimental pk_a values for each compound (* extrapolated pk_a values).

As can be seen in this graph, most of compounds with fluoro-inositol or inositol cores (orange and blue boxes respectively) appeared to be better GCase inhibitors in the assay with imiglucerase (represented as positive values in the graph) at both pH's. The exception were the hydroxynonyl inositol derivative **(R)-89y** that resulted better inhibitor in the detergent-free assay at both pH's and difluorobutyl inositol derivative **76x** that at pH 5.2 seemed to be better inhibitor in the detergent-free assay, while at pH 7.0 showed better GCase inhibition in the assay with imiglucerase.

All the DNJ derivatives (purple) also showed better GCase inhibition in the assay with imiglucerase and detergents at pH 7.0. In contrast, as can be seen with the negative values in

the graph, at pH 5.2 the DNJ derivatives, except the fluorobutyl derivative **(R)-87x,** presented lower IC_{50} values in the detergent-free assay than in the assay with imiglucerase.

In conclusion, as can be observed in Graph. 13, no direct correlation between the influence of the assay conditions and pK_a of the amine in the core, side chain length or configuration of the β-substitution on the side chain could be established. The only clear effect seems to reside on the structure of the scaffold core, which results in a different behavior in the assays and could suggest a different interaction mode with the enzymes for inositol vs. iminosugar inhibitors.

3.3.2.2 Determination of GBA2 inhibition

NB-DNJ is described to be a good GBA2 inhibitor, with good selectivity with respect to GBA1 enzyme[24]. For this reason, we decided to also analyze the effect of the compounds synthesized in the previous sections on GBA2 activity. For this purpose, the compounds were tested as GBA2 inhibitors in a cell homogenate assay similar to the one conducted to analyze the GBA1 inhibition, but using CHO cell homogenates with GBA2 overexpression at pH 6 (the GBA2 activity profile of the cell homogenates at different pH is showed in Graph. 10A).

Thus, in Graph. 14 we have represented the percentages of GBA2 inhibition in front of different concentrations of inhibitor for the less potent GBA2 inhibitors. For those compounds that showed the best percentages of GBA2 inhibition, IC_{50} values were determined and the results are represented in Graph. 15.

When comparing the different cores, it seems that the best GBA2 inhibitors are those with DNJ moiety (purple in Graph. 14, and Graph. 15), while the fluoro-inositol derivatives (orange in Graph. 14) are weaker inhibitors for this enzyme.

On the other hand, the inositol and fluoro-inositol butyl derivatives (compounds **67x** and **47x**) resulted to be similar or weaker GBA2 inhibitors than the corresponding cores without *N*-substitution (compounds **69** and **64** respectively) while NB-DNJ resulted better GBA2 inhibitor than DNJ (compound **27**). In contrast, in the case of GBA1 inhibition, the inositol and fluoro-inositol *N*-butyl derivatives were better inhibitors and NB-DNJ showed similar inhibitory capacity than their respective cores without *N*-substitution. Moreover, it should be highlighted that the *N*-nonyl derivatives were more potent inhibitors than the corresponding *N*-butyl derivatives, both for GBA1 and GBA2 enzymes.

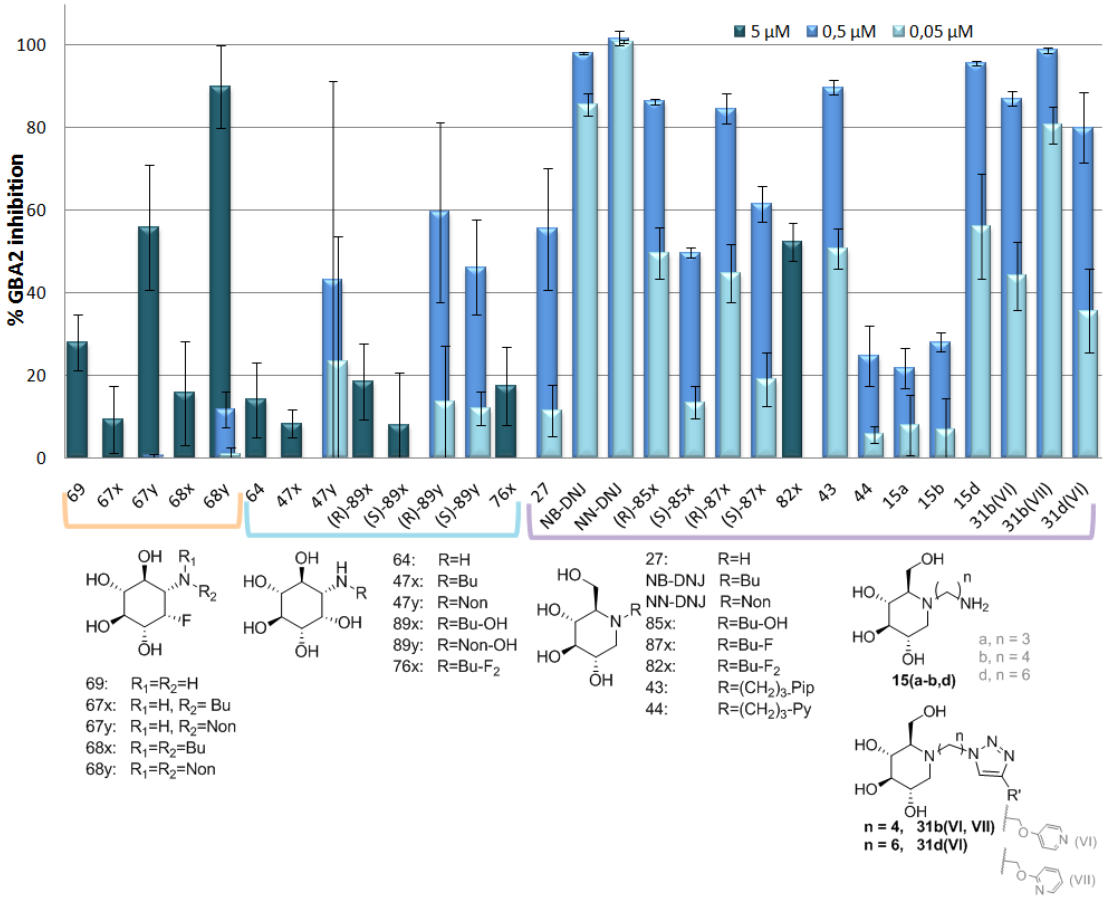

Graphic 14 Percentage of GBA2 inhibition in CHO (GBA2 overexpressed) cell homogenates assay at pH 6. (mean and standard deviation of three different assays with quadruplicates). Compounds with better GBA2 inhibition are not shown in this graph, but their IC_{50} values can be found in Graph. 15.

As shown in Graph. 15, the DNJ butyl derivatives with β-substitution (compounds **(*R*)-85x**, **(*S*)-85x**, **(*R*)-87x** and **(*S*)-87x**) were less potent GBA2 inhibitors than NB-DNJ, with lower inhibition for compounds having *S* configuration over the *R* ones, with similar inhibitory capacity for compounds with hydroxyl or fluoro substitution. In addition, it should be noticed that the butyl derivative with two fluorine substituted in the β-position of the side chain (compound **82x**), showed moderate (52%) inhibition of GBA2 at 5 µM. Although this value showed weaker GBA2 inhibitory capacity in comparison with the derivative without substitution in the side chain (NB-DNJ) it showed good selectivity for GBA2 in front of imiglucerase, as the IC_{50} for this compound against imiglucerase was 170 µM at pH 7.0 and higher than 400 µM at pH 5.2 .

A

	IC_{50} (nM)
NB-DNJ	11,4 ± 1,2
NN-DNJ	0,310 ± 0,039
47y	3800 ± 1500
16d(I)	2,70 ± 0,44
16d(II)	29,7 ± 3,3
16d(III)	9,53 ± 0,71
24d	0,74 ± 0,12
31d(I)	1,69 ± 0,37
31d(II)	3,8 ± 1,1
31d(III)	5,2 ± 1,3
31d(IV)	4,18 ± 0,84
31d(V)	0,55 ± 0,13
31d(VI)	177 ± 22
(R)-85y	0,395 ± 0,050
(S)-85y	0,284 ± 0,055
(R)-87y	0,164 ± 0,026
(S)-87y	0,587 ± 0,052
82x	7000 ± 2300

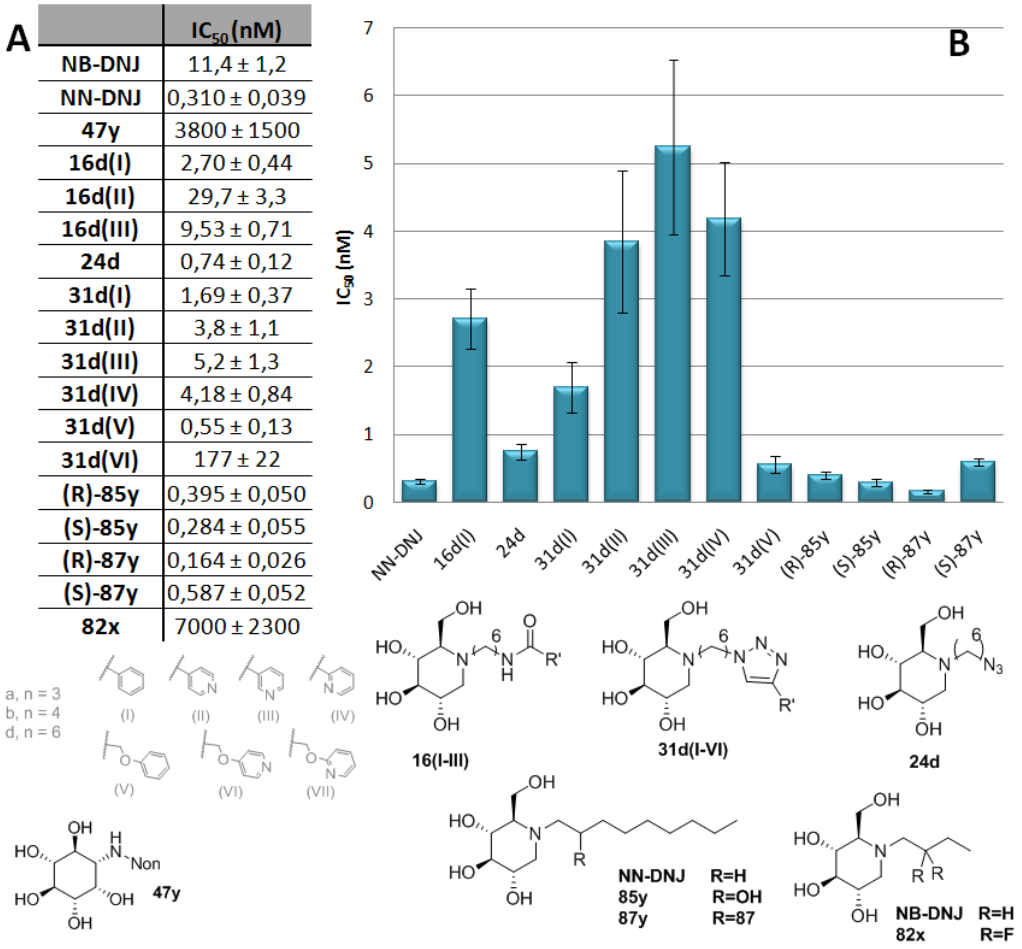

Graphic 15 GBA2 inhibition in CHO (GBA2 overexpressed) cell homogenates assay at pH 6 (mean and standard deviation of at least two different assays with quadruplicates). **(A)** IC_{50} values. **(B)** Representation of IC_{50} of the most potent GBA2 inhibitors analyzed in this section.

Regarding the DNJ derivatives with substitution at the end of the side chain, compound **43** resulted better GBA1 and GBA2 inhibitor than compound **44** and compounds **15(a-b)** showed low inhibition of both enzymes at 5 µM. Surprisingly, compound **15d** showed excellent GBA2 inhibition at 0.5 µM (96% inhibition) while having low (14%) and moderate (62%) imiglucerase inhibition at 50 µM at pH 5.2 and pH 7.0 respectively, indicative of good selectivity for GBA2 in front of imiglucerase.

Moreover, although the DNJ amido derivatives (compounds **16d(I-III)**) and the DNJ triazol derivatives with a terminal phenyl, pyridine or methoxyphenyl group (compounds **31d(I-V)**) resulted both better imiglucerase and GBA2 inhibitors than compounds with a terminal methoxypyridine (**31b(VI-VII**) and **31d(VI)**), all synthesized DNJ derivatives presented higher

affinity for GBA2 enzyme than for imiglucerase, showing good selectivity for GBA2. For example triazol DNJ derivatives with a methoxypyridine at the end of the side chain (compounds **31b(VI**), **31b(VII)** and **31d(VI)**) presented GBA2 inhibition higher than 80% at 0.5 μM while their IC_{50} values against imiglucerase were higher than 50 μM, and compounds **16d(I-III)** and **31d(I-V)** showed IC_{50} values against imiglucerase in the micromolar range (Table 2) while their IC_{50} values against GBA2 enzyme are in the nanomolar range (Graph. 15).

Finally, the most potent GBA2 inhibitors resulted to be the nonyl DNJ derivatives with or without β-substitution (NB-DNJ, **(R)-85y**, **(S)-85y**, **(R)-87y**, **(S)-87y**) as well as the azide **24d** and triazol derivative **31d(V)**. All of them presented subnanomolar IC_{50} values, as shown in Graph. 15.

3.3.3 Intact cell assays

3.3.3.1 Tuning up of the assay and analysis of GBA2 inhibition in HAP1_001 (GBA1-KO) cells

In order to study the permeability and effect of our compounds in cells, we decided to carry out an assay in intact cell. In this way, we initially tried to perform an assay similar to the one that was previously described for GCase inhibition in intact human fibroblasts[145]. Thus, HAP1 (GBA1-KO) cells were seeded and 24 h preincubated for 24 h in presence of the inhibitor or DMSO (control). After, the culture medium was replaced by a 50% mixture of PBS and 200 mM acetate buffer (pH 4.0) and 4-MUG was added and the fluorescence resulting of its cleavage was monitored in real time. After 2 h of assay, enzymatic reactions were stopped by lysing the cells with glycine/NaOH buffer (100 mM, pH 10.6) and the fluorescence measured again. No significant changes in the fluorescence measurements between the control (cells without inhibitor) and the blank (wells without cells) were observed neither during the 2h measurement in real time nor in the measurement at basic pH after cell lysate.

Then, we decided to try a similar assay in culture medium instead of PBS/acetate buffer (pH 4) and studying the fluorescence for longer incubation periods after 4-MUG addition. Thus, the GBA1-KO cells were preincubated for 2 h in presence of the inhibitor or DMSO (control) in fresh medium without FCS. It must be highlighted the importance of using medium without FCS, as FCS contains glycosidases that would hydrolyze the 4-MUG. Next, a solution of 4-MUG in water was added and fluorescence of each well was monitored in real time 0.5, 5, 8, 20 and

27 hours after 4-MUG addition. Between each fluorescence lecture and the next one the plate was placed again in the incubator at 37 ºC under a 5% CO_2 atmosphere.

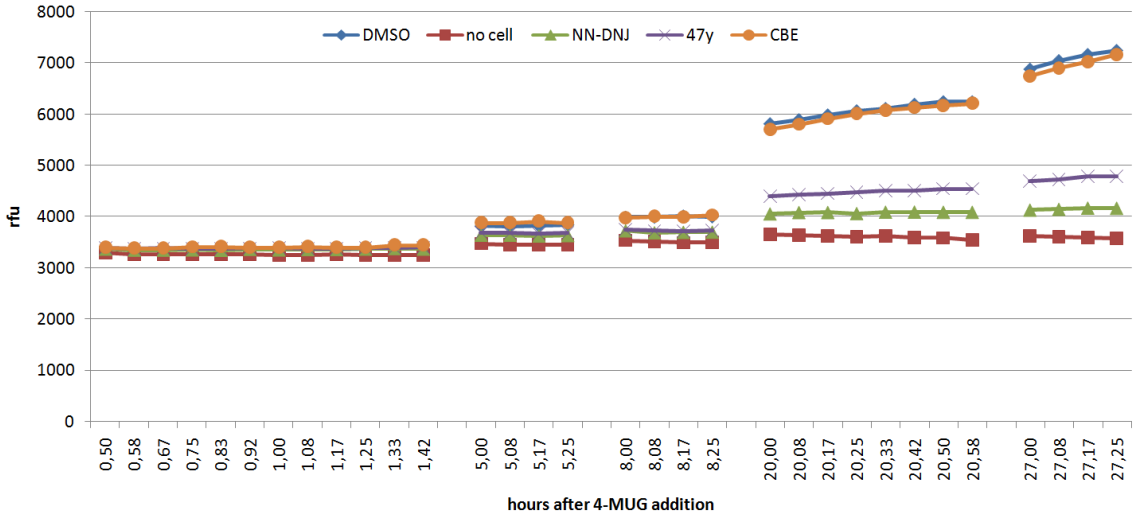

Graphic 16 GBA activity in HAP1 GBA1-KO intact cell. Inhibitors: 10 µM NN-DNJ, 10 µM 47y, 30 µM CBE. Positive control (100% GBA activity): DMSO; negative control (0% GBA activity): no cells.

As can be noticed in Graph. 16, there is no appreciable difference of fluorescence between the positive and negative controls 2h after 4-MUG addition, and between 5 and 8 hours there is a slight difference but not enough to quantify properly the percentage of GBA inhibition. Finally, in the measurements after 20 and 27 h after 4-MUG addition, we found that the conditions to measure the difference of fluorescence were appropriate for evaluation of GBA inhibition. As expected, given that CBE is a selective GBA1 inhibitor and cells used in this assay were GBA1-KO, cells cultured in presence of CBE showed the same GBA activity than the positive control (DMSO). On the contrary, the wells where cells were cultured in presence of 10 µM NN-DNJ or **47y** showed an important decrease of the fluorescence, suggesting an inhibition of GBA2 enzyme by these compounds.

To the best of our knowledge, the assays to determine GBA inhibition in intact cell published since now were carried out in intact cell but analyzing the fluorescence after lysing the cells (for example by addition of glycine/NaOH buffer (100 mM, pH 10.6)). Promisingly, this new assay is advantageous since allows the determination of GBA activity in intact cells *in situ* without requiring cell lysing.

Once the assay was tuned up, we decided to study the GBA2 inhibition by analyzing the fluorescence 24h after 4-MUG addition in presence of different inhibitors. As can be observed in Graph. 17, all tested compounds (**67y**, **(R)-89y**, **47y**, **(R)-89y**, NB-DNJ, NN-DNJ, (**R)-85y** and

(S)-85y) showed good GBA2 inhibition at 10 µM in HAP1 GBA1-KO intact cells. It should be noticed that none of the tested compounds (neither 10 µM NB-DNJ) fully blocked the β-glucosidase activity, showing around 30% of GBA activity remaining. This fact could be explained considering that those cells were GBA1 Knock-out and although they did not express GBA1 enzyme, they could present GBA3 activity.

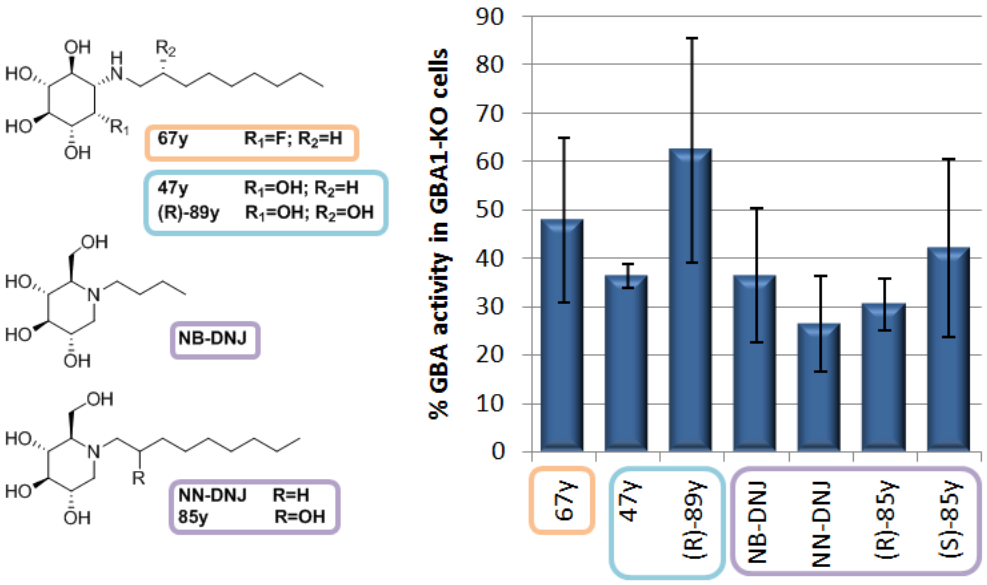

Graphic 17 GBA activity in HAP1 GBA1-KO intact cell after 26h of incubation with 10 µM inhibitor. Mean + SD of three independent assays with duplicates.

On the other hand, as shown in Graph. 18, after the GBA2 inhibition assay, the supernatants were removed and placed in a different 24-well plate. The layers with cells remained attached at the bottom of the plate and were washed twice with PBS. Then, new media without FCS, the inhibitors and 4-MUG were added to the plate with cells and the fluorescence was monitored, again, for 2h showing basal fluorescence values. On the other hand, the fluorescence of the supernatants previously placed in a new plate without cells was also monitored. These supernatants presented fluorescence values proportionally to the GBA activity observed in the GBA2 inhibition assay, although showing a slight decrease of fluorescence along the time. This result suggests that the cleaved 4-MU is excreted from the cell and it accumulates in the culture media, not inside the cell. This fact is quite interesting, as it could allow the analysis of fluorescence in a different plate from the one were cells are cultured, meaning that the cells could be maintained in a more controlled environment, minimizing the possibility of

contaminations and, what could be even more interesting, opening the door to analyze the recovery of cellular GBA activity after inhibitor removal.

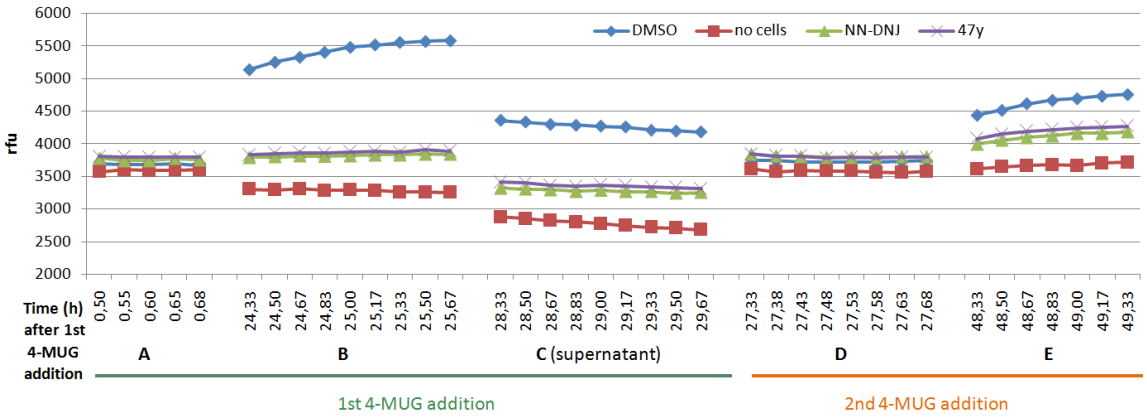

Graphic 18 Variation of fluorescence. **(A)** Plate with cells after 1st 4-MUG addition. **(B)** Plate with cells 24 h after 1st 4-MUG addition. **(C)** Supernatant placed in a plate without cells 25 h after 4-MUG addition. Lecture after 3 h in the new plate. **(D)** Plate with cells after removal of culture medium and addition of fresh medium with inhibitors and 4-MUG. **(E)** Plate with cells after 24 h of the second addition of 4-MUG.

Finally, the analysis of the plate with cells 24 h after the second addition of culture media with inhibitor and 4-MUG showed again difference of fluorescence between the positive and negative controls, but with lower values. It should be highlighted that at this point, after 48 h maintaining cells in a media without FCS, we observed extensive died cells and for this reason these data were not taken into account to determine the percentage of inhibition.

In summary, we have set up an assay to determine GBA2 activity in intact cell, based in the analysis of the fluorescence of 4-MU cleaved by GBA enzymes, and without the need of any cell lysing. All the assayed compounds showed GBA2 inhibition in the same range than NB-DNJ when tested at 10 µM. At this concentration GBA2 activity should be fully blocked by NB-DNJ and all the assayed compounds showed nanomolar IC_{50} values against GBA2 in the assay performed previously in cell homogenates. For this reason we hypothesize that the 30% of GBA activity not blocked in this assay could be GBA3 activity. On the other hand, we have seen that once 4-MUG was cleaved, 4-MU was excreted and accumulated outside the cells, allowing the analysis of GBA activity by monitoring either the fluorescence of the plate with cells or the fluorescence of the corresponding supernatants.

3.3.3.2 Analysis of GBA1 inhibition and activity recovery in HAP1_001 (GBA2-KO) cells

Taking into account the experience obtained with GBA2 inhibition assay in GBA1-KO intact cell, we tried to perform the assay with GBA2-KO intact cell similarly, but going one step further and trying to analyze the recovery of cellular GBA activity after inhibitor removal.

Previous studies that analyzed the recovery of GBA activity were based on culturing the cells with the inhibitor in several plates, removing the inhibitor from all the plates at one time point, and lysing each plate in a different day, after inhibitor removal[161]. Interestingly, as our assay does not need the lysate of the cells, the recovery of the activity could be studied with the same cells in a single 24-well plate.

Thus, HAP1 GBA2-KO cells were preincubated in presence or absence of inhibitor for 2 h. Next 4-MUG was added and the plate was incubated again for 24 h before fluorescence monitorization. After that, the supernatant was removed and fresh medium with FCS was added to prevent the death cells. After 18 h of incubation, the medium was again replaced by medium without FCS, and 4-MUG was added without any addition of inhibitor. After 24 h of incubation, the fluorescence was monitored again to analyze the percentage of GBA activity 1.5 days after the removal of the inhibitors. Last steps (addition of fresh medium with FCS, 18 h incubation, replacement of the medium, 4-MUG addition, 24 h of incubation and lecture of fluorescence) were repeated in order to analyze the GBA activity 3 days after the inhibitor removal. In this way, the capacity of GBA1 inhibition of several compounds and the capacity of recovery of GBA activity after inhibitor release were tested (data shown in Graph. 19).

As expected, NB-DNJ 10 µM showed no GBA1 inhibition and those cells presented an activity similar to the positive control (DMSO) both during the lectures carried out in presence of NB-DNJ or after removal of this compound.

Regarding CBE interaction, 30 µM concentration of this compound showed the expected fully blockage of GBA1 activity. Although CBE is described as GBA1 irreversible inhibitor, cells previously cultured in presence of 30 µM CBE showed 80% and 100% of GBA activity in comparison with the DMSO control 1.5 and 3 days after removal of the CBE present in the culture medium. This fact is in concordance with a previous study[161] where murine peritoneal cells were cultured in presence of CBE. In

that case β-glucosidase activity recovered to half maximum 2.2 days after removal of CBE in murine peritoneal cells.

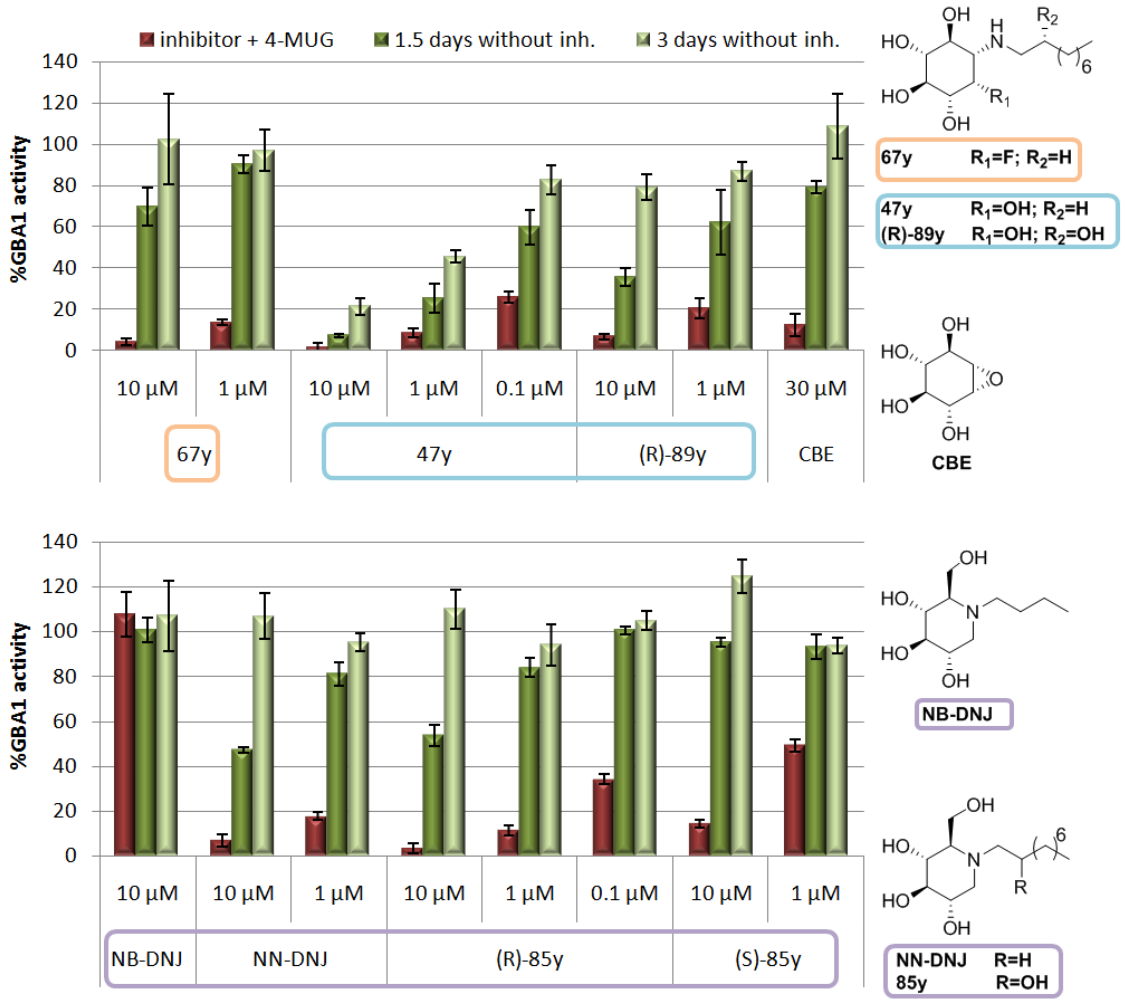

Graphic 19 GBA1 activity in GBA2-KO intact cells.

All tested compounds showed excellent GBA1 inhibition when tested both at 10 µM and 1 µM, showing GBA inhibitions higher than 80% in all cases except **(*S*)-85y** that presented inhibition around 50% at 1 µM, and NB-DNJ that showed no inhibition, as mentioned before. Compounds that appeared to be the best inhibitors (nonyl inositol **47y** and nonyl-OH DNJ derivative **(*R*)-85y**) were also assayed at 0.1 µM showing, respectively, 74 and 66% of GBA1 inhibition after incubating the cells in presence of these inhibitors for 26 h.

All compounds except *N*-nonyl inositol (**47y**) showed ratios around 50% of GBA1 activity recovery 1.5 days after removal of the inhibitor, and at least 80% of GBA1 activity after 3 days. As expected, the lower the concentration of inhibitor, the better recovery of GBA1 activity was observed.

It should be noticed that although *N*-nonyl inositol (**47y**) is not an irreversible GBA1 inhibitor, cells incubated with this compound did not achieve the 100% of GBA1 activity in any of the assayed concentrations (10, 1 and 0.1 µM) 3 days after inhibitor removal. This compound showed no signs of cytotoxicity in Human WT fibroblasts when tested at 200µM for 24 h[111] but presented low cell viability at 500 µM. For this reason, we decided to analyze the state of the HAP cells after GBA1 inhibition and recovery assay in order to prevent a potential loss of GBA activity due to cell death.

Thus, once the GBA1 activity assay was finished, the culture medium was removed and cells were tripsinated, stained with trypan blue and cell viability was analyzed under a microscope. Live cells would be not stained by the dye, while dead cells would show a distinctive blue color. No different amount of dead cells was observed in wells with cells previously treated with **47y** in comparison with the control cells (treated with DMSO), suggesting that cell death was not the cause of the reduced GBA activity after inhibitor removal.

Another explanation for this reduced GBA activity would be that inositol derivative **47y** could penetrate the cell membrane but was not easily excreted from inside the cell, creating an intracellular concentration higher than expected. Thus, when culture medium with 4-MUG and inhibitor was removed, some of the inhibitor would remain inside the cell, being able to still block high proportion of GBA1 enzyme.

In summary, we have been able to tune up a new assay to analyze GBA1 inhibition and the recovery of this activity after inhibitor removal in intact cell, without the need of cell lysing. All the tested compounds penetrated the cell membrane and showed good GBA1 inhibition at 10 and 1 µM. Compounds **47y** and **(*R*)-85y** were also assayed at 0.1 µM showing, respectively, 74 and 66% of GBA1 inhibition. All the tested compounds, even CBE, showed a recovery of GBA1 activity after inhibitor removal, although inositol

derivative **47y** showed the lowest ratio of activity recovery, perhaps due to low ratio of excretion of this compound out of the cell.

4. CONCLUSIONS

Això ha estat possible perqué algú un dia ho va somniar.

Anònim

4.1 Study of the influence of the pK_a of the amino substitution in the side chain of DNJ derivatives

- A small library of DNJ-derivatives with and without protonable substituents at the end of the side chain were synthesized in order to evaluate the influence of the pK_a of this group in the imiglucerase inhibition.

- Compounds **16d(I-III)**, **24d**, **31d(I-V)** and **43** resulted better imiglucerase inhibitors than NB-DNJ(IC_{50} 430 µM at pH 5.2 and 145 µM at pH at pH 7.0) although not as potent as NN-DNJ(IC_{50} 1.0 µM at pH 5.2 and 0.25 µM at pH at pH 7.0).

- The triazole and azido derivatives **31d(I-IV)** and **24d** resulted better imiglucerase inhibitors than its corresponding amido and amino derivatives (compounds **16(I-III)** and **15d** respectively).

- The pK_a of **31b(VI)** and **31b(VII)**and other homologous triazole and amide derivatives without the DNJ core (compounds **34(II-IV)** and **35(II-IV, VI-VII)**) were experimentally determined, giving a range of pK_as of the terminal pyridines between 2.6 and 4.9. The derivatives with a terminal pyridine did not show higher Δ values in the imiglucerase assay than their corresponding homologues without this moiety.

- Derivative **44** presented experimental pK_a values of 4.85 and 6.18. Although a dibasic compound with these pK_a values would be expected to be neutral at pH 7.0 and ionized at pH 5.2, this compound did not show difference on its imiglucerase activity according to the pH of the assay. Its difference of inhibitory capacity (Δ = 2.0) was lower than other compounds without this ionizable group as compound **43** (Δ =3.2).

- The DNJ derivatives were evaluated as GCS inhibitors. Compounds **16d(I-III)**, **24d** and **31(I-V)** presented higher GCS inhibitory capacities than NB-DNJ, a drug that is actually administered as GCS inhibitor for treatment of GD.

- A family of compounds with potential dual interaction GCS inhibition and chaperone for GCasehas been discovered, having good selectivity against other commercial glycosidases and low cellular toxicity.

4.2 Study of the influence of the pK_a of the sugarmimethic core

- Small libraries of sugar mimetic compounds having DNJ ((2*R*,3*R*,4*R*,5*S*)-2-(hydroxymethyl)piperidine-3,4,5-triol), fluoroinositol ((1*R*,2*S*,3*R*,4*S*,5*S*,6*S*)-5-amino-6-fluorocyclohexane-1,2,3,4-tetraol) and *myo*-inositol ((1*S*,2*R*,3*S*,4*S*,5*S*,6*S*)-6-aminocyclohexane-1,2,3,4,5-pentaol) cores were synthesized. Different substituents were introduced in the β-position of the amine with the aim of modulating its pK_a and to study its influence in the inhibition of GCase.

- The in vitro screening in front imiglucerase revealed the hydroxynonyl DNJ derivative **(*R*)-85y** as the most potent imiglucerase inhibitor (78 nM IC_{50} at pH 5.2 and 45 nM at pH 7.0) described so far from the family of DNJ.

- The potency of the DNJ derivatives having an hydroxyl substituent defining a*R* configuration in theβ-carbon of the side chain of the DNJ derivatives (**(*R*)-85x** and **(*R*)-85y**) is higher than those with *S* configuration and those unsubstituted.In contrast,the inositol derivatives **(*R*)-89x** or **(*R*)-89y** did not show this diasteromeric effects. Most of the compounds analyzed also exhibit higher activity as inhibitors at pH 7.0 than pH 5.2 in the assay with imiglucerase and detergents.

- The pK_as of most of the synthesized compounds with different β-substitution were experimentally determined and it was evaluated the influence of those substituents in the pKa of the nitrogen of the sugarmimetic core. The derivatives with the same β-substitution showed similar pK_a values, independently of the carbon configuration (*R* or *S*) and the length of the chain (butyl or nonyl).

- The analysis of the pK_as and the Δ values for the inhibitors does not establish a direct correlation between both parameters. Even though, a tendency could be perceived as the compounds with higher Δ (compounds **(*R*)-89y**, **(*S*)-89y**, **67y**, **47y** and **47x**) presented pK_a between 7.2 and 8.9.

- Compound **67y** showed highest difference of imiglucerase inhibitory capacity according to the pH of the assay among all the tested compounds, showing an IC_{50} value 10 times lower when the assay was performed, in presence of detergents, at pH 7.0 than when it was carried out at pH5.2.

- The selectivity in front of GCS and other commercial glycosidases as well as the toxicity of the β-substituted compounds were also studied. In general, compounds with potent GCase inhibitory capacity (IC_{50} < 50 μM) showed good selectivity in front GCS and other commercial glycosidases, and acceptable safety windows.

4.3 GBA inhibition in detergent-free assays

- Evidence is provided on the importance of the assay conditions when determining the GCase inhibitory potency of compounds at different pHs. We demonstrate that the IC_{50} values obtained with recombinant enzyme with sodium taurocholate and Triton X-100® and the IC_{50} values obtained with cell homogenates without addition of exogenous detergents lead to totally different conclusions over the influence of the pH in GCase enzyme inhibition.

- Some representative compounds were tested as GBA1 inhibitors in a detergent-free assay with HAP1 (GBA2-KO) cell homogenates. Under these assay conditions, only inositol derivatives resulted better inhibitors at pH 7.0 than pH 5.2. In general, the Δ values obtained in the detergent-free assay were lower than those observed in the assay with imiglucerase and detergents.

- The *N*-butyl (**47x**), and *N*-hydroxybutyl (**(*R*)-89x** and **(*S*)-89x**) inositol derivatives showed the highest Δ values (4.7, 3.5 and 2.6 respectively) in the detergent-free assay.

- DNJ nonyl derivatives with hydroxyl (**85y**) or fluorine (**87y**) β-substitution showed the same Δ value for the *R* and *S* structures (0.3 for the hydroxyl derivatives, and 0.1 for the fluorine ones) in the assay with cell homogenates, regardless of their different potencies. In contrast, the Δ values for butyl derivatives **(*R*)-85x** and **(*R*)-87x**do not correlate with those of the *N*-nonyl ones, in spite of having very similar pK_a values. This would indicate that the inhibitor p$K_a$is not determinant for a high Δ value. ,

- No strongrelationship between the GCase inhibitionwith either the pK_a of the amine in the core, the side chain length or the configuration of the side chain β-substitution could be establishedindependently of the assay conditions.

- The capacity of GBA2 inhibition of the synthesized compounds was analyzed in cell homogenates, showing that DNJ derivatives are a family of potent and selective GBA2 inhibitors, most of them with nanomolar activity and with some sub-nanomolar inhibitors.

- A new GBA inhibition assay in intact cell has been developed, allowing the analysis of GBA1 or GBA2 activity directly in the culture plate or taking the supernatants in an alternative plate, without the need of lysate cells, in presence or after removing the inhibitor. This assay allows the study of the GBA cellular activity recovery due treatment and removal with inhibitors using a single cell batch. .

- The data obtained in the new assay in intact cell suggested that 4-MUG penetrates the cell but when it is cleaved, the fluorogenic 4-MU is not accumulated inside the cell but excreted to the medium.

- Some representative compounds were tested as GBA2 inhibitors in intact cell assays, showing full blockage of this enzyme when cells were cultured for 26 h with 10 μM concentrations of inhibitor.

- All the compounds tested as GBA1 inhibitors in the intact cell assays showed good GBA1 inhibition at 10 μM and 1 μM. Most of them, includingCBE, showed moderate or high recovery of GBA activity after 1.5 days of inhibitor removal. On the contrary, **47y** showed significant lower recovery of GBA activity after inhibitor removal, suggesting a high intracellular retention of this compound.

5. EXPERIMENTAL SECTION

If you always do what you always did, you will always get what you always got.

Albert Einstein

Experimental section contents

5.1 Synthesis and product characterization.

5.1.1 General methods

5.1.1.1 Compound purification and characterization

5.1.1.2 pK_a determination

5.1.1.3 Microwave reactions

5.1.1.4 General synthetic procedures

5.1.2 Synthesis of DNJ derivatives with substitution at the end of the side chain

5.1.2.1 Synthesis of DNJ amino and amido derivatives (compounds **15(a-d)** and **16d**)

5.1.2.2 Synthesis of DNJ azido and triazole derivatives (compounds **24** and **31**)

5.1.2.2.1 Failed attempts for synthesis of DNJ azido derivatives **24**. Synthesis of compounds **18**, **19**, **20**, **26**, **25**, **27**, **23** and **22**

5.1.2.2.2 Synthesis of **24d** and triazole derivatives **31**

5.1.2.3 Synthesis of amido derivatives **34(II-IV)** and **38** and triazole derivatives **35**

5.1.2.4 Synthesis of compounds **43** and **44**

5.1.3 Synthesis of compounds with different pK_a in the sugarmimethic core

5.1.3.1 Synthesis of *myo*-inositol benzylated core (compounds **49**, **53**-**60**, **62** and **63**)

5.1.3.2 Synthesis of fluoroinositol derivatives (compounds **66**, **67x**, **67y**, **68x** and **68y**)

5.1.3.3 Synthesis of benzylated *myo*-inositol and DNJ derivatives

5.1.3.3.1 Benzylated *N*-butil inositol derivatives (synthesis of compounds **72** and **74**).

5.1.3.3.2 Benzylated 2,2-difluorobutyl inositol and DNJ derivatives (synthesis of compounds **73**, **75**, **80** and **81**)

5.2 Biological assays.

5.2.1 Assays with purified enzyme

5.2.2.1 Imiglucerase inhibition assay with detergents

5.2.2.2 General procedure for the inhibition assay against other commercial glycosidases

5.2.2 Cell lines and culture

5.2.3 Assays with cell homogenates

5.2.3.1 Determination of glucosylceramide synthase activity in A549 cell homogenates

5.2.3.2 Determination of GBA1 inhibition in HAP1_001 (GBA2-KO) cell homogenates

5.2.3.3 Determination of GBA2 Inhibition in CHO_G4A11 (GBA2 over expressed) cell homogenates

5.2.4 Assays with intact cell

5.2.4.1 Cytotoxicity assay in WT-human fibroblasts

5.2.4.2 GBA Inhibition Assay in HAP1_001 (GBA2-KO or GBA1-KO) intact cell

5.1 Synthesis and product characterization

5.1.1 General methods

All moisture-sensitive reactions were carried out under nitrogen. All the materials were obtained commercially and used without further purification. Solvents were dried prior to use with Pure Solv-EN^{TM} system or distilled and dried by standard methods.

5.1.1.1 Compound purification and characterization

When possible, reactions or purifications were monitored by **thin-layer chromatography**(TLC) carried out on silica gel (Alugram Sil G/UV) using UV light (254 nm) or ethanolic solution of phosphomolybdic acid as visualizing agents.

Purifications by ***flash* chromatography** were done using:

a) silica gel 60 (40-63 microns, Panreac)
b) Biotage® KP-Sil column when using Flash^{+} Biotage® purification system
c) Biotage® SNAP Cartridges when using Biotage® Isolera PrimeTM *flash* purification system.

IR spectra were registered as film and were recorded with a Thermo Nicolet Avatar 360 FT-IR Spectometer.

$[\alpha]_D$ values were measured in microaperture mode with a Perkin–Elmer 341 polarimeter with Na/NaI lamp (589 nm) and 1 dm of lengh cell (1 ml of capacity). $[\alpha]_D$ are expressed in degrees and calculated as *c* x 100 / (d x m) (where *c* is the concentration of the sample (in g/100 ml), *d* is the optical way (in dm) and *m* is the measured value (mean of 10 measurements)).

NMR spectra were recorded on an Agilent VNMRS-400 (^{1}H at 400.10 MHz and ^{13}C at 100.62 MHz). The following abbreviations were used to designate multiplicities: s=singlet, d=doublet, t=triplet, q=quartet, m=multiplet, q=quintuplet, br=broad, dd=double-doublet, ddd=double-double-doublet. Chemical shifts were expressed in ppm relative to TMS and coupling constant (*J*) in Hz.

Chiral-HPLC were run on a HPLC-UV Breeze coupled to a UV/visible Waters 2489 detector (λ= 220nm). 30 µl of sample 1 mg/ml in Hx/IPA 9:1 were injected in a Daicel Chiralpack IA column. Mobil phase: isocratic Hx/IPA 9:1, flow: 0.7 ml/min, run time: 18 min.

HPLC-PDA-MS were performed with a High-Performance Liquid Chromatography Thermo Ultimate 3000SD (Thermo Scientific Dionex) coupled to a photodiode array detector and a mass spectrometer LTQ XL ESI-ion trap (Thermo Scientific); 5µl of sample 0.5 mM in MeOH were injected in a Zorbax Extend –C18 (3.5 µm, 2.1x50mm) column at 30ºC. Mobil phase: A=0.1% NH_4OH (30%) in water, B= 0.1% NH_4OH (30%) in ACN. Flow 0.6 ml/min, 5%B-100% B 3 min, 100%B 3 min, total runtime 10 min. Data from PDA spectra were analyzed at 210 nm. Data from mass spectra were analyzed by electrospray ionization in positive and negative mode every 0.3 s (m/z 50-1500) and peaks are given m/z (% of basis peak).

Purifications by **preparative HPLC** were performed with Delta prep (DP4KF) instrument(Waters) coupled to a Waters fraction collector (III). Column Gemini® Phenomenex C18 (particle size 5 µm, pore size 100 Å, 250x10 mm). Flow: 10 ml/min. Fractions were collected in tubes and analyzed separately by **HPLC-ELS** (Waters 2695 Alliance HPLC System coupled to a PL-ELS-1000 detector) or **HPLC-PDA-MS**.

High-resolution mass spectra (HRMS) were analyzed by FIA (flux injected analysis) with Ultrahigh-Performance Liquid Chromatography (UPLC) Aquity (Waters) coupled to LCT Premier Orthogonal Accelerated Time of Flight Mass Spectrometer (TOF) (Waters). Data from mass spectra were analyzed by electrospray ionization in positive and negative mode. Spectra were scanned between 50 and 1500 Da with values every 0.2 seconds and peaks are given m/z. Data was acquired with MassLynx software version 4.1 (Waters). These analyses were performed by the mass spectrometry service of IQAC-CSIC.

5.1.1.2 pK_a determination

General method for pKa determination: 1-2 mg of compound (hydrochloride) was dissolved in 1.5 ml of water in a 3 ml vial with magnetic stirring. This mixture was titrated with NaOH 0.01N using Titrando-888 (Metrohm®) with pH-microelectrode. The pHs of the mixture were monitorized and the ending point and pKa values were determined using Tiamo® software. The ending point (EP1) was defined as the inflexion point of the titration curve, while pK_a was

determined as the pH of the sample when half of the volume added at the ending point was added (HP1).

For compound **44**, the pK_a was determined as follows: 1.23 mg of **44** were dissolved in 3 ml of aqueous NaCl 150mM in a 25ºC thermostated vessel with magnetic stirring. Then, 120 µl of HCl 0.1M were added and the mixture tritrated with successive additions of 3 µl of NaOH 0.1M under a weak nitrogen stream by using Titrando-888 (Metrohm®) with pH-microelectrode. The evolution of pH was monitored and recorded with Tiamo® software. Data analysis was performed by Dr. Ignacio Alfonso from Supramolecular Chemistry Group, at IQAC-CSIC, using the computer program HYPERQUAD®.

5.1.1.3 Microwave reactions

Reactions under microwave irradiation were carried out in a CEM Discover Focused™ Microwave reactor. The instrument consists in a continuous focused microwave power delivery system with operator selectable power output from 0-300W. Reactions were performed in glass vessels of 10 mL sealed with septum. The temperature of the content of the vessel was monitored using an IR sensor and the indicated temperature corresponds to the maximal temperature reached during each experiment. The content of the vessels are stirred by means of rotating magnetic plate located below the floor of the microwave cavity and a Teflon coated magnetic stir bar in the vessel. The specified time corresponds to the total irradiation time. Efficient cooling is accomplished by means of pressurized air during entire experiment.

5.1.1.4 General synthetic procedures

General methodologies for debenzylation:

Method A[127]: hydrogenation with $Pd(OH)_2/C$

Palladium hydroxide (20% on carbon) (0.2 equivalent-mol) and HCl aq (6 equivalent-mol) were added to a 0.08 M solution of the corresponding benzylated derivative. The suspension was stirred at room temperature under 1.5 atm of H_2. When the debenzylation was completed, the catalyst was filtered over a pad of Celite®, and the solvent was removed by evaporation under reduced pressure to give the desired product.

Method B[132]: debenzylation with BCl_3

A 1M solution of BCl_3 in heptane (8 equivalent-mol) was added to a solution of the corresponding benzylated derivative (1 equivalent-mol) in DCM (0.02 M) at -78ºC. The resulting mixture was stirred at -78 ºC over 3 h. After, it was allowed to reach room temperature for 2 h. After this, the reaction was cooled again to -78 ºC. Then MeOH (0.01 M) was added and the mixture was stirred at rt overnight. The next day, the solvent was distilled off under reduced pressure. The crude was redissolved in MeOH/H_2O 2:1 (0.02 M) and filtered through an anionic resin (IRA-400 (OH^-)), and purified by column chromatography if needed.

General procedure for acylations:

EDC (1.5 equivalent-mol), HOBT (1.5 equivalent-mol) and Et_3N (2.5 equivalent-mol) were added to a solution of the corresponding acid (1.1equivalent-mol) in AcOEt (0.2 M). The mixture was stirred for 15 min at room temperature. Then, this suspension was added dropwise to a solution of the corresponding amine (1 equivalent-mol) in AcOEt. The mixture was stirred overnight at room temperature. After that, the mixture was partitioned over H_2O and the two layers were separated. The aqueous phase was extracted again with AcOEt. The combined organic phases were washed with aq. $NaHCO_3$sat (2x), dried over anh. Na_2SO_4 and filtered. The solvent was distilled off under reduced pressure and the residue was purified by *flash* chromatography, if necessary.

5.1.2 Synthesis of DNJ derivatives with substitution at the end of the side chain

5.1.2.1 Synthesis of DNJ amino and amido derivatives (compounds 15(a-d) and 16d)

- **General method[125] for the synthesis of azidoalcohol derivatives 11(a-d)**:

To a mixture of the corresponding bromoalcohol (1 equivalent-mol) in DMF (0.8 M), 4 equivalent-mol of sodium azide were added. The reaction mixture was stirred at 70 ºC for 16 h. Then, it was cooled to room temperature and diluted with water (100 ml) and saturated aqueous solution of $NaHCO_3$ (50 ml). The mixture was extracted with AcOEt (3 x 50 ml). The combined organic layers were dried over $Na_2SO_{4anh}$and filtered. The solvent was removed under reduced vacuum and the obtained residue was purified by *flash* chromatography on silica gel (Flash$^+$ Biotage®, KP-Sil 40+S column, eluent DCM), giving the corresponding azidoalcohol **11(a-d)**.

Synthesis of 3-azidopropan-1-ol (11a)

Following the general method for the synthesis of azidoalcohol derivatives, from 0.6 ml of 3-bromopropan-1-ol, 244 mg of **11a** were obtained as a yellowish oil (35% yield), with an ^{1}H NMR spectra in concordance with the previously reported[162].

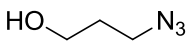

11a: ^{1}H NMR (400 MHz, $CDCl_3$) δ 3.76 (q, *J* = 5.5 Hz, 2H), 3.45 (t, *J* = 6.6 Hz, 2H), 1.83 (p, *J* = 6.3 Hz, 2H), 1.58 – 1.46 (m, 1H).

Synthesis of4-azidobutan-1-ol (11b)

Following the general method for the synthesis of azidoalcohol derivatives, from 0.6 ml of 4-bromobutan-1-ol, 362 mg of **11b** were obtained as a colorless oil (48% yield), with an ^{1}H NMR and ^{13}C NMR spectra in concordance with the previously reported[125].

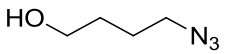

11b: ^{1}H NMR (400 MHz, $CDCl_3$) δ 3.67 (q, *J* = 5.5 Hz, 2H), 3.31 (t, *J* = 6.4 Hz, 2H), 1.76 – 1.59 (m, 4H), 1.40 – 1.31 (m, 1H).^{13}C NMR (101 MHz, $CDCl_3$) δ 62.23, 51.28, 29.77, 25.38.

Synthesis of 5-azidopentan-1-ol (11c)

Following the general method for the synthesis of azidoalcohol derivatives, from 0.75 ml of 5-bromopentan-1-ol, 442 mg of **11c** were obtained as a greenish oil (51% yield), with an ^{1}H NMR spectra in concordance with the previously reported[125].

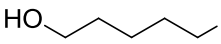

11c: ^{1}H NMR (400 MHz, $CDCl_3$) δ 3.65 (t, *J* = 6.4 Hz, 2H), 3.27 (t, *J* = 6.9 Hz, 2H), 1.69 – 1.54 (m, 4H), 1.51 – 1.39 (m, 2H), 1.34 – 1.22 (m, 1H).

Synthesis of 6-azidohexan-1-ol (11d)

Following the general method for the synthesis of azidoalcohol derivatives, from 0.72 ml of 6-bromohexan-1-ol, 595 mg of **11d**were obtained as a yellowish oil (75% yield), with an ^{1}H NMR spectra in concordance with the previously reported[163].

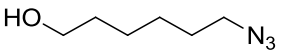

11d: ^{1}H NMR (400 MHz, $CDCl_3$) δ 3.63 (t, *J* = 6.5 Hz, 2H), 3.25 (t, *J* = 6.9 Hz, 2H), 1.66 – 1.51 (m, 4H), 1.43 – 1.32 (m, 5H).

- **General method[126] for the synthesis of azidotosylate derivatives12 (a-d)**:

At 0 ºC, toluenesulfonic chloride (1.05 equivalent-mol) was added to a solution of the azidoalcohol (1 equivalent-mol) and Et_3N (3 equivalent-mol) in dry DCM. The reaction mixture was stirred overnight at room temperature. Next day, it was diluted with AcOEt and washed with 10% aqueous solution of sodium hydrogensulphate. The aqueous phase was extracted with AcOEt (3x). The combined layers were washed with saturated aqueous solution of $NaHCO_3$ and dried over Na_2SO_{4anh}. The solvent was removed by distillation under reduced pressure, and the crude purified by *flash* chromatography on silica gel (Flash$^+$ Biotage®, KP-Sil 40+S column, eluent Hx/AcOEt 6:1) to give the corresponding azidotosylate **12(a-d)**.

Synthesis of 3-azidopropyl 4-methylbenzenesulfonate (12a)

Following the general method for the synthesis of the azidotosylate derivatives, from 483 mg of **11a,** 709 mg of **12a** were obtained as a colorless oil (58% yield).

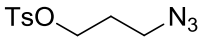

12a: ^{1}H NMR (400 MHz, $CDCl_3$) δ 7.85 – 7.74 (m, 2H), 7.39 – 7.32 (m, 2H), 4.11 (t, *J* = 5.9 Hz, 2H), 3.38 (t, *J* = 6.5 Hz, 2H), 2.46 (s, 3H), 1.97 – 1.77 (m, 2H).^{13}C NMR (101 MHz, $CDCl_3$) δ 144.99, 132.73, 129.90, 127.87, 66.94, 47.25, 28.43, 21.63. HRMS calculated for $C_{10}H_{14}NO_3S$: 228.0694 $[M\text{-}N_2]^+$; found: 228.0699.

Synthesis of4-azidobutyl 4-methylbenzenesulfonate (12b)

Following the general method for the synthesis of the azidotosylate derivatives, from 382 mg of **11b,** 495 mg of **12b** were obtained as a colorless oil (55% yield).

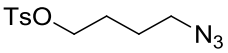

12b: ^{1}H NMR (400 MHz, $CDCl_3$) δ 7.77 (d, *J* = 8.2 Hz, 2H (2 x CH_{Ar}-C-SO_3)), 7.34 (d, *J* = 7.9 Hz, 2H (2 x CH_{Ar}-C-Me)), 4.04 (t, *J* = 6.1 Hz, 2H (CH_2-OTs)), 3.24 (t, *J* = 6.6 Hz, 2H (CH_2-N_3)), 2.44 (s, 3H (CH_3)), 1.79 – 1.56 (m, 4H ($C\underline{H_2}$-$C\underline{H_2}$-CH_2-N_3)). ^{13}C NMR (101 MHz, $CDCl_3$) δ 144.84; 132.96 (2 x C_{Ar}); 129.85 (2 x $\underline{C}H_{Ar}$-C-Me); 127.85 (2 x $\underline{C}H_{Ar}$-C-SO_3); 69.61 (CH_2-OTs); 50.63 (CH_2-N_3); 26.11 ($\underline{C}H_2$-CH_2-OTs); 25.00 ($\underline{C}H_2$-CH_2-N_3); 21.62 (CH_3). HRMS calculated for $C_{11}H_{16}NO_3S$: 242.0851 $[M\text{-}N_2]^+$; found: 242.0865.

Synthesis of 5-azidopentyl 4-methylbenzenesulfonate (12c)

Following the general method for the synthesis of the azidotosylate derivatives, from 480 mg of **11c,**908 mg of **12c**were obtained as a yellow oil (86% yield).

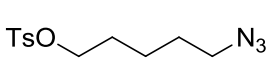

12c: ^{1}H NMR (400 MHz, $CDCl_3$) δ 7.79 (d, *J* = 8.3 Hz, 1H), 7.35 (dd, *J* = 8.6, 0.7 Hz, 1H), 4.03 (t, *J* = 6.3 Hz, 1H), 3.23 (t, *J* = 6.8 Hz, 1H), 2.45 (s, 2H), 1.74 – 1.61 (m, 1H), 1.61 – 1.47 (m, 2H), 1.44 – 1.35 (m, 1H).HRMS calculated for $C_{12}H_{18}NO_3S$: 256.1007 $[M\text{-}N_2]^+$; found: 256.0999.

Synthesis of 6-azidohexyl 4-methylbenzenesulfonate (12d)

Following the general method for the synthesis of the azidotosylate derivatives, from 595 mg of **11d,** 1.025 g of **12d** were obtained as a brown oil (83% yield).

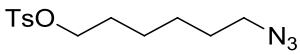

12d: ^{1}H NMR (400 MHz, $CDCl_3$) δ 7.77 (d, *J* = 8.2 Hz, 2H), 7.33 (d, 2H), 4.01 (t, *J* = 6.4 Hz, 2H), 3.21 (t, *J* = 6.8 Hz, 2H), 2.44 (s, 3H), 1.70 – 1.46 (m, 4H), 1.41 – 1.24 (m, 4H).^{13}C NMR (101 MHz, $CDCl_3$) δ 144.68, 133.14, 129.79, 127.84, 70.28, 51.20, 28.67, 28.59, 26.04, 24.95, 21.60. HRMS calculated for $C_{13}H_{20}NO_3S$: 270.1164 $[M\text{-}N_2]^+$; found: 270.1175.

Synthesis of (2*R*,3*R*,4*R*,5*S*)-1-(6-azidohexyl)-3,4,5-tris(benzyloxy)-2-((benzyloxy)methyl)piperidine (14d)

- Analysis of different conditions for the *N*-alkylation of DNJ with tosylates. Synthesis of 14d:

A) Thermic reaction

Based on previously reported procedure[124], 63.7 mg (0.214 mmol) of azidotosylate **12d** and 99 mg (0.714 mmol) of K_2CO_3 were added to a solution of 100 mg (0.179 mmol) of **13** in 1 ml of **ACN or DMSO**. The reaction mixture was heated to **85ºC or 120ºC** for **12 h or 48h** under argon atmosphere. After, the reaction was cooled to room temperature and the solvent was evaporated under reduced pressure. Water and **DCM or AcOEt** were added to the residue and the whole mixture was stirred for 10 min, and then partitioned. The aqueous layer was extracted with **DCM or AcOEt** (3x). The combined organic extracts were dried over Na_2SO_{4anh}, filtrated and the solvent was removed by distillation under reduced pressure. After Purification by *flash* chromatography on silica gel eluting with Hx/AcOEt 5:1 (Flash$^+$ Biotage®, KP-Sil 12+M column), **14d** was obtainedas yellowish oil.

Trial	solvent	conditions	Work-up	mg **14d**:	yield
I	ACN	85ºC 12 h	DCM	16.9	15%
II	ACN	85ºC **48 h**	**AcOEt**	36.4	31%
III	**DMSO**	**120ºC 48 h**	AcOEt	11.9	10%

Table 13 Synthesis of **14d** under different conditions via thermic reactions.

B) Microwave irradiation

In a 10ml vessel with a magnetic stir bar, it was introduced a solution of 100 mg (0.179 mmol) of **13** dissolved in 1 ml of ACN. Then, **1.2 or 1.7 equivalent-mol** of azidotosylate **12d**, 99 mg (0.714 mmol) of K_2CO_3 were introduced. For one trial, **3 mg** (0.018 mmol) of KI were also introduced at this point. The vessel was sealed with a septum and submitted to MW irradiation (T max = 85ºC, power = 150 w, t = 2 h). After, water and AcOEt were added to the vessel and the whole mixture was stirred for 10 min, and finally partitioned. The aqueous layer was extracted with AcOEt (3x). The combined organic extracts were dried over Na_2SO_{4anh}, filtrated

and the solvent was removed by distillation under reduced pressure. The resulting residue was purified by *flash* chromatography on silica gel eluting with Hx/AcOEt 5:1 (Flash$^+$ Biotage®, KP-Sil 12+M column).

Trial	eq **12d**	eq KI	solvent	MW conditions	mg **14d**	yield
IV	1.2	--	ACN	Tmax=85ºC, 150 w 2 h	38.4	33%
V	**1.7**	**0.1**	ACN	Tmax=85ºC, 150 w 2 h	62.0	53%

Table 14 Synthesis of **14d** under different conditions via microwave irradiation.

(Note that the procedure followed in *Trial V* for the synthesis of **14d**, was also used to synthesize other derivatives, named as *Method A for the N-alkylation with tosylates).*

The analytical data for **14d** were in agreement with those reported in the literature[132]:

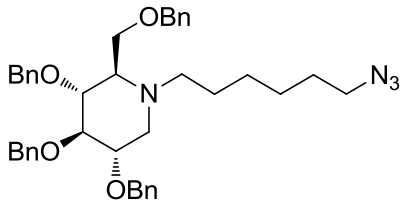

14d: ^{1}H NMR (400 MHz, $CDCl_3$) δ 7.39 – 7.21 (m, 18H), 7.20 – 7.08 (m, 2H), 5.00 – 4.75 (m, 3H), 4.74 – 4.57 (m, 2H), 4.55 – 4.36 (m, 3H), 3.75 – 3.39 (m, 5H), 3.22 (t, *J* = 6.9 Hz, 2H), 3.07 (dd, *J* = 11.2, 4.9 Hz, 1H), 2.73 – 2.46 (m, 2H), 2.36 – 2.14 (m, 2H), 1.63 – 1.50 (m, 2H), 1.45 – 1.09 (m, 8H). ^{13}C NMR (101 MHz, $CDCl_3$) δ 139.00, 138.54, 137.78, 128.41, 128.35, 128.33, 128.30, 128.28, 127.83, 127.80, 127.60, 127.50, 127.40, 87.35, 78.60, 78.52, 75.28, 75.16, 73.41, 72.75, 65.43, 63.76, 54.46, 52.20, 51.31, 28.78, 26.99, 26.57, 23.59. HRMS calculated for $C_{40}H_{49}N_4O_4$: 649.3754 $[M+H]^+$; found: 649.3688.

- **Method A for the *N*-alkylation with tosylates. Synthesis of 14 (a-d)**:

A 0.2M solution of **13** (1.0 equivalent-mol.) in ACN was introduced in a 10ml vessel with a magnetic stir bar. Then, 1.7equivalent-mol of the corresponding azidotosylate, 4 equivalent-mol of K_2CO_3 and 0.1equivalent-mol of KI were added. The vessel was sealed with a septum and submitted to MW irradiation (T max = 85ºC, power = 150 w, t = 2 h). After, water and AcOEt were added to the vessel and the whole mixture was stirred for 10 min, and finally partitioned. The aqueous layer was extracted with AcOEt (3x). The combined organic extracts were dried over $Na_2SO_{4anh,}$and filtrated. The solvent was removed by distillation under reduced pressure and the resulting residue was purified by *flash* chromatography on silica gel (Flash$^+$ Biotage®, KP-Sil 40+S column).

- **Method B for the *N*-alkylation with tosylates. Synthesis of 14 (b-c)**:

A 0.2M solution of **13** (1.0 equivalent-mol) in ACN was introduced in a 10 ml vessel with a magnetic stir bar. Then, 1.7equivalent-mol of the corresponding azidotosylate and 4 equivalent-mol of DIPEA were added. The vessel was sealed with a septum and submitted to MW irradiation (T max = 85ºC, power = 150 w, t = 2 h). After, the solvent was removed under reduced pressure. The obtained crude was partitioned with DCM and a saturated aqueous solution of $NaHCO_3$. The aqueous layer was extracted with DCM (3x). The combined organic extracts were dried over anhydrous Na_2SO_4, and filtrated. The solvent was removed by distillation under reduced pressure and the resulting residue was purified by *flash* chromatography on silica gel (Flash$^+$ Biotage®, KP-Sil 40+S column).

Synthesis of(2*R*,3*R*,4*R*,5*S*)-1-(3-azidopropyl)-3,4,5-tris(benzyloxy)-2-((benzyloxy)methyl)piperidine (14a)

According to *Method A for the N-alkylation with tosylates*, from 250 mg of **13** hydrochloride and 194 mg (0.759 mmol) of **12a**, after a *flash* chromatography eluting with Hx/AcOEt 6:1, 140 mg of **14a** were obtained as a colorless oil (52% yield). Moreover, 53 mg of **13** were recovered after eluting the column with Hx/AcOEt 3:2.

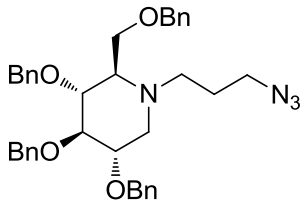

14a: ^{1}H NMR (400 MHz, $CDCl_3$) δ 7.35 – 7.23 (m, 18H), 7.16 – 7.12 (m, 2H), 4.99 – 4.80 (m, 3H), 4.67 (q, *J* = 11.6 Hz, 2H), 4.52 – 4.38 (m, 3H), 3.73 – 3.41 (m, 5H), 3.28 – 3.12 (m, 2H), 3.04 (dd, *J* = 11.2, 4.9 Hz, 1H), 2.86 – 2.74 (m, 1H), 2.60 (ddd, *J* = 13.9, 9.3, 5.0 Hz, 1H), 2.35 – 2.28 (m, 1H), 2.20 (t, *J* = 10.8 Hz, 1H), 1.75 – 1.56 (m, 2H). ^{13}C NMR (101 MHz, $CDCl_3$) δ 138.91, 138.42, 137.66, 128.37, 128.33, 128.29, 127.82, 127.66, 127.54, 127.42, 87.22, 78.52, 78.33, 75.29, 75.18, 73.38, 72.81, 65.83, 64.01, 54.53, 49.64, 49.38, 23.95.IR (neat) : 2095 cm^{-1}(N_3) cm^{-1}. $[\alpha]^{25}_D$ -4º (*c* 0.9, $CHCl_3$).

Synthesis of (2*R*,3*R*,4*R*,5*S*)-1-(4-azidobutyl)-3,4,5-tris(benzyloxy)-2-((benzyloxy)methyl)piperidine (14b)

According to *Method A for the N-alkylation with tosylates*, from 330 mg of **13** hydrochloride and 270 mg (1.002 mmol) of **12b**, after a *flash* chromatography eluting with Hx/AcOEt 5:1, 34 mg of **14b** were obtained as a colorless oil (9% yield). Moreover, 127 mg of **13** were recovered after eluting the column with Hx/AcOEt 3:2.

According to *Method B for the N-alkylation with tosylates*, from 300 mg of **13** hydrochloride and 254 mg (0.911 mmol) of **12b**, after a *flash* chromatography eluting with Hx/AcOEt 4:1, 53 mg of **14b** were obtainedas a colorless oil(16% yield). After eluting the column with Hx/AcOEt 1:1, 117 mg of **13** were recovered.

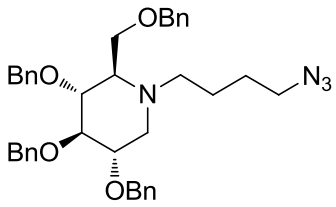

14b: ^{1}H NMR (400 MHz, $CDCl_3$) δ 7.44 – 7.18 (m, 18H_{Ar}), 7.19 – 7.11 (m, 2H_{Ar}), 5.00 – 4.77 (m, 3H (CH_2Bn)), 4.75 – 4.61 (m, 2H (CH_2Bn)), 4.53 – 4.39 (m, 3H (CH_2Bn)), 3.72 – 3.52 (m, 4H (2xCH-OBn and CH-C$\underline{H_2}$-OBn)), 3.47 (t, *J* = 9.0 Hz, 1H (CH-OBn)), 3.23 – 3.14 (m, 2H (CH_2-N_3)), 3.06 (dd, *J* = 11.6, 5.0 Hz, 1H (CH-C$\underline{H_{2a}}$-N)), 2.78 – 2.62 (m, 1H (N-C$\underline{H_{2a}}$-$(CH_2)_3$-N_3)), 2.62 – 2.47 (m, 1H (N-C$\underline{H_{2b}}$-$(CH_2)_3$-N_3)), 2.37 – 2.26 (m, 1H (C$\underline{H}$-CH_2-OBn)), 2.26 – 2.14 (m, 1H (CH-C$\underline{H_{2b}}$-N)), 1.56 – 1.35 (m, 4H (N-CH_2-C$\underline{H_2}$-C$\underline{H_2}$-CH_2-N_3)). ^{13}C NMR (101 MHz, $CDCl_3$) δ 138.93, 138.46, 137.66 (4 x C_{Ar}); 128.53, 128.41, 128.38, 128.33, 128.30, 127.92, 127.84, 127.82, 127.75, 127.66, 127.61, 127.55, 127.44, 126.95 (20 x CH_{Ar}); 87.26, 78.50, 78.48 (3 x CH-OBn); 75.30, 75.20, 73.39, 72.82 (4 x CH_2-Ph); 65.58 (CH_2-OBn); 63.89 (CH-N); 54.31 (CH-$\underline{C}H_2$-N); 51.62 (CH_2-$\underline{C}H_2$-N); 51.12(CH_2-$\underline{C}H_2$-N_3); 26.67, 21.16 (N-CH_2-$\underline{C}H_2$-$\underline{C}H_2$-CH_2-N_3). IR (neat): 2095 cm^{-1}(N_3) cm^{-1}. HRMS calculated for $C_{38}H_{45}N_4O_4$: 621.3441 $[M+H]^+$; found: 621.3466. $[\alpha]^{24}_D$ -4° (*c* 1.2, $CHCl_3$).

Synthesis of (2*R*,3*R*,4*R*,5*S*)-1-(5-azidopentyl)-3,4,5-tris(benzyloxy)-2-((benzyloxy)methyl)piperidine (14c)

According to *Method A for the N-alkylation with tosylates*, from 330 mg of **13** hydrochloride and 284 mg (1 mmol) of **12c**, after a *flash* chromatography eluting with Hx/AcOEt 5:1 and 3:1, 84 mg of **14c** were obtained (23% yield) as a colorless oil. Moreover, 100 mg of **13** were recovered after eluting the column with Hx/AcOEt 3:2.

According to *Method B for the N-alkylation with tosylates*, from 227 mg of **13** and 209 mg (0.737 mmol) of **12b**, after a *flash* chromatography eluting with Hx/AcOEt 4:1, 161 mg of **14c** were obtained (59% yield). After eluting the column with Hx/AcOEt 1:1, 15 mg of **13** were recovered.

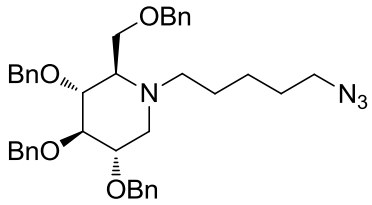

14c: ^{1}H NMR (400 MHz, $CDCl_3$) δ 7.38 – 7.21 (m, 18H), 7.18 – 7.07 (m, 2H), 4.99 – 4.76 (m, 3H), 4.72 – 4.58 (m, 2H), 4.52 – 4.37 (m, 3H), 3.68 – 3.39 (m, 5H), 3.19 (t, *J* = 6.9 Hz, 2H), 3.05 (dd, *J* = 11.2, 4.9 Hz, 1H), 2.75 – 2.59 (m, 1H), 2.58 – 2.47 (m, 1H), 2.28 (d, *J* = 9.5 Hz, 1H), 2.19 (t, *J* = 10.8 Hz, 1H), 1.53 – 1.09 (m, 6H). ^{13}C NMR (101 MHz, $CDCl_3$) δ 138.97, 138.50, 137.72, 128.35, 128.28, 127.82, 127.61, 127.51, 127.40, 87.32, 78.49, 75.27, 75.16, 73.40, 72.76, 65.45, 63.80, 54.45, 52.07, 51.33, 28.68, 24.57, 23.38. IR (neat): 2096 cm^{-1}(N_3) cm^{-1}. $[\alpha]^{24}_{D}$ -3° (*c* 1.0, $CHCl_3$).

Synthesis of (2*R*,3*R*,4*R*,5*S*)-1-(3-aminopropyl)-2-(hydroxymethyl)piperidine-3,4,5-triol dihydrochloride (15a)

According to *Method A: hydrogenation with Pd(OH)$_2$/C*, from a solution of 140 mg (0.231 mmol) of **14a** in MeOH**,** after 16h of reaction, 57 mg of **15a** were obtained as a colorless oil (87% yield).

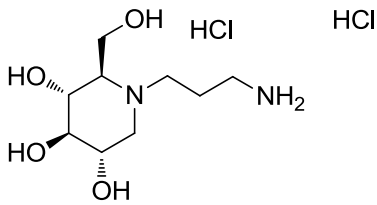

15a: ^{1}H NMR (400 MHz, D_2O) δ 4.05 – 3.79 (m, 2H), 3.74 – 3.60 (m, 1H), 3.58 – 3.43 (m, 2H), 3.43 – 3.30 (m, 2H), 3.23 – 3.15 (m, 1H), 3.15 – 3.05 (m, 1H), 3.03 – 2.90 (m, 3H), 2.15 – 1.91 (m, 2H).^{13}C NMR (101 MHz, D_2O) δ 75.66, 66.93, 65.80, 65.66, 53.72, 52.96, 48.78, 36.40, 21.08. HPLC (ESI) 77.4% rt: 0.82'; m/z: 221.14. HRMS calculated for $C_9H_{21}N_2O_4$: 221.1501 $[M+H]^+$; found: 221.1503. $[\alpha]^{28}_{D}$ -2° (*c* 0.45, H_2O).

Synthesis of (2*R*,3*R*,4*R*,5*S*)-1-(4-aminobutyl)-2-(hydroxymethyl)piperidine-3,4,5-triol dihydrochloride (15b)

According to *Method A: hydrogenation with Pd(OH)$_2$/C*, from a solution of 91 mg (0.147 mmol) of **14b** in THF/MeOH 1:1, after 48h of reaction, 50 mg of **15b** were obtained as a yellow oil (100% yield).

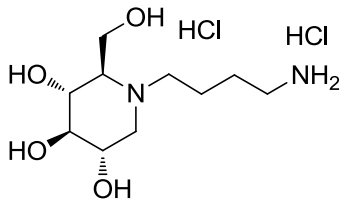

15b: ^{1}H NMR (400 MHz, D_2O) δ 4.06 – 3.85 (m, 2H (CH_2-OH)), 3.80 – 3.65 (m, 1H (C<u>H</u>-OH)), 3.65 – 3.47 (m, 2H (2 x C<u>H</u>-OH)), 3.44 (t, *J* = 9.4 Hz, 1H (CH-C<u>H$_{2a}$</u>-N)), 3.40 – 3.28 (m, 1H (N-C<u>H$_{2a}$</u>-CH_2)), 3.25 – 3.08 (m, 2H (N-C<u>H$_{2b}$</u>-CH_2 and C<u>H</u>-CH_2OH)), 3.07 – 2.91 (m, 3H (CH-C<u>H$_{2b}$</u>-N and C<u>H$_2$</u>-NH_2)), 1.92 – 1.58 (m, 4H (N-CH_2-C<u>H$_2$</u>-C<u>H$_2$</u>-CH_2-NH_2)). ^{13}C NMR (101 MHz, D_2O) δ 75.71, 66.95, 65.89 (3 x CH-OH), 65.39 (C<u>H</u>-CH_2OH); 53.62 (CH_2-OH); 52.94 (CH-C<u>H$_2$</u>-N); 52.29 (N-C<u>H$_2$</u>-CH_2); 38.67 (CH_2-NH_2); 23.82, 19.84 N-CH_2-C<u>H$_2$</u>-C<u>H$_2$</u>-CH_2-NH_2).HRMS calculated for $C_{10}H_{23}N_2O_4$: 235.1658 $[M+H]^+$; found: 235.1678. IR (neat): 3367 (OH st), 2947(CH st) cm^{-1}. $[\alpha]^{26}_{D}$ -3° (*c* 0.18, MeOH).

Synthesis of (2*R*,3*R*,4*R*,5*S*)-1-(5-aminopentyl)-2-(hydroxymethyl)piperidine-3,4,5-triol dihydrochloride (15c)

According to *Method A: hydrogenation with Pd(OH)$_2$/C*, from a solution of 315 mg (0.496 mmol) of **14c** in THF/MeOH 1:1, after 48h of reaction, 133 mg of **15c** were obtained as a colorless oil (83% yield).

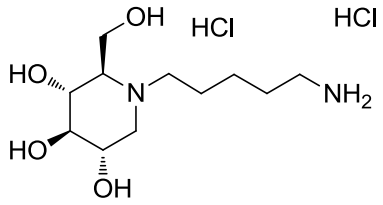

15c: ^{1}H NMR (400 MHz, MeOD) δ 4.10 (d, *J* = 12.6 Hz, 1H), 3.99 – 3.88 (m, 1H), 3.77 – 3.65 (m, 1H), 3.58 (t, *J* = 9.8 Hz, 1H), 3.52 – 3.32 (m, 3H), 3.25 – 3.17 (m, 1H), 3.11 – 2.87 (m, 4H), 1.93 – 1.66 (m, 4H), 1.58 – 1.39 (m, 2H). ^{13}C NMR (101 MHz, MeOD) δ 76.68, 67.38, 66.36, 66.05, 53.56, 52.61, 38.92, 26.61, 25.23, 23.11, 22.23.HRMS calculated for $C_{11}H_{25}N_2O_4$: 249.1814 $[M+H]^+$; found: 249.1792. $[\alpha]^{28}_{D}$ -5° (*c* 0.45, H_2O).

Synthesis of (2*R*,3*R*,4*R*,5*S*)-1-(6-aminohexyl)-2-(hydroxymethyl)piperidine-3,4,5-triol dihydrochloride (15d)

According to *Method A: hydrogenation with Pd(OH)$_2$/C*, from a solution of 104 mg (0.160 mmol) of **14d** in MeOH, after 16h of reaction, 55.28 mg of **15d**were obtained as a brown foam (100% yield).

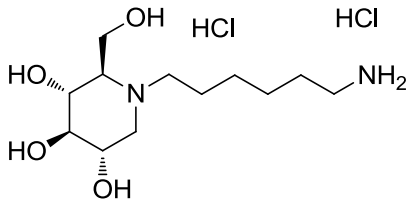

15d: ^{1}H NMR (400 MHz, MeOD) δ 4.10 (d, *J* = 12.5 Hz, 1H (C<u>H$_{2a}$</u>-OH)), 3.95 – 3.82 (m, 1H (C<u>H$_{2b}$</u>-OH)), 3.77 – 3.63 (m, 1H (C<u>H</u>-OH)), 3.64 – 3.51 (m, 1H (C<u>H</u>-OH)), 3.50 – 3.32 (m, 3H (C<u>H</u>-OH, CH-C<u>H$_{2a}$</u>-N and N-C<u>H$_{2a}$</u>-CH$_2$)), 3.25 – 3.15 (m, 1H (N-C<u>H$_{2b}$</u>-CH$_2$)), 3.08 – 2.87 (m, 4H (C<u>H</u>-CH$_2$-OH, CH-C<u>H$_{2b}$</u>-N and C<u>H$_2$</u>-NH$_2$)), 1.95 – 1.61 (m, 4H (N-CH$_2$-C<u>H$_2$</u>-CH$_2$-CH$_2$-C<u>H$_2$</u>-CH$_2$-NH$_2$)), 1.56 – 1.35 (m, 4H (N-CH$_2$-CH$_2$-C<u>H$_2$</u>-C<u>H$_2$</u>-CH$_2$-CH$_2$-NH$_2$)). ^{13}C NMR (101 MHz, MeOD) δ 76.66, 67.39, 66.37 (3x CH-OH); 66.08 (<u>C</u>H-CH$_2$-OH); 53.63 (CH$_2$-OH); 53.49 (CH-<u>C</u>H$_2$-N); 52.84 (N-<u>C</u>H$_2$-CH$_2$); 39.13 (CH$_2$-NH$_2$), 26.86, 25.66, 25.47, 22.52 (N-CH$_2$-(<u>C</u>H$_2$)$_4$-CH$_2$NH$_2$).HRMS calculated for $C_{12}H_{27}N_2O_4$: 263.1971 $[M+H]^+$; found: 263.1963.IR (neat) : 3334 (OH st), 2947(CH st) cm^{-1}. $[\alpha]^{23}_{D}$ -3º (*c* 1.0, MeOH).

- **General method for the synthesis of the amide derivatives (16d(I-III)):**

For thepreparation of the polymer-bound activated ester[164],0.143 mmol of the corresponding acid was added to a mixture containing 66.7 mg (0.143 mmol) of PyBrOP in 177 µl of DMF. Next, 50 µl (0.286 mmol) of DIPEA were added and the mixture was added to with 83 mg of 1-HOBT polymer-bound (100-300mesh, 1.0 mmol/g loading, matrix polystyrene, cross linked with 2%DVB), previously preswollen with DMF. This mixture was shaken for 3 h. Then, the mixture was filtered and the resin washed with DMF 3 times. A second activation step was performed under the same conditions as the first one, and the resin was washed first with DMF (5x) and then with DMSO (5x).

On the other hand, a solution of 16 mg (0.048 mmol) of **15d** in 5 ml of MeOH/H_2O 9:1 was treated with 95 mg of resin IRA-900 $NaCO_3^-$ form (3.5 mmol/g resin). The mixture was shaken for 3 h and then filtrated. The resin was washed with 2 ml of MeOH/H_2O 9:1 and the solvent of the combined filtrated was distilled off under reduced pressure[165]. The residue was taken up in 500 µl of DMSO and added to the previously activated HOBT polymer-bound. The mixture was shaken at room temperature during 16 h. After, the supernatant was separated from the resin by filtration. The polymeric beads were washed with 200 µl of DMSO and the washing solutions were combined with the supernatant previously recovered. The solvent of the filtrate was removed by liofilization. The residue was then redissolved in 1 ml of MeOH and filtered through 40 mg of anionic resin IRA-400 (OH^-), then the solvent was distilled off under reduced pressure and the obtained residue was washed with $CHCl_3$, giving the corresponding amide.

Synthesis of *N*-(6-((2*R*,3*R*,4*R*,5*S*)-3,4,5-trihydroxy-2-(hydroxymethyl)piperidin-1-yl)hexyl)benzamide (16d(I))

According to *General method for the synthesis of the amide derivatives*, using 17.48 mg of benzoic acid for each polymer-bound activation, 1.70 mg of **16d(I)** were obtained as a yellowish foam (10% yield).

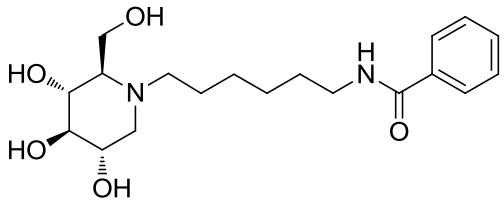

16d(I): ^{1}H NMR (400 MHz, MeOD) δ 7.81 – 7.75 (m, 2H), 7.53 – 7.46 (m, 1H), 7.46 – 7.39 (m, 2H), 3.89 – 3.73 (m, 2H), 3.48 – 3.39 (m, 1H), 3.39 – 3.31 (m, 2H), 3.13 – 3.06 (m, 1H), 2.96 (dd, *J* = 11.2, 4.9 Hz, 1H), 2.84 – 2.72 (m, 1H), 2.60 – 2.48 (m, 1H), 2.14 (t, *J* = 10.8 Hz, 1H), 2.08 (dt, *J* = 9.6, 2.8 Hz, 1H), 1.62 (p, *J* = 7.2 Hz, 2H), 1.54 – 1.30 (m, 6H). ^{13}C NMR (101 MHz, MeOD) δ 131.06, 128.07, 126.75, 79.16, 70.64, 69.34, 65.97, 58.09, 56.29,52.26, 39.49, 29.01, 26.86, 26.52, 23.76.HPLC (UV) 79.0% rt: 2.19'. HRMS calculated for $C_{19}H_{31}N_2O_5$: 367.2233 $[M+H]^+$; found: 367.2246. $[\alpha]^{24}_{D}$ -9° (*c* 0.44, MeOH).

Synthesis of *N*-(6-((2*R*,3*R*,4*R*,5*S*)-3,4,5-trihydroxy-2-(hydroxymethyl)piperidin-1-yl)hexyl)isonicotinamide (16d(II))

According to *General method for the synthesis of the amide derivatives*, using 17.63 mg of isonicotinic acid for each polymer-bound activation, 2.14 mg of **16d(II)** were obtained as a brown foam (12% yield).

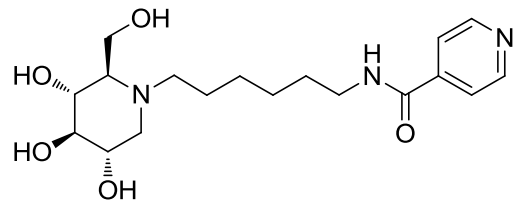

16d(II):^{1}H NMR (400 MHz, MeOD) δ 8.70 – 8.60 (m, 2H), 7.79 – 7.66 (m, 2H), 3.92 – 3.70 (m, 2H), 3.48 – 3.40 (m, 1H), 3.41 – 3.30 (m, 3H), 3.10 (t, *J* = 9.0 Hz, 1H), 2.96 (dd, *J* = 11.2, 4.9 Hz, 1H), 2.84 – 2.71 (m, 1H), 2.61 – 2.47 (m, 1H), 2.13 (t, *J* = 10.9 Hz, 1H), 2.07 (dt, *J* = 9.6, 2.8 Hz, 1H), 1.63 (p, *J* = 7.2 Hz, 2H), 1.55 – 1.23 (m, 6H). ^{13}C NMR (101 MHz, MeOD) δ 149.48, 121.42, 79.17, 70.64, 69.34, 66.00, 58.11, 56.29, 52.24, 39.63, 28.83, 26.82, 26.48, 23.76.HRMS calculated for $C_{18}H_{30}N_3O_5$: 368.2185 $[M+H]^+$; found: 368.2201. $[\alpha]^{24}_{D}$ -11° (*c* 0.44, MeOH).

Synthesis of *N*-(6-((2*R*,3*R*,4*R*,5*S*)-3,4,5-trihydroxy-2-(hydroxymethyl)piperidin-1-yl)hexyl)nicotinamide (16d(III))

According to *General method for the synthesis of the amide derivatives*, using 17.63 mg of nicotinic acid for each polymer-bound activation, 1.46 mg of **16d(III)** were obtained as a yellowish foam (8% yield).

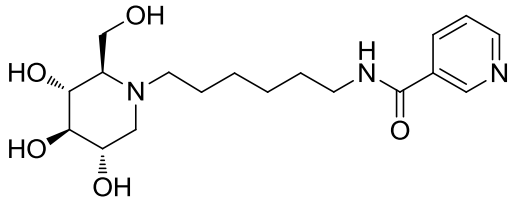

16d(III): ^{1}H NMR (400 MHz, MeOD) δ 8.97 (dd, *J* = 2.3, 0.9 Hz, 1H (H-2_{Ar})), 8.69 (dd, *J* = 5.0, 1.6 Hz, 1H (H-6_{Ar})), 8.24 (dd, *J* = 8.0, 0.7 Hz, 1H (H-4_{Ar})), 7.55 (ddd, *J* = 8.0, 4.9, 0.9 Hz, 1H (H-5_{Ar})), 3.96 – 3.77 (m, 2H (CH-C$\underline{H_2}$-OH)), 3.52 – 3.34 (m, 4H (2 x C$\underline{H}$-OH and C$\underline{H_2}$-NH-CO)), 3.17 – 3.08 (m, 1H (CH-OH)), 3.00 (dd, *J* = 11.2, 4.9 Hz, 1H (CH-C$\underline{H_{2a}}$-N)), 2.88 – 2.74 (m, 1H (N-C$\underline{H_{2a}}$-CH_2)), 2.65 – 2.51 (m, 1H (N-C$\underline{H_{2b}}$-CH_2)), 2.22 – 2.06 (m, 2H (CH-C$\underline{H_{2b}}$-N and C$\underline{H}$-CH_2-OH)), 1.66 (p, *J* = 7.3 Hz, 2H (C$\underline{H_2}$-CH_2-NHCO)), 1.58 – 1.32 (m, 6H (N-CH_2-(C$\underline{H_2}$)$_3$-$(CH_2)_2$-NHCO)). ^{13}C NMR (101 MHz, MeOD) δ 151.08 (CH_{Ar} (C-6)); 147.59 (CH_{Ar} (C-2)); 135.51 (CH_{Ar} (C-5)); 123.68 (CH_{Ar} (C-4)); 79.16, 70.64, 69.34 (3 x CH-OH); 66.00 (C$\underline{H}$-CH_2-OH); 58.10 (CH_2-OH); 56.29 (CH-C$\underline{H_2}$-N); 52.25 (N-C$\underline{H_2}$-CH_2); 39.58 (C$\underline{H_2}$-NHCO); 28.90, 26.83, 26.50, 23.77 (N-CH_2-(C$\underline{H_2}$)$_4$-CH_2). HRMS calculated for $C_{18}H_{30}N_3O_5$: 368.2185 $[M+H]^+$; found: 368.2194.IR (neat) : 3301, 2928, 2856, 1643, 1593, 1549, 1311 cm^{-1}. $[\alpha]^{24}{}_D$ -10º (*c* 0.48, MeOH).

5.1.2.2 Synthesis of DNJ azido and triazole derivatives(compounds 24 and 31)

5.1.2.2.1 Failed attempts for synthesis of DNJ azido derivatives 24. Synthesis of compounds 18, 19, 20, 26, 25, 27, 23 and 22

Synthesis of 5-hydroxypentyl 4-methylbenzenesulfonate (19) and pentane-1,5-diyl bis(4-methylbenzenesulfonate) (18)[133]

To a cooled (0 °C) solution of 2 ml pentane-1,5-diol (19.09 mmol), DMAP (0.075 g, 0.611 mmol) and Et_3N (1.3 ml, 9.54 mmol) in *t*-BME (13 ml, 115 mmol), a cooled (0 °C) solution of Ts-Cl (1.82 g, 9.54 mmol) in 5 ml of DCM was slowly added. The reaction mixture was stirred at 0 °C for 2 h after which it was warmed to rt within a 1 h period and stirred for an additional 18 h. Then, 4 ml of water were carefully added to the reaction mixture, followed by 8 ml of 1 M aqueous HCl. After stirring the mixture for 30 min, the organic layer was isolated and washed with saturated aqueous NaCl (2 × 3.9 ml) and dried over Na_2SO_{4anh} and filtered. The solvent was distilled off under reduced pressure, using moderate heating (Tmax < 40 ºC: the product slowly decomposes when heated) to produce a colorless oil.

The residue was treated with 2-propanol (5 ml) and was stirred for 1 h at rt during which the ditosylate byproduct precipitated as a white solid. The mixture was then cooled at -5 °C for 2 h after which the precipitate was removed by filtration and washed with precooled 2-propanol. The solvent of mother liquor and washings was removed by distillation under reduced pressure using moderate heating (T_{max}< 40 °C). 1.73 g of **19** (colorless oil, 70% yield) and 333 mg of the ditosylate byproduct **18** (white solid, 9% yield) were obtained, with ^{1}H NMR data in concordance with the previously described in the literature[133].

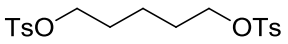

18:^{1}H NMR (400 MHz, $CDCl_3$) δ 7.75 (d, *J* = 8.3 Hz, 4H), 7.33 (d, *J* = 8.0 Hz, 4H), 3.95 (t, *J* = 6.3 Hz, 4H), 2.44 (s, 6H), 1.66 – 1.56 (m, 4H), 1.41 – 1.28 (m, 2H).

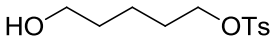

19: ^{1}H NMR (400 MHz, $CDCl_3$) δ 7.77 (d, *J* = 8.3 Hz, $2H_{Ar}$), 7.33 (d, *J* = 8.0 Hz, $2H_{Ar}$), 4.02 (t, *J* = 6.4 Hz, 2H ($C\underline{H}_2$-OTs), 3.59 (t, *J* = 6.4 Hz, 2H ($C\underline{H}_2$-OH)), 2.43 (s, 3H (CH_3)), 1.73 – 1.61 (m, 2H ($C\underline{H}_2$-CH_2-OTs)), 1.56 – 1.47 (m, 2H ($C\underline{H}_2$-CH_2-OH)), 1.43 – 1.33 (m, 2H ($C\underline{H}_2$-CH_2-CH_2-OH).

Synthesis of 5-oxopentyl 4-methylbenzenesulfonate (20)[133]

A solution of KBr (0.085 g, 0.715 mmol) in 300 µl of H_2O was added to a solution of **19** (1.539 g, 5.96 mmol) and TEMPO (10.24 mg, 0.066 mmol) in8 ml of DCM .The mixture was cooled to 5ºC.

Separately, NaOCl 12% in water (4.42 ml, 8.94 mmol) was diluted with enough $NaHCO3_{sat}$ (aprox 9.6%) in water (4.41 ml, 8.94 mmol) to reach a pH between 8.5 and 9.5 and then cooled to 5 ºC. Controlled addition of an equimolar amount of NaOCl was essential to prevent over oxidation. The NaOCl/$NaHCO_3$ solution was slowly added at 5 ºC to the mixture containing the alcohol, which caused an initial orange coloration of the reaction mixture that slowly disappeared. The reaction mixture was stirred for an additional 60 min at 5 ºC. Then, the reaction mixture was warmed to 20 ºC, and the aqueous layer was separated and extracted with 3 ml of DCM. Aqueous 2M HCl (12.5 ml) containing KI (0.017 g, 0.101 mmol) was slowly added to the combined organic layers. The aqueous layer was removed, and the organic layer was successively extracted with aqueous $Na_2S_2O_3$ 10% (9 ml), saturated aqueous $NaHCO_3$ (9 ml), and water (9 ml). The organic layer was isolated, dried over Na_2SO_{4anh} and filtered, and the solvent of the filtrate was removed by distillation under reduced pressure with moderate heating (T_{max}< 40ºC). The residue was purified by *flash* chromatography on silica gel (Flash+

Biotage®, Flash 40+M column, eluent DCM), giving 1.33 g of **20** as brown oil (87% yield). ^{1}H NMR data in concordance with the previously described in the literature[133].

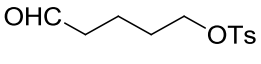

20: ^{1}H NMR (400 MHz, $CDCl_3$) δ 9.71 (d, *J* = 1.4 Hz, 1H (CHO)), 7.77 (d, *J* = 8.3 Hz, $2H_{Ar}$), 7.39 – 7.29 (m, $2H_{Ar}$), 4.02 (t, *J* = 5.8 Hz, 2H ($C\underline{H}_2$-OTs)), 2.42 (d, *J* = 9.2 Hz, 5H ($C\underline{H}_3$ and $C\underline{H}_2$-CHO)), 1.72 – 1.60 (m, 4H (CH_2-($C\underline{H}_2$)$_2$-CH_2-CHO).^{13}C NMR (101 MHz, $CDCl_3$) δ 201.44 (CHO); 144.80, 132.97 (2 x C_{Ts}); 129.84, 127.85 (4 x CH_{Ts}); 69.84 ($\underline{C}H_2$-OTs); 42.90 ($\underline{C}H_2$-CHO); 28.15 ($\underline{C}H_2$-$\underline{C}H_2$-OTs); 21.61 (CH_3); 18.03 ($\underline{C}H_2$-CH_2-CHO).

Synthesis of azidopentanal (25)

76 mg (1.170 mmol) of NaN_3 were added to a solution of **20** (143 mg, 0.558 mmol) in 1.5 ml of dry DMF. The reaction mixture was stirred at 0ºC for 5 h. Then, the reaction mixture was diluted with diethyl ether/hexane (1:1), washed twice with water and twice with brine, dried over $Na_2SO_{4\ anh}$, and the solvent distilled off under reduced pressure. After purification of the residue by *flash* chromatography on silica gel (Flash+ Biotage®, Flash 12+S column, eluent Hx/AcOEt 10:1), 30 mg of **25** (colorless oil, 42%yield) were obtained, and 15 mg of **19** were recovered without react. ^{1}H NMR data were in concordance with the previously described in the literature[166].

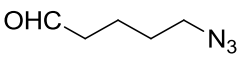

25: ^{1}H NMR (400 MHz, $CDCl_3$) δ 9.76 (s, 1H), 3.29 (t, *J* = 6.6 Hz, 2H), 2.48 (td, *J* = 7.0, 1.5 Hz, 2H), 1.76 – 1.58 (m, 4H).

Synthesis of (2*R*,3*R*,4*R*,5*S*)-2-(hydroxymethyl)piperidine-3,4,5-triol hydrochloride (27)

According to *Method A: hydrogenation with Pd(OH)$_2$/C*, from a solution of 500 mg (0.843 mmol) of **13**(HCl) in EtOH,after 48h of reaction, 179 mg of **27**were obtained as a white solid (100% yield)), with an ^{1}H NMR spectra in concordance with the previously reported[167].

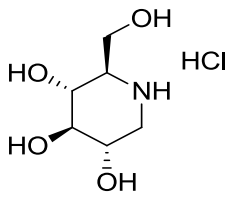

27: ^{1}H NMR (400 MHz, MeOD) δ 3.90 – 3.76 (m, 2H), 3.66 – 3.57 (m, 1H), 3.48 – 3.41 (m, 1H), 3.34 (t, *J* = 9.1 Hz, 1H), 3.30 – 3.25 (m, 1H), 3.06 – 2.98 (m, 1H), 2.84 (dd, *J* = 12.4, 11.4 Hz, 1H).^{13}C NMR (101 MHz, MeOD) δ 76.95, 68.19, 67.31, 60.45, 57.74, 46.16. HPLC (ESI) 90.8% rt: 0.38'; m/z: 164.00. HRMS calculated for $C_6H_{14}NO_4$: 164.0923 $[M+H]^+$; found: 164.0931.

Attempts of synthesis of (2*R*,3*R*,4*R*,5*S*)-1-(5-azidopentyl)-2-(hydroxymethyl)piperidine-3,4,5-triol (24c) via reductive amination between 13 and 20[133]. Synthesis of (1R,2R,3R,4S)-2,3,4-trihydroxy-1-(hydroxymethyl)-6-azaspiro[5.5]undecan-6-ium (23).

2 ml of NaOH 1N were added to a suspension of 100 mg (0.179 mmol) of **13** in 3 ml of AcOEt. After stirring at rt for 10 min, the two layers were separated, and the organic phase was washed successively with NaOH 1M and NaCl. The organic layer was dried over Na_2SO_{4anh} and filtered. The solvent was distilled off under reduced pressure and the residue was redissolved in 2 ml of EtOH. Then, 48 mg (0.187 mmol) of **20**, 102 µl (1.785 mmol) of acetic acid, and 11.4 mg (0.027 mmol) of Pd/C (10%) were added. The mixture was stirred at rt under H_2 atmosphere (1.5 atm) during 24 h. After that, 11.4 mg (0.027 mmol) of Pd/C (10%), 1.7 ml HCl 1M and 1 ml of EtOH were added and the mixture was stirred again at rt under H_2 atmosphere (1.5 atm) during 48 h. Then, the mixture was filtered over a pad of Celite®, and the solvent was distilled off under reduced pressure, giving a mixture of compounds that seemed to contain the cyclized compound **23** and the DNJ tosylate derivative **22**.

Attempt A: 300 mg of strongly basic resin IRA-400-Cl were introduced in a 5 ml syringe with frit. The resin was activated by treatment 2 ml of NaOH 1M (three times). After, the resin was washed with H_2O several times, until neutral washings. Then, 50 mg of the residue obtained in the step before (containing **22** and **23**) were dissolved in 2 ml of MeOH/H_2O 9:1 and added to the syringe with resin. Then, the syringe was shacked for 15 min. After that, the mixture was filtered and the resin was washed three times with 1 ml of of MeOH/H_2O 9:1. The filtrates were combined and the solvent was distilled off under reduced pressure giving a residue that seemed to be only the cycled compound **23**.

Attempt B[135]: 59 mg of the residue obtained after the onepot amination reductive and debenzylation (mixture containing **22** and **23**) were dissolved in 250 µl of dry DMF. 19.18 mg of NaN_3 (0.295 mmol) were added to this solution.The mixture was stirred at 80 °C for 16 h. After, 2 ml of water were added and the solvent was removed by liofilization. The residue was treated with 15 mg of strongly acidic resin Dowex 50 W X 8[168], and eluted with NH_4OH (30% Aq), giving a residue that seemed to be only the cycled compound **23**.

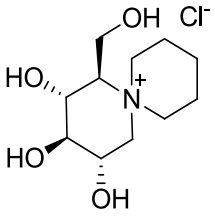

23: ^{1}H NMR (400 MHz, MeOD) δ 4.26 (d, J = 13.3 Hz, 1H), 4.17 – 3.73 (m, 5H), 3.65 (t, J = 12.5 Hz, 1H), 3.52 – 3.39 (m, 2H), 3.28 – 3.19 (m, 1H), 2.92 (t, J = 10.7 Hz, 1H), 2.18 – 1.89 (m, 2H), 1.82 (d, J = 12.0 Hz, 3H), 1.69 – 1.51 (m, 1H).

Attempt of synthesis of (2*R*,3*R*,4*R*,5*S*)-1-(5-azidopentyl)-2-(hydroxymethyl)piperidine-3,4,5-triol (24c) by reductive amination between 27 and 25.

15.70 mg (0.076 mmol) of **27**(HCl), 30 mg (0.236 mmol) of **25** 7.10 mg of AcONa and 1 ml of EtOH, were introduced in a round bottomed flask. The mixture was stirred at 25 °C for 3h. After, $NaBH(AcO)_3$ (36.7 mg, 0.173 mmol) was added and the mixture was stirred overnight at room temperature. Then, the solvent was distilled off under reduced pressure and the residue was treated with the strongly acidic resin Dowex 50 W X 8[168]. After washing the resin with water, the retained compounds were eluted with NH_4OH (30%aq). The desired compound **24c** was not obtained, and 8 mg of **27** as free base were recovered.

5.1.2.2.2 Synthesis of 24d and triazole derivatives 31

Synthesis of(2*R*,3*R*,4*R*,5*S*)-1-(6-azidohexyl)-2-(hydroxymethyl)piperidine-3,4,5-triol formate (24d)[124]

25.0 mg (0.125 mmol) of **13**, 63.3 mg (0.213 mmol) of the azidotosilate **12d**, 69.2 mg (0.501 mmol) of K_2CO_3, 2.1 mg (0.013 mmol) of KI, 0.6 ml of ACN and 0.2 ml of DMF were introduced in a 10ml vessel with a magnetic stir bar. The vessel was sealed with a septum and submitted to MW irradiation (T max = 85ºC, power = 150 w, t = 2 h). After, the mixture was filtrated and the precipitate washed with MeOH. The solvent of the filtrate was distilled off under reduced pressure and the residue was purified with preparative HPLC (mobile phase: A=H_2O + 0.2% formic acid,B= ACN + 0.2% formic acid. Gradient from 95:5 to 10:90 A/B in 5 minutes). 7.26 mg of **24d** were obtained as colorless oil (17% yield).

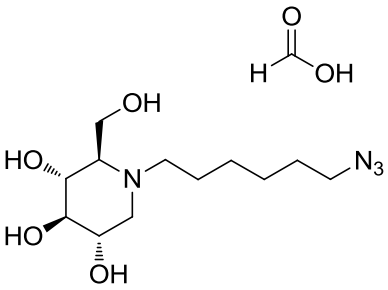

24d: ^{1}H NMR (400 MHz, MeOD) δ 8.49 (s, 1H (H-COOH)), 4.01 – 3.82 (m, 2H (CH_2-OH)), 3.63 – 3.50 (m, 1H (CH-OH)), 3.46 (t, *J* = 9.4 Hz, 1H (CH-OH)), 3.30 – 3.14 (m, 4H (CH_2-N_3, CH-OH, CH-CH_{2a}-N)), 3.12 – 2.97 (m, 1H (N-CH_{2a}-$(CH_2)_5$-N_3)), 2.91 – 2.78 (m, 1H (N-CH_{2b}-$(CH_2)_5$-N_3)), 2.57 – 2.43 (m, 2H (CH-CH_{2b}-N, CH-CH_2-OH)), 1.70 – 1.55 (m, 4H (N-CH_2-CH_2-CH_2-CH_2-CH_2-CH_2-N_3)), 1.53 – 1.26 (m, 4H (N-CH_2-CH_2-CH_2-CH_2-CH_2-CH_2-N_3)).^{13}C NMR (101 MHz, MeOD) δ 167.74 (HCOOH); 77.89, 68.96, 67.78, 66.00 (4 x CH); 55.82 (CH_2-OH); 54.77 (CH-CH_2-N); 52.37 (N-CH_2-$(CH_2)_5$-N_3); 50.88 (CH_2-N_3); 28.32 (CH_2-CH_2-N_3); 26.21, 26.07 (N-CH_2-CH_2-CH_2-CH_2-CH_2-CH_2-N_3), 23.22 (N-CH_2-CH_2). HRMS calculated for $C_{12}H_{25}N_4O_4$: 289.1876 $[M+H]^+$; found: 289.1861. $[\alpha]^{24}_{D}$ -11° (*c* 0.75, MeOH).

Synthesis of 4-(prop-2-yn-1-yloxy)pyridine (30(VI))

A mixture of pyridin-4-ol (500 mg, 5.26 mmol) and K_2CO_3 (872 mg, 6.31 mmol) in toluene (52 ml) was stirred at room temperature for 10 minutes. After that, 3-bromoprop-1-yne (633 µl, 6.31 mmol) was added. The resulting mixture was stirred for 30 min and then filtered and the solvent was distilled off under reduced pressure. After purification by *flash* cromathogratpy on silica gel (eluent: DCM/MeOH 20:1), 315 mg of **30(VI)** were obtainedas a yellowish oil (45% yield). The^{1}H NMR spectra was in concordance with the previously reported[169].

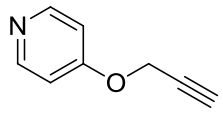

30(VI): ^{1}H NMR (400 MHz, $CDCl_3$) δ 7.40 (d, *J* = 7.7 Hz, 2H), 6.41 (d, *J* = 7.7 Hz, 2H), 4.56 (d, *J* = 2.6 Hz, 2H), 2.62 (t, *J* = 2.6 Hz, 1H). HRMS calculated for C_8H_8NO ($[M+H]^+$): 134.0606; found: 134.0607.

Synthesis of 2-(prop-2-yn-1-yloxy)pyridine (30(VII))

Similarly to the synthesis of **30(VI)**, from 500 mg of pyridine-2-ol (5.26 mmol), 400 mg of **30(VII)** were obtained as yellowish oil (57% yield).

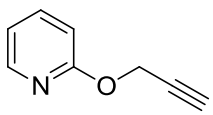

30(VII): ^{1}H NMR (400 MHz, $CDCl_3$) δ 7.63 (dd, *J* = 6.9, 2.1 Hz, 1H), 7.35 (ddd, *J* = 8.8, 6.6, 2.0 Hz, 1H), 6.59 (d, *J* = 9.0 Hz, 1H), 6.24 (td, *J* = 6.7, 1.4 Hz, 1H), 4.76 (d, *J* = 2.6 Hz, 2H), 2.48 (t, *J* = 2.6 Hz, 1H). ^{13}C NMR (101 MHz, $CDCl_3$) δ 161.97, 139.76, 135.76, 120.62, 106.36, 76.86, 75.37, 37.61.

Synthesis of compounds 31d(I-VI):

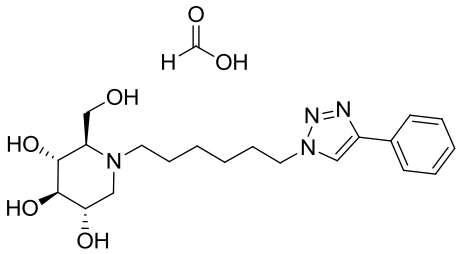

(2*R*,3*R*,4*R*,5*S*)-2-(hydroxymethyl)-1-(6-(4-phenyl-1H-1,2,3-triazol-1-yl)hexyl)piperidine-3,4,5-triol formate (31d(I))

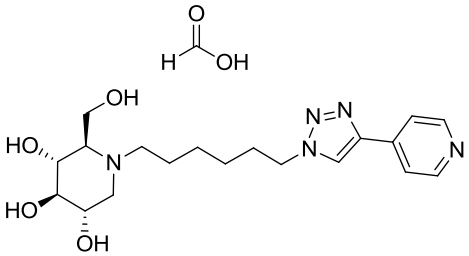

(2*R*,3*R*,4*R*,5*S*)-2-(hydroxymethyl)-1-(6-(4-(pyridin-4-yl)-1H-1,2,3-triazol-1-yl)hexyl)piperidine-3,4,5-triol formate (31d(II))

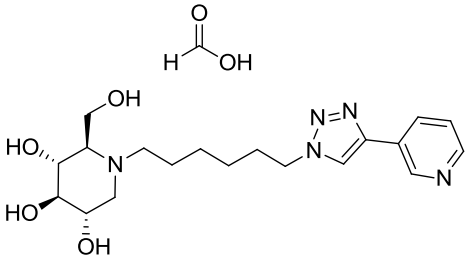

(2*R*,3*R*,4*R*,5*S*)-2-(hydroxymethyl)-1-(6-(4-(pyridin-3-yl)-1H-1,2,3-triazol-1-yl)hexyl)piperidine-3,4,5-triol formate (31d(III))

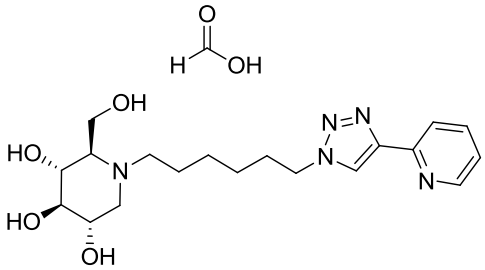

(2*R*,3*R*,4*R*,5*S*)-2-(hydroxymethyl)-1-(6-(4-(pyridin-2-yl)-1H-1,2,3-triazol-1-yl)hexyl)piperidine-3,4,5-triol formate (31d(IV))

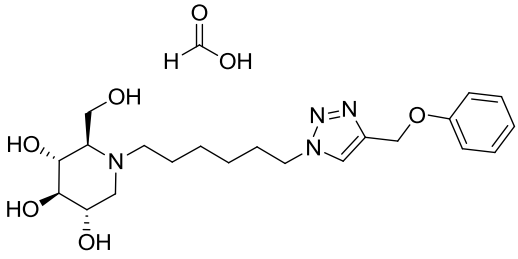

(2*R*,3*R*,4*R*,5*S*)-2-(hydroxymethyl)-1-(6-(4-(phenoxymethyl)-1H-1,2,3-triazol-1-yl)hexyl)piperidine-3,4,5-triol formate (31d(V))

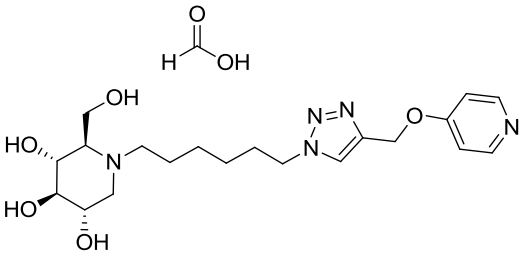

2*R*,3*R*,4*R*,5*S*)-2-(hydroxymethyl)-1-(6-(4-((pyridin-4-yloxy)methyl)-1H-1,2,3-triazol-1-yl)hexyl)piperidine-3,4,5-triol formate (31d(VI))

General procedure: To a mixture of 1.14 mg (3.41 µmol) of azide **24d** and 1.17 mg (8.18 µmol) of $Cu_2O(I)$ in 30 µl of water, a solution of 3.75 µmol of the desired alkyne in 4.29 µl of THF was added. The resulting mixture was stirred at room temperature or heated until the reaction was finished. The completion of the reaction was checked by HRMS, and the biological assays were performed without further purification or compound isolation.

compound	alkyne	reaction conditions	$[M+H]^+$	calculated	found
31d(I)	0.412 µl ethynylbenzene	5 days rt + 15 h 60ºC	$C_{20}H_{31}N_4O_4$	391.2345	391.2356
31d(II)	0.379 µl 4-ethynylpyridine	24 h , rt	$C_{19}H_{30}N_5O_4$	392.2298	392.2299
31d(III)	0.387 mg 3-ethynylpyridine	24 h, rt	$C_{19}H_{30}N_5O_4$	392.2298	392.2306
31d(IV)	0.379 µl 2-ethynylpyridine	30 min, rt	$C_{19}H_{30}N_5O_4$	392.2298	392.2296
31d(V)	0.481µl (prop-2-yn-1-yloxy)benzene	48 h, rt	$C_{21}H_{33}N_4O_5$	421.2451	421.2442
31d(VI)	0.499 mg **30f**	24 h, rt	$C_{20}H_{32}N_5O_5$	422.2403	422.2387

Table 15 Synthesis of compounds **31**.

Synthesis of 4-((1-(4-((2*R*,3*R*,4*R*,5*S*)-3,4,5-tris(benzyloxy)-2-((benzyloxy)methyl)piperidin-1-yl)butyl)-1H-1,2,3-triazol-4-yl)methoxy)pyridine(32b(VI))

To a mixture of (**14b**) (60 mg, 0.097 mmol) and $Cu_2O(I)$ (2.77 mg, 0.019 mmol) in Water/THF 1:1 (805 µl), 14.16 mg of **30(VI)** (0.106 mmol) in THF (805 µl) were added and the resulting mixture was stirred at 60ºC overnight.Next day the mixture was filtrated and the solvent was distilled off under reduced pressure. After purification by *flash* chromatography on silicagel (Eluent: AcOEt), 40 mg (44% yield) of **32b(VI)** were obtained with 20% of impurity by ^{1}H NMR. This compound was used in the next step without further purification.

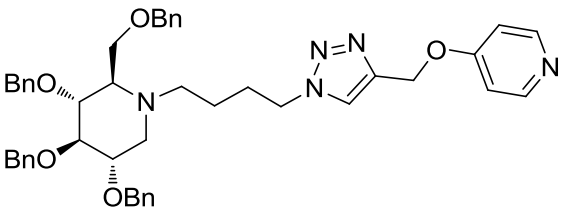

32b(VI): ^{1}H NMR (400 MHz, $CDCl_3$) δ 7.39 (d, *J* = 7.1 Hz, 2H (2 x H(Py))), 7.34 – 7.18 (m, 18H (H_{Ar})), 7.15 (dd, *J* = 7.6, 1.9 Hz, 2H (H_{Ar})), 6.37 (d, *J* = 7.5 Hz, 2H (2 x CH(Py))), 4.98 – 4.77 (m, 5H (CH_2-OPy, CH_2-Ph)), 4.71 – 4.57 (m, 2H (CH_2-Ph)), 4.49 – 4.39 (m, 3H (CH_2-Ph)), 4.24 (t, *J* = 7.3 Hz, 2H (CH_2-C$\underline{H_2}$-Triazole)), 3.73 – 3.40 (m, 5H (CH_2-OBn and 3 x CH-OBn)), 2.99 (dd, *J* = 11.2, 4.8 Hz, 1H (CH-C$\underline{H_{2a}}$-N)), 2.82 – 2.63 (m, 1H (CH_2-N-C$\underline{H_{2a}}$-CH_2)), 2.60 – 2.39 (m, 1H (CH_2-N-C$\underline{H_{2b}}$-CH_2)), 2.28 (dt, *J* = 9.4, 2.6 Hz, 1H (CH-C$\underline{H_{2b}}$-N)),), 2.10 (t, *J* = 10.8 Hz, 1H (C$\underline{H}$-CH_2-OBn)), 1.89 – 1.62 (m, 2H (C$\underline{H_2}$-CH_2-triazole)), 1.49 – 1.31 (m, 2H, CH_2-N-CH_2-C$\underline{H_2}$)). ^{13}C NMR (101 MHz, $CDCl_3$) δ 178.80 (C (Py)); 141.64, 139.62, 138.77, 138.39, 138.34, 137.74 (2 x CH (Py) + 4 C (Ph)); 128.38, 128.36, 128.34, 128.31, 128.28, 128.26, 127.95, 127.86, 127.81, 127.73, 127.70, 127.62, 127.52, 127.44 (20 x CH (Bn)); 122.17 (CH (triazole)); 119.02 (2x CH (Py)); 87.16 , 78.54, 78.34 (3 x CH-OBn), 75.37, 75.22, 73.32, 72.83 (4 x CH_2-Ph); 66.01 (CH_2-OBn); 64.23(C$\underline{H}$-CH_2-OBn); 54.15 (C$\underline{H}$-CH_2-N), 51.38 (CH_2-N-C$\underline{H_2}$-CH_2); 50.90(CH_2-N(triazole)); 50.16 (CH_2-OPy), 27.92(C$\underline{H_2}$-CH_2-triazole), 21.50 (CH_2-N-CH_2-C$\underline{H_2}$).

Synthesis of 2-((1-(4-((2*R*,3*R*,4*R*,5*S*)-3,4,5-tris(benzyloxy)-2-((benzyloxy)methyl)piperidin-1-yl)butyl)-1H-1,2,3-triazol-4-yl)methoxy)pyridine (32b(VII))

Similarly to the synthesis of **32b(VI)**, from 14.16 mg (0.106 mmol) of **30(VII)**, after purification by *flash* chromatography, 66 mg (75% yield) of **32b(VII)** were obtained with 20% of impurity (by ^{1}H NMR). This compound was used in the next step without further purification.

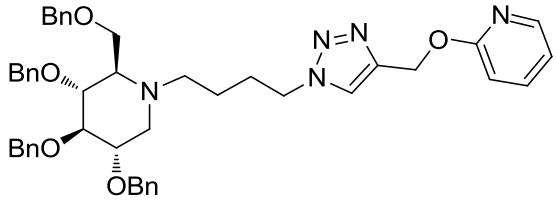

32b(VII): ^{1}H NMR (400 MHz, $CDCl_3$) δ 7.65 (s, 1H), 7.57 (dd, *J* = 6.8, 2.0 Hz, 1H), 7.34 – 7.18 (m, 19H), 7.13 (dd, *J* = 7.6, 1.9 Hz, 2H), 6.54 (d, *J* = 9.1 Hz, 1H), 6.15 (td, *J* = 6.7, 1.4 Hz, 1H), 5.16 (s, 2H), 5.00 – 4.71 (m,3H), 4.70 – 4.53 (m, 2H), 4.49 – 4.32 (m, 3H), 4.24 – 4.12 (m, 2H), 3.65 – 3.37 (m, 5H), 2.99 (dd, *J* = 11.2, 4.8 Hz, 1H), 2.76 – 2.59 (m, 1H), 2.56 – 2.41 (m, 1H), 2.25 (d, *J* = 9.4 Hz, 1H), 2.17 – 2.04 (m, 1H), 1.84 – 1.62 (m, 2H), 1.45 – 1.29 (m, 2H).^{13}C NMR (101 MHz, $CDCl_3$) δ 162.38, 142.60, 139.97, 138.90, 138.45, 137.73, 137.64, 128.41, 128.37, 128.35, 128.33, 128.30, 128.28, 128.22, 127.90, 127.83, 127.81, 127.79, 127.77, 127.64, 127.61, 127.53, 127.46, 127.42, 123.70, 120.77, 106.46, 87.20, 78.51, 78.34, 75.29, 75.17, 73.34, 72.79, 65.70, 63.97, 54.24, 51.22, 49.99, 44.58, 27.94, 21.21.

Synthesis of (2R,3R,4R,5S)-2-(hydroxymethyl)-1-(4-(4-((pyridin-4-yloxy)methyl)-1H-1,2,3-triazol-1-yl)butyl)piperidine-3,4,5-triol (31b(VI))

According to *Method B: debenzylation with BCl_3*, from 40 mg (0.053 mmol) of **32(VI),** after filtration of the crude through 408 mg of strong basic resin Amberlite-IRA400 and purification by *flash* chromatography (Biotage® Isolera PrimeTM, SNAP KP-C18-HS cartridge, gradient: A/B 100:0 to 0:100, A:H_2O+0.1%NH_4OH, B: ACN+ 0.1% NH_4OH), 9 mg of **31b(VI)**(36% yield)were obtainedas colorless oil, containing 17% of impurity by ^{1}H NMR.

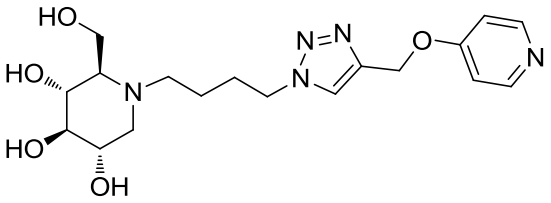

31b(VI): ^{1}H NMR (400 MHz, MeOD) δ 8.07 (s, 1H), 7.88 (d, *J* = 7.6 Hz, 2H), 6.43 (d, *J* = 7.6 Hz, 2H), 5.25 (s, 2H), 4.43 (t, *J* = 7.0 Hz, 2H), 3.89 – 3.73 (m, 2H), 3.42 (ddd, *J* = 10.4, 9.0, 4.8 Hz, 1H), 3.34 – 3.24 (m, 1H), 3.09 (t, *J* = 9.0 Hz, 1H), 2.91 (dd, *J* = 11.1, 4.9 Hz, 1H), 2.87 – 2.78 (m, 1H), 2.57 – 2.46 (m, 1H), 2.15 – 2.00 (m, 2H), 1.95 – 1.80 (m, 2H), 1.53 – 1.41 (m, 2H). ^{13}C NMR (101 MHz, MeOD) δ 179.47, 141.65, 123.71, 117.24, 79.15, 70.60, 69.32, 66.20, 58.20, 56.19, 51.33, 50.71, 49.85, 27.64, 21.13.HPLC (ESI) 86.9% rt: 0.37'; m/z: 394.22. HRMS calculated for $C_{18}H_{28}N_5O_5$: 394.2090 $[M+H]^+$; found: 394.2101. IR (neat): 3302, 2926, 1636, 1540, 1446, 1381, 1180. $[\alpha]^{25}{}_D$ -10º (*c* 1.0, MeOH).

Synthesis of (2*R*,3*R*,4*R*,5*S*)-2-(hydroxymethyl)-1-(4-(4-((pyridin-2-yloxy)methyl)-1H-1,2,3-triazol-1-yl)butyl)piperidine-3,4,5-triol (31b(VII))

According to *Method B: debenzylation with BCl_3*, from 66 mg (0.088 mmol) of **32(VII),** after filtration of the crude through 675 mg of strong basic resin Amberlite-IRA400 and purification by *flash* chromatography (Biotage® Isolera PrimeTM, SNAP KP-C18-HS cartridge, gradient: A/B 100:0 to 0:100, A:H_2O+0.1%NH_4OH, B: ACN+ 0.1% NH_4OH), 12 mg of **31b(VII)**(30% yield)were obtainedas colorless oil, containing 13% of impurity by ^{1}H NMR.

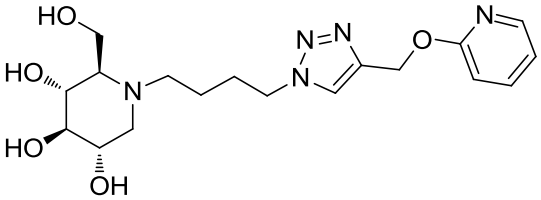

31b(VII): ^{1}H NMR (400 MHz, MeOD) δ 7.96 (s, 1H), 7.76 (dd, *J* = 6.8, 2.0 Hz, 1H), 7.50 (ddd, *J* = 8.9, 6.7, 2.0 Hz, 1H), 6.53 (d, *J* = 9.1 Hz, 1H), 6.38 (td, *J* = 6.8, 1.3 Hz, 1H), 5.22 (s, 2H), 4.39 (t, *J* = 7.0 Hz, 2H), 3.79 (qd, *J* = 11.9, 2.9 Hz, 2H), 3.51 – 3.35 (m, 1H), 3.34 – 3.22 (m, 1H), 3.09 (t, *J* = 9.0 Hz, 1H), 2.90 (dd, *J* = 11.2, 4.9 Hz, 1H), 2.86 – 2.72 (m, 1H), 2.58 – 2.42 (m, 1H), 2.16 – 1.94 (m, 2H), 1.94 – 1.74 (m, 2H), 1.53 – 1.34 (m, 2H). ^{13}C NMR (101 MHz, MeOD) δ 163.00, 142.45, 141.04, 138.28, 123.96, 119.41, 107.36, 79.13, 70.61, 69.31, 66.12, 58.17, 56.18, 51.33, 49.74, 44.01, 27.66, 21.05.HRMS calculated for $C_{18}H_{28}N_5O_5$: 394.2090 $[M+H]^+$; found: 394.2083. IR (neat): 3346, 2917, 1650, 1573, 1541, 1463. $[\alpha]^{25}{}_D$ -10° (*c* 1.0, MeOH).

5.1.2.3 Synthesis of amido derivatives34(II-IV) and 38 and triazole derivatives 35

Synthesis of *N*-(5-hydroxypentyl)isonicotinamide (34(II))

According to *General procedure for acylations,* from 100 mg of 5-aminopentanol and 131 mg of isonicotinic acid, after a purification by *flash* chromatography (silica gel, gradient from 100% DCM to DCM/MeOH 10:1), 7 mg of **34(II)** were obtained as a yellow oil (3% yield).

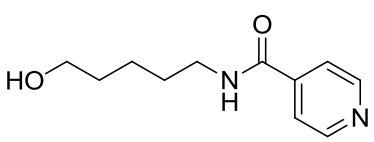

34(II): ^{1}H NMR (400 MHz, $CDCl_3$) δ 8.73 – 8.69 (m, 2H), 7.67 – 7.54 (m, 2H), 6.45 (s, 1H), 3.66 (t, *J* = 6.3 Hz, 2H), 3.47 (td, *J* = 7.0, 5.8 Hz, 2H), 1.70 – 1.56 (m, 4H), 1.52 – 1.42 (m, 2H). ^{13}C NMR (101 MHz, $CDCl_3$) δ 165.52, 150.36, 141.90, 120.89, 62.51, 40.06, 31.97, 29.10, 23.13.

Synthesis of *N*-(5-hydroxypentyl)nicotinamide (34(III))

According to *General procedure for acylations,* from 100 mg of 5-aminopentanol and 131 mg of nicotinic acid, after a purification by *flash* chromatography (Biotage® Isolera PrimeTM,SNAP-Sil 12g cartridge, gradient from 100% DCM to DCM/MeOH 10:1),9 mg of **34(III)** were obtained as a yellow oil (4% yield).

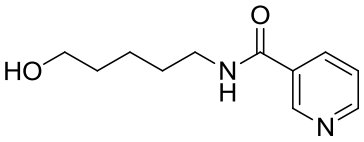

34(III): ^{1}H NMR (400 MHz, $CDCl_3$) δ 8.99 (s, 1H), 8.70 (s, 1H), 8.14 (dt, *J* = 7.9, 1.8 Hz, 1H), 7.39 (dd, *J* = 7.8, 4.8 Hz, 1H), 6.64 (s, 1H), 3.67 (t, *J* = 6.2 Hz, 2H), 3.49 (td, *J* = 7.0, 5.7 Hz, 2H), 1.74 – 1.55 (m, 4H), 1.55 – 1.42 (m, 2H). ^{13}C NMR (101 MHz, $CDCl_3$) δ 165.56, 151.80, 147.55, 135.42, 130.54, 123.60, 62.47, 40.01, 31.98, 29.13, 23.15.

Synthesis of *N*-(5-hydroxypentyl)benzamide(34(IV))

Similarly to *General procedure for acylation* but without aqueous extraction,from 100 mg of 5-aminopentanol and 131 mg of picolinic acid, 193 mg of **34(IV)** were obtained as yellow oil (96% yield). In this case, after the reaction the solvent of the crude was removed by distillation without previous aqueous extraction. The residue was purified by *flash* chromatography (Flash^{+} Biotage®, KP-Sil 40+S column, Hx:AcOEt 1:3).

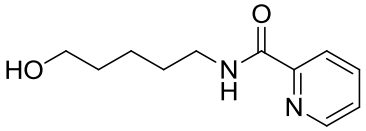

34(IV): ^{1}H NMR (400 MHz, $CDCl_3$) δ 8.51 (ddd, *J* = 4.8, 1.8, 0.9 Hz, 1H (CH (Py))), 8.16 (dt, *J* = 7.9, 1.1 Hz, 1H (CH(Py))), 8.09 (s, 1H (NH-CO)), 7.82 (td, *J* = 7.7, 1.7 Hz, 1H (CH(Py))), 7.39 (ddd, *J* = 7.6, 4.8, 1.3 Hz, 1H (CH (Py))), 3.63 (t, *J* = 6.4 Hz, 2H, ($C\underline{H_2}$-OH)), 3.46 (q, *J* = 6.9 Hz, 2H ($C\underline{H_2}$-NH-CO)), 2.35 (s, 1H (OH)), 1.69 – 1.56 (m, 4H ($C\underline{H_2}$-CH_2-$C\underline{H_2}$-CH_2-OH)), 1.52 – 1.40 (m, 2H ($C\underline{H_2}$-CH_2-CH_2-OH)). ^{13}C NMR (101 MHz, $CDCl_3$) δ 164.35 (CO); 149.87 ($\underline{C}$-CO); 147.96, 137.34, 126.06, 122.16 (4 x CH (Py)); 62.49 (CH_2-OH); 39.28 (CH_2-NH); 32.25 ($\underline{C}H_2$-CH_2-OH); 29.41 ($\underline{C}H_2$-CH_2-NH); 23.11 ($\underline{C}H_2$-CH_2-CH_2-OH). IR (neat): 3372, 2933, 2860, 1657, 1529.

Synthesis of 4-(3-(pyridin-4-yl)propanamido)butyl 3-(pyridin-4-yl)propanoate (38)

According to *General procedure for acylations*, from 100 mg of 4-aminopentanol and 187 mg of 3-(pyridin-4-yl)propanoic acid, after a purification by phase reverse chromatography (Biotage® Isolera PrimeTM, SNAP-C18 cartridge, gradient from100% H_2O to 100% ACN), 70 mg of **38** were obtained as a yellow oil (28% yield).

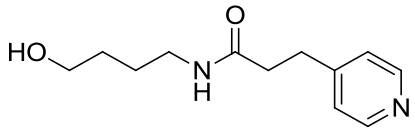

38: ^{1}H NMR (400 MHz, MeOD) δ 8.41 (d, *J* = 6.2 Hz, 2H (CH (Py))), 7.31 (d, *J* = 6.2 Hz, 2H (CH (Py))), 3.53 (t, *J* = 6.1 Hz, 2H (C$\underline{H_2}$-OH)), 3.15 (t, *J* = 6.6 Hz, 2H (C$\underline{H_2}$-NHCO)), 2.97(t, *J* = 7.5 Hz, 2H (CH_2-Py)), 2.53 (t, *J* = 7.5 Hz, 2H (C$\underline{H_2}$-CH_2-Py), 1.58 – 1.38 (m, 4H, C$\underline{H_2}$-C$\underline{H_2}$-CH_2-OH). ^{13}C NMR (101 MHz, MeOD) δ 172.71 (CO); 151.51 (C_q (Py)); 148.49, 124.17 (4 x CH (Py)); 60.99 (CH_2-OH); 38.71 (C$\underline{H_2}$-NHCO); 35.76 (C$\underline{H_2}$-CO); 30.52 (CH_2-Py)); 29.36 (C$\underline{H_2}$-CH_2-OH); 25.39 (C$\underline{H_2}$-CH_2-NHCO). IR (neat): 3281, 2934, 2866, 1641, 1605, 1558, 1418.

Synthesis of compounds 35 (II-IV, VI-VII):

- **General procedure:**To a mixture of **11c** (46 mg, 0.356 mmol) and Cu_2O(I) (10.19 mg, 0.071 mmol) in 3.5 ml of H_2O, 0.392 mmol of the corresponding alkyne in 512 µl of THF were added. The resulting mixture was stirred at 60ºC overnight. Next day the mixture was filtrated and the solvent was removed by distillation under reduced pressure The obtained residue was purified by *flash* chromatography on silica gel (Biotage® Isolera PrimeTM, SNAP-Sil cartridge, gradient from 100% DCM to DCM/MeOH 10:1) or chromatography on reverse phase (Biotage® Isolera PrimeTM, SNAP-C18 cartridge, gradient from 100% H_2O to 100% ACN).

5-(4-(pyridin-4-yl)-1H-1,2,3-triazol-1-yl)pentan-1-ol (35(II))

From 40.4 mg of 4-ethynylpyridine, after a purification by *flash* chromatography on silica gel, 53.0 mg of **35(II)** were obtained(64% yield).

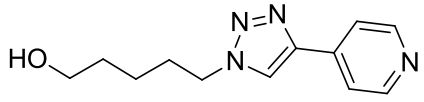

35(II): ^{1}H NMR (400 MHz, $CDCl_3$) δ 8.74 – 8.53 (m, 2H), 7.90 (s, 1H), 7.69 (d, *J* = 4.7 Hz, 2H), 4.40 (t, *J* = 7.1 Hz, 2H), 3.62 (t, *J* = 6.3 Hz, 2H), 2.41 (s, 1H), 1.97 (p, *J* = 7.3 Hz, 2H), 1.67 – 1.54 (m, 2H), 1.50 – 1.37 (m, 2H). ^{13}C NMR (101 MHz, $CDCl_3$) δ 150.14, 145.08, 138.15, 121.15, 120.04, 62.06, 50.52, 31.83, 29.99, 22.82.

5-(4-(pyridin-3-yl)-1H-1,2,3-triazol-1-yl)pentan-1-ol (35(III))

From 40.4 mg of 3-ethynylpyridine, after a purification by *flash* chromatography on silica gel, 43.0 mg of **35(III)** were obtained (52% yield).

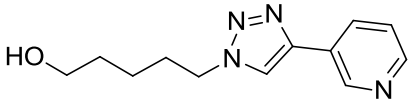

35(III): ^{1}H NMR (400 MHz, $CDCl_3$) δ 8.95 (s, 1H (H-2(Py)), 8.52 (s, 1H (H-6(Py)), 8.16 (d, *J* = 7.9 Hz, 1H (H-4(Py)), 7.86 (s, 1H (H (triazole))), 7.33 (dd, *J* = 7.5, 4.8 Hz, 1H (H-5(Py)), 4.40 (t, *J* = 7.1 Hz, 2H (CH_2-triazole)), 3.62 (t, *J* = 6.2 Hz, 2H ($C\underline{H_2}$-OH)), 1.97 (p, *J* = 7.3 Hz, 2H ($C\underline{H_2}$-CH_2-triazole)), 1.59 (p, *J* = 6.4 Hz, 2H ($C\underline{H_2}$-CH_2-OH)), 1.44 (q, *J* = 8.2 Hz, 2H ($C\underline{H_2}$-CH_2-CH_2-OH)). ^{13}C NMR (101 MHz, $CDCl_3$) δ 148.99, 146.82 (2 x CH(Py)); 144.55 (C(triazole)); 133.01 (CH(Py)); 126.86 (C(Py)); 123.83 (CH(Py)); 120.00 (CH-triazole); 62.06 (CH_2-OH); 50.45 (CH_2-triazole); 31.86, 30.02, 22.84 (CH_2-($\underline{C}H_2$)$_3$-CH_2-OH). IR (neat): 3367, 3127, 2937, 2863, 1456, 1439, 1408, 1226, 1051.

5-(4-(pyridin-2-yl)-1H-1,2,3-triazol-1-yl)pentan-1-ol (35(IV))

From 40.4 mg of 2-ethynylpyridine, after a purification by *flash* chromatography on silica gel, 67.7 mg of **35(IV)** were obtained(82% yield).

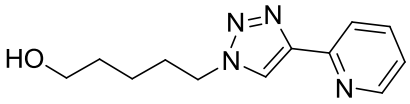

35(IV): ^{1}H NMR (400 MHz, $CDCl_3$) δ 8.51 (ddd, *J* = 4.9, 1.6, 0.8 Hz, 1H), 8.13 (d, *J* = 8.6 Hz, 2H), 7.74 (td, *J* = 7.8, 1.8 Hz, 1H), 7.19 (ddd, *J* = 7.6, 4.9, 1.2 Hz, 1H), 4.38 (t, *J* = 7.1 Hz, 2H), 3.59 (t, *J* = 6.4 Hz, 2H), 2.67 (s, 1H), 2.01 – 1.85 (m, 2H), 1.61 – 1.51 (m, 2H), 1.46 – 1.33 (m, 2H). ^{13}C NMR (101 MHz, $CDCl_3$) δ 150.14, 149.14, 148.05, 137.09, 122.85, 122.00, 120.27, 62.06, 50.36, 31.88, 29.93, 22.76.

5-(4-((pyridin-4-yloxy)methyl)-1H-1,2,3-triazol-1-yl)pentan-1-ol (35(VI))

From 52.2 mg of **30(VI)**, after purification by *flash* chromatography in reverse phase, 76.8 mg of **35(VI)** were obtained (83% yield).

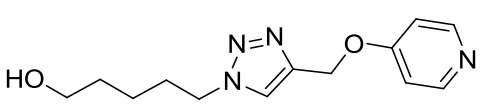

35(VI): ^{1}H NMR (400 MHz, $CDCl_3$) δ 7.69 (s, 1H (CH(triazole)), 7.57 (d, *J* = 6.8 Hz, 2H (2 X CH(Py)), 6.38 (d, *J* = 7.4 Hz, 2H (2 X CH(Py)), 5.06 (s, 2H (CH_2-OPy)), 4.32 (t, *J* = 7.1 Hz, 2H (CH_2-triazole)), 3.51 (t, *J* = 6.3 Hz, 2H ($C\underline{H_2}$-OH)), 1.88 (p, *J* = 7.3 Hz, 2H ($C\underline{H_2}$-CH_2-triazole)), 1.56 – 1.42 (m, 2H ($C\underline{H_2}$-CH_2-OH)), 1.41 – 1.23 (m, 2H 2H ($C\underline{H_2}$-$(CH_2)_2$-OH)). ^{13}C NMR (101 MHz, $CDCl_3$) δ 179.21(C_q (triazole)); 141.47 (C_q (Py)); 140.51 (2 x CH (Py)); 122.99 (CH (triazole)); 118.28 (2 x CH (Py)); 61.51 (CH_2-OH); 51.33 (CH_2-OPy); 50.50 (CH_2-$\underline{C}H_2$-triazole); 31.38 (CH_2-$\underline{C}H_2$-OH); 29.67 ($\underline{C}H_2$-CH_2-triazole); 22.60 ($\underline{C}H_2$-$(CH_2)_2$-OH)).

5-(4-((pyridin-2-yloxy)methyl)-1H-1,2,3-triazol-1-yl)pentan-1-ol (35(VII))

From 52.2 mg of **30(VII)**, after a purification by *flash* chromatography on silica gel, 13.1 mg of **35(VII)** were obtained (14% yield).

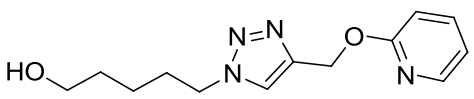

35(VII): ^{1}H NMR (400 MHz, $CDCl_3$) δ 7.77 (s, 1H), 7.60 (dd, *J* = 6.8, 1.9 Hz, 1H), 7.32 (ddd, *J* = 8.9, 6.6, 2.0 Hz, 1H), 6.55 (d, *J* = 9.2 Hz, 1H), 6.20 (dd, *J* = 6.7, 1.0 Hz, 1H), 5.17 (s, 2H), 4.32 (t, *J* = 7.2 Hz, 2H), 3.62 (t, *J* = 6.3 Hz, 2H), 2.02 – 1.84 (m, 3H), 1.61 – 1.51 (m, 2H), 1.46 – 1.33 (m, 2H).

5.1.2.4 Synthesis of compounds 43 and 44

Synthesis of 3-(pyridin-4-yl)propyl 4-methylbenzenesulfonate (42)

At 0ºC, *p*-Tosyl-Cl (142 mg, 0.742 mmol) was added to a solution of the 3-(pyridin-4-yl)propan-1-ol (97 mg, 0.707 mmol) and K_2CO_3 (117 mg, 0.849 mmol) in DCM (1.5 ml). The reaction mixture was stirred at 0ºC for 45 min. Then, 2 ml of H_2O were added and the two phases were separated. The organic phase was dried over Na_2SO_4 $_{anh}$ and the solvent removed by distillation under reduced pressure. The residue was purified by *flash* chromatography (gradient from 100% DCM to DCM/MeOH 9:1), obtaining 72 mg of **42** as a colorless oil, which presented around 15% impurity but was used in the next step without further purification.

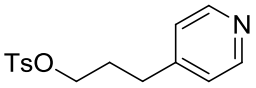

42: ^{1}H NMR (400 MHz, $CDCl_3$) δ 8.46 (d, *J* = 5.7 Hz, 2H), 7.78 (d, *J* = 8.3 Hz, 2H), 7.35 (d, *J* = 8.1 Hz, 2H), 7.02 (d, *J* = 5.9 Hz, 2H), 4.03 (t, *J* = 6.1 Hz, 2H), 2.74 – 2.60 (m, 2H), 2.46 (s, 3H), 2.11 – 1.84 (m, 2H).

Synthesis of 3-(pyridin-4-yl)propanal (40)

A solution of dry DMSO (124 µl, 1.750 mmol) in 0.5 ml of dry DCM was added to a solution of oxalyl dichloride (102 µl, 1.181 mmol) in DCM (0.3 ml) at -78 °C. After stirring for 15 min, a solution of 3-(pyridin-4-yl)propan-1-ol (60 mg, 0.437 mmol) in dry DCM (0.3 ml) was added dropwise. The reaction mixture was stirred at -78 °C for 60 min, then dry Et_3N (427 µl, 3.06 mmol) was added and the solution was warmed to rt. After this, H_2O was added and the two phases were separated. The organic phase was dried over Na_2SO_{4anh} and the solvent was removed under reduced pressure. The residue was purified by *flash* chromatography (DCM/MeOH 20:1), obtaining 48 mg of **40** as a brown foam, which presented around 15% impurity but was used in the next step without further purification.

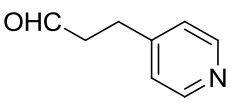

40: ^{1}H NMR (400 MHz, $CDCl_3$) δ 9.81 (s, 1H), 8.50 (d, *J* = 6.1 Hz, 2H), 7.12 (d, *J* = 4.4 Hz, 2H), 2.94 (t, *J* = 7.3Hz, 2H), 2.82 (tt, *J* = 7.4, 1.0 Hz, 2H).

Synthesis of 4-(3-((2*R*,3*R*,4*R*,5*S*)-3,4,5-tris(benzyloxy)-2-((benzyloxy)methyl)piperidin-1-yl)propyl)pyridine (41)

Method A: According to*Method A for the N-alkylation with tosylates*, from 52.5 mg (0.094 mmol) of **13** hydrochloride and 58 mg (0.159 mmol) of **42**, after a *flash* chromatography eluting with Hx/AcOEt 3:1 and 1:1, 5 mg of **41** were obtained as a yellowish oil (8% overall yield from 3-(pyridin-4-yl)propan-1-ol). Moreover, 23 mg of **13** were also recovered from this reaction.

Method B: In a round bottomed flask, sodium acetate (7.77 mg, 0.095 mmol) and a solution of **13**(HCl) (53.0 mg, 0.095 mmol) in DCM were introduced. After stirring for a couple of minutes, the aldehyde **40** (48 mg, 0.284 mmol) was added. The mixture was stirred at 25 °C for 1h. Afterthat, $NaBH(AcO)_3$ (80 mg, 0.379 mmol) was added and the mixture was stirred at room temperature overnight. The next day, an aqueous saturated solution of Na_2CO_3 was added and the two phases separated. The organic phase was dried over anhydrous Na_2SO_4 and the solvent removed by distillation under reduced pressure. The residue was purified by *flash* chromatography (Hx/AcOEt 3:2), obtaining 9 mg of **41** as a yellow oil (15% overall yield from 3-(pyridin-4-yl)propan-1-ol).

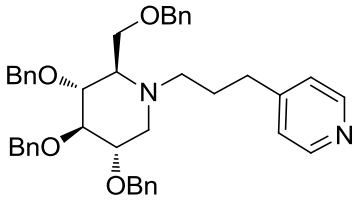

41: ^{1}H NMR (400 MHz, $CDCl_3$) δ 8.47 (s, 2H), 7.39 – 7.20 (m, 18H), 7.11 (dd, *J* = 7.4, 2.2 Hz, 2H), 7.02 (d, *J* = 4.8 Hz, 2H), 5.01 – 4.76 (m, 3H), 4.74 – 4.57 (m, 2H), 4.45 – 4.31 (m, 3H), 3.75 – 3.40 (m, 5H), 3.04 (dd, *J* = 11.3, 4.9 Hz, 1H), 2.81 – 2.68 (m, 1H), 2.66 – 2.28 (m, 4H), 2.21 (t, *J* = 10.8 Hz, 1H), 1.82 – 1.61 (m, 2H). HRMS calculated for $C_{42}H_{47}N_2O_4$ ($[M+H]^+$): 643.3536; found: 643.3597. $[\alpha]^{24}{}_D$ -3° (*c* 1.6, $CHCl_3$).

Synthesis of (2*R*,3*R*,4*R*,5*S*)-2-(hydroxymethyl)-1-(3-(piperidin-4-yl)propyl)piperidine-3,4,5-triol dihydrochloride (43)

According to *Method A: hydrogenation with $Pd(OH)_2/C$*, from 9 mg (0.014 mmol) of **41,** after 4 days of reaction 5.43 mg of **43**were obtained as a yellow foam (100% yield).

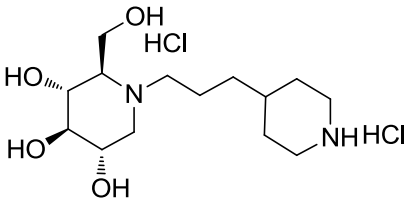

43: ^{1}H NMR (400 MHz, MeOD) δ 4.10 (d, *J* = 11.4 Hz, 1H (C$\underline{H}_{2a}$-OH)), 3.90 (d, *J* = 12.1 Hz, 1H (C$\underline{H}_{2b}$-OH)), 3.76 – 3.63 (m, 1H (C$\underline{H}$-OH)), 3.58 (t, *J* = 8.9 Hz, 1H (C$\underline{H}$-OH)), 3.50 – 3.41 (m, 1H (CH-C$\underline{H}_{2a}$-N)), 3.42 – 3.33 (m, 4H (C$\underline{H}$-OH, N-C$\underline{H}_{2a}$-CH_2 and 2 x CH-C$\underline{H}_{2a}$(Pip))), 3.21 – 3.14 (m, 1H (N-C$\underline{H}_{2b}$-CH_2)), 3.07 – 2.93 (m, 4H (C$\underline{H}$-CH_2-OH, CH-C$\underline{H}_{2b}$-N and 2 x CH-C$\underline{H}_{2b}$(Pip)), 2.02 – 1.92 (m, 2H (2 x C$\underline{H}_{2a}$-NH (Pip)), 1.86 – 1.64 (m, 3H (N-CH_2-C$\underline{H}_2$ and CH (Pip))), 1.47 – 1.35 (m, 4H (CH_2-Piperidine and 2 x C$\underline{H}_{2b}$-NH (Pip))). ^{13}C NMR (101 MHz, MeOD) δ 76.70, 67.39, 66.37, 66.19 (C$\underline{H}$-CH_2-OH and 3 x CH-OH); 53.74, 53.67 (CH_2-OH and CH-C$\underline{H}_2$-N); 53.05 (N-C$\underline{H}_2$-CH_2); 43.94 (2 x CH-C$\underline{H}_2$(Pip)); 33.00 (CH (Pip)); 32.31 (CH_2-Piperidine), 28.48, 28.40 (2 x CH_2-NH (Pip)); 19.98 (N-CH_2-C$\underline{H}_2$-CH_2).HRMS calculated for $C_{14}H_{29}N_2O_4$: 289.2127 $[M+H]^+$; found: 289.2134. $[\alpha]^{26}_D$ -6° (*c* 0.3, MeOH).

Synthesis of (2*R*,3*R*,4*R*,5*S*)-2-(hydroxymethyl)-1-(3-(pyridin-4-yl)propyl)piperidine-3,4,5-triol (44)

According to *Method B: debenzylation with BCl_3*, from 34 mg (0.053 mmol) of **41** after filtration of the crude through 400 mg of strong basic resin Amberlite-IRA400 and purification by *flash* chromatography (Biotage® Isolera PrimeTM, SNAP KP-C18-HS cartrige, gradient: A/B from 100:0 to 0:100, Eluent: A:H_2O+0.1%NH_4OH, B: ACN + 0.1% NH_4OH), 7 mg of **44** were obtained as yellowish foam (42% yield).

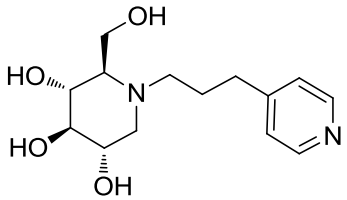

44: ^{1}H NMR (400 MHz, MeOD) δ 8.41 (d, *J* = 6.1 Hz, 2H (2 x CH_{Py})), 7.32 (d, *J* = 6.2 Hz, 2H (2 x CH_{Py})), 3.90 – 3.75 (m, 2H (C$\underline{H}_2$-OH)), 3.50 – 3.41 (m, 1H (C$\underline{H}$-OH)), 3.37 – 3.33 (m, 1H (C$\underline{H}$-OH)), 3.13 (t, *J* = 9.0 Hz, 1H (C$\underline{H}$-OH)), 2.98 (dd, *J* = 11.2, 4.9 Hz, 1H (CH-C$\underline{H}_{2a}$-N)), 2.93 – 2.81 (m, 1H (N-C$\underline{H}_{2a}$-CH_2)), 2.74 – 2.57 (m, 3H (N-C$\underline{H}_{2b}$-CH_2 and C$\underline{H}_2$-Py)), 2.21 – 2.10 (m, 2H, (CH-C$\underline{H}_{2b}$-N and C$\underline{H}$-CH_2-OH)), 1.89 – 1.80 (m, 2H (CH_2-C$\underline{H}_2$-CH_2)). ^{13}C NMR (101 MHz, MeOD) δ 152.82 (C_{Ar}); 148.41, 124.19 (4 x CH_{Ar}); 79.10, 70.65, 69.34 (3 x CH-OH); 66.06 (C$\underline{H}$-CH_2-OH); 58.23 (CH-C$\underline{H}_2$-OH); 56.29 (CH-C$\underline{H}_2$-N); 51.64 (N-C$\underline{H}_2$-CH_2); 32.45 (CH_2-Py); 24.92 (CH_2-C$\underline{H}_2$-CH_2).HPLC (UV) 75.8% rt: 1.49'. HRMS calculated for $C_{14}H_{23}N_2O_4$: 283.1658 $[M+H]^+$; found: 283.1660. IR (neat): 3307, 2924, 1605, 1560, 1417, 1081, 1033, 1014. $[\alpha]^{26}_D$ -10° (*c* 0.7, MeOH).

5.1.3 Synthesis of compounds with different pK_a in the sugarmimethic core

5.1.3.1 Synthesis of *myo*-inositol benzylated core (compounds 49, 53-60, 62 and 63)

Synthesis of (1*SR*,4*SR*,5*RS*,6*RS*)-5,6-dibromocyclohex-2-ene-1,4-diol ((±)-53)[150]

A solution of p-benzoquinone (50.2 g, 464 mmol) in DCM (1 l) was cooled to 0 ºC and then dibromine (25.2 ml, 492 mmol) was added dropwise over 15 minutes. The resulting mixture was stirred and allowed to reach room temperature for 2 hours. Then, TLC was done and it was checked that no starting benzoquinone remained. The solvent of the reaction mixture was removed under reduced pressure to give the dibromo-dione **(±)-52** as a brown solid, that was redissolved in 900 ml of diethyl ether and the solution cooled to -5 ºC (NaCl and ice bath). Then, a solution of sodium borohydride (38.5 g, 1019 mmol) in 270 ml of water was carefully added dropwise. After that, the resulting mixture was allowed to reach room temperature and stirred overnight. Next day, the crude was diluted with water (3.5 l) and extractions were done with diethyl ether (10 extractions). Then, the collected organic layer were dried over $MgSO_4$, filtered and the solvent was removed under reduced pressure to give 58 g of **(±)-53**as a white solid (46% yield).

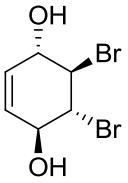

(±)-53: ^{1}H NMR (400 MHz, MeOD) δ 5.69 (d, *J* = 0.5 Hz, 2H), 4.43 – 4.32 (m, 2H), 4.11 – 4.02 (m, 2H).

Synthesis of (1*RS*,2*SR*,3*SR*,4*RS*)-cyclohex-5-ene-1,2,3,4-tetrayl tetraacetate ((±)-49)

58 ml of acetic acid were added to a solution of 6.78 g (24.93 mmol) of **(±)-53** and 19.58 g (199 mmol) of AcOK in 23.5 ml (249 mmol) of acetic anhydride. The mixture was stirred 48h at 145 °C. After, the mixture was cooled to rt, diluted with 25 ml of MeOH and stirred for 10 minutes. Then, the solvent was distilled off under reduced pressure. The resulting paste was dissolved with AcOEt and washed with water, sat. aq. $NaHCO_3$ solution, and brine. The organic layer was dried over Na_2SO_4 and filtered. The solvent was removed under reduced pressure and the residue was purified by *flash* chromatography on silica gel (Flash$^+$ Biotage®, KP-Sil 40+M column, Hx/AcOEt 5:2), giving 2.5 g of **(±)-49** as a white solid (31% yield).

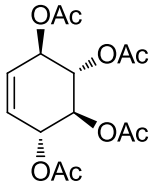

(±)-49: ^{1}H NMR (400 MHz, $CDCl_3$) δ 5.68 (d, *J* = 0.5 Hz, 2H), 5.60 – 5.55 (m, 2H), 5.34 – 5.28 (m, 2H), 2.04 (s, 6H), 2.02 (s, 6H).

Synthesis of (1*S*,2*S*,3*R*,6*R*)-3,6-dihydroxycyclohex-4-ene-1,2-diyl diacetate ((-)-54) and (1*S*,2*R*,3*R*,4*S*)-cyclohex-5-ene-1,2,3,4-tetrayl tetraacetate ((+)-49)

2 g (6.36 mmol) of racemic tetraester **(±)-49** dissolved in 200 ml of tBME were treated with 4 g of Lipozyme® in the presence of n-BuOH (2.3 ml, 25.5 mmol). The mixture was stirred for 48 h at 40ºC and 300 rpm. After, the mixture was filtrated and the solvent of the filtrate was distilled off under reduced pressure. After purification by *flash* cromatography on silicagel (Isolera®; elutent: Hx/AcOEt 2:3; column SNAP 50g), 572 mg of diol **(-)-54** (white solid, 78% yield) and 816 mg of tetraacetate **(+)-49** (white solid, 82% yield) were obtained, with analytical data in concordance with those previously reported[149].

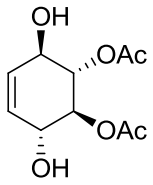

(-)-54:^{1}H NMR (400 MHz, $CDCl_3$) δ 5.72 (d, *J* = 0.5 Hz, 2H), 5.04 – 4.94 (m, 2H), 4.40 (d, *J* = 5.3 Hz, 2H), 2.45 (s, 2H), 2.10 (s, 6H). ^{13}C NMR (101 MHz, $CDCl_3$) δ 171.39, 129.04, 75.40, 70.85, 20.83. $[\alpha]^{26}_{D}$-159º(*c*0.3, $CHCl_3$).

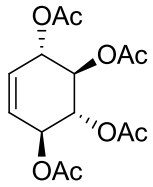

(+)-49: ^{1}H NMR (400 MHz, $CDCl_3$) δ 5.68 (d, *J* = 0.6 Hz, 2H), 5.60 – 5.55 (m, 2H), 5.34 – 5.28 (m, 2H), 2.04 (s, 6H), 2.02 (s, 6H). $[\alpha]^{26}_{D}$+141º (*c* 1.1, $CHCl_3$).

Synthesis of (1*S*,2*R*,3*R*,4*S*)-cyclohex-5-ene-1,2,3,4-tetraol (55)

3.1 g (9.86 mmol) of **(+)-49** were dissolved in 100 ml of MeOH. The mixture was cooled with an ice bath and then 68 mg (2.96 mmol) of Na were added in small portions. The mixture was stirred overnight at rt. Next day, the solvent was partially removed by vacuum and diethyl ether was added. The crude was kept inside the fridge overnight. Then, the solvent was removed by filtration, giving 1.26 g of **55** as a brown solid precipitate (87% yield), with ^{1}H NMR spectra in concordance with the previously reported[147].

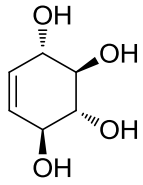

55: ^{1}H NMR (400 MHz, MeOD) δ 5.55 (s, 2H), 4.09 – 3.98 (m, 2H), 3.38 – 3.32 (m, 2H).

Synthesis of (1*R*,2*R*,3*S*,4*S*,5*R*,6*S*)-7-oxabicyclo[4.1.0]heptane-2,3,4,5-tetraol (56)

1.33 g (9.09 mmol) of **55**were dissolved in 125 ml of MeOH. Then, the mixture was cooled to 0ºC and 4.70 g (27.3 mmol) of mCPBA were added. The mixture was stirred at room temperature overnight. Next day, the solvent was distilled off under reduced pressure and the residue was triturated with DCM to dissolve exces mCPBA and 3-clorobenzoic acid. The remaining solid was washed several times with DCM and the remaining traces of solvent were removed under reduced pressure at rt. Finally, 1.30 g of **56** were obtained as white solid (88% yield), with ^{1}H NMR spectra in concordance with the previously reported[147].

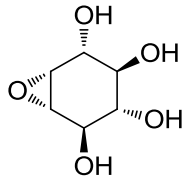

56: ^{1}H NMR (400 MHz, MeOD) δ 3.76 (dd, *J* = 8.2, 1.9 Hz, 1H), 3.67 (dd, *J* = 7.9, 0.8 Hz, 1H), 3.28 – 3.28 (m, 1H), 3.26 – 3.10 (m, 2H), 3.06 (d, *J* = 3.7 Hz, 1H).

Synthesis of (1*R*,2*R*,3*S*,4*S*,5*R*,6*S*)-2,3,4,5-tetrakis(benzyloxy)-7-oxabicyclo[4.1.0]heptane (57)[147]

9.51 ml (80 mmol) of benzyl bromide were carefully added to a solution of 1.30 g (7.99 mmol) of **56** and 2.88 g (71.9 mmol) of NaH (60% in mineral oil) in 50 ml of DMF at 30ºC. The mixture was stirred overnight at 30ºC. Then, the solvent was distilled off under reduced pressure and the residue was partitioned between AcOEt/H_2O. The organic layer was washed with brine and dried over $Na2SO_4$. The solvent was distilled off under reduced pressure. The residue was treated with 20ml of Hx and the soluble impurities were removed by filtration. 3.56 g of **57** were obtained as a white solid (85% yield), with ^{1}H NMR spectra in concordance with the previously reported[147].

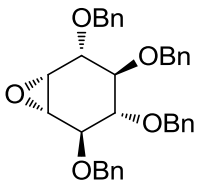

57: ^{1}H NMR (400 MHz, $CDCl_3$) δ 7.43 – 7.18 (m, 20H), 4.87 – 4.68 (m, 8H), 3.88 (ddd, *J* = 7.9, 3.3, 1.3 Hz, 2H), 3.61 (dd, *J* = 10.4, 8.5 Hz, 1H), 3.45 (dd, *J* = 10.5, 7.9 Hz, 1H), 3.31 (ddd, *J* = 3.9, 1.8, 0.8 Hz, 1H), 3.18 (d, *J* = 3.8 Hz, 1H).

Synthesis of (1*R*,2*R*,3*S*,4*R*,5*R*,6*S*)-2-azido-3,4,5,6-tetrakis(benzyloxy)cyclohexanol (58) and (1*S*,2*S*,3*S*,4*R*,5*R*,6*S*)-2-azido-3,4,5,6-tetrakis(benzyloxy)cyclohexanol (59)

15.62 g (147 mmol) of $LiClO_4$ were added to a solution of 3.66 g (6.99 mmol) of **57** in 70 ml of ACN. Then, 4.55g (69.9 mmol) of NaN_3 were added, and the reaction was stirred at reflux overnight. Then, the mixture was cooled to 0ºC and quenched by the addition of water. Then the ACN was removed by distillation under reduced pressure and the aqueous mixture was extracted with AcOEt. The combined organic layers were washed with brine and dried over Na_2SO_4. The solvent was distilled off under reduced pressure, and after *flash* column chromatography on silica eluting with hexane/EtOAc (6:1), 2.13 g of **58** (colorless oil, 54% yield) and 633 mg of **59** (colorless oil, 16% yield) were obtained, with ^{1}H NMR spectra in concordance with the previously reported[147].

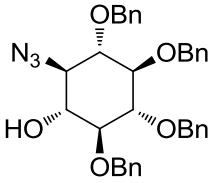

58: ^{1}H NMR (400 MHz, $CDCl_3$) δ 7.40 – 7.15 (m, 20H), 4.94 – 4.72 (m, 8H), 3.57 (dt, *J* = 7.7, 2.7 Hz, 1H), 3.54 – 3.47 (m, 1H), 3.39 (tt, *J* = 4.1, 2.4 Hz, 4H).

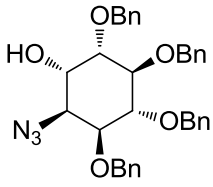

59: ^{1}H NMR (400 MHz, $CDCl_3$) δ 7.38 – 7.25 (m, 20H), 4.90 – 4.56 (m, 8H), 4.05 – 3.98 (m, 2H), 3.94 (t, *J* = 3.4 Hz, 1H), 3.83 (t, *J* = 9.1 Hz, 1H), 3.73 (td, *J* = 9.1, 0.7 Hz, 1H), 3.66 (dd, *J* = 9.3, 3.0 Hz, 1H).

Synthesis of (1*R*,2*S*,3*S*,4*R*,5*S*,6*R*)-2-azido-3,4,5,6-tetrakis(benzyloxy)cyclohexyl methanesulfonate (60)[147]

A solution of 152 mg (0.269 mmol) of **58** in 2.5 ml of dry THF was cooled to 0ºC. Then 112 µl (0.806 mmol) of Et_3N and 31.4 µl (0.403 mmol) of MsCl were added and the mixture was stirred overnight at rt. Next day the mixture was filtrated and the solved was distilled off under reduced pressure. The residue was redissolved in diethyl ether and filtered again to remove the insoluble triethylamine salts. The solvent of the filtrate was again removed by distillation

under reduced pressure, giving 172 mg of 60 (white oil, 99% yield). The H-NMR was compatible with those previously reported in the literature[147] and the obtained compound was used in the next step without further purification.

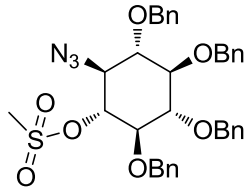

60: ^{1}H NMR (400 MHz, $CDCl_3$) δ 7.34 – 7.25 (m, 18H), 7.22 – 7.17 (m, 2H), 5.01 – 4.69 (m, 8H), 4.40 (dd, *J* = 10.3, 9.3 Hz, 1H), 3.64 – 3.35 (m, 5H), 3.02 (s, 3H).

Synthesis of (1*S*,2*S*,3*S*,4*R*,5*S*,6*S*)-2-azido-3,4,5,6-tetrakis(benzyloxy)cyclohexyl acetate (62)

1.27 g (15.53 mmol) of AcONa and 300 µl of H_2O were added to a solution of 1g (1.553 mmol) of **60** in 15 ml of DMF. The mixture was stirred at 150ºC overnight. Next day, the crude was cooled to rt and partitioned over AcOEt/H_2O. The organic phase was washed twice with H_2O and dried over anh. Na_2SO_4 and filtered. The solvent was distilled off under reduced pressure and the residue was purified by *flash* chromatography on silicagel (Flash$^+$ Biotage®, KP-Sil 40+M column, Hx/AcOEt 6:1). 630 mg of **62** were obtained as colorless oil (67% yield).

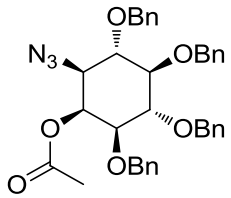

62: ^{1}H NMR (400 MHz, $CDCl_3$) δ 7.34 – 7.25 (m, 20H), 5.69 (t, *J* = 2.8 Hz, 1H), 4.94 – 4.69 (m, 7H), 4.48 (d, *J* = 11.1 Hz, 1H), 3.93 – 3.75 (m, 2H), 3.59 – 3.46 (m, 2H), 3.42 (dd, *J* = 10.4, 2.7 Hz, 1H), 2.15 (s, 3H).

Synthesis of (1*S*,2*R*,3*S*,4*R*,5*R*,6*S*)-2-amino-3,4,5,6-tetrakis(benzyloxy)cyclohexanol (63)

A solution of 530 mg (0.872 mmol) of **62** in 10 ml of anh. THF was added dropwise over a suspension of 83 mg (2.180 mmol) of LAH in 6 ml of anhydrous THF at 0ºC. After the addition, the mixture was stirred at this temperature for 60 minutes. Then, the reaction was quenched by addition of AcOEt and $Na_2SO_4 \cdot 10H_2O$. Finally, the crude was filtrated and the solvent removed by distillation under reduced pressure. The residue was was purified by silica *flash*

chromatography (elution with CH_2Cl_2-MeOH-TEA (99:1:0.7)). 460 mg of **63** were obtained as white solid (98% yield), with the analytical data according to the previously described[147].

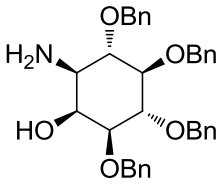

63: ^{1}H NMR (400 MHz, $CDCl_3$) δ 7.35 – 7.23 (m, 20H), 5.02 – 4.79 (m, 5H), 4.69 (s, 2H), 4.65 (d, *J* = 11.2 Hz, 1H), 4.12 (t, *J* = 2.7 Hz, 1H), 3.93 (t, *J* = 9.5 Hz, 1H), 3.63 (t, *J* = 9.7 Hz, 1H), 3.52 – 3.40 (m, 2H), 2.62 (dd, *J* = 10.0, 2.6 Hz, 1H). ^{13}C NMR (101 MHz, $CDCl_3$) δ 138.66, 138.52, 138.43, 137.88, 128.53, 128.52, 128.48, 128.38, 128.34, 127.96, 127.94, 127.90, 127.88, 127.87, 127.86, 127.82, 127.75, 127.57, 127.56, 84.60, 81.86, 81.65, 81.24, 75.89, 75.71, 75.62, 72.66, 69.30, 53.79).HRMS calculated for $C_{34}H_{38}NO_5$ ($[M+H]^+$): 540.2750; found: 540.2735. Mp = 165-168ºC. IR (neat): 3029, 2893, 2867, 1453, 1357, 1071, 695. . $[\alpha]^{24}_D$ -24º (*c* 1.0, $CHCl_3$).

5.1.3.2 Synthesis of fluoroinositol derivatives (compounds 66, 67x, 67y,68x and 68y)

Synthesis of ((((1*R*,2*S*,3*R*,4*S*,5*S*,6*S*)-5-azido-6-fluorocyclohexane-1,2,3,4-tetrayl)tetrakis(oxy))tetrakis(methylene))tetrabenzene (66)[170]

Triflic anhydride (8.96 µl, 0.053 mmol) was added at −5 °C to a solution of azidoalcohol **58** (25 mg, 0.044 mmol) in 221 µl of anh. DCM containing 8.94 µl of anh.Py (0.110 mmol). The mixture was stirred at rt for 1 h. The mixture was successively washed with 1 M HCl, aq $NaHCO_3$, and water. The organic phase was dried over anhydrous Na_2SO_4 and the solvent was distilled off under reduced pressure at T<35 °C, to give 24 mg of the azido-triflate as a yellow oil.

The azido-triflate residue was redisolved in 200 µl of THF, and 53 µl of TBAF 1M in THF (0.053 mmol) were added to the solution. The mixture was stirred overnight at rt. After, the mixture was poured onto ice and extracted with AcOEt. The extract was washed with H_2O, dried over Na_2SO_4 and the solvent was distilled off under reduced pressure. The residue was purified by *flash* chromatography (Flash$^+$ Biotage® purification system, Biotage KP-Sil® 12+S column, Hx/AcOEt 8:1). 18 mg of **66** were obtained as a white paste (77% yield).

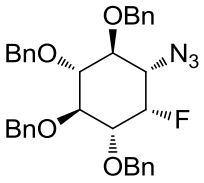

66: ^{1}H NMR (400 MHz, $CDCl_3$) δ 7.43 – 7.15 (m, 20H_{Ar}), 4.95 – 4.74 (m, 9H (4 x C<u>H</u>$_2$-Ph and C<u>H</u>-F)), 3.92 (dtd, *J* = 15.2, 10.0, 1.4 Hz, 2H (C<u>H</u>-OBn)), 3.56 – 3.26 (m, 3H (2 x C<u>H</u>-OBn and C<u>H</u>-N_3)). ^{13}C NMR (101 MHz, $CDCl_3$) δ 138.21, 138.15, 137.53, 137.34 (4 x C_{Ar}); 128.56, 128.42, 128.39, 128.16, 128.05, 128.00, 127.92, 127.85, 127.73, 127.70, 127.64 (20 x CH_{Ar}); 90.18 (CH-F), 88.36, 83.66, 80.93, 80.89, 79.68, 79.64, 78.83, 78.66 (4 x <u>C</u>H-OBn); 76.16, 75.95, 75.91, 72.96 (4 x <u>C</u>H_2-Ph), 62.21, 62.04 (1 x CH-N3). ^{19}F NMR (376 MHz, $CDCl_3$) δ -209.05 (dt, *J* = 51.1, 29.1 Hz).HRMS calculated for $C_{34}H_{35}NO_4F$ ([M-N_2+H]$^+$): 540.2550; found: 540.2573. IR (neat) : 2105 cm^{-1}(N_3). $[\alpha]^{26}_D$ +9° (*c* 1.0, $CHCl_3$).

Synthesis of (1*S*,2*R*,3*S*,4*R*,5*S*,6*S*)-5-fluoro-6-(nonylamino)cyclohexane-1,2,3,4-tetraol (67y) and (1*R*,2*S*,3*R*,4*S*,5*S*,6*S*)-5-(dinonylamino)-6-fluorocyclohexane-1,2,3,4-tetraol hydrochloride (68y)

Similarly to **68x**, from 77 mg (0.136 mmol) of **66**, but adding 30.3 µl (0.176 mmol) of nonanal, after purification by *flash* chromatography (Biotage Isolera Prime TM purification system, column SNAP KP-C18-HS 12g, mobile phase: A: H2O+0.1%NH_4OH, B: ACN + 0.1% NH_4OH, gradient A/B from 100:0 to 0:100), 8 mg of **67y** were obtained as white paste (19% yield). The fraction with the disubstituted compound was treated with 1 ml of HCl in dioxane (1M) giving 8 mg of **68y** as a white paste (13% yield).

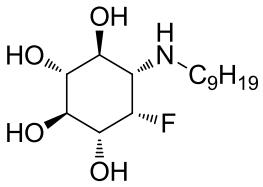

67y: ^{1}H NMR (400 MHzMeOD) δ 4.85 (dt, *J* = 52.0, 1.9 Hz, 1H), 3.63 – 3.35 (m, 3H), 3.22 (t, *J* = 9.1 Hz, 1H), 2.79 (dt, *J* = 11.3, 7.4 Hz, 1H), 2.66 – 2.44 (m, 2H), 1.53 (p, *J* = 7.3 Hz, 2H), 1.38 – 1.19 (m, 12H), 0.93 – 0.76 (m, 2H). ^{13}C NMR (101 MHzMeOD) δ 91.06, 89.30, 75.80, 72.74, 72.70, 71.71, 71.54, 71.27, 71.23, 59.87, 59.70, 31.60, 29.23, 29.16, 28.96, 28.95, 26.85, 22.28, 12.98.^{19}F NMR (376 MHz, MeOD) δ -213.87 (dt, *J* = 52.0, 29.9 Hz). HPLC (ESI) 94.1% rt: 2.88'; m/z: 308.15. HRMS calculated for $C_{15}H_{31}NO_4F$: 308.2237 [M+H]$^+$; found: 308.2225. IR (neat): 3260, 2917, 2850. . $[\alpha]^{26}_D$ -20° (*c* 0.81, MeOH).

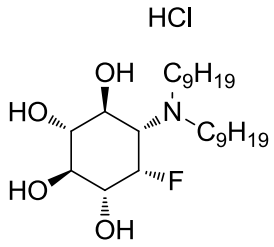

68y: ^{1}H NMR (400 MHz, MeOD) δ 5.22 (d, *J* = 52.2 Hz, 1H), 4.01 – 3.89 (m, 1H), 3.76 – 3.30 (m, 6H), 1.74 (s, 3H), 1.45 – 1.19 (m, 25H), 0.93 – 0.81 (m, 6H). ^{13}C NMR (101 MHz, MeOD) δ 90.03, 88.24, 75.32, 72.35, 71.11, 70.94, 66.65, 62.09, 61.92, 52.87, 31.56, 29.06, 29.03, 28.87, 28.79, 26.35, 22.27, 12.97.^{19}F NMR (376 MHz, MeOD) δ -207.50 (dt, *J* = 53.1, 31.1 Hz). HRMS calculated for $C_{24}H_{49}NO_4F$: 434.3646 $[M+H]^+$; found: 434.3666. IR (neat): 3355, 2923, 2854. $[\alpha]^{26}_D$ -15º (*c* 0.71, MeOH).

Synthesis of (1*R*,2*S*,3*R*,4*S*,5*S*,6*S*)-5-(dibutylamino)-6-fluorocyclohexane-1,2,3,4-tetraol hydrochloride (68x)

To a solution of 19.32 mg (0.034 mmol) of 66 in EtOH (0.06M), 2.2 mg of Pd/C (2.04 µmol) and 14.5 µl of acetic acid (0.340 mmol) were added. The mixture was stirred for 1 h at rt under H_2 atmosphere (1 atm). After this time, 5.51 µl of butyraldehyde (0.061 mmol) were added and the mixture was stirred 24h at rt, under 1.5 atm of H_2. Next day, the vessel was purged with N_2, and 2.2 mg of Pd/C (2.04 µmol), 180 µl of EtOH and 340 µl of HCl_{aq} (1 M) were added. The mixture was stirred 36h at rt, under 1.5 atm of H_2. When the debenzylation was completed, the catalyst was filtered over a pad of Celite®, and the solvent was removed by distillation under reduced pressure to give 7 mg of **68x**, as white paste (62% yield).

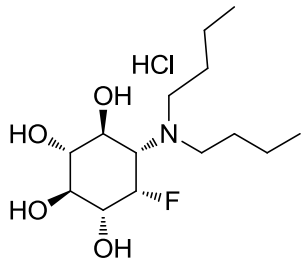

68x: ^{1}H NMR (400 MHz, MeOD) δ 5.23 (d, *J* = 52.5 Hz, 1H (CH-F)), 3.96 (dd, *J* = 11.2, 8.6 Hz, 1H (CH-OH)), 3.65 – 3.31 (m, 7H (3 x CH-OH, CH-N, CH_{2a}-N and CH_{2ab}-N)), 3.17 – 3.06 (m, 1H (CH_{2b}-N)),1.82 – 1.62 (m, 4H (2 x $C\underline{H}_2$-CH_2-CH_3)), 1.50 – 1.33 (m, 4H (2 x $C\underline{H}_2$-CH_3)), 0.99 (q, *J* = 7.1 Hz, 6H (2 x CH_3)). ^{13}C NMR (101 MHz, MeOD) δ 89.98, 88.19 (1 x CH-F); 75.30, 72.34, 71.08, 70.91, 66.65 (4 x CH-OH); 62.10, 61.93 (1 x CH-N); 52.91, 52.57 (2 x CH_2-N); 27.16, 26.26 (2 x $\underline{C}H_2$-CH_2-CH_3); 19.63 ($\underline{C}H_2$-CH_3); 12.45 (CH_3).^{19}F NMR (376 MHz, MeOD) δ -207.56 (dt, *J* = 56.7, 30.3 Hz). IR (neat) : 3356, 2962 cm^{-1}.HRMS calculated for $C_{14}H_{29}NO_4F$: 294.2081 $[M+H]^+$; found: 294.2076. IR (neat): 3356, 2962. . $[\alpha]^{25}_D$ -9º (*c* 0.57, MeOH).

Synthesis of (1*R*,2*S*,3*R*,4*S*,5*S*,6*S*)-5-(butylamino)-6-fluorocyclohexane-1,2,3,4-tetraol (67x)

Similarly to **68x**, from 20 mg (0.035 mmol) of **66**, but adding only 3.33 µl (0.037 mmol) of butyraldehyde, it was obtained a mixture that contained around 10% of **68x** as impurity. After purification by preparative HPLC (mobile phase: A: H2O+0.1% NH_4OH, B: ACN+ 0.1% NH_4OH gradient A/B from 100:0 to 0:100, total run time 15 min), 2.3 mg of **67x** were obtained as white paste (28% yield).

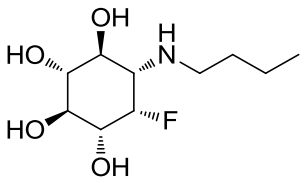

67x: ^{1}H NMR (400 MHz, MeOD) δ 4.84 (dt, *J* = 51.9, 2.0 Hz, 1H (C<u>H</u>-F)), 3.61 – 3.34 (m, 3H (3 x C<u>H</u>-OH)), 3.21 (t, *J* = 9.1 Hz, 1H (C<u>H</u>-OH)), 2.77 (dt, *J* = 11.3, 7.3 Hz, 1H (C<u>H</u>$_{2a}$-NH)), 2.63 – 2.41 (m, 2H (C<u>H</u>$_{2b}$-NH and C<u>H</u>-NH)), 1.63 – 1.43 (m, 2H (C<u>H</u>$_2$-CH_2-CH_3)), 1.44 – 1.28 (m, 2H (C<u>H</u>$_2$-CH_3)), 0.93 (t, *J* = 7.3 Hz, 3H (CH_3)).^{13}C NMR (101 MHz, MeOD) δ 91.13 (CH-F); 89.37, 75.87, 72.76, 71.80, 71.62, 71.39 (4 x CH-OH); 59.96, 59.79 (CH-NH); 46.50 (CH_2-NH), 31.36 (<u>C</u>H_2-CH_2-CH_3); 19.97 (<u>C</u>H_2-CH_3); 12.82 (CH_3).^{19}F NMR (376 MHz, MeOD) δ -214.01 (dt, *J* = 51.7, 29.8 Hz). HPLC (ESI) 98.2% rt: 1.03'; m/z: 238.16. HRMS calculated for $C_{10}H_{21}NO_4F$: 238.1455 $[M+H]^+$; found: 238.1463. IR (neat): 3363, 3258, 2922. . $[\alpha]^{24}_D$ -24º (*c* 0.24, MeOH).

5.1.3.3 Synthesis of benzylated *myo*-inositol and DNJ derivatives

5.1.3.3.1 Benzylated *N*-butil inositol derivatives (synthesis of compounds 72 and 74). Synthesis of *N*-((1*R*,2*S*,3*R*,4*R*,5*S*,6*S*)-2,3,4,5-tetrakis(benzyloxy)-6-hydroxycyclohexyl)butyramide (72)

According to General procedure for acylations, from 17.96 mg (0.204 mmols) of butyric acid and 100 mg of **63**, after purification by *flash* chromatography on silica gel (eluent:Hx/AcOEt 3:2), 62 mg of **72** were obtained as beige solid (55% yield).

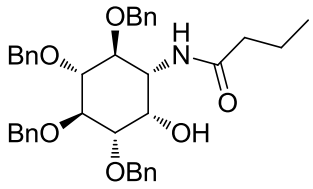

72: ^{1}H NMR (400 MHz, $CDCl_3$) δ 7.41 – 7.25 (m, 20H_{Ar}), 5.62 (d, *J* = 8.6 Hz, 1H (NH)), 4.91 – 4.78 (m, 5H (C$\underline{H}_2$-Ph), 4.72 – 4.58 (m, 3H (C$\underline{H}_2$-Ph), 4.09 (t, *J* = 2.8 Hz, 1H (C$\underline{H}$-OH)), 4.10 – 3.99 (m, 1H (C$\underline{H}$-NH)), 3.86 (td, *J* = 9.4, 1.0 Hz, 1H (C$\underline{H}$-OBn)), 3.73 (ddd, *J* = 10.4, 9.2, 1.0 Hz, 1H (C$\underline{H}$-OBn)), 3.59 (d, *J* = 9.3 Hz, 1H (C$\underline{H}$-OBn)), 3.58 – 3.49 (m, 1H (C$\underline{H}$-OBn)), 2.04 – 1.95 (m, 2H (C$\underline{H}_2$-CH_2-CH_3).), 1.64 – 1.49 (m, 2H (CH_2-C$\underline{H}_2$-CH_3).), 0.89 (t, *J* = 7.4 Hz, 3H (CH_3)). ^{13}C NMR (101 MHz, $CDCl_3$) δ 172.89 (C=O); 138.55, 138.42, 138.39, 137.58 (4 x C_{Ar}); 128.53, 128.43, 128.37, 128.37, 128.06, 128.03, 127.95, 127.87, 127.84, 127.70, 127.64, 127.61 (20 x CH_{Ar}); 84.13, 81.29, 80.81, 78.84 (4 x $\underline{C}$H-OBn); 75.89, 75.88, 75.08, 72.95 (4 x $\underline{C}H_2$-Ph); 68.95(CH-OH); 51.06 (CH-NH); 38.69 ($\underline{C}H_2$-CH_2-CH_3); 19.03 (CH_2-$\underline{C}H_2$-CH_3); 13.77 (CH_2-CH_2-$\underline{C}H_3$). HRMS calculated for $C_{38}H_{43}NO_6$ ([M+Na]$^+$): 632.2988; found: 632.2937. IR (neat): 3250, 3050, 2920, 1620, 1090, 1080. $[\alpha]^{25}_{D}$ -25º (*c* 1.5, $CHCl_3$).

Synthesis of (1*S*,2*S*,3*R*,4*R*,5*S*,6*R*)-2,3,4,5-tetrakis(benzyloxy)-6-(butylamino)cyclohexanol (74)

180 µ of borane/THF complex (0.180 mmol) were added to a solution of **72** (44 mg, 0.072 mmol) in 2 ml of THF. The mixture was stirred overnight at 70 °C under argon atmosphere. Next day, 2 ml of MeOH were added and the mixture was stirred 2 h more at 70 °C. After that, the solvent was removed by distillation under reduced pressure and the residue was partitioned in 2 ml of AcOEt and 2 ml of water. After separation of the two layers, the organic layer was washed with brine, dried over anhydrous Na_2SO_4 and filtered. The solvent was distilled off under reduced pressure, and the crude was treated with Hx/AcOEt 3:1 and filtered. The solvent was distilled off under reduced pressure rending 22 mg of **74** as colorless oil (51% yield).

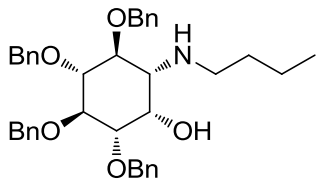

74: ^{1}H NMR (400 MHz, $CDCl_3$) δ 7.45 – 7.17 (m, 20H), 4.95 (dd, *J* = 10.9, 4.7 Hz, 2H), 4.86 – 4.62 (m, 5H), 4.18 (d, *J* = 2.8 Hz, 1H), 4.03 (t, *J* = 9.5 Hz, 1H), 3.75 (t, *J* = 9.5 Hz, 1H), 3.53 (t, *J* = 9.3 Hz, 1H), 3.42 (dd, *J* = 9.6, 2.7 Hz, 1H), 2.81 – 2.40 (m, 5H), 1.43 – 1.12 (m, 4H), 0.86 (q, *J* = 7.3, 6.7 Hz, 3H). ^{13}C NMR (101 MHz, $CDCl_3$) δ 138.69, 138.49, 138.26, 138.17, 128.58, 128.43, 128.40, 128.38, 128.34, 128.32, 128.29, 128.17, 128.03, 127.93, 127.87, 127.84, 127.72, 127.64, 127.57, 127.53, 84.78, 81.51, 80.90, 79.54, 75.93, 75.63, 75.60, 72.43, 65.19, 60.83, 47.08, 29.68, 20.16, 13.81. HRMS calculated for $C_{38}H_{43}NO_5$ ([M+H]$^+$): 596.3376; found 596.3375. IR (neat): 2925, 1454, 1069. $[\alpha]^{23}_{D}$ -17º (*c* 2.16, $CHCl_3$).

5.1.3.3.2 Benzylated 2,2-difluorobutyl inositol and DNJ derivatives (synthesis of compounds 73, 75, 80 and 81)

Synthesis of 2,2-difluoro-N-((1*R*,2*S*,3*R*,4*R*,5*S*,6*S*)-2,3,4,5-tetrakis(benzyloxy)-6-hydroxycyclohexyl)butanamide (73)

Similarly to synthesis of **72**, from 25.3 mg (0.204 mmols) of 2,2-difluorobutanoic acid and 100 mg of **63**, 61 mg of **73** were obtained as beige solid (51% yield).

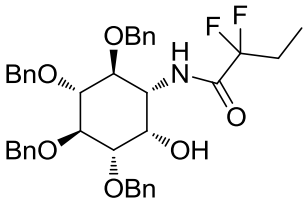

73: ^{1}H NMR (400 MHz, $CDCl_3$) δ 7.42 – 7.17 (m, 20H_{Ar}), 6.74 (d, *J* = 8.7 Hz, 1H (NH)), 4.94 – 4.80 (m, 5H (C$\underline{H}_2$-Ph)), 4.76 – 4.60 (m, 3H (C$\underline{H}_2$-Ph)), 4.18 – 4.04 (m, 2H (C$\underline{H}$-OH and C$\underline{H}$-NH)), 3.93 – 3.76 (m, 2H (2 x C$\underline{H}$-OBn)), 3.64 – 3.49 (m, 2H (2 x C$\underline{H}$-OBn)), 2.12 – 1.94 (m, 2H (C$\underline{H}_2$-CH_3)), 0.95 (t, *J* = 7.5 Hz, 3H (CH_3)). ^{13}C NMR (101 MHz, $CDCl_3$) δ 164.53, 164.24, 163.95 (1 x C=O); 138.44, 138.29, 137.92, 137.40 (4 x C_{Ar}), 128.59, 128.39, 128.37, 128.14, 127.91, 127.84, 127.83, 127.78, 127.77, 127.66 (20 x CH_{Ar}); 120.98, 118.47, 115.97 (1 x $\underline{C}F_2$); 83.97, 81.18, 80.67, 78.71 (4 x $\underline{C}$H-OBn); 75.94, 75.85, 75.39, 73.18 (4 x $\underline{C}H_2$-Ph); 68.77 ($\underline{C}$H-OH); 51.47 ($\underline{C}$H-NH); 27.48, 27.24, 27.00 (1 x $\underline{C}H_2$-CH_3); 5.75, 5.70, 5.64 (1 x $\underline{C}H_3$). HRMS calculated for $C_{38}H_{42}NO_6F_2$ ($[M+H]^+$): 646.2980; found 646.3010. IR (neat): 3287, 1678, 1660, 1555, 1134, 1072. $[\alpha]^{25}_{D}$ -13º (*c*1.2, $CHCl_3$).

Synthesis of (1*S*,2*S*,3*R*,4*R*,5*S*,6*R*)-2,3,4,5-tetrakis(benzyloxy)-6-((2,2-difluorobutylamino)cyclohexanol (75)

Similarly to synthesis of **74** and afterpurification by column chromatography on silica gel (eluent: Hx/AcOEt 3:1), from 55 mg of **73**, 30 mg of **75** were obtained as a colorless oil (51% yield).

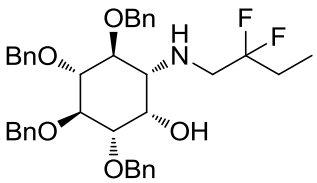

75: ^{1}H NMR (400 MHz $CDCl_3$) δ 7.41 – 7.20 (m, 20H), 5.01 – 4.65 (m, 8H), 4.27 (s, 1H), 4.00 (t, *J* = 9.4 Hz, 1H), 3.87 (td, *J* = 9.8, 2.6 Hz, 1H), 3.52 (t, *J* = 9.3 Hz, 1H), 3.43 (dd, *J* = 9.6, 2.7 Hz, 1H), 3.10 (t, *J* = 14.0 Hz, 2H), 2.71 (d, *J* = 10.1 Hz, 1H), 1.84 (td, *J* = 17.0, 7.9 Hz, 2H), 0.95 (t, *J* = 7.5 Hz, 3H). ^{13}C NMR (101 MHz, $CDCl_3$) δ 138.59, 138.37, 138.02, 137.92, 128.59, 128.57, 128.45, 128.41, 128.39, 128.37, 128.33, 128.18, 127.97, 127.90, 127.84, 127.76, 127.68, 127.65, 127.60, 127.57, 84.51, 81.29, 80.56, 79.03, 75.90, 75.66, 75.50, 72.55, 65.43, 60.68, 50.53, 50.26, 49.98, 28.13, 27.88, 27.63, 6.11, 6.05. HRMS calculated for $C_{38}H_{44}NO_5F_2$ ($[M+H]^+$): 632.3188; found 632.3184. IR (neat): 2918, 1454, 1069. $[\alpha]^{23}_{D}$ -14º (*c* 1.59, $CHCl_3$).

Synthesis of 1-((2*R*,3*R*,4*R*,5*S*)-3,4,5-tris(benzyloxy)-2-((benzyloxy)methyl)piperidin-1-yl)butan-2-one (80)

312 µl (1.785 mmol) of DIPEA and 81 mg of 1-bromobutan-2-one (0.536 mmol) were added to a solution of 250 mg (0.446 mmol) of **10** in 1.5 ml of DMF. The mixture was stirred for 60 min. under microwave irradiation (Power = 150 w, T_{max} = 85ºC). After, the crude was partitioned by addition of water and AcOEt. The organic phase was then dried over anhydrous Na_2SO_4, filtered and the solvent was distilled off under reduced pressure, giving 274 mg of 80 as brown paste (100% yield).

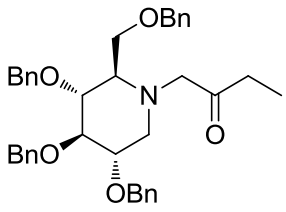

80: ^{1}H NMR (400 MHz, $CDCl_3$) δ 7.34 – 7.10 (m, 20H), 5.01 – 4.74 (m, 3H), 4.69 – 4.57 (m, 2H), 4.49 – 4.25 (m, 3H), 3.68 – 3.35 (m, 7H), 2.97 – 2.77 (m, 2H), 2.72 (t, *J* = 10.8 Hz, 1H), 2.23 – 2.10 (m, 2H), 0.90 (t, *J* = 7.3 Hz, 3H). HRMS calculated for $C_{38}H_{44}NO_5$ ($[M+H]^+$): 594.3219; found 594.3141. IR (neat): 3030, 2894, 1714, 1453, 1140. $[\alpha]^{28}_D$ +5º (*c*0.45, $CHCl_3$).

Synthesis of (2*R*,3*R*,4*R*,5*S*)-3,4,5-tris(benzyloxy)-2-((benzyloxy)methyl)-1-(2,2-difluorobutyl)piperidine (81)

55.3 µl of deoxofluor® 50% in toluene (0.093 mmol) and 0.5 µl of EtOH (8.42 µmol) were added to a solution of 25 mg (0.042 mmol) of **80** in 200 µl of dry 1,2-dicloroethane. The mixture was stirred at rt overnight. After, the reaction was cooled to 0ºC and quenched with water. The two layers were separated, and the organic was layer washed with brine and dried over $MgSO_4$. The solvent removed by distillation under reduced pressure and the residue was purified by *flash* chromatography on silica gel (Flash+ Biotage®, KP-Sil 12+M, eluent: Hx/AcOEt7:1), giving 4 mg of **81** as brown paste (15% yield).

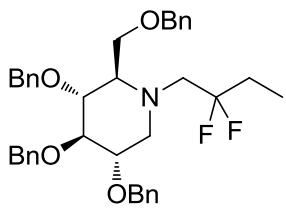

81: ^{1}H NMR (400 MHz, $CHCl_3$) δ 7.38 – 7.20 (m, 18H), 7.15 (dd, *J* = 7.6, 1.9 Hz, 2H), 4.97 – 4.72 (m, 3H), 4.64 (d, *J* = 1.0 Hz, 2H), 4.52 – 4.33 (m, 3H), 3.75 – 3.40 (m, 5H), 3.23 (dd, *J* = 11.9, 4.6 Hz, 1H), 3.10 (t, *J* = 16.0 Hz, 1H), 2.95 (s, 1H), 2.66 (s, 1H), 2.50 (d, *J* = 11.8 Hz, 1H), 1.69 (dtd, *J* = 33.6, 14.5, 13.6, 7.3 Hz, 2H), 0.90 (t, *J* = 7.5 Hz, 3H). HRMS calculated for $C_{38}H_{44}NO_4F_2$ ($[M+H]^+$): 616.3238; found 616.3255.

5.1.3.3.3 Benzylated 2-hydroxybutyl DNJ derivatives (synthesis of compounds (*R*)-84x and (*S*)-84x)

Synthesis of (*R*)-1-((2*R*,3*R*,4*R*,5*S*)-3,4,5-tris(benzyloxy)-2-((benzyloxy)methyl)piperidin-1-yl)butan-2-ol ((*R*)-84x) and (*S*)-1-((2*R*,3*R*,4*R*,5*S*)-3,4,5-tris(benzyloxy)-2-((benzyloxy)methyl)piperidin-1-yl)butan-2-ol ((*S*)-84x)

Method A: To a solution of 62 mg of **80** (0.104 mmol) in 1.2 ml THF/MeOH 3:1, a solution of 9 mg (0.209 mmol) of $NaBH_4$ in MeOH was added dropwise. The mixture was stirred overnight at 50ºC. Then, the solvent was removed by distillation under reduced pressure and the residue was partitioned between water and AcOEt. The organic phase was washed with brine, dried over anhydrous Na_2SO_4 and filtered. The solvent was distilled off under reduced pressure and the residue was purified by *flash* chromatography on silica gel (Flash$^+$ Biotage®, KP-Sil 12+M column, eluent: Hx/AcOEt 4:1) giving 20 mg of **(*R*)-84x** and 16 mg of **(*S*)-84x**, both as a colorless oil (32% and 26% yield respectively).

Method B: 63 mg (0.112 mmols) of **10** were treated with a saturated aqueous solution of Na_2CO_3, then the benzylated compound was extracted with DCM. The organic phase was dried over Na_2SO_4, filtered, and the solvent was removed by distillation under reduced pressure. The residue was dissolved in 1 ml of ACN and 14.53 µl (0.169 mmol) of (R)-2-ethyloxirane and 59.8 mg (0.562 mmol) of $LiClO_4$ were added to the solution. The mixture was stirred at 80ºC overnight. Next day, the solvent was removed by distillation under reduced pressure. The residue was partitioned on AcOEt/H_2O. The organic phase was washed with brine, dried over anhydrous Na_2SO_4, filtered, and the solvent was distilled off under reduced pressure. The residue was purified by *flash* chromatography on silicagel (Flash$^+$ Biotage®, KP-Sil 12+M column, eluent: Hx/AcOEt 3:1) giving 33 mg of **(*R*)-84x** as a colorless oil (47% yield). After eluting the column with Hx/AcOEt 2:3, 10 mg of **10** as a free base were recovered.

Similarly, starting from 14.53 µl of (*S*)-ethyloxirane, 25 mg of **(*S*)-84x** were obtained (37% yield) and 19 mg of **10** were recovered.

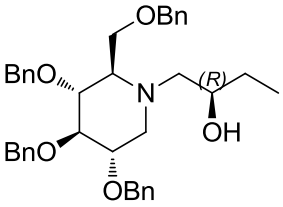

(*R*)-84x: ^{1}H NMR (400 MHz, $CDCl_3$) δ 7.40 – 7.19 (m, 18H_{Ar}), 7.15 (dd, *J* = 7.5, 2.0 Hz, 2H_{Ar}), 5.02 – 4.76 (m, 3H (CH_2-Ph)), 4.74 – 4.62 (m, 2H (CH_2-Ph)), 4.54 – 4.36 (m, 3H (CH_2-Ph)), 3.72 – 3.45 (m, 6H (CH-OH, CH_2-OBn and 3 x CH-OBn)), 3.20 (dd, *J* = 11.4, 4.5 Hz, 1H (CHOBn-CH_{2a}-N)), 2.70 (t, *J* = 11.8 Hz, 1H (N-CH_{2a}-CH-OH)), 2.38 (d, *J* = 9.2 Hz, 1H (CH-CH_2-OBn), 2.21 (d, *J* = 12.9 Hz, 1H (N-CH_{2b}-CH-OH)), 2.13 (t, *J* = 10.8 Hz, 1H (CHOBn-CH_{2b}-N))), 1.51 – 1.32 (m, 2H (CH_2-CH_3)), 0.96 (t, *J* = 7.5 Hz, 3H (CH_3)). ^{13}C NMR (101 MHz, $CDCl_3$) δ 138.83, 138.37, 138.35, 137.61 (4 x C_{Ar}); 128.42, 128.38, 128.35, 128.33, 128.15, 127.85, 127.79, 127.77, 127.70, 127.61, 127.47 (20 x CH_{Ar}); 86.94, 78.48 (3 x CH-OBn); 75.31, 75.28, 73.21, 72.94 (4 x CH_2-Ph), 68.72 (CH-OH); 65.90 (CH_2-OBn); 65.23 (N-CH-CH_2-OBn); 57.58 (N-CH_2-CH-OH); 54.84 (N-CH_2-CH-OBn); 27.49 (CH_2-CH_3); 9.88 (CH_3). HRMS calculated for $C_{38}H_{46}NO_5$ ([M+H]$^+$): 596.3376; found 596.3412. IR (neat): 3461, 2913, 2874, 1454, 1093, 1071. $[\alpha]^{22}_{D}$ -5º (*c* 1.46, $CHCl_3$).

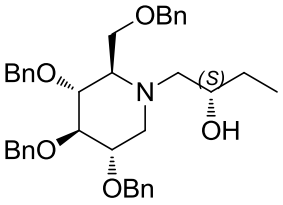

(*S*)-84x^{1}H NMR (400 MHz, $CDCl_3$) δ 7.36 – 7.21 (m, 18H_{Ar}), 7.15 (dd, *J* = 7.4, 2.1 Hz, 2H_{Ar}), 4.94 (d, *J* = 11.0 Hz, 1H (CH_2-Ph)), 4.82 (dd, *J* = 16.4, 10.9 Hz, 2H (CH_2-Ph)), 4.70 – 4.60 (m, 2H (CH_2-Ph)), 4.51 – 4.38 (m, 3H (CH_2-Ph)), 3.72 – 3.60 (m, 3H (CH_2-OBn and CH-OBn)), 3.59 – 3.41 (m, 3H (2 x CH-OBn and CH-OH), 3.05 (dd, *J* = 12.3, 4.7 Hz, 1H CHOBn-CH_{2a}-N), 2.76 – 2.61 (m, 2H (N-CH_{2a}-CH-OH and CH-CH_2-OH)), 2.54 – 2.36 (m, 2H (N-CH_{2b}-CH-OH and CHOBn-CH_{2b}-N)), 1.44 – 1.31 (m, 2H (CH_2-CH_3), 0.91 (t, *J* = 7.5 Hz, 3H (CH_3). ^{13}C NMR (101 MHz, $CDCl_3$) δ 138.82, 138.36, 138.30, 137.47, 128.40, 128.35, 128.33, 128.30, 128.29, 128.15, 127.90, 127.83, 127.81, 127.79, 127.75, 127.71, 127.68, 127.61, 127.49, 127.45, 86.88, 78.13, 77.50, 75.28, 75.05, 73.24, 72.78, 70.03 (CH-OH), 67.43, 65.10, 57.50 (N-CH_2-CH-OH), 55.78, 27.94 (CH_2-CH_3), 9.96. HRMS calculated for $C_{38}H_{46}NO_5$ ([M+H]$^+$): 596.3376; found 596.3410. IR (neat): 3461, 2918, 2872, 1453, 1093, 1070. $[\alpha]^{22}_{D}$ +17º (*c* 1.56, $CHCl_3$).

5.1.3.3.4 Synthesis of heptyloxiranes (compounds (*R*)-94, (*S*)-94, (*R*)-83y and *(S)*-83y)

Synthesis of (*R*)-1-chlorononan-2-ol ((*R*)-94)

4 ml (8.0 mmol) of a 2M solution of hexylmagnesium bromide in diethyl ether were added dropwise to a solution of 102 mg (0.533 mmol) of CuI(I) and 0.418 ml (5.33 mmol) of(*R*)-2-(chloromethyl)oxirane in 7 ml of THF at -78ºC, and under argon atmosphere. After the addition, the mixture was allowed to heat to 0ºC in 4h. After, the mixture was poured into a cold saturated aqueous solution of NH_4Cl. Then, the two layers were separated and the aqueous layer was washed twice with diethyl ether. The combined organic phase was washed

with brine, cried over anhydrous $Na_2SO_4$and filtered. The solvent was removed by distillation under reduced pressure and the residue was purified by *flash* chromatography on silica gel eluted with Hx/AcOEt 15:1, giving 272 mg of **(*R*)-94** as colorless oil (29% yield).

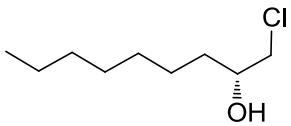

(*R*)-94: ^{1}H NMR (400 MHz, $CDCl_3$) δ 3.85 – 3.72 (m, 1H (C<u>H</u>-OH)), 3.62 (dd, *J* = 11.1, 3.2 Hz, 1H (C<u>H</u>$_{2a}$-Cl)), 3.46 (dd, *J* = 11.1, 7.2 Hz, 1H (C<u>H</u>$_{2b}$-Cl)), 2.11 (s, 1H (O<u>H</u>)) 1.62 – 1.20 (m, 12H (($C\underline{H}_2)_6$-CH_3)), 0.94 – 0.80 (m, 3H (CH_3)). ^{13}C NMR (101 MHz, $CDCl_3$) δ 71.44 (CH-OH); 50.58 (CH_2-Cl); 34.20, 31.73, 29.43, 29.13, 25.49, 22.60 (($\underline{C}H_2)_6$-CH_3); 14.04 (CH_3).

Synthesis of (*S*)-1-chlorononan-2-ol ((*S*)-94)

Similarly to **(*R*)-94**, from 209 µl (2.67 mmol) of (*S*)-2-(chloromethyl)oxirane, 150 mg of **(*S*)-94** were obtained as colorless oil (32% yield).

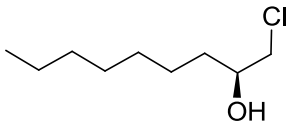

(*S*)-94: ^{1}H NMR (400 MHz, $CDCl_3$) δ 3.83 – 3.72 (m, 1H (C<u>H</u>-OH)), 3.62 (dd, *J* = 11.1, 3.2 Hz, 1H (C<u>H</u>$_{2a}$-Cl)), 3.45 (dd, *J* = 11.1, 7.2 Hz, 1H (C<u>H</u>$_{2b}$-Cl), 2.09 (d, *J* = 4.9 Hz, 1H (OH)), 1.50 – 1.16 (m, 12H (($C\underline{H}_2)_6$-CH_3)), 0.91 – 0.78 (m, 3H (CH_3)). ^{13}C NMR (101 MHz, $CDCl_3$) δ 71.43 (CH-OH); 50.58 (CH_2-Cl); 34.19, 31.72, 29.42, 29.12, 25.48, 22.59 (($\underline{C}H_2)_6$-CH_3); 14.03 (CH_3).

Synthesis of (*R*)-2-heptyloxirane ((*R*)-83y)

299 mg (7.47 mmol) of pulverized NaOH were added to a solution of 267 mg (1.494 mmol) of **(*R*)-94** in 2 ml of diethyl ether. The mixture was vigorously stirred at rt overnight. Next day, water was added and the mixture partitioned. The aquous phase was extracted twice with diethyl ether. The combined organic phase were dried over Na_2SO_4 and filtered. The solvent was finally removed by soft distillation under reduced pressure at rt, giving 100 mg of yellowish oil **((*R*)-83y**, 47% yield, with H-NMR spectra in concordance with the previously reported[171].

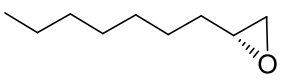

(*R*)-83y: ^{1}H NMR (400 MHz, $CDCl_3$) δ 2.93 – 2.85 (m, 1H (CH-O)), 2.73 (dd, *J* = 5.0, 4.0 Hz, 1H (CH_{2a}-O), 2.45 (dd, *J* = 5.0, 2.7 Hz, 1H (CH_{2b}-O), 1.52 – 1.23 (m, 12H (($C\underline{H}_2)_6$-CH_3), 0.89 – 0.83 (m, 3H (CH_3)).

Synthesis of (*S*)-2-heptyloxirane ((*S*)-83y)

Similarly to **(*R*)-83y**, from 150 mg (0.834 mmol) of **(*S*)-94**, 59 mg of **(*S*)-83y** were obtained as yellowish oil (49% yield), with NMR spectra in concordance with those previously reported[172].

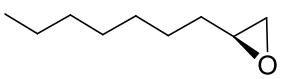

(*S*)-83y ^{1}H NMR (400 MHz, $CDCl_3$) δ 2.95 – 2.81 (m, 1H (CH-O)), 2.72 (dd, *J* = 5.0, 4.0 Hz, 1H (CH_{2a}-O), 2.44 (dd, *J* = 5.1, 2.8 Hz, 1H (CH_{2b}-O), 1.53 – 1.17 (m, 12H (($C\underline{H}_2)_6$-CH_3), 0.91 – 0.78 (m, 3H (CH_3)). ^{13}C NMR (101 MHz, $CDCl_3$) δ 52.38 (CH-O); 47.10 (CH_2-O); 32.45, 31.72, 29.36, 29.17, 25.93, 22.59 (($\underline{C}H_2)_6$-CH_3); 14.04 (CH_3).

5.1.3.3.5 Synthesis of derivatives with β-hydroxy substitution, via epoxide ring-opening. Synthesis of compounds (*R*)-84x, (*S*)-84x, (*R*)-88x, (*S*)-88x, (*R*)-84y, (*S*)-84y, (*R*)-88y, and (*S*)-88y.

Similarly to synthesis of **(R)-84x** (method B), the compounds described below were synthesized in the conditions indicated in Table 16.

(1*S*,2*S*,3*R*,4*R*,5*S*,6*R*)-2,3,4,5-tetrakis(benzyloxy)-6-(((*R*)-2-hydroxybutyl)amino)cyclohexanol ((*R*)-88x)

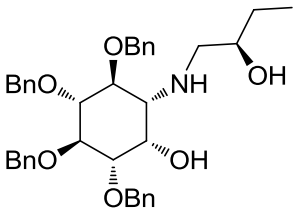

(*R*)-88x: Colorless oil, ^{1}H NMR (400 MHz, $CDCl_3$) δ 7.41 – 7.14 (m, $20H_{Ar}$), 4.99 – 4.59 (m, 8H (4 x $C\underline{H}_2$-Ph)), 4.17 – 4.05 (m, 1H (CH-C$\underline{H}$-OH), 3.96 (t, *J* = 9.5 Hz, 1H (C$\underline{H}$-OBn)), 3.71 (t, *J* = 9.7 Hz, 1H (C$\underline{H}$-OBn)), 3.52 (t, *J* = 9.3 Hz, 1H (C$\underline{H}$-OBn)), 3.43 (dd, *J* = 9.6, 2.8 Hz, 2H (C$\underline{H}$-OBn and CH_2-C$\underline{H}$-OH)), 2.70 (dd, *J* = 12.3, 3.0 Hz, 1H ($C\underline{H}_{2a}$-NH)), 2.57 – 2.41 (m, 2H ($C\underline{H}_{2b}$-NH and C$\underline{H}$-NH)), 1.46 – 1.33 (m, 2H ($C\underline{H}_2$-CH_3)), 0.90 (t, *J* = 7.5 Hz, 3H (CH_3)). ^{13}C NMR (101 MHz, $CDCl_3$) δ 138.59, 138.43, 138.10, 137.94 (4 x C_{Ar}); 128.59, 128.42, 128.38, 128.34, 128.20, 127.98, 127.94, 127.87, 127.80, 127.71, 127.59, 127.57 (20 x CH_{Ar}); 84.63, 81.48, 80.95, 79.51 (4 x $\underline{C}$H-OBn); 75.90, 75.73, 75.67, 72.69 (4 x $\underline{C}H_2$-Ph); 70.98 (CH_2-$\underline{C}$H-OH); 65.76 (CH-$\underline{C}$H-OH); 59.84 ($\underline{C}$H-NH); 52.20 ($\underline{C}H_2$-NH); 27.49 ($\underline{C}H_2$-CH_3); 9.88 (CH_3).

compound	amine core	epoxide	T	eluent chromatography	obtained amount (yield)
(*R*)-84x	63 mg **10** (0.112 mmol)	14.53 µl (*R*)-ethyoxyrane (0.169 mmol)	80 ºC	Hx/AcOEt 3:1	33 mg (47%)
(*S*)-84x	63 mg **10** (0.112 mmol)	14.53 µl (*S*)-ethyoxyrane (0.169 mmol)	80 ºC	Hx/AcOEt 3:1	25 mg (37%)
(*R*)-88x	200 mg **63** (0.371 mmol)	47.9 µl (*R*)-ethyoxyrane (0.556 mmol)	80 ºC	200 ml AcOEt and 200 ml AcOEt/MeOH 95:5	45 mg (19.6%)
(*S*)-88x	200 mg **63** (0.371 mmol)	47.9 µl (*S*)-ethyoxyrane (0.556 mmol)	80 ºC	200 ml AcOEt and 200 ml AcOEt/MeOH 95:5	59 mg (26%)
(*R*)-84y	187 mg **10** (0.333 mmol)	71.1 mg **(*R*)-83y** (0.500 mmol)	**50 ºC**	500 ml Hx/AcOEt 4:1 and 400 ml Hx/AcOEt34:1	83 mg (37%)
(*S*)-84y	147 mg **10** (0.268 mmol)	57.1 mg **(*S*)-83y** (0.402 mmol)	**50 ºC**	500 ml Hx/AcOEt 4:1 and 400 ml Hx/AcOEt34:1	67 mg (38%)
(*R*)-88y	113 mg **63** (0.209 mmol)	44.7 mg **(*R*)-83y** (0.314 mmol)	80 ºC	Hx/AcOEt 1:5	83 mg (58%)
(*S*)-88y	162 mg **63** (0.300 mmol)	64 mg **(*S*)-83y** (0.450 mmol)	80 ºC	Hx/AcOEt 1:5	105 mg (51%)

Table 16 Synthesis of derivatives with β-hydroxy substitution, via epoxide ring-opening.

(1*S*,2*S*,3*R*,4*R*,5*S*,6*R*)-2,3,4,5-tetrakis(benzyloxy)-6-(((*S*)-2-hydroxybutyl)amino)cyclohexanol ((*S*)-88x)

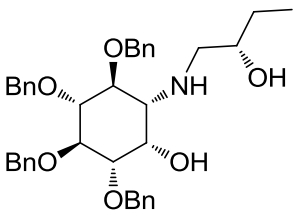

(*S*)-88x: Colorless oil, ^{1}H NMR (400 MHz, $CDCl_3$) δ 7.44 – 7.20 (m, 20H), 4.98 – 4.61 (m, 8H), 4.17 (t, *J* = 2.8 Hz, 1H), 3.96 (t, *J* = 9.4 Hz, 1H), 3.75 (t, *J* = 9.7 Hz, 1H), 3.58 – 3.48 (m, 2H (C<u>H</u>-OBn and CH_2-C<u>H</u>-OH), 3.44 (dd, *J* = 9.5, 2.8 Hz, 1H (C<u>H</u>-OBn)), 2.85 (dd, *J* = 11.9, 3.2 Hz, 1H (C<u>H_{2a}</u>-NH)), 2.56 (dd, *J* = 10.2, 2.6 Hz, 1H (C<u>H_{2b}</u>-NH)), 2.45 (dd, *J* = 12.0, 8.8 Hz, 2H), 1.44 – 1.30 (m, 2H), 0.89 (t, *J* = 7.5 Hz, 3H). ^{13}C NMR (101 MHz, $CDCl_3$) δ 138.55, 138.38, 137.99, 137.89, 128.56, 128.44, 128.40, 128.34, 128.29, 127.97, 127.95, 127.91, 127.83, 127.71, 127.61, 127.59, 84.46, 81.35, 80.88, 79.46, 75.90, 75.79, 75.67, 72.75, 71.61 (CH_2-C<u>H</u>-OH), 66.01, 61.03, 52.76 (C<u>H_2</u>-NH), 27.82 (C<u>H_2</u>-CH_3), 9.80.

(*R*)-1-((2*R*,3*R*,4*R*,5*S*)-3,4,5-tris(benzyloxy)-2-((benzyloxy)methyl)piperidin-1-yl)nonan-2-ol ((*R*)-84y)

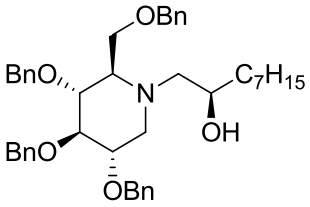

(*R*)-84y: Colorless oil, ^{1}H NMR (400 MHz, $CDCl_3$) δ 7.45 – 7.19 (m, 18H_{Ar}), 7.18 – 7.09 (m, 2H_{Ar}), 4.99 – 4.74 (m, 3H (C<u>H_2</u>-Ph)), 4.67 (q, *J* = 11.5 Hz, 2H (C<u>H_2</u>-Ph)), 4.52 – 4.33 (m, 3H (C<u>H_2</u>-Ph)), 3.73 – 3.45 (m, 6H (3 x C<u>H</u>-OBn, C<u>H</u>-OH and C<u>H_2</u>-OBn)), 3.18 (dd, *J* = 11.5, 4.5 Hz, 1H (CHOBn-C<u>H_{2a}</u>-N)), 2.68 (dd, *J* = 13.0, 10.3 Hz, 1H (N-C<u>H_{2a}</u>-CH-OH)), 2.36 (dt, *J* = 9.3, 2.4 Hz, 1H (C<u>H</u>-CH_2-OBn), 2.19 (dd, *J* = 12.9, 2.4 Hz, 1H (N-C<u>H_{2b}</u>-CH-OH)), 2.12 (t, *J* = 10.8 Hz, 1H (CHOBn-C<u>H_{2b}</u>-N)), 1.63 – 1.20 (m, 12H ((C<u>H_2</u>)$_6$-CH_3)), 0.97 – 0.82 (m, 3H (CH_3)). ^{13}C NMR (101 MHz, $CDCl_3$) δ 138.83, 138.38, 137.63 (4 x C_{Ar}); 128.41, 128.37, 128.34, 128.32, 128.15, 127.84, 127.77, 127.75, 127.69, 127.59, 127.46 (20 x CH_{Ar}); 86.97, 78.51(3 x CH-OBn); 75.31 , 75.27, 73.18, 72.94 (4 x C<u>H</u>-Ph); 67.49 CH-OH); 65.91(C<u>H_2</u>-OBn); 65.20 (C<u>H</u>-CH_2-OBn); 57.97 (N-C<u>H_2</u>-CH-OH); 54.86 (CHOBn-C<u>H_2</u>-N); 34.74, 31.83, 29.82, 29.27, 25.62, 22.66 (6 x (C<u>H_2</u>)$_6$-CH_3); 14.10 (CH_3).$[\alpha]^{26}_{D}$-6° (*c*1.05, $CHCl_3$).

(*S*)-1-((2*R*,3*R*,4*R*,5*S*)-3,4,5-tris(benzyloxy)-2-((benzyloxy)methyl)piperidin-1-yl)nonan-2-ol ((*S*)-84y)

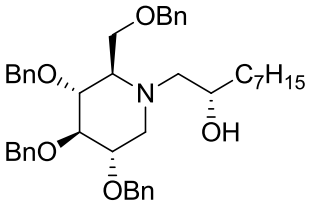

(*S*)-84y: Colorless oil, ^{1}H NMR (400 MHz, $CDCl_3$) δ 7.38 – 7.02 (m, 20H), 4.93 (d, *J* = 11.0 Hz, 1H), 4.81 (dd, *J* = 15.9, 10.9 Hz, 2H), 4.71 – 4.58 (m, 2H), 4.48 – 4.36 (m, 3H), 3.70 – 3.59 (m, 3H), 3.58 – 3.43 (m, 3H), 3.06 (dd, *J* = 12.2, 4.7 Hz, 1H), 2.74 – 2.62 (m, 2H), 2.52 – 2.37 (m, 2H), 1.67 – 1.15 (m, 13H), 0.88 (t, *J* = 6.5 Hz, 3H). ^{13}C NMR (101 MHz, $CDCl_3$) δ 138.37, 138.31, 137.49, 128.39,128.38, 128.34, 128.32, 128.12, 127.83, 127.80, 127.78, 127.70, 127.60, 127.47, 86.88, 78.14, 77.53, 75.27, 75.05, 73.23, 72.75, 68.72, 67.46, 65.13, 58.01, 55.84, 35.15, 31.83, 29.78, 29.27, 25.66, 22.65, 14.09. HRMS calculated for $C_{43}H_{56}NO_5$ ([M+H]$^+$): 666.4158; found 666.4164. $[\alpha]^{20}_D$ +18° (*c*1.1, $CHCl_3$).

(1*S*,2*S*,3*R*,4*R*,5*S*,6*R*)-2,3,4,5-tetrakis(benzyloxy)-6-(((*R*)-2-hydroxynonyl)amino)cyclohexanol ((*R*)-88y)

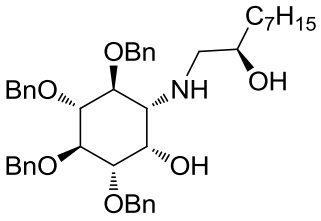

(*R*)-88y: Colorless oil, ^{1}H NMR (400 MHz, $CDCl_3$) δ 7.42 – 7.20 (m, 20H), 5.33 – 4.57 (m, 8H), 4.10 (q, *J* = 7.2 Hz, 2H), 3.97 (t, *J* = 9.5 Hz, 1H), 3.68 (d, *J* = 9.8 Hz, 1H), 3.51 (t, *J* = 9.4 Hz, 1H), 3.41 (dd, *J* = 9.6, 2.8 Hz, 1H), 2.65 (dd, *J* = 12.2, 3.0 Hz, 1H), 2.50 – 2.33 (m, 2H), 1.44 – 1.18 (m, 12H), 0.96 – 0.75 (m, 3H).

(1*S*,2*S*,3*R*,4*R*,5*S*,6*R*)-2,3,4,5-tetrakis(benzyloxy)-6-(((*S*)-2-hydroxynonyl)amino)cyclohexanol ((*S*)-88y)

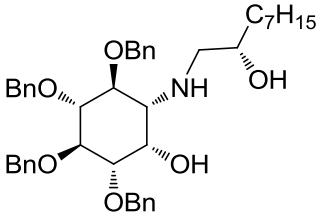

(*S*)-88y:Colorless oil, ^{1}H NMR (400 MHz, $CDCl_3$) δ 7.42 – 7.18 (m, 20H_{Ar}), 5.01 – 4.88 (m, 3H (CH_2-Ph)), 4.84 (dd, *J* = 10.8, 2.6 Hz, 2H (CH_2-Ph)), 4.79 – 4.64 (m, 3H (CH_2-Ph)), 4.14 (t, *J* = 2.7 Hz, 1H (CH-C<u>H</u>-OH), 3.99 (t, *J* = 9.5 Hz, 1H (C<u>H</u>-OBn)), 3.73 (t, *J* = 9.7 Hz, 1H (C<u>H</u>-OBn)), 3.55 (q, *J* = 9.4, 8.2 Hz, 2H (C<u>H</u>-OBn and CH_2-C<u>H</u>-OH)), 3.44 (dd, *J* = 9.6, 2.8 Hz, 1H (C<u>H</u>-OBn)), 2.78 (dd, *J* = 11.9, 3.2 Hz, 1H (C<u>H</u>$_{2a}$-NH)), 2.51 (dd, *J* = 10.2, 2.6 Hz, 1H (C<u>H</u>-NH)), 2.41 (dd, *J* = 11.9, 8.6 Hz, 1H (C<u>H</u>$_{2b}$-NH)), 1.48 – 1.18 (m, 12H (C<u>H</u>$_2$)$_6$-CH_3), 0.94 – 0.83 (m, 3H (CH_3)). ^{13}C NMR (101 MHz, $CDCl_3$) δ 138.66, 138.53, 138.19, 138.03 (4 x C_{Ar}); 128.55, 128.44, 128.40, 128.35, 128.25, 127.97, 127.91, 127.87, 127.80, 127.74, 127.59, 127.57 (20 x CH_{Ar}); 84.69, 81.54, 81.09, 80.11 (4 x <u>C</u>H-OBn); 75.93, 75.87, 75.71, 72.72 (4 x <u>C</u>H_2-Ph); 70.81 (CH_2-<u>C</u>H-OH); 66.37 (CH-<u>C</u>H-OH); 61.02 (CH-NH); 53.32 (CH_2-NH); 35.09, 31.82, 29.65, 29.25, 25.60, 22.66 ((<u>C</u>H_2)$_6$-CH_3); 14.11 (CH_3).

5.1.3.3.6 Synthesis of benzylated derivatives with 2-fluoro substitution (compounds (*R*)-86x, (*S*)-86x, (*R*)-86y and (*S*)-86y).

- **General procedure for fluorination:** A solution of deoxofluor (50% in toluene) was added to a solution of the hydroxylated compound in dry DCM. The mixture was stirred at rt during 2 or 16h. then, the reaction was cooled to 0ºC and quenched with water. The two layers were separated and the organic layer dried over anhydrous Na_2SO_4.The solvent was distilled off under reducer pressure and the residue was purified by *flash* chromatography on silica gel.

compound	amount deoxofluor	hydroxylated starting compound	time of reaction	Mobil phase	obtained amount (yield)
(*R*)-86x	58.9 µl (0.197 mmol)	53 mg **(*S*)-84x** (0.091 mmol)	16 h	Hx/AcOEt 6:1	22 mg (41%)
(*S*)-86x	59.7 µl (0.200 mmol)	54 mg **(*R*)-84x** (0.091 mmol)	16 h	Hx/AcOEt 6:1	28 mg (52%)
(*R*)-86y	202 µl (0.338 mmol)	45 mg **(*S*)-84y** (0.068 mmol)	2 h	Hx/AcOEt 8:1	13 mg (29%)
(*S*)-86y	224 µl (0.375 mmol)	50 mg **(*R*)-84y** (0.075 mmol)	2 h	Hx/AcOEt 8:1	17 mg (34%)

Table 17 Synthesis of compounds **86x** and **86y**.

(2*R*,3*R*,4*R*,5*S*)-3,4,5-tris(benzyloxy)-2-((benzyloxy)methyl)-1-((*R*)-2-fluorobutyl)piperidine ((*R*)-86x)

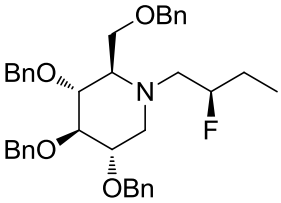

(*R*)-86x: White paste, ^{1}H NMR (400 MHz, $CDCl_3$) δ 7.38 – 7.20 (m, 18H), 7.13 (dd, *J* = 7.5, 2.0 Hz, 2H), 5.01 – 4.76 (m, 3H), 4.73 – 4.50 (m, 3H), 4.46 – 4.36 (m, 3H), 3.72 – 3.60 (m, 3H), 3.50 (dt, *J* = 17.9, 9.1 Hz, 2H), 3.13 (dd, *J* = 11.4, 4.9 Hz, 1H), 2.91 – 2.66 (m, 2H), 2.50 (d, *J* = 9.4 Hz, 1H), 2.38 (t, *J* = 10.8 Hz, 1H), 1.64 – 1.43 (m, 3H), 0.92 (t, *J* = 7.4 Hz, 3H). ^{13}C NMR (101 MHz, $CDCl_3$) δ 138.98, 138.52, 138.46, 137.69, 128.41, 128.36, 128.35, 128.29, 128.28, 127.86, 127.81, 127.80, 127.62, 127.49, 127.40, 94.36, 92.67, 87.24, 78.53, 78.26, 77.32, 77.20, 77.00, 75.30, 75.13, 73.37, 72.71, 65.69, 65.67, 64.54, 55.58, 55.38, 54.96, 29.68, 26.80, 26.58, 9.21, 9.15. HRMS calculated for $C_{38}H_{45}NO_4F$ ($[M+H]^+$): 598.333; found 598.3282. IR (neat): 2921, 1454, 1094. $[\alpha]^{24}_{D}$ +4° (*c*1.14, $CHCl_3$).

(2*R*,3*R*,4*R*,5*S*)-3,4,5-tris(benzyloxy)-2-((benzyloxy)methyl)-1-((*S*)-2-fluorobutyl)piperidine ((*S*)-86x)

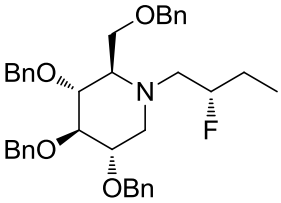

(*S*)-86x: White paste, ^{1}H NMR (400 MHz, $CDCl_3$) δ 7.34 – 7.23 (m, 18H), 7.17 – 7.11 (m, 2H), 4.99 – 4.72 (m, 3H), 4.69 – 4.56 (m, 3H), 4.53 – 4.40 (m, 3H), 4.37 (d, *J* = 12.1 Hz, 1H), 3.66 – 3.55 (m, 2H), 3.54 – 3.45 (m, 3H), 3.18 (dd, *J* = 11.7, 4.7 Hz, 1H), 2.97 – 2.65 (m, 2H), 2.57 – 2.40 (m, 2H), 1.50 – 1.29 (m, 2H), 0.86 (t, *J* = 7.5 Hz, 3H). ^{13}C NMR (101 MHz, $CDCl_3$) δ 138.96, 138.47, 137.60, 137.12, 128.36, 128.33, 128.27, 128.26, 128.25, 128.11, 128.01, 127.93, 127.81, 127.61, 127.55, 127.50, 127.40, 91.89, 87.16, 78.52, 78.35, 75.29, 75.16, 73.29, 72.54, 66.67, 63.53, 56.07, 55.78, 26.47, 26.29, 9.14. IR (neat): 2910, 1454, 1095. $[\alpha]^{22}_{D}$ -2° (*c*0.45, $CHCl_3$).

(2*R*,3*R*,4*R*,5*S*)-3,4,5-tris(benzyloxy)-2-((benzyloxy)methyl)-1-((*R*)-2-fluorononyl)piperidine ((*R*)-86y)

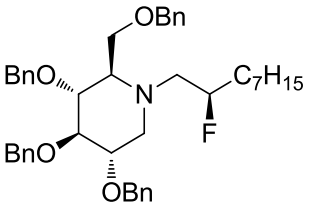

(*R*)-86y: Colorless oil, ^{1}H NMR (400 MHz, $CDCl_3$) δ 7.38 – 7.05 (m, 20H), 4.98 – 4.76 (m, 3H), 4.77 – 4.55 (m, 3H), 4.40 (d, J = 10.9 Hz, 1H), 3.71 – 3.60 (m, 3H), 3.58 – 3.40 (m, 2H),3.12 (dd, J = 11.3, 4.9 Hz, 1H), 2.89 – 2.64 (m, 2H), 2.48 (dd, J = 9.3, 2.1 Hz, 1H), 2.37 (t, J = 10.8 Hz, 1H), 1.52 – 1.11 (m, 12H), 0.88 (d, J = 6.6 Hz, 3H). ^{13}C NMR (101 MHz, $CDCl_3$) δ 138.98, 138.46, 137.71, 128.39, 128.33, 128.27, 127.83, 127.80, 127.77, 127.59, 127.47, 127.38, 93.33, 91.64, 87.24, 78.55, 78.26, 77.29, 77.18, 75.29, 75.11, 73.35, 72.68, 65.69, 64.52, 55.94, 55.73, 54.97, 33.74, 33.54, 31.75, 29.39, 29.12, 24.88, 24.84, 22.62, 14.07. ^{19}F NMR (376 MHz, $CDCl_3$) δ -181.34 (dtt, J = 50.0, 33.3, 17.2 Hz). HRMS calculated for $C_{43}H_{55}NO_4F$ ($[M+H]^+$): 668.4155; found 668.4115. $[\alpha]^{20}_D$ +5° (*c* 0.66, $CHCl_3$).

(2*R*,3*R*,4*R*,5*S*)-3,4,5-tris(benzyloxy)-2-((benzyloxy)methyl)-1-((*S*)-2-fluorononyl)piperidine ((*S*)-86y)

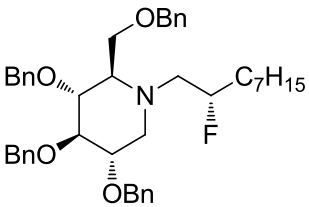

(*S*)-86y: Colorless oil, ^{1}H NMR (400 MHz, $CDCl_3$) δ 7.36 – 7.04 (m, 17H), 5.04 – 4.73 (m, 3H), 4.71 – 4.50 (m, 1H), 4.50 – 4.41 (m, 2H), 4.37 (d, *J* = 12.1 Hz, 1H), 3.66 – 3.54 (m, 2H), 3.54 – 3.45 (m, 3H), 3.18 (dd, *J* = 11.9, 4.7 Hz, 1H), 2.97 – 2.67 (m, 2H), 2.59 – 2.41 (m, 2H), 1.52 – 1.11 (m, 12H), 0.88 (t, *J* = 6.9 Hz, 3H). ^{13}C NMR (101 MHz, $CDCl_3$) δ 138.97, 138.50, 138.48, 137.60, 128.36, 128.32, 128.27, 128.25, 127.85, 127.83, 127.78, 127.57, 127.54, 127.40, 92.54, 90.85, 87.18, 78.53, 78.39, 75.30, 75.16, 73.29, 72.53, 66.70, 63.48, 56.46, 56.26, 55.74, 33.41, 33.21, 31.76, 29.38, 29.10, 24.88, 24.84, 22.62, 14.08. ^{19}F NMR (376 MHz, $CDCl_3$) δ -179.52 (dtt, *J* = 50.8, 35.3, 17.8 Hz). HRMS calculated for $C_{43}H_{55}NO_4F$ ($[M+H]^+$): 668.4155; found 668.4142. $[\alpha]^{26}_D$ -2° (*c*0.66, $CHCl_3$).

5.1.3.4 Debenzylation of compounds obtained in this section. Synthesis of 64, 69, 47x, 76x, 82x, (*R*)-85x, (*S*)85x, (*R*)-87x, (*S*)-87x, (*R*)-89x, (*S*)-89x, (*R*)-85y, (*S*)-85y, (*R*)-87y, (*S*)-87y, (*R*)-89y and (*S*)-89y).

Debenzylations were performed according to *Method A: hydrogenation with $Pd(OH)_2/C$*, with the specific conditions indicated in the next table:

compound	solvent reaction	benzylated compound	time of reaction	obtained amount (yield)
64	EtOH	40 mg **63** (0.074 mmol)	48 h	12.28 mg (77%)
69	THF/MeOH 1:1	15 mg **66** (0.026 mmol)	48 h	4.61 mg (80%)
47x	THF/MeOH 1:1	47.3 mg **74** (0.079 mmol)	48 h	17.81 mg (83%)
76x	THF/MeOH 1:1	47.2 mg **75** (0,074 mmol)	48 h	22.62 mg (100%)
82x	MeOH	15.1 mg **81**(0.024 mmol)	16 h	6.53 mg (92%)
(*R*)-85x	THF/MeOH 1:1	36.3 mg **(*R*)-84x** (0.060 mmol)	16 h	12.81 mg (78%)
(*S*)-85x	THF/MeOH 1:1	31.2 mg **(*S*)-84x** (0.052 mmol)	16 h	14.01 mg (99%)
(*R*)-87x	THF/MeOH 1:1	28.5 mg **(*R*)-86x** (0.048 mmol)	16 h	10.22 mg (78%)
(*S*)-87x	THF/MeOH 1:1	34.7 mg **(*S*)-86x** (0.058 mmol)	16 h	16.01 mg (100%)

Table 18 Debenzylation of the synthesized derivatives.

compound	solvent reaction	benzylated compound	time of reaction	obtained amount (yield)
(*R*)-89x	THF/MeOH 1:1	15.0 mg **(*R*)-88x** (0.025 mmol)	48 h	5.36 mg (75%)
(*S*)-89x	THF/MeOH 1:1	25.2 mg **(*S*)-88x** (0.041 mmol)	48 h	11.96 mg (100%)
(*R*)-85y	THF/MeOH 1:1	31.8 mg **(*R*)-84y** (0.048 mmol)	48 h	16.19 mg (99%)
(*S*)-85y	THF/MeOH 1:1	21.7 mg **(*S*)-84y** (0.033 mmol)	48 h	9.73 mg (87%)
(*R*)-87y	THF/MeOH 1:1	9.2 mg **(*R*)-86y** (0.013 mmol)	16 h	4.71 mg (100%)
(*S*)-87y	THF/MeOH 1:1	18.7 mg **(*S*)-86y** (0.026 mmol)	16 h	9.27 mg (96%)
(*R*)-89y	THF/MeOH 1:1	83.2 mg **(*R*)-88y** (0.122 mmol)	48 h	38.01 mg (87%)
(*S*)-89y	THF/MeOH 1:1	105.4 mg **(*S*)-88y** (0.169 mmol)	48 h	55.04 mg (91%)

Table 18 (cont) Debenzylation of the synthesized derivatives.

(1*S*,2*R*,3*S*,4*S*,5*S*,6*S*)-6-aminocyclohexane-1,2,3,4,5-pentaol hydrochloride (64)

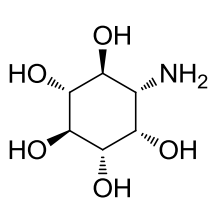

64: Yellowish paste. ^{1}H NMR (400 MHz, D_2O) δ 4.03 (t, *J* = 2.8 Hz, 1H (C<u>H</u>-OH)), 3.59 (t, *J* = 10.1 Hz, 1H (C<u>H</u>-OH)), 3.53 – 3.36 (m, 2H (2 x C<u>H</u>-OH)), 3.20 (t, *J* = 9.3 Hz, 1H (C<u>H</u>-OH)),3.14 (dd, *J* = 10.9, 2.8 Hz, 1H (C<u>H</u>-NH_2)). ^{13}C NMR (101 MHz, D_2O) δ 74.49, 71.80, 71.39, 69.14, 68.34 (5 x CH-OH); 53.51 (CH-NH_2). IR: 3363, 1631, 1116, 1044. HPLC (ESI) 86.6% rt: 0.38'; m/z: 180.10. HRMS calculated for $C_6H_{14}NO_5$: 180.0872 $[M+H]^+$; found: 180.0881.$[\alpha]^{26}_D$ -10° (*c*0.49, MeOH).

(1*R*,2*S*,3*R*,4*S*,5*S*,6*S*)-5-amino-6-fluorocyclohexane-1,2,3,4-tetraol hydrochloride (69)

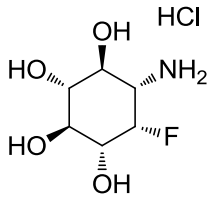

69: Yellowish paste. ^{1}H NMR (400 MHz, MeOD) δ 4.92 (d, *J* = 54.1 Hz, 1H (CH-F)), 3.67 – 3.47 (m, 3H (3 x C<u>H</u>-OH)), 3.38 – 3.18 (m, 2H (C<u>H</u>-NH_2)). ^{13}C NMR (101 MHz, MeOD) δ 91.77, 90.00 (1 x CH-F); 75.00, 72.29, 72.25, 70.74, 70.57, 69.48, 69.45 (4 x CH-OH); 53.10, 52.92 (CH-NH_2).HPLC (ESI) 89.8% rt: 0.37'; m/z: 182.06. HRMS calculated for $C_6H_{13}NO_4F$: 182.0829 $[M+H]^+$; found: 182.0838. IR: 3332, 1626, 1518, 1118, 1047. $[\alpha]^{24}_{D}$ -5° (*c*0.58, MeOH).

(1*S*,2*R*,3*S*,4*S*,5*S*,6*S*)-6-(butylamino)cyclohexane-1,2,3,4,5-pentaol hydrochloride (47x)

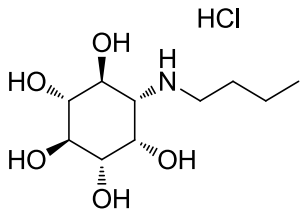

47x: Yellowish paste. ^{1}H NMR (400 MHz, MeOD) δ 4.18 (s, 1H (C<u>H</u>-OH)), 3.77 (t, J = 9.5 Hz, 1H (C<u>H</u>-OH)), 3.58 (t, J = 9.3 Hz, 1H (C<u>H</u>-OH)), 3.42 (d, J = 9.6 Hz, 1H (C<u>H</u>-OH)), 3.22 (t, J = 9.2 Hz, 1H (C<u>H</u>-OH)), 3.16 – 3.03 (m, 3H (C<u>H</u>-NH-C<u>H_2</u>)), 1.83 – 1.60 (m, 2H (C<u>H_2</u>-CH_2-CH_3)), 1.53 – 1.36 (m, 2H (CH_2-C<u>H_2</u>-CH_3), 0.99 (t, J = 7.1 Hz, 3H (CH_3)).^{13}C NMR (101 MHz, MeOD) δ 75.37, 72.12, 72.09, 69.45, 66.55 (5 x <u>C</u>H-OH); 59.73 (CH-NH); 44.90 (NH-CH_2); 27.52 (<u>C</u>H_2-CH_2-CH_3), 19.56 (CH_2-<u>C</u>H_2-CH_3), 12.52 (CH_3HPLC (UV) 88.5% rt: 0.78'. HRMS calculated for $C_{10}H_{22}NO_5$: 236.1498 $[M+H]^+$; found: 236.1508.$[\alpha]^{25}_{D}$ -21° (*c*1.0, MeOH).

(2*R*,3*R*,4*R*,5*S*)-1-(2,2-difluorobutyl)-2-(hydroxymethyl)piperidine-3,4,5-triol hydrochloride (82x)

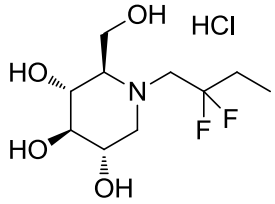

82x: Yellowish paste. ^{1}H NMR (400 MHz, MeOD) δ 4.14 – 3.93 (m, 3H (CH-C<u>H_2</u>-OH and N-C<u>H_{2a}</u>-CF_2)), 3.87 – 3.65 (m, 3H (N-C<u>H_{2b}</u>-CF_2, CH-C<u>H_{2a}</u>-N and C<u>H</u>-OH)), 3.61 (t, *J* = 9.5 Hz, 1H (C<u>H</u>-OH)), 3.36 (t, *J* = 9.0 Hz, 1H (C<u>H</u>-OH)), 3.23 – 3.05 (m, 2H (C<u>H</u>-CH_2-OH and CH-C<u>H_{2b}</u>-N)), 2.04 (td, *J* = 17.4, 16.8, 7.8 Hz, 2H (C<u>H_2</u>-CH_3)), 1.06 (t, *J* = 7.2 Hz, 3H (CH_3)). ^{13}C NMR (101 MHz, MeOD) δ 122.22 (CF_2); 76.58 (CH-OH); 68.59 (<u>C</u>H-CH_2-OH); 67.18, 65.88 (2 x CH-OH); 56.01 (CH-<u>C</u>H_2-N); 54.94 (<u>C</u>H-CH_2-OH); 34.61(N-<u>C</u>H_2-CF_2); 28.76 (<u>C</u>H_2-CH_3); 4.65 (CH_3). HPLC (UV) 89.6% rt: 1.53'. HRMS calculated for $C_{10}H_{20}NO_4F_2$: 256.1360 $[M+H]^+$; found: 256.1355.IR (neat): 3317, 1643. $[\alpha]^{25}_{D}$ +4° (*c*1.04, MeOH).

(2*R*,3*R*,4*R*,5*S*)-1-((*R*)-2-hydroxybutyl)-2-(hydroxymethyl)piperidine-3,4,5-triol hydrochloride ((*R*)-85x)

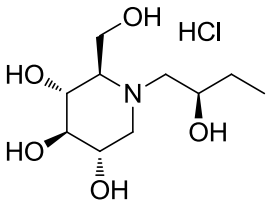

(*R*)-85x: Brown paste.^{1}H NMR (400 MHz, MeOD) δ 4.07 (d, *J* = 12.5 Hz, 1H (CH-C$\underline{H}_{2a}$-OH)), 3.99 – 3.89 (m, 2H (CH-C$\underline{H}_{2b}$-OH and CH_2-C$\underline{H}$OH-CH_2)), 3.80 – 3.68 (m, 1H (CH-C$\underline{H}$-OH)), 3.67 – 3.54 (m, 2H (CH-C$\underline{H}$-OH and CH-CH-C$\underline{H}_{2a}$-N)), 3.42 – 3.34 (m, 2H (CH-C$\underline{H}$-OH and N-C$\underline{H}_{2a}$-CHOH-CH_2)), 3.20 (d, *J* = 13.0 Hz, 1H (N-C$\underline{H}_{2b}$-CHOH-CH_2)), 3.15 – 2.99 (m, 2H (C$\underline{H}$-CH_2-OH and CH-CH-C$\underline{H}_{2b}$-N), 1.61 – 1.40 (m, 2H (C$\underline{H}_2$-CH_3)), 0.99 (t, *J* = 7.2 Hz, 3H (CH_3)).^{13}C NMR (101 MHz, MeOD) δ 76.69 (CH-C$\underline{H}$-OH); 67.44 (CH-C$\underline{H}_2$-OH); 67.28, 66.27 (2 x CH-C$\underline{H}$-OH); 65.71(N-CH_2-C$\underline{H}$OH-CH_2); 58.45 (N-C$\underline{H}_2$-CHOH-CH_2); 54.12 (C$\underline{H}$-CH_2-OH); 53.61 (CH-CH-C$\underline{H}_2$-N); 27.97(C$\underline{H}_2$-CH_3), 8.46 (CH_3).HPLC (ESI) 88.2% rt: 0.70'; m/z: 236.16. HRMS calculated for $C_{10}H_{22}NO_5$: 236.1498 $[M+H]^+$; found: 236.1489. IR (neat): 3324. $[\alpha]^{26}_D$ -8° (*c* 0.34, MeOH).

(2*R*,3*R*,4*R*,5*S*)-1-((*S*)-2-hydroxybutyl)-2-(hydroxymethyl)piperidine-3,4,5-triol hydrochloride ((*S*)-85x)

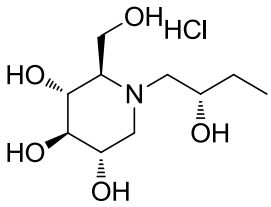

(*S*)-85x: Brown paste.^{1}H NMR (400 MHz, MeOD) δ 4.14 – 3.94 (m, 3H (CH-CH_2-OH and N-CH_2-C$\underline{H}$OH-CH_2), 3.77 – 3.67 (m, 2H), 3.57 (t, *J* = 9.3 Hz, 1H), 3.44 (d, *J* = 13.0 Hz, 1H (N-C$\underline{H}_{2a}$-CHOH-CH_2), 3.39 – 3.31 (m, 1H), 3.26 – 3.21 (m, 1H), 3.19 – 2.92 (m, 2H (N-C$\underline{H}_{2b}$-CHOH-CH_2 and CH-CH-C$\underline{H}_{2b}$-N), 1.60 – 1.42 (m, 2H), 0.98 (t, *J* = 7.0, 6.1 Hz, 3H). ^{13}C NMR (101 MHz, MeOD) δ 76.69, 67.68 (N-CH_2-C$\underline{H}$OH-CH_2), 67.49, 67.44, 66.32, 58.15, 55.36, 53.98, 28.49, 8.31HPLC (ESI) 87.2% rt: 0.52'; m/z: 236.21. HRMS calculated for $C_{10}H_{22}NO_5$: 236.1498 $[M+H]^+$; found: 236.1499. IR (neat): 3312. $[\alpha]^{26}_D$ +16° (*c*0.27, MeOH).

(2*R*,3*R*,4*R*,5*S*)-1-((*R*)-2-fluorobutyl)-2-(hydroxymethyl)piperidine-3,4,5-triol hydrochloride ((*R*)-87x)

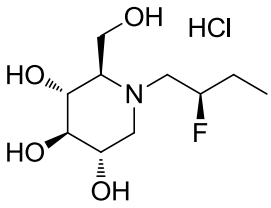

(*R*)-87x: Brown paste. ^{1}H NMR (400 MHz, MeOD) δ 5.01 (d, *J* = 52.5 Hz, 1H (CH-F)), 4.02 (dd, *J* = 74.1, 12.4 Hz, 2H), 3.79 – 3.54 (m, 4H), 3.54 – 3.40 (m, 1H), 3.40 – 3.31 (m, 1H), 3.23 – 3.03 (m, 2H), 1.87 – 1.61 (m, 2H), 1.03 (t, *J* = 7.1 Hz, 3H). ^{13}C NMR (101 MHz, MeOD) δ 91.18, 89.48 (CH-F); 76.52, 67.55, 67.39, 66.25, 56.60, 56.40, 55.15, 53.64, 26.01, 25.80, 7.70, 7.65.^{19}F NMR (376 MHz, MeOD) δ -181.70 – -184.20 (m).HPLC (UV) 93.6% rt: 1.12'. HRMS calculated for $C_{10}H_{21}NO_4F$: 238.1455 $[M+H]^+$; found: 238.1453.IR (neat): 3342. $[\alpha]^{26}_D$ +4° (*c*0.36, MeOH).

(2*R*,3*R*,4*R*,5*S*)-1-((*S*)-2-fluorobutyl)-2-(hydroxymethyl)piperidine-3,4,5-triol hydrochloride ((*S*)-87x)

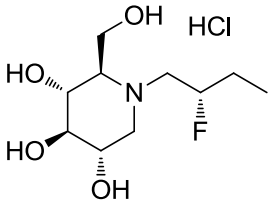

(*S*)-87x: Brown paste. ^{1}H NMR (400 MHz, MeOD) δ 5.04 (d, *J* = 51.6 Hz, 1H (CH-CF)), 4.00 (dd, *J* = 68.4, 12.4 Hz, 2H (CH-C$\underline{H}_2$-OH)), 3.77 – 3.53 (m, 4H (2 x C$\underline{H}$-OH, N-C$\underline{H}_{2a}$-CHF and CHOH-C$\underline{H}_{2a}$-N)), 3.52 – 3.33 (m, 2H (N-C$\underline{H}_{2b}$-CHF and C$\underline{H}$-OH)), 3.17 (d, *J* = 10.4 Hz, 1H (C$\underline{H}$-CH_2-OH)), 3.08 (t, *J* = 11.6 Hz, 1H (CHOH-C$\underline{H}_{2b}$-N)), 1.84 – 1.61 (m, 2H (C$\underline{H}_2$-CH_3)), 1.04 (t, *J* = 7.0 Hz, 3H (CH_3). ^{13}C NMR (101 MHz, MeOD) δ 89.18, 87.48 (CH-F); 76.66, 67.24, 67.13, 66.25 (3 x CH-OH and C$\underline{H}$-CH_2OH); 56.43, 56.23 (N-C$\underline{H}_2$-CHF); 54.16, 53.98 (CH-C$\underline{H}_2$-OH and CHOH-C$\underline{H}_2$-N); 25.76, 25.56 (C$\underline{H}_2$-CH_3); 7.81, 7.76 (CH_3). ^{19}F NMR (376 MHz, MeOD) δ -185.88 – -187.40 (m).HPLC (UV) 95.6% rt: 0.95'. HRMS calculated for $C_{10}H_{21}NO_4F$: 238.1455 $[M+H]^+$; found: 238.1455.IR (neat): 3340.$[\alpha]^{26}_D$ -5° (*c*0.54, MeOH).

(1*S*,2*R*,3*S*,4*S*,5*S*,6*S*)-6-((2,2-difluorobutylamino)cyclohexane-1,2,3,4,5-pentaol hydrochloride (76x)

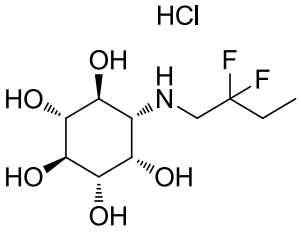

76x: Greenish paste ^{1}H NMR (400 MHz, MeOD) δ 4.23 (s, 1H (C$\underline{H}$-OH)), 3.93 – 3.73 (m, 2H (C$\underline{H}$-OH and C$\underline{H}_{2a}$-NH)), 3.71 – 3.51 (m, 2H (C$\underline{H}$-OH and C$\underline{H}_{2b}$-NH)), 3.39 (d, *J* = 9.2 Hz, 1H (C$\underline{H}$-OH)), 3.28 – 3.15 (m, 2H (C$\underline{H}$-OH and C$\underline{H}$-NH)), 2.12 – 1.91 (m, 2H (C$\underline{H}_2$-CH_3)), 1.06 (t, *J* = 6.6 Hz, 3H (CH_3)). ^{13}C NMR (101 MHz, MeOD) δ 123.95, 121.54, 119.13 (1 x C$\underline{F}_2$); 75.37, 72.13, 72.11, 68.88, 67.32 (5 x C$\underline{H}$-OH); 60.70 (C$\underline{H}$-NH); 48.20, 47.94, 47.72 (1 x NH-C$\underline{H}_2$), 28.44, 28.20, 27.97 (1 x C$\underline{H}_2$-CH_3), 4.81 (CH_3).^{19}F NMR (376 MHz, MeOD) δ -104.49 – -107.97 (m).HPLC (ESI) 75.0% rt: 0.84'; m/z: 272.20. HRMS calculated for $C_{10}H_{20}NO_5F_2$: 272.1310 $[M+H]^+$; found: 272.1314. IR (neat): 3300, 1635, 1034. $[\alpha]^{25}_D$ -16° (*c*1.0, MeOH).

(1*S*,2*R*,3*S*,4*S*,5*S*,6*S*)-6-(((*R*)-2-hydroxybutyl)amino)cyclohexane-1,2,3,4,5-pentaol hydrochloride ((*R*)-89x)

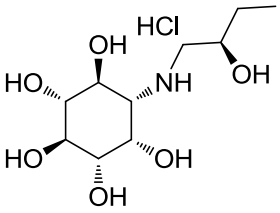

(*R*)-89x: Yellowish paste.^{1}H NMR (400 MHz, MeOD) δ 4.17 (t, *J* = 2.6 Hz, 1H (CH-C<u>H</u>-OH)), 3.85 – 3.71 (m, 2H (CH-C<u>H</u>-OH and CH_2-C<u>H</u>-OH)), 3.56 (t, *J* = 9.4 Hz, 1H (CH-C<u>H</u>-OH)), 3.39 (dd, *J* = 9.8, 2.5 Hz, 1H (CH-C<u>H</u>-OH)), 3.24 – 3.10 (m, 3H (CH-C<u>H</u>-OH, C<u>H_{2a}</u>-NH and C<u>H</u>-NH)), 2.97 (dd, *J* = 12.6, 10.1 Hz, 1H (C<u>H_{2b}</u>-NH), 1.62 – 1.42 (m, *J* = 7.7, 7.0 Hz, 2H (C<u>H_2</u>-CH_3)), 0.98 (t, *J* = 7.4 Hz, 3H (C<u>H_3</u>)). ^{13}C NMR (101 MHz, MeOD) δ 75.32, 72.19, 72.07, 69.11, 67.07, 66.29 (6 x <u>C</u>H-OH); 59.85 (<u>C</u>H-NH); 49.71 (<u>C</u>H_2-NH); 27.66 (<u>C</u>H_2-CH_3); 8.44(CH_3). HPLC (ESI) 95.7% rt: 0.47'; m/z: 252.10. HRMS calculated for $C_{10}H_{22}NO_6$: 252.1447 $[M+H]^+$; found: 252.1451. IR (neat): 3350, 1654, 1101. $[\alpha]^{25}_{D}$ -17° (*c* 0.7, MeOH).

(1*S*,2*R*,3*S*,4*S*,5*S*,6*S*)-6-(((*S*)-2-hydroxybutyl)amino)cyclohexane-1,2,3,4,5-pentaol hydrochloride ((*S*)-89x)

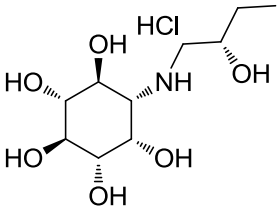

(*S*)-89x: Yellowish paste. ^{1}H NMR (400 MHz MeOD) δ 4.19 (t, *J* = 2.7 Hz, 1H (CH-C<u>H</u>-OH)), 3.82 – 3.69 (m, 2H (CH-C<u>H</u>-OH and CH_2-C<u>H</u>-OH)), 3.56 (t, *J* = 9.3 Hz, 1H (CH-C<u>H</u>-OH)), 3.39 (dd, *J* = 9.7, 2.7 Hz, 1H (CH-C<u>H</u>-OH)), 3.33 – 3.30 (m, 1H (C<u>H_{2a}</u>-NH)), 3.20 (t, *J* = 9.2 Hz, 2H (CH-C<u>H</u>-OH and C<u>H</u>-NH)), 2.92 (dd, *J* = 12.5, 10.4 Hz, 1H (C<u>H_{2b}</u>-NH)), 1.63 – 1.42 (m, 2H (C<u>H_2</u>-CH_3)), 0.98 (t, *J* = 7.4 Hz, 3H (C<u>H_3</u>)). ^{13}C NMR (101 MHz, MeOD) δ 75.30, 72.24, 72.07, 69.30, 68.03, 66.55 (6 x <u>C</u>H-OH); 60.68 (<u>C</u>H-NH), 50.03 (<u>C</u>H_2-NH), 27.84 (<u>C</u>H_2-CH_3); 8.34 (CH_3). HPLC (ESI) 81.7% rt: 0.46'; m/z: 252.19. HRMS calculated for $C_{10}H_{22}NO_6$: 252.1447 $[M+H]^+$; found: 252.1458. IR (neat): 3341, 1652, 1104, 1036. $[\alpha]^{25}_{D}$ -9° (*c* 1.0, MeOH).

(2*R*,3*R*,4*R*,5*S*)-2-(hydroxymethyl)-1-((*R*)-2-hydroxynonyl)piperidine-3,4,5-triol hydrochloride ((*R*)-85y)

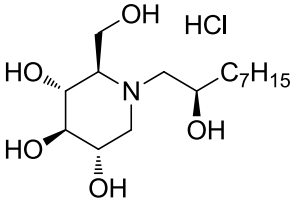

(*R*)-85y: Yellowish powder. ^{1}H NMR (400 MHz, MeOD) δ 4.14 – 3.90 (m, 3H), 3.78 – 3.68 (m, 1H), 3.62 (t, *J* = 8.9 Hz, 2H), 3.42 – 3.32 (m, 2H), 3.19 (d, *J* = 12.6 Hz, 1H), 3.07 (t, *J* = 10.4 Hz, 2H), 1.57 – 1.17 (m, 12H), 0.95 – 0.81 (m, 3H). ^{13}C NMR (101 MHz, MeOD) δ 76.71, 67.48, 67.26, 66.26, 64.44, 58.72, 54.14, 53.57, 35.10, 31.53, 29.22, 28.91, 24.84, 22.27, 12.99.HPLC (UV) 96.9% rt: 2.68'. HRMS calculated for $C_{15}H_{32}NO_5$: 306.2280 $[M+H]^+$; found: 306.2278.IR (neat): 3315, 2927, 2855. $[\alpha]^{26}_{D}$ -9° (*c* 1.0, MeOH).

(2*R*,3*R*,4*R*,5*S*)-2-(hydroxymethyl)-1-((*S*)-2-hydroxynonyl)piperidine-3,4,5-triol hydrochloride ((*S*)-85y)

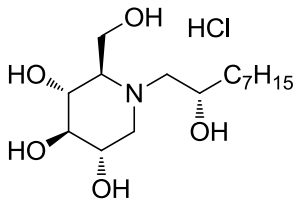

(*S*)-85y: Colorless paste. ^{1}H NMR (400 MHz, MeOD) δ 4.15 – 3.94 (m, 3H), 3.79 – 3.67 (m, 2H), 3.57 (t, *J* = 9.7 Hz, 1H), 3.46 – 3.40 (m, 1H), 3.38 – 3.32 (m, 1H), 3.24 (d, *J* = 10.0 Hz, 1H), 3.17 – 2.93 (m, 2H), 1.55 – 1.22 (m, 12H), 0.88 (t, *J* = 6.9 Hz, 3H). ^{13}C NMR (101 MHz, MeOD) δ 76.69, 67.48, 67.42, 66.47, 66.31, 58.42, 55.33, 53.92, 35.57, 31.52, 29.13, 28.89, 24.66, 22.26, 12.96.HPLC (UV) 89.0% rt: 2.58'. HRMS calculated for $C_{15}H_{32}NO_5$: 306.2280 $[M+H]^+$; found: 306.2290.$[\alpha]^{26}_D$ +11º (*c* 1.0, MeOH).

(2*R*,3*R*,4*R*,5*S*)-1-((*R*)-2-fluorononyl)-2-(hydroxymethyl)piperidine-3,4,5-triol hydrochloride ((*R*)-87y)

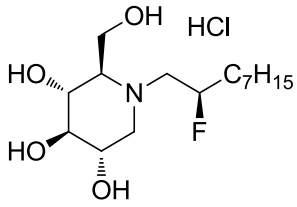

(*R*)-87y: Yellow oil. ^{1}H NMR (400 MHz, MeOD) δ 5.19 – 4.97 (m, 1H (CH-F)), 4.12 (d, *J* = 12.5 Hz, 1H (CH-C$\underline{H}_{2a}$-OH)), 3.92 (dd, *J* = 12.3, 3.0 Hz, 1H (CH-C$\underline{H}_{2b}$-OH)), 3.76 – 3.64 (m, 2H (N-C$\underline{H}_{2a}$-CH-F and (CH-C$\underline{H}$-OH)), 3.63 – 3.53 (m, 2H (CH-C$\underline{H}$-OH and CHOH-C$\underline{H}_{2a}$-N)), 3.53 – 3.40 (m, 1H (N-C$\underline{H}_{2b}$-CH-F)), 3.36 (t, *J* = 9.2 Hz, 1H (CH-C$\underline{H}$-OH)), 3.11 (t, *J* = 11.2 Hz, 2H (CHOH-C$\underline{H}_{2b}$-N and C$\underline{H}$-CH_2-OH)), 1.82 – 1.19 (m, 12H (($C\underline{H}_2$)$_6$-CH_3)), 0.88 (t, *J* = 6.8 Hz, 3H (CH_3)). ^{13}C NMR (101 MHz, MeOD) δ 90.20, 88.49 (C$\underline{H}$-F); 76.53, 67.37, 66.25 (3 x CH-OH and C$\underline{H}$-CH_2-OH); 56.80 (N-C$\underline{H}_2$-CH-F); 55.12 (CHOH-C$\underline{H}_2$-N); 53.55(CH-C$\underline{H}_2$-OH); 32.68, 32.47, 31.45, 28.79, 28.76, 24.09, 22.22 (($C\underline{H}_2$)$_6$-CH_3); 12.94 (CH_3). ^{19}F NMR (376 MHz, MeOD) δ -181.69 (ddq, *J* = 50.9, 32.8, 16.4 Hz). HPLC (UV) 95.2% rt: 2.84'. HRMS calculated for $C_{15}H_{31}NO_4F$: 308.2237 $[M+H]^+$; found: 308.2246. $[\alpha]^{26}_D$ +1º (*c* 0.47, MeOH).

(2*R*,3*R*,4*R*,5*S*)-1-((*S*)-2-fluorononyl)-2-(hydroxymethyl)piperidine-3,4,5-triol hydrochloride ((*S*)-87y)

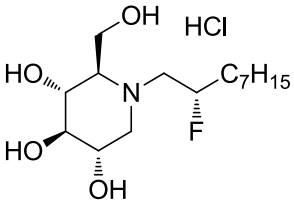

(*S*)-87y: Beige solid. ^{1}H NMR (400 MHz, MeOD) δ 5.09 (d, *J* = 51.9 Hz, 1H (CH-F)), 3.99 (dd, *J* = 69.0, 12.2 Hz, 2H (CH-C$\underline{H}_2$-OH)), 3.77 – 3.52 (m, 4H (CHOH-C$\underline{H}_{2a}$-N, N-C$\underline{H}_{2a}$-CHF and 2 x CH-C$\underline{H}$-OH)), 3.51 – 3.30 (m, 3H (CH-C$\underline{H}$-OH and N-C$\underline{H}_{2b}$-CHF)), 3.16 (d, *J* = 10.4 Hz, 1H (C$\underline{H}$-CH$_2$-OH)), 3.07 (t, *J* = 11.7 Hz, 1H (CHOH-C$\underline{H}_{2b}$-N)), 1.80 – 1.23 (m, 12H (C$\underline{H}_2$)$_6$-CH$_3$)), 0.89 (d, *J* = 6.5 Hz, 3H (CH$_3$)). ^{13}C NMR (101 MHz, MeOD) δ 88.17, 86.48 (1 x C$\underline{H}$-F); 76.66, 67.24 (2 x CH-C$\underline{H}$-OH); 67.14 (C$\underline{H}$-CH$_2$-OH); 66.25 (CH-C$\underline{H}$-OH); 56.58, 56.38 (1 x N-C$\underline{H}_2$-F); 54.07 (CHOH-C$\underline{H}_2$-N); 53.92 (CH-C$\underline{H}_2$-OH); 32.46, 32.26, 31.45, 28.89, 28.77, 24.25, 24.21, 22.23 (6 x (C$\underline{H}_2$)$_6$-CH$_3$); 12.95 (CH$_3$). ^{19}F NMR (376 MHz, MeOD) δ -185.00 – -187.38 (m). HPLC (UV) 83.3% rt: 2.84'. HRMS calculated for $C_{15}H_{31}NO_4F$: 308.2237 $[M+H]^+$; found: 308.2251. $[\alpha]^{26}_D$ -1° (*c* 0.85, MeOH).

(1*S*,2*R*,3*S*,4*S*,5*S*,6*S*)-6-(((*R*)-2-hydroxynonyl)amino)cyclohexane-1,2,3,4,5-pentaol hydrochloride ((*R*)-89y)

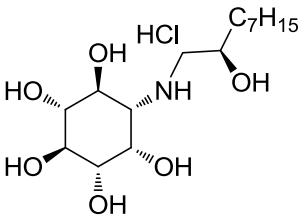

(*R*)-89y: Yellowish paste.^{1}H NMR (400 MHz, MeOD) δ 4.15 (t, *J* = 2.8 Hz, 1H (CH-C$\underline{H}$-OH)), 3.92 – 3.82 (m, 1H (CH$_2$-C$\underline{H}$-OH)), 3.76 (dd, *J* = 10.6, 9.2 Hz, 1H (CH-C$\underline{H}$-OH)), 3.56 (t, *J* = 9.5 Hz, 1H (CH-C$\underline{H}$-OH)), 3.37 (dd, *J* = 9.7, 2.8 Hz, 1H (CH-C$\underline{H}$-OH)), 3.23 – 3.09 (m, 3H (CH-C$\underline{H}$-OH, C$\underline{H}$-NH and C$\underline{H}_{2a}$-NH)), 2.96 (dd, *J* = 12.7, 10.1 Hz, 1H (C$\underline{H}_{2b}$-NH)), 1.50 – 1.25 (m, 12H ((C$\underline{H}_2$)$_6$-CH$_3$))), 0.94 – 0.82 (m, 3H (CH$_3$)). ^{13}C NMR (101 MHz, MeOD) δ 75.35, 72.18, 72.08, 69.08, 66.29 (5 x CH-C$\underline{H}$-OH); 65.75 (CH$_2$-C$\underline{H}$-OH); 59.83 (C$\underline{H}$-NH); 49.99 (C$\underline{H}_2$-NH); 34.83, 31.52, 29.18, 28.90, 24.86, 22.26 ((C$\underline{H}_2$)$_6$-CH$_3$); 12.95 (C$\underline{H}_3$). HPLC (ESI) 100% rt: 2.55'; m/z: 322.21. HRMS calculated for $C_{15}H_{32}NO_6$: 322.2230 $[M+H]^+$; found: 322.2234.

(1*S*,2*R*,3*S*,4*S*,5*S*,6*S*)-6-(((*S*)-2-hydroxynonyl)amino)cyclohexane-1,2,3,4,5-pentaol hydrochloride ((*S*)-89y)

(*S*)-89y: Yellowish paste.^{1}H NMR (400 MHz, MeOD) δ 4.17 (t, *J* = 2.8 Hz, 1H), 3.88 – 3.78 (m, 1H (CH$_2$-C$\underline{H}$-

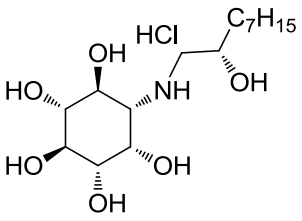

OH), 3.74 (dd, *J* = 10.7, 9.2 Hz, 1H), 3.55 (t, *J* = 9.5 Hz, 1H), 3.37 (dd, *J* = 9.7, 2.9 Hz, 1H), 3.27 – 3.22 (m, 1H (C$\underline{H}_{2a}$-NH)), 3.21 – 3.14 (m, 2H), 2.90 (dd, *J* = 12.5, 10.4 Hz, 1H (C$\underline{H}_{2b}$-NH)), 1.57 – 1.42 (m, 3H), 1.41 – 1.20 (m, 9H), 0.95 – 0.80 (m, 3H). ^{13}C NMR (101 MHz, MeOD) δ 75.34, 72.23, 72.09, 69.26, 66.71, 66.54, 60.61, 50.21, 35.01, 31.52, 29.15, 28.88, 24.73, 22.26, 12.95. HPLC (UV) 97.0% rt: 2.51'. HRMS calculated for $C_{15}H_{32}NO_6$: 322.2230 $[M+H]^+$; found: 322.2234.

5.2 Biological assays

5.2.1 Assays with purified enzyme

The glycosidases α-glucosidase (from baker's yeast), β-glucosidase (from crude almond), α-galactosidase (from green coffee beans), and β-galactosidase (from bovine liver) that were used in the inhibition studies, as well as 4-methylumbelliferyl-β-D glucoside and the corresponding p-nitrophenyl glycoside substrates, were purchased from Sigma. Imiglucerase (Cerezyme®; recombinant human GCase analogue) was kindly provided by Genzyme.

5.2.2.1 Imiglucerase inhibition assay with detergents

Imiglucerase (Genzyme) activity was determined with 4-MUG as previously reported[138]. Briefly, enzyme solutions (25 μL from a stock solution containing 0.1 mg mL−1) in the presence of 0.25% (w/v) sodium taurocholate and 0.1% (v/v) Triton X-100 in McIlvaine buffer (100 mM sodium citrate and 200 mM sodium phosphate buffer, pH 5.2 or 7) were incubated at 37 °C without (control) or with inhibitor at a final volume of 40 μL for 30 min. After addition of 60 μL of substrate (4-MUG 4 mM in McIlvaine buffer, pH 5.2 or 7), the samples were incubated at 37 °C for 10 min. Enzymatic reactions were stopped by the addition of aliquots (150 μL) of glycine/NaOH buffer (100 mM, pH 10.6). The amount of 4-MU formed was determined with a SpectraMax M5 fluorometer (Molecular Devices Corporation) at 355 nm (excitation) and 460 nm (emission). IC_{50} values were determined with Excel® by plotting percentage of activity versus log [I], using at least four different inhibitor concentrations or with Graphpad Prism 6 ® by non-lineal fitting analysis (least squares fitting method, log [inh] vs response, 3 parameters).

5.2.2.2 General procedure for the inhibition assay against other commercial glycosidases[138]

Commercial glycosidase solutions were prepared with the appropriated buffer and incubated in 96-well plates at 37 °C without (control) or with inhibitor for 5 min. After addition of the corresponding substrate solution, incubations were prolonged for different time periods: 3 min for α-glucosidase (from baker's yeast) and β-glucosidase (from almond), 13 min for α-galactosidase and 5 min for β-galactosidase, and stopped by addition of Tris or Na_2CO_3 solution, depending on the enzymatic inhibition assay.

The amount of p-nitrophenol formed was determined at 405 nm with a Spectramax M5 (Molecular Devices Corporation) spectrophotometer. For α-glucosidase, the activity was determined with p-nitrophenyl-α-D-glucopyranoside (1 mM) in sodium phosphate buffer (100 mM, pH 7.2). For β-glucosidase, the activity was determined with p-nitrophenyl-β-D-glucopyranoside (1 mM) in sodium acetate buffer (100 mM, pH 5.0). β-Galactosidase activity was determined with p-nitrophenyl-β-D-galactopyranoside (1 mM) in sodium phosphate buffer (100 mM, 0.1 mM $MgCl_2$, pH 7.2). α-Galactosidase activity was determined with p-nitrophenyl-α-D-galactopyranoside (1 mM) in sodium phosphate buffer (100 mM, pH 6.8). The commercial glycosidase solutions were prepared as follows: α-glucosidase (0.1 mg/ml buffer); β-glucosidase (0.24 mg/ml buffer); α-galactosidase 7.4 µL in buffer (1.99 ml) and β-galactosidase (0.5 mg/ml buffer). Data analysis was performed using Graphpad Prism® vs 6.

As a summary:

T=37ºC	**α-glucosidase (saccharomyces cerevisiae, baker's yeast)**	**β-glucosidase (almond)**	**α-galactosidase (green coffee beans)**	**β-galactosidase (bovine liver)**
buffer	147.5 µl phosphate buffer pH 7.2 (100 mM)	147.5 µl acetate buffer pH 5.0 (100 mM)	44.1 µl phosphate buffer pH 6.8 (100 mM)	147.5 µl phosphate buffer pH 7.2 (100 mM+ 0.1 mM $MgCl_2$)
µl inhibitor	2.5 µl solution 10 mM in DMSO	2.5 µl solution 10 mM in DMSO	0.9 µl solution 10 mM in DMSO	2.5 µl solution 10 mM in DMSO
preincubation	3 min.	3 min.	3 min.	3 min.
µl enzyme	50 µl (0.1 mg/ml)	50 µl (0.2 mg/ml)	20 µl (7.4 µl /1.99 ml buffer)	50 µl (0.5 mg/ml)
incubation	5 min.	5 min.	5 min.	5 min.
substrate	50 µl of 4-nitrophenyl-α-D-glucopyranoside 5 mM	50 µl of 4-nitrophenyl-β-D-glucopyranoside 5 mM	25 µl of 4-nitrophenyl-α-D-galactopyranoside 5 mM	50 µl of 4-nitrophenyl-β-D-galactopyranoside 5 mM
2nd incubation	3 min.	3 min.	13 min.	5 min.
stop solution	50 µl Tris solution 1 M	50 µl Tris solution 1 M	180 µl $Na2CO_3$ 1 M	50 µl Tris solution 1 M
Measurement	absorvance 405 nm	absorvance 405 nm	absorvance 405 nm	absorvance 405 nm

Table 19 Assay conditions for analysis of different glycosidases activity.

5.2.2 Cell lines and culture

Wild-Type human fibroblasts were cultured in Dulbecco's modified Eagle's medium (DMEM; D5796) supplemented with 10% fetal bovine serum (FBS) and 1% penicillin−streptomycin at 37 °C in 5% CO_2/ 95% air to confluence. Those cells used were between the 14th and 30th passage.

A549 cells were grown according to standard cell culture methods (HAM's F12 with 10% FBS, and 1% penicillin-streptomycine),at 37 °C in 5% CO_2/ 95% air to confluence.

HAP1_001 (GBA1-KO or GBA2-KO) cells were provided by Minerva Max Planck Research Group "Molecular Physiology", Research Center Caesar, Bonn. Cells were cultured in IMDM (Iscove's Modified Dubelco's Medium 1X) with L-Glutamine and 25mM HEPES with addition of 10% of FCS and 1% of Penicillin-Streptomycin, at 37 °C in 5% CO_2/ 95% air to confluence.

CHO G4A11 (GBA2 over expressed) cells were provided by Minerva Max Planck Research Group "Molecular Physiology", Research Center Caesar, Bonn. Cells were cells were grown in HAM's F12 medium with 10% FBS and 1% Genecitin (G418 40 mg/ml), at 37 °C in 5% CO2/ 95% air to confluence.

5.2.3 Assays with cell homogenates

5.2.3.1 Determination of glucosylceramide synthase activity in A549 cell homogenates[173]

A549 cells were grownto confluence, collected by trypsinization and washed twice with sodium phosphate (PBS) (10 mM, 137 mM NaCl, pH 7.4). This cell culture and the pellet preparation were performed by the Cell Culture Service based at the Center of Research and Development (CID) of the Spanish Council for Scientific Research (CSIC) in Barcelona.

The cell pellets were resuspended in 50 mM TRIS-HCl buffer (pH 7.4) and 10 mM $MgCl_2$ by sonication (three times, 30 s). The cell lysate (100 µL) was incubated with inhibitor (0.25 mM final concentration) for 10 min at 37 °C. Then, 25 µL of NAD (16 mM in TRIS-HCl, pH 7.4 and 10 mM $MgCl_2$), 25 µL of UDP-Glucose (2 mM in TRIS-HCl 50 mM, pH 7.4 and 10 mM $MgCl_2$), and 52 µL of NBD C6-ceramide complexed to BSA at a 1:1 ratio (20 µM in 50 mM TRIS-HCl buffer,

pH = 7.4, 10 mM $MgCl_2$)) were added. After 15 min incubation at 37°C, the reactions were stopped by adding 800 µL of MeOH and centrifuged at 10 000 rpm for 3 min.

The supernatant was transferred to HPLC vials. HPLC analyses were performed with a Waters 2695 Alliance System coupled to a Waters 2475 Fluorescence detector (Milford, MA) using a C18-Zorbax Eclipse Plus column (3.5 µm, 4.6 x 75 mm) and eluted with a gradient of H_2O/ACN, both with a 0.1% of trifluoroacetic acid (2 min 70/30, 4 min gradient to 25/75, and 7 min at 25/75); flow: 1 ml/min.. The detector was set at an excitation wavelength of 470 nm and measured the emission wavelength at 530 nm. Empower Software (Waters Corporation) was utilized for data acquisition and processing. Data analysis was performed using Graphpad Prism® vs 6.

5.2.3.2 Determination of GBA1 inhibition in HAP1_001 (GBA2-KO) cell homogenates

The HAP1 pellet was resuspended and lysated (3 cycles of sonication of 20 seconds) to a concentration of 5 µg protein/µl in hypotonic buffer (10 mM HEPES/NaOH, 0.5 mM EDTA, pH 7.4 and 1:500 m-PIC). The assay was performed in a 384-wells Greiner plate, providing per well 25 µl of cell homogenate, with or without inhibitors, diluted in Mc Ilvaine buffer (pH 5.2 or 7.0) to a protein concentration of 0.77 µg/µl. The assay was initiated by adding 5 µl of 4-MUG (10 mM), resulting in a final substrate concentration of 1.67 mM. The hydrolysis of 4-MUG was monitored in real time, and recorded as a change in relative fluorescence units (rfu)/min by a Fluostar Omega reader (BMG Labtech) at 30 °C using the filter pair 355 nm/460 nm for excitation and emission, respectively. Each analysis was performed as a quadruplicate in parallel, and in three different days. Data analysis was performed using Graphpad Prism® vs 6. IC_{50} values were determined by non-lineal fitting analysis (least squares fitting method, log [inh] vs response, 3 parameters).

5.2.3.3 Determination of GBA2 Inhibition in CHO_G4A11 (GBA2 over expressed) cell homogenates

The CHO pellet was resuspended and lysated (3 cycles of sonication of 20 seconds) to a concentration of 2 µg protein/µl in hypotonic buffer (10 mM HEPES/NaOH, 0.5 mM EDTA, pH 7.4 and 1:500 m-PIC). The assay was performed in a 384-wells Greiner plate, providing per well

25 µl of cell homogenate, with or without inhibitors, diluted in Mc Ilvaine buffer (pH 6.0) to a protein concentration of 0.31 µg/µl. The assay was initiated by adding 5 µl of 4-MUG (10 mM), resulting in a final substrate concentration of 1.67 mM. The hydrolysis of 4-MUG was monitored in real time, and recorded as a change in relative fluorescence units (rfu)/min by a Fluostar Omega reader (BMG Labtech) at 30 °C using the filter pair 355 nm/460 nm for excitation and emission, respectively. Each analysis was performed as a quadruplicate in parallel, and in three different days. Data analysis was performed using Graphpad Prism® vs 6.

5.2.4 Assays with intact cell

5.2.4.1 Cytotoxicity assay in WT-human fibroblasts[173]

Wild-type human fibroblasts were seeded at a density of 25 000 cells per well in 96-well plates. Media were renewed after 24 h, and compounds were added to give final concentrations of 200 or 500 µM. All compounds were dissolved in DMSO, and control experiments were performed with DMSO. Cells were incubated at 37 °C in 5% CO_2 for 24 h. Then, the media were replaced with 100 µL of 3-(4,5- dimethylthiazol-2-yl)-2,5-diphenyltetrazolium bromide (MTT) solution (5 mg/ml en PBS), and the mixture was incubated for an additional 3 h at 37 °C in 5% CO_2/95% air. Then, the media was removed and it was added 100 µL of DMSO on each well. After 3h, absorbance was measured at 570 nm with a SpectraMax M5 (Molecular Devices Corporation) in 96-well format. The number of viable cells was quantified by the estimation of its dehydrogenase activity, which reduces MTT to waterinsoluble formazan, which was dissolved in DMSO. WT-fibroblasts culture and this assay were performed by the Cell Culture Service based at the Center of Research and Development of the Spanish Council for Scientific Research in Barcelona.

5.2.4.2 GBA Inhibition Assay in HAP1_001 (GBA2-KO or GBA1-KO) intact cell

In a 24-well plate there were seeded $20x10^4$ HAP1_001 cells per well in their culture medium (except wells that will be negative control). After 16h the medium was replaced by 400 ml of medium without FCS, and the cells were incubated in presence of compounds or DMSO (positive control). After 2 h, 28 µl of 4-MUG 30 mM in water were added, and the plate was incubated for 24 h. After, the amount of 4-MU formed was determined with by reading the fluorescence with a Fluostar Omega reader (BMG Labtech) at 30 °C using the filter pair 355 nm/460 nm for excitation and emission, respectively.

Then, the medium was removed by aspiration and fresh medium with 10% FCS and 1% P/S was added. The plate was incubated overnight and next day the medium was replaced by medium without FCS, 28 µl of 4-MUG 30 mM were added, and the plate was incubated for another 24 h. After that, the fluorescence was read again. This step was repeated to obtain the fluorescence after 3 days without compound.

HAP1-001 (GBA2-KO) cells were used for determination of GBA1 inhibition, while for determination of GBA2 inhibition the cells used were HAP1-001 (GBA1-KO).

6. RESUM EN CATALÀ

Hi ha un llenguatge que va més enllà de les paraules….

Paulo Coello, *L'alquimista*.

Contingut del resum en català

6.1 Introducció

6.2 Objectius

6.3 Resultats i discussió

6.3.1 Estudi de la influència del pK_a de la cadena lateral

6.3.2 Estudi de la influència del pK_a del nucli central de l'inhibidor.

6.3.3 Assajos sense detergents

6.3.3.1 Assajos en homogenats cel·lulars

6.3.3.2 Assajos en cèl·lula intacta

6.4 Conclusions

6.1 Introducció

La malaltia de Gaucher és un desordre hereditari autosòmic recessiu. Els seus símptomes són diversos i poden incloure engrandiment del fetge i la pleura, problemes d'ossos, anèmia, problemes respiratoris i, en casos més greus, problemes amb el sistema nerviós central i, fins i tot la mort[1,2]. Els afectats per aquesta malaltia presenten un incorrecte plegament de l'enzim glucosilceramidasa (GCase) degut a algunes mutacions en el gen responsable de la seva síntesi. L'incorrecte plegament de la GCase fa que no es transporti correctament fins al lisosoma. La GCase és responsable de la hidròlisi de glucosilceramida (GluCer) al lisosoma, i per tant, en els malalts de Gaucher es produeix una acumulació de GluCer no degradada, que és el que condueix a la manifestació clínica de la malaltia.

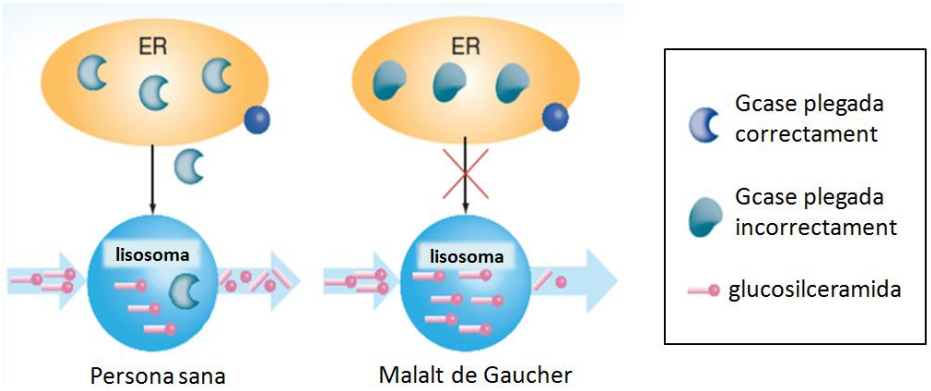

Figura 1 Comparativa del metabolisme de la GluCer en una persona sana I un malalt de Gaucher. Figura adaptada de Trapero *et al*[1].

La GluCer és un glicoesfingolípid que es sintetitza a l'aparell de Golgi per la transferasa glucosilceramida sintasa (GCS), a partir de UDP-glucosa i ceramida[18], i és un precursor bàsic per la síntesi d'altres glicoesfingolipids més complexes[13-15]. Així mateix, la GluCer pot ser degradada per tres hidrolases diferents: la glucosilceramidasa lisosomal (GBA1), la no lisosomal (GBA2) i la citosòlica (GBA3)[174]. Cal remarcar, però, que la malaltia de Gaucher només es desenvolupa a partir de mutacions en el gen *gba1*, mentre que mutacions en els gens *gba2* o *gba3* no sembla que condueixin a aquestes manifestacions clíniques.

La GCase és una β-glucosidasa que actua amb retenció de configuració (Figura 2). El seu cicle catalític té lloc en dos passos on els Glu235 i Glu340 del centre actiu juguen els papers de àcid/base i nucleòfil respectivament[36].

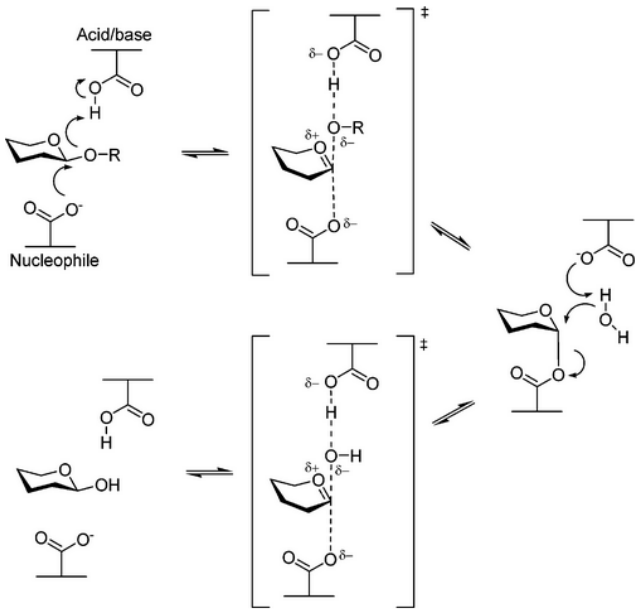

Figura 2 Mecanisme general de hidròlisi d'un β-glucòsid amb retenció de configuració[36].

Entre les diferents aproximacions terapèutiques per als malalts de Gaucher cal destacar la teràpia de reemplaçament enzimàtic (ERT), la teràpia de reducció de substrat (SRT), i la teràpia amb chaperones farmacològiques[1] (Figura 3).

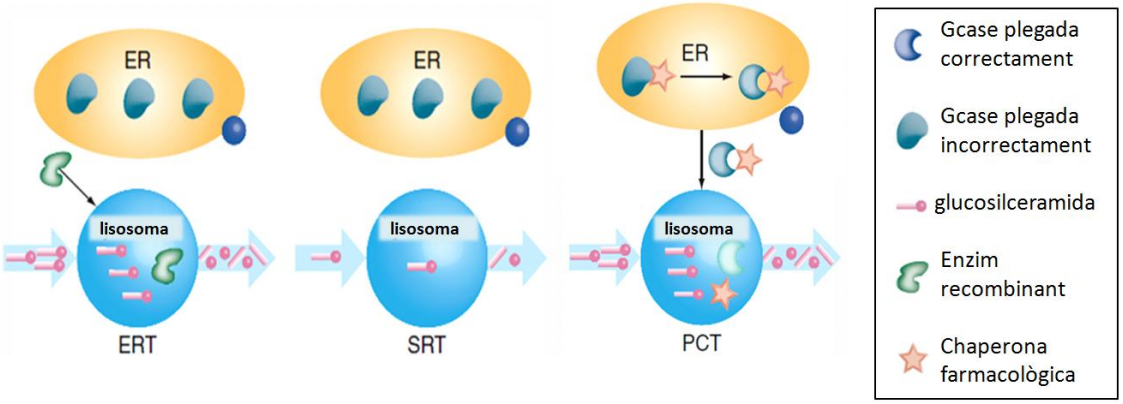

Figura 3 Algunes teràpies potencials per al tractament de la malaltia de Gaucher. Figura adaptada de Trapero *et al*[1].

La primera aproximació (ERT) consisteix en administrar als pacients per via intravenosa un enzim que substitueixi i pugui suplir les funcions de la seva GCase. El principals problemes d'aquesta teràpia són la limitada disponibilitat del enzim a administrar, el seu elevat cost, el fet que l'administració de l'enzim s'ha de realitzar cada dues setmanes i en dependències

hospitalàries, i que no serveix per tractar les variants associades als malalts de Gaucher de tipus 3 amb afectació cerebral.

La SRT consisteix en l'administració de medicaments que bloquegin la síntesi de GluCer i per tant minimitzin la seva acumulació als lisosomes. Tot i que aquesta teràpia sembla que té el potencial per oferir medicaments orals capaços de creuar la barrera hematoencefàlica (BBB), cap dels dos medicaments aprovats actualment com a SRT per a la malaltia de Gaucher ha demostrat eficàcia per a tractar les variants neuronopàtiques de la malaltia. A més a més, aquesta aproximació terapèutica comporta uns efectes secundaris intrínsecs degut a que una reducció en la quantitat de GluCer sintetitzada afecta també a la síntesi dels diferents glicolípids dels quals és precursora.

L'aproximació de les chaperones farmacològiques (PC) es basa en administrar un inhibidor que s'uneixi a la GCase al reticle endoplasmàtic, l'ajudi a adquirir el seu correcte plegament facilitant el seu transport fins al lisosoma i, per tant, facilitant la hidròlisi lisosomal de la GluCer mitjançant la GCase. Aquesta teràpia podria proporcionar compostos capaços de travessar la BBB, i sense els efectes secundaris intrínsecs de la SRT deguts a la disminució de GluCer.
Per altra banda, alguns estudis han demostrat que les PC poden augmentar la estabilitat d'alguns enzims utilitzats per a la ERT, com la imiglucerasa. Malgrat que actualment encara no hi ha cap fàrmac aprovat per a l'administració com a PCT per al tractament de la malaltia de Gaucher, hi ha diversos compostos en fase clínica, per a demostrar la seva eficàcia com a PC per a aquesta malaltia o per altres malalties de dipòsit lisosomal com les malalties de Fabry o Pompe.

Una chaperona farmacològica ideal per al tractament de la malaltia de Gaucher hauria de complir les següents premisses:

- Ser un inhibidor competitiu de la GCase amb alta afinitat per l'enzim al reticle endoplasmàtic (pH neutre), per tal d'induir el correcte plegament de la proteïna i facilitar el seu transport del reticle fins al lisosoma.
- Tenir una dissociació de la GCase fluida en les condicions del lisosoma, per facilitar la interacció entre l'enzim i la GluCer.
- Ser selectiu per a la GCase, per tal de minimitzar possibles efectes secundaris.
- Tenir una bons biodistribució i atravessar la barrera hematoencefàlica, per tal de ser útil per al tractament de les variants neuronopàtiques de la malaltia.
- Presentar una baixa toxicitat.

6.2 Objectius

El principal objectiu d'aquesta tesi és **dissenyar i sintetitzar inhibidors potents de GCase amb major afinitat per la GCase a pH neutre que a pH àcid, que puguin ser potencials chaperones farmacològiques per al tractament de la malaltia de Gaucher.**

Aquest objectiu inclou els següents objectius específics:

A) Estudi de la influència del pK_a de la cadena lateral en el forat hidrofóbic de la GCase.

Amb aquest propòsit es dissenyarà una petita llibreria de derivats de DNJ amb diferents grups protonables en la cadena *N*-alquilada, amb diferents pK_as.

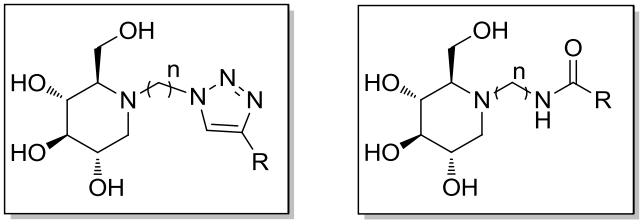

Figura 4 Estructures generals dels compostos proposats per a l'estudi de la influencia del pKa de la cadena lateral.

B) Estudi de la influència del pK_a del nucli estructural de l'inhibidor.

Per tal d'assolir aquest objectiu, es dissenyaran i sintetitzaran diferents derivats d'iminosucres i aminociclitols amb diferents β-substitucions en la cadena lateral, per a obtenir compostos amb estructures similars i diferents pK_as.

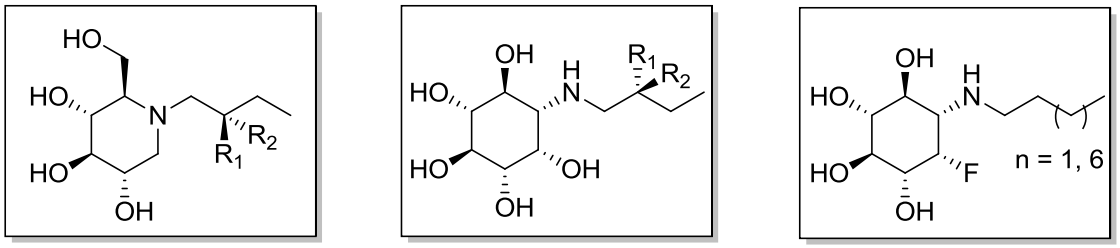

R_1, R_2 = H, OH, F

Figura 5 Compostos proposats per a l'estudi de la influència del pK_a en el nucli central de l'inhibidor.

Per altra banda, donat que alguns derivats de DNJ han resultat ser bons inhibidors de GCS, un objectiu secundari per a aquesta tesi serà **obtenir inhibidors potents de GCS, enfocats cap a l'ús com a SRT o, fins i tot, com a compostos duals (inhibidors de GCS i chaperones farmacològiques) per al tractament de la malaltia de Gaucher.**

6.3 Resultats i discussió

6.3.1 Estudi de la influència del pK_a de la cadena lateral

Les estructures cristal·logràfiques de NB-DNJ i NN-DNJ unides a la GCase han estat determinades[112]. D'aquesta manera és possible conèixer com aquests compostos s'uneixen realment a l'enzim. Tal i com es pot apreciar a la Figura 6, tots dos compostos s'uneixen de manera similar al centre actiu de la pGCase (GCase humana recombinada expressada en cèl·lules vegetals cultivades) amb l'iminosucre fent ponts d'hidrogen amb les cadenes laterals dels residus del centre actiu. Les cadenes alquíliques de tos dos compostos estan orientades cap a la entrada del centre actiu. La diferència d'afinitat entre els dos compostos sembla ser deguda a una major hidrofobicitat global de la NN-DNJ respecte la NB-DNJ, junt amb el fet que la superfície hidrofòbica a la entrada del centre actiu afavoreix l'entrada dels lligands més hidrofòbics.

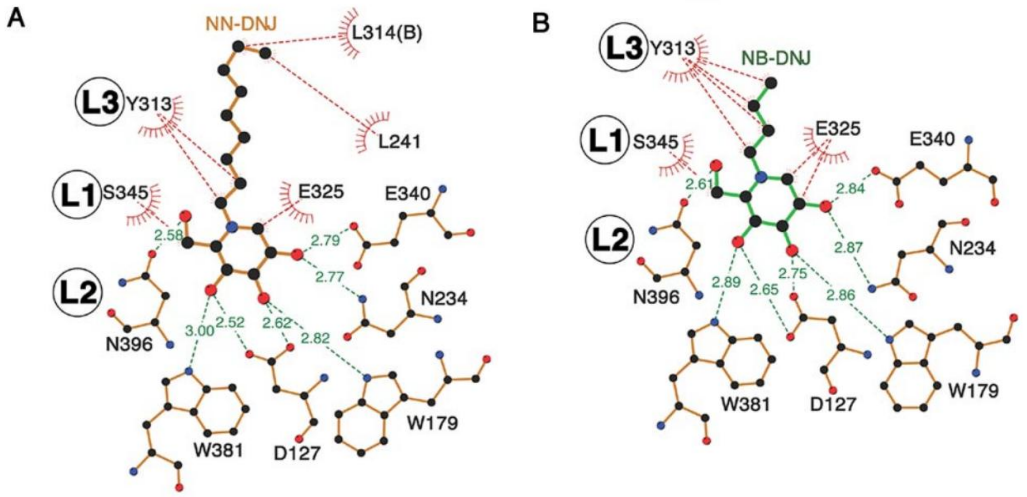

Figura 6 Comparativa de la unió d'inhibidors no covalents a la GCase. **(A)** NN-DNJ/pGCase (PDB ID: 2V3E) **(B)** NB-DNJ/pGCase (PDB ID: 2V3D). Les línies verdes representen ponts d'hidrogen i les vermelles interaccions hidrofòbiques. Adaptat de Brumstein *et al*[112].

Aquesta aparent afinitat de l'enzim per compostos hidrofòbics unit al fet que el reticle endoplasmàtic té una pH neutre mentre que el pH del lisosoma és lleugerament acídic, sembla suggerir que sintetitzant compostos amb diferent hidrofobicitat en la cadena depenent del pH del medi pot conduir a la obtenció de compostos amb diferent afinitat i per tant diferent capacitat d'inhibició de la GCase segons el pH del medi. Així doncs, en aquesta secció, per a l' obtenció d'aquests compostos amb diferent hidrofobicitat ens centrarem en la introducció de substituents amb diferents pK_as al final de la cadena lateral, introduint aquests substituents mitjançant reaccions de síntesi d'amides en fase sòlida o bé cicloaddicions de Huisgen 1,3-dipolars.

En primer lloc es van sintetitzar els derivats amb amina terminal **15**, tal i com es detalla al següent esquema, a partir del derivat benzilat de la DNJ [124-126] (**13**).

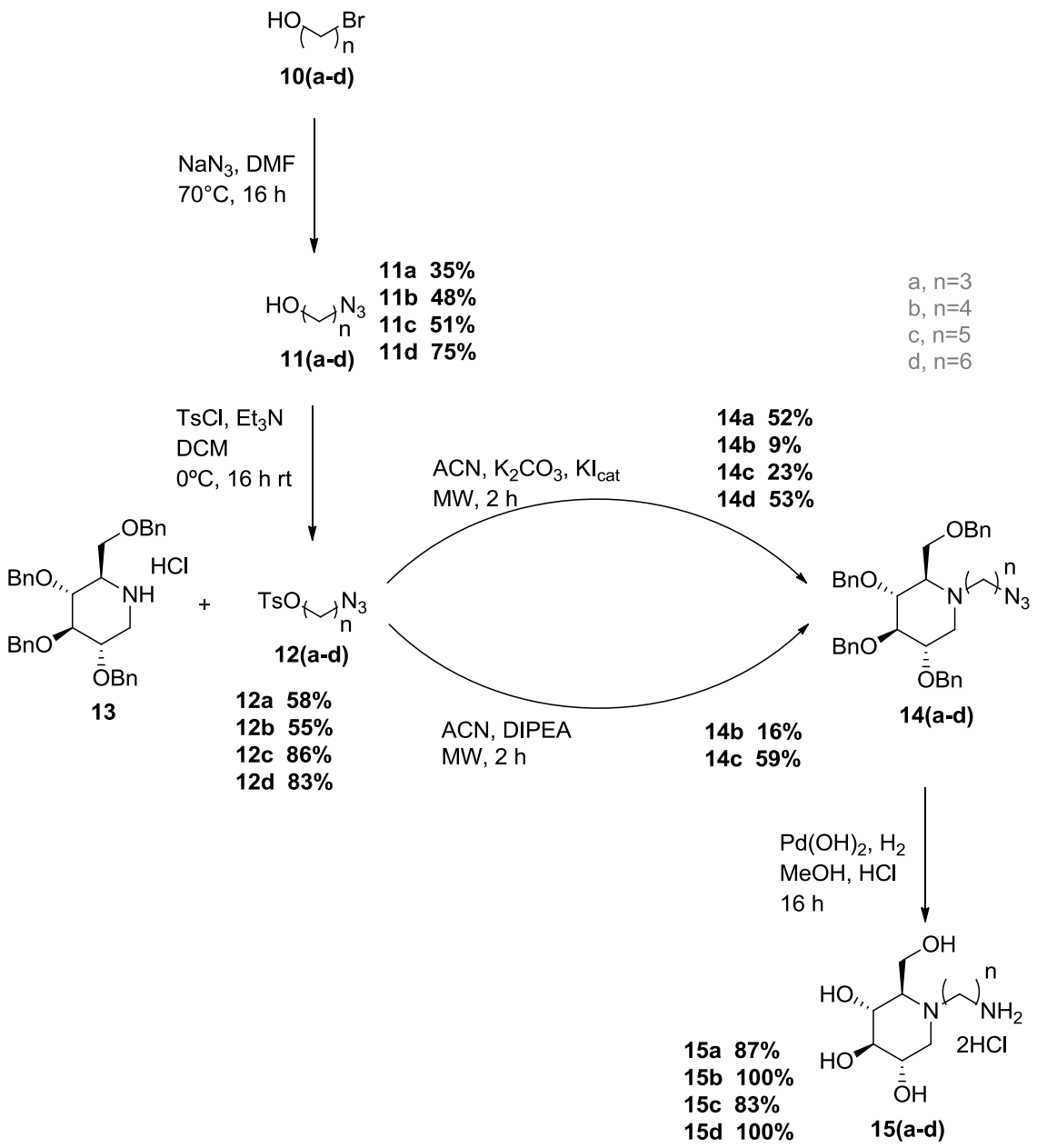

Esquema 1 Síntesi dels derivats **15(a-d)**.

Per a la síntesi dels derivats amida es va optar per reaccions amb HOBT suportat en una matriu de poliestiré i PyBrOP com a agent activant amb l'objectiu d'obtenir els compostos desitjats sense necessitat de cap purificació cromatogràfica i esperant poder realitzar els assajos biològics *in vitro* directament amb els crus de reacció. Lamentablement, degut a la insolubilitat de l'amina **15d** en els dissolvents apropiats per treballar amb la resina, es van utilitzar unes condicions que no van conduir als compostos desitjats amb suficient puresa per ser assajats

directament. Després de les conseqüents purificacions, els derivats amida **16d(I-III)** es van obtenir amb baixos rendiments (entre el 8 i 12%).

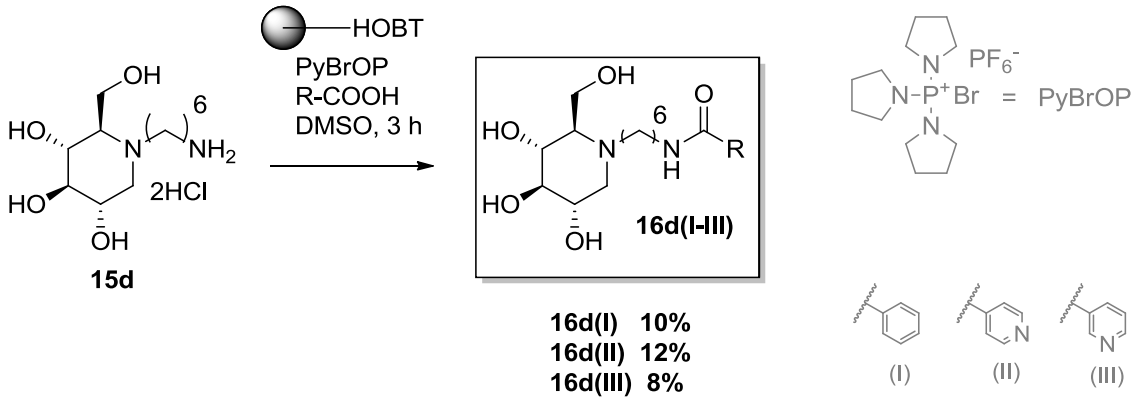

Esquema 2 Síntesi dels compostos **16d(I-III)**.

Degut a el baix rendiment de les reaccions i al fet que va caldre tractar els residus obtinguts per a purificar els compostos desitjats, es va decidir no sintetitzar més derivats d'aquest tipus, partint de les altres amines **15** mostrades en l'esquema 1, fins haver realitzat els assajos *in vitro* dels compostos sintetitzats.

Pel que fa a la síntesi dels derivats amb el grup triazol **31**, primerament es van intentar obtenir mitjançant una 1,3-cicloaddició de Huisgen entre les azides **24** i l'alquí corresponent per tal d'introduir la diversitat en l'ultima etapa de reacció i, aprofitar que es tracta d'una reacció click per fer directament els assajos biològics *in vitro*, sense necessitat de purificar els crus de reacció. Per aquest motiu es va intentar abordar la síntesi de les azides **24** amb diferents aproximacions.

Després de provar diferents condicios, el compost **24d** va ser sintetitzat amb un 17% de rendiment mitjançant la alquilació de la DNJ (**27**) amb l'azidotosilat **12d** utilitzant radiació de microones, i posterior purificació per HPLC preparatiu. La quantitat obtinguda va ser baixa degut al baix rendiment i la dificultat en la purificació.

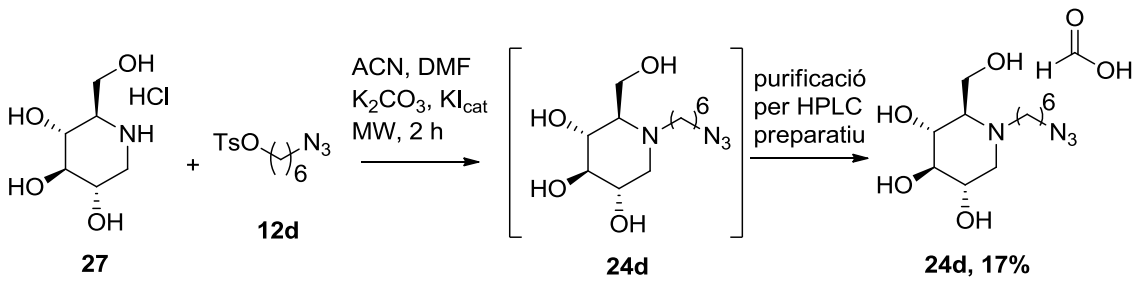

Esquema 3 Síntesi del compost **24d.**

Un cop obtingut el derivat **24d**, es va poder procedir a la síntesi dels compostos **31d(I-IV)** mitjançant la 1,3-cicloaddició de Huisgen entre l'azida **24d** i l'alquí corresponent, catalitzada amb Cu_2O. Es va fer un seguiment de les reaccions per HRMS, observant-se la necessitat de diferents temps i temperatures de reacció per assolir la completa formació dels productes d'interès, tal i com es resumeix a l'esquema 4.

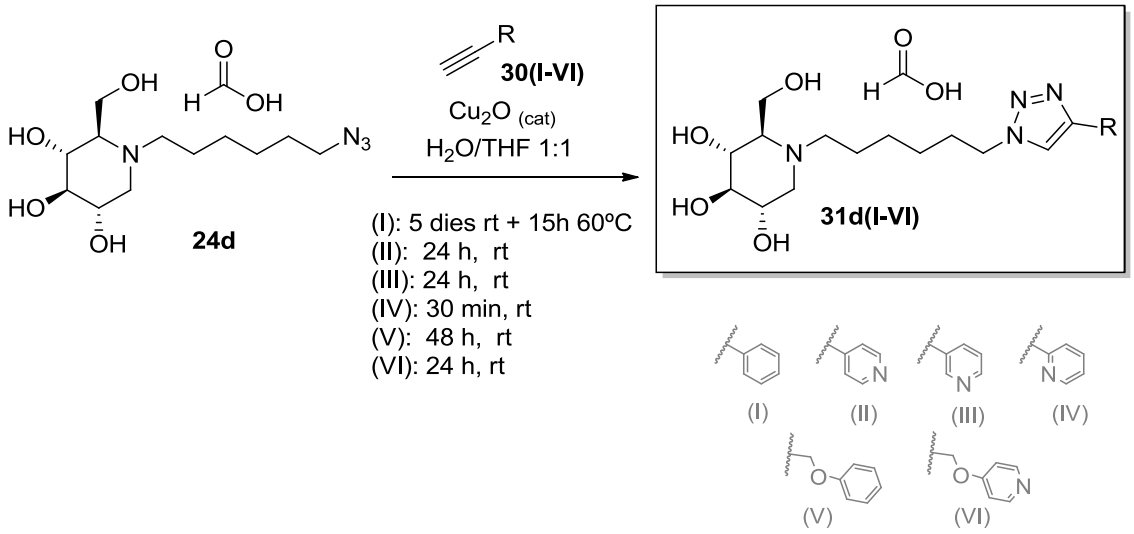

Esquema 4 Síntesi dels compostos **31d(I-VI)**.

Arribats a aquest punt, degut a la dificultat de síntesi dels derivats azida **24** amb bons rendiments i grans quantitats, es va decidir no sintetitzar més derivats d'aquest tipus seguint aquest procediment fins analitzar els resultats dels assajos biològics in vitro dels compostos obtinguts. Tot i així, es va procedir a sintetitzar els compostos **31b(VI-VII)** en major quantitat, fent primer la reacció click a partir del derivat benzilat de la DNJ i després la etapa de desbenzilació, per tal de poder-los caracteritzar correctament i determinar experimentalment el seu pK_a (Esquema 5).

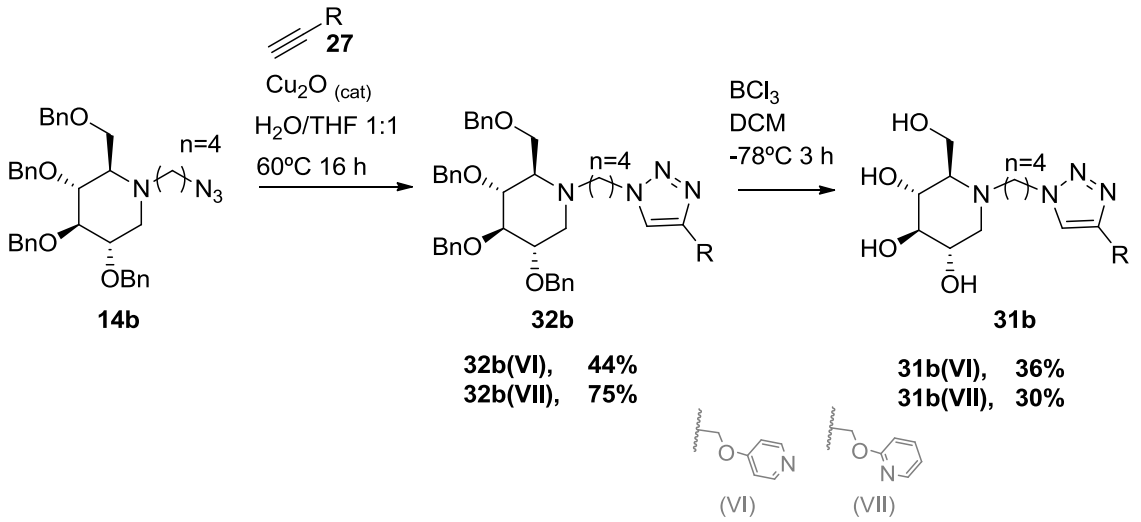

Esquema 5 Síntesi dels compostos **31b(VI-VII).**

Així doncs, per tal d'estudiar si els compostos sintetitzat realment mostren major afinitat per la GCase al reticle endoplasmàtic (pH neutre) que al lisosoma (pH al voltant de 5,2), es va analitzar la seva capacitat d'inhibir la imiglucerasa a ambdós pHs. La imiglucerasa és una GCase humana recombinant obtinguda a partir de cèl·lules de hamster chinès, que s'utilitza habitualment en la teràpia ERT per al tractament de la malaltia de Gaucher. En aquest assaig es va mesurar la capacitat dels compostos sintetitzats d'inhibir la hidròlisi del 4-metilumbel·liferil-β-D-glucopiranòsid (4-MUG) per part de la imiglucerasa a pH 7,0 i a pH 5,2 en presència de detergents com el taurocolat sòdic i el Triton X-100, per intentar emular els lipids i detergents naturalment presents a les cèl·lules i que són necessaris per a la correcta activitat enzimàtica.

Tal i com es pot observar a la Taula 1, tots els compostos assajats presenten millor afinitat per l'enzim a pH 7,0 que a pH 5,2 en aquestes condicions d'assaig.

	pH 5,2 IC_{50} (μM)	pH 7,0 IC_{50} (μM)	Δ
NB-DNJ	430	145	3,0
NN-DNJ	1,03	0,25	4,2
15a	>50	>50	-
15b	>50	>50	-
15d	>50	>50	-
16d(I)	22,8	5,6	4,1
16d(II)	35,4	18,7	1,9
16d(III)	42,6	24,2	1,8
24d	15,7	5,5	2,8
31b(VI)	>50	>50	-
31b(VII)	>50	>50	-
31d(I)	8,5	1,6	5,2
31d(II)	22,6	7,1	3,2
31d(III)	27,2	6,3	4,4
31d(IV)	6,4	1,6	4,0
31d(V)	2,4	0,8	2,8
31d(VI)	>50	>50	-

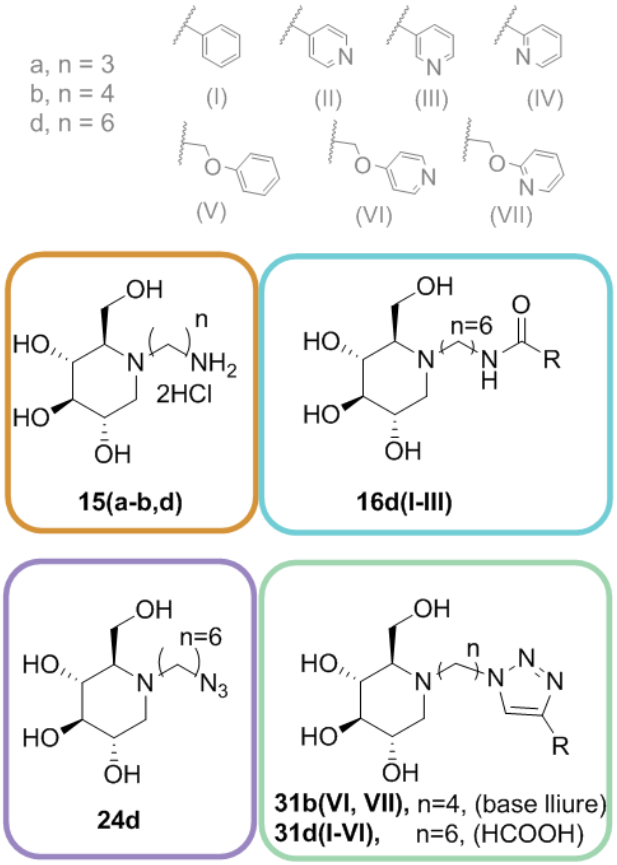

Taula 1 Inhibició de imiglucerasa.

Tal i com caldria esperar degut a la seva polaritat, els compostos **15(a-b, d)** (amb una amina primària al final de la cadena) presenten valors d'IC_{50} superiors a 50 μM, mentre que el compost **24d** (amb una azida termina, en lloc d'amina) presenta major afinitat per l'enzim, amb valors de IC_{50} de 15,7 i 5,5 μM a pH 5,2 i pH 7,0 respectivament. Similarment, la majoria de compostos amb una piridina terminal van mostrar valors considerablement més alts que els seus homòlegs amb un grup fenílic.

Desgraciadament, no s'observa el desitjat increment de la diferència d'afinitat per la GCase segons el pH de l'assaig (Δ) que esperàvem veure en els compostos amb piridines terminals. De fet, tal i com s'observa al Gràfic 1, els compostos amb grups piridina tenen valors Δ menors que els seus homòlegs amb grups fenils, al contrari del que buscàvem.

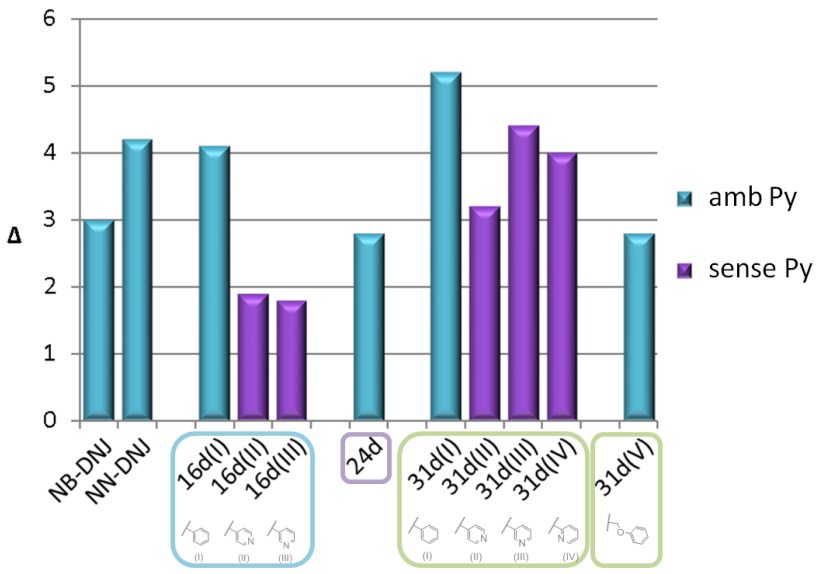

Gràfic 1 Representació gràfica dels valors de Δ per a diferents compostos.

Una possible explicació per a aquest fet és que els pK_a dels compostos són menors del que esperàvem, tal i com es va poder comprovar a partir de la determinació experimental de pK_as dels compostos **31b(VI-VII)** i dels derivats **34(II-IV)** i **35(II-IV, VI-VII)**, precursors dels compostos d'interès sense l'en nucli de DNJ (Taula 2). Per aquesta raó es va decidir sintetitzar el derivat **44**, després de comprovar que el 3(piridin-4-il)propan-1-ol presentava un pK_a experimental de 5.9.

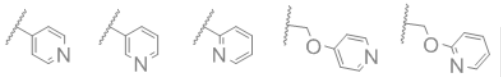

compost (BH^+)	pK_a
31b(VI)	2,62 ± 0,06 6,03 ± 0,05
31b(VII)	2,66 ± 0,19 6,21 ± 0,09
34(II)	3,95 ± 0,30
34(III)	3,89 ± 0,34
34(IV)	3,04 ± 0,07
35(II)	4,86 ± 0,21
35(III)	4,22 ± 0,04
35(IV)	4,21 ± 0,61
35(VI)	3,12 ± 0,13
35(VII)	3,04 ± 0,13
38	5,37 ± 0,09
39	5,94 ± 0,15

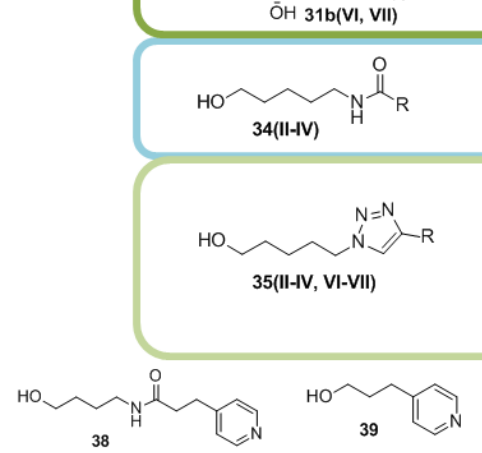

Taula 2 Valors dels pK_a determinats experimentalment per a diferents compostos.

El derivat **44** es va intentar obtenir per desbenzilació del compost **41**. Aquest últim es va sintetitzar en paral·lel (Esquema 6) tant per aminació reductiva entre l'aldehid **40** i l'amina **13** (15% rendiment), com per alquilació de **13** amb el tosilat **42** (8% rendiment). Malauradament, quan es va intentar desbenzilar **41** per hidrogenació catalitzada amb $Pd(OH)_2/C$ en medi àcid fort, es va hidrogenar també la piridina, obtenint-se el compost **43**. Finalment, el derivat **44** es va obtenir desbenzilant **41** amb BCl_3.

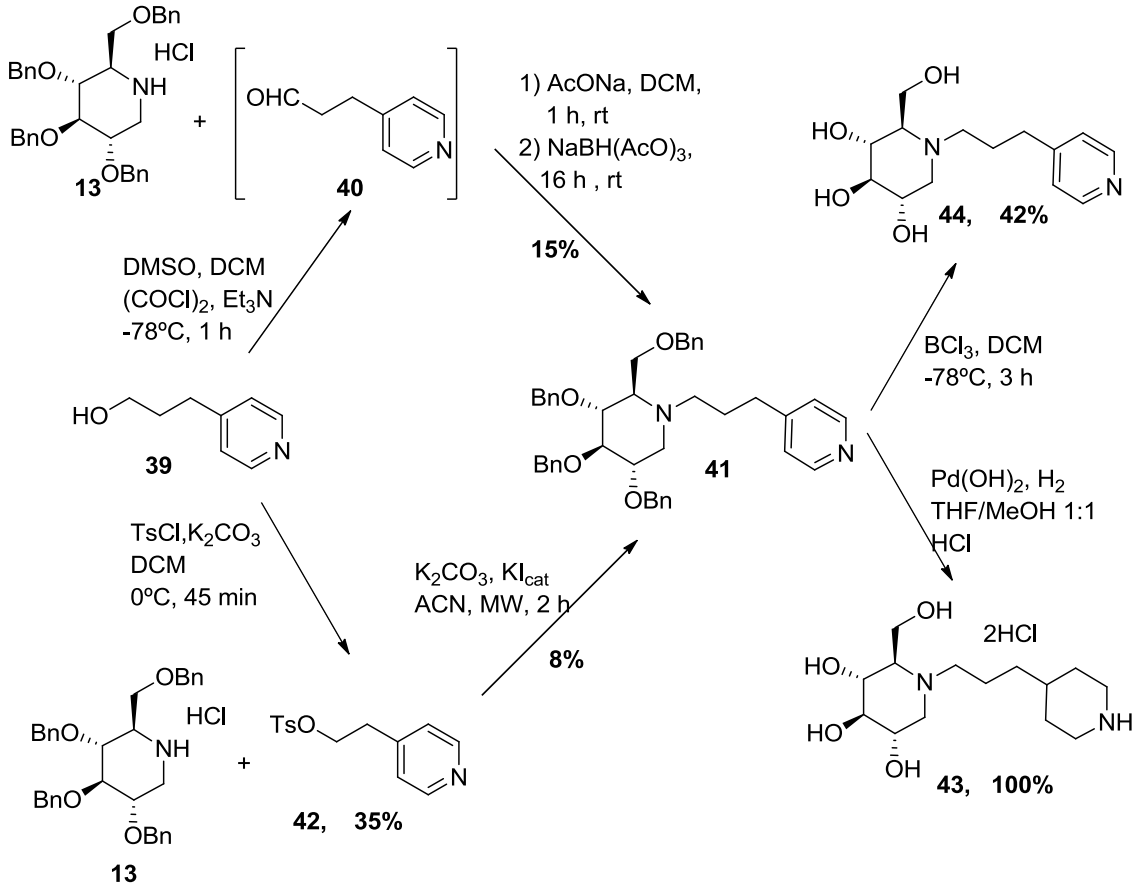

Esquema 6 Síntesi dels compostos **43** i **44**.

Arribats a aquest punt, es va determinar la capacitat inhibitòria de GCase dels compostos **43** i **44** a pH 5,2 i pH 7,0, així com els valors de pK_a del compost **44** (Taula 3).

Compost	IC_{50} (pH 5,2; µM)	IC_{50} (pH 7,0; µM)	Δ	pK_a
43	105	33	3,2	n.d.
44	414	203	2,0	4,850 ± 0,023 6,178 ± 0,023

Taula 3 Inhibició de imiglucerasa i pK_as dels compostos **43** i **44**.

Tal i com es pot veure en el diagrama de distribució d'espècies d'un compost diprotonable amb pK_a s 4,85 i 6,18 (Figura 7), aquest compost estaria desprotonat a pH 7,0, mentre que a pH 5,2 es trobaria en un 65% monoprotonat i un 30% diprotonat. Això voldria dir que, tal i com desitjàvem, aquest compost seria neutre a pH 7,0 i ionitzat a pH 5,2 i per tant caldria esperar que a aquest últim pH tingués menys afinitat per la GCase que a pH 7,0.

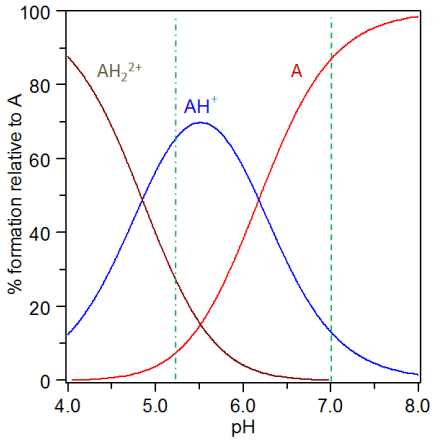

Figura 7 Diagrama de distribució d'espècies (marró = diprotonat, blau = monoprotonat, vermell = diprotonat) per a un compost diprotonable amb valors de pK_a 4,85 i 6,18. En verd, pH 5,2 (- · -) i pH 7,0 (- - -).

Tant el compost amb piridina terminal (**44**) com el derivat amb piperidina **43** van presentar major inhibició de la imiglucerasa a pH 7,0 que a pH 5,2. En canvi, tot i que esperaríem que el derivat **44** mostrés una major diferència d'activitat entre els 2 pH's de l'assaig (Δ) gràcies al seu pK_a, aquest compost va presentar un valor Δ menor que el derivat amb piperidina terminal (**43**), el qual esperaríem que presentés una inhibició de la GCase similar a ambdós pH's. Aquest resultat sembla suggerir que aquesta aproximació per obtenir compostos amb una major diferència d'afinitat per la GCase a pH 7,0 que a pH 5,2 no funciona tal i com inicialment esperàvem, probablement degut al fet que la afinitat dels compostos per un enzim està determinada per una combinació de factors i en la nostra aproximació estem tenint en compte

un factor preponderant que potser no està jugant el paper fonamental que nosaltres esperàvem.

Per altra banda, els compostos sintetitzats en aquest capítol van ser també analitzats com a inhibidors de la Glucosilceramida sintasa (GCS). Els percentatges d'inhibició de GCS dels compostos més potents es troben representats al següent gràfic.

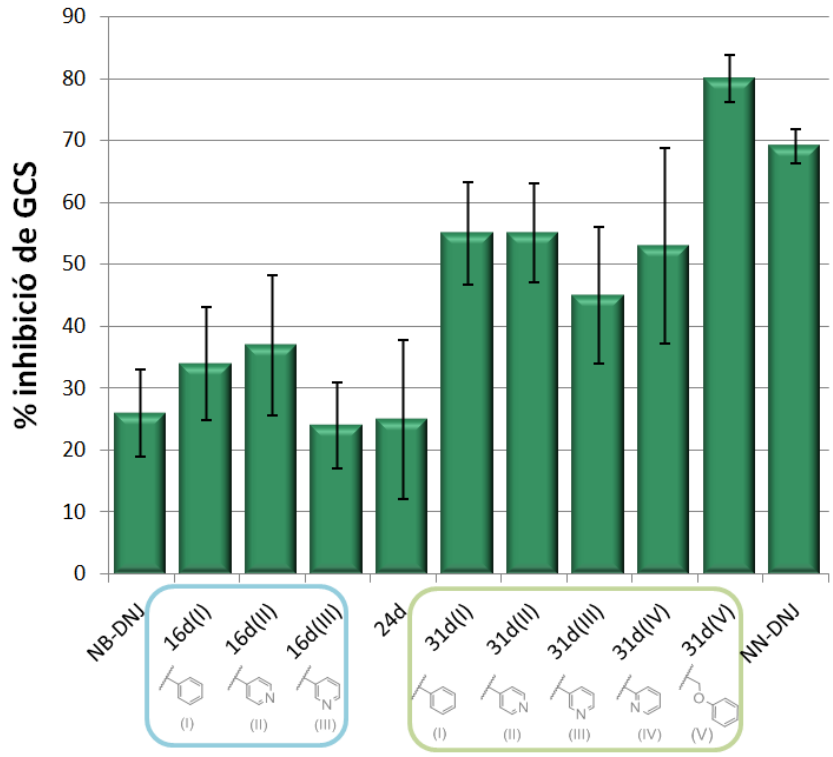

Gràfic 2 Capacitat inhibidora de GCS d'alguns compostos.

Cal remarcar que les famílies de compostos **16d(I-III)** i **31d(I-IV**) van resultar inhibidors de la GCS amb una potència similar o fins i tot superior a la NB-DNJ, un compost que s'administra actualment com a inhibidor de la GCS per al tractament de la malaltia de Gaucher. A més a més, tot i que els compostos amb una alcoxipiridina terminal (derivats **31d(VI**) i **31b(VI, VII)** no van presentar una inhibició de GCS significant a 100 µM, el seu homòleg **31d(V)**, amb un grup fenil en lloc de piridina, va resultar el millor inhibidor de GCS d'entre tots els compostos provats en aquest capítol, amb una IC_{50} de 2 µM.

Per altra banda, és important destacar que els compostos **16(I-III)** i **31d(I-V)** presenten valors de IC50 dins del mateix rang tant per GCS com per inhibició de imiglucerasa. Aquesta propietat resulta molt interessant ja que permetria l'ús d'aquests compostos com a compostos duals per

al tractament de la malaltia de Gaucher, inhibint la síntesi de GluCer alhora que podrien funcionar com a chaperones farmacològiques per la GCase.

Finalment, es va estudiar la capacitat d'inhibició d'altres glicodidases comercials per part dels compostos sintetitzats per tal d'estudiar la seva selectivitat. Tots els compostos amb interès com a inhibidors de imiglucerasa van presentar selectivitat per a aquest enzim en front β-glucosidasa d'ametlla, α-galactosidasa de grans de café verds i β-galactosidasa de fetge boví. A més a més, la majoria de compostos també van presentar bona selectivitat per la imiglucerasa en front la α-glucosidasa de *Saccharomyces cerevisiae*, excepte la família de compostos **31d**, la qual va presentar també certa afinitat per aquest enzim. Cap dels compostos estudiats en aquest apartat va presentar una toxicitat elevada a 200 μM, i els compostos d'interès com a inhibidors de imiglucerasa o GCS van presentar uns bons rangs de seguretat.

6.3.2 Estudi de la influència del pK_a del nucli central de l'inhibidor

Les glicosidases solen presentar dos àcids carboxílics en el centre actiu i generalment només realitzen la seva funció hidrolasa quan un d'ells està protonat en la forma àcida neutra i l'altre està desprotonat en la forma aniònica de carboxilat. En el cas de la GCase, el residu Glu340 actua com a nucleòfil i s'espera que estigui inicialment en forma de carboxilat, mentre que el Glu235 es trobaria inicialment protonat i actuaria com a àcid en la reacció enzimàtica. La necessitat d'un estat de protonació específic d'aquests residus glutamats implica una dependència del pH per a l'activitat de l'enzim. Per altra banda, la posició del nitrogen en els derivats de DNJ mimetitza l'oxigen endocíclic de la glucosa de la GluCer[143]. Per aquest motiu, s'esperaria que canvis en l'estat de protonació d'aquest nitrogen situat en el nucli de DNJ puguin modificar la interacció d'aquests inhibidors amb la GCase.

Per tal de modular i estudiar la influència del pK_a de l'amina del nucli central de l'inhibidor, es va decidir sintetitzar derivats de DNJ i *myo*-inositol amb i sense hidroxil o fluor en la posició β de la cadena lateral. Amb el mateix propòsit, també es va decidir sintetitzar derivats de *N*-butil i *N*-nonil amb un nucli similar al *myo*-inositol, però amb el grup hidroxil en la posició 2 de l'anell substituït per un àtom de fluor.

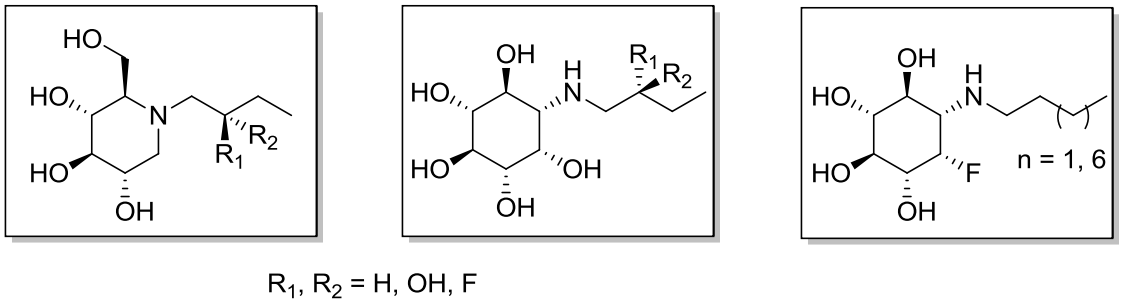

Figura 8 Representació dels compostos objectiu per a l'estudi de la influencia del pK_a de l'amina del nucli central de l'inhibidor.

La obtenció dels derivats d'inositol es va iniciar amb la síntesi del tetraacetat **(±)-49** a partir de la *p*-benzoquinona, seguin procediments prèviament descrits a la literatura[150]. Un cop obtingut el tetraester racèmic, es va fer una resolució enzimàtica[149] amb Lipozyme®, per tal de poder continuar la síntesi amb el tetraacetat **(+)-49** enantiomèricament pur.

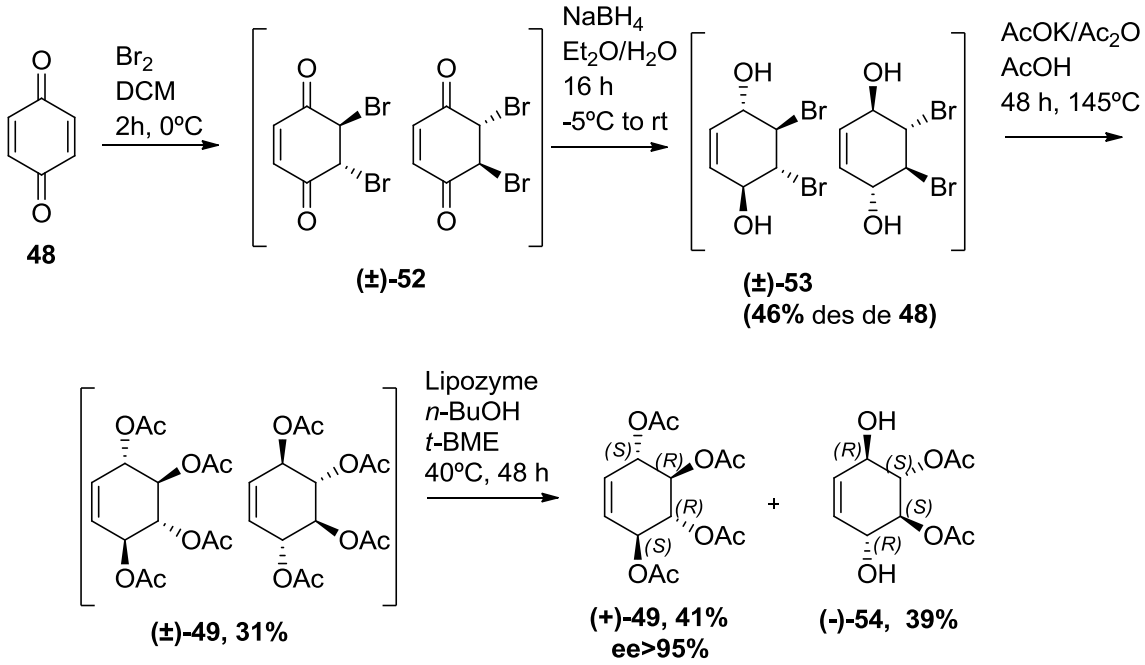

Esquema 7 Síntesi del tetraacetat racèmic **(±)-49** i posterior resolució enzimàtica.

Seguidament, es va procedir a la síntesi del derivat azidoalcohol **58**, seguint procediments prèviament descrits a la literatura[147] (Esquema 8). A continuació, es va formar el mesilat del grup hidroxil lliure d'aquesta ciclitolazida, per tal de procedir a la inversió d'aquest grup hidroxil, tractant el compost **60** amb una barreja de DMF/H_2O a 140ºC, tal i com estava

descrita a la literatura[147]. Desgraciadament, aquesta reacció no va tenir lloc en aquestes condicions ni tampoc utilitzant radiació de microones. Finalment, la síntesi del compost **63** va ser assolida mitjançant la formació del derivat acetat **62** i posterior reducció simultània del grup azida i de l'ester. A partir del derivat benzilat **63** es sintetitzaran altres derivats N-substituits, però també es va considerar interesant analitzar els derivats sense substitució en el nitrogen de cadascuna de les famílies estudiades per tal d'avaluar possibles efectes intrínsecs del anell inositol que no fossin específics de l'efecte de la cadena lateral. Per aquest motiu el es va procedir a desbenzilar el compost **63**, obtenint el derivat desprotegit **64**.

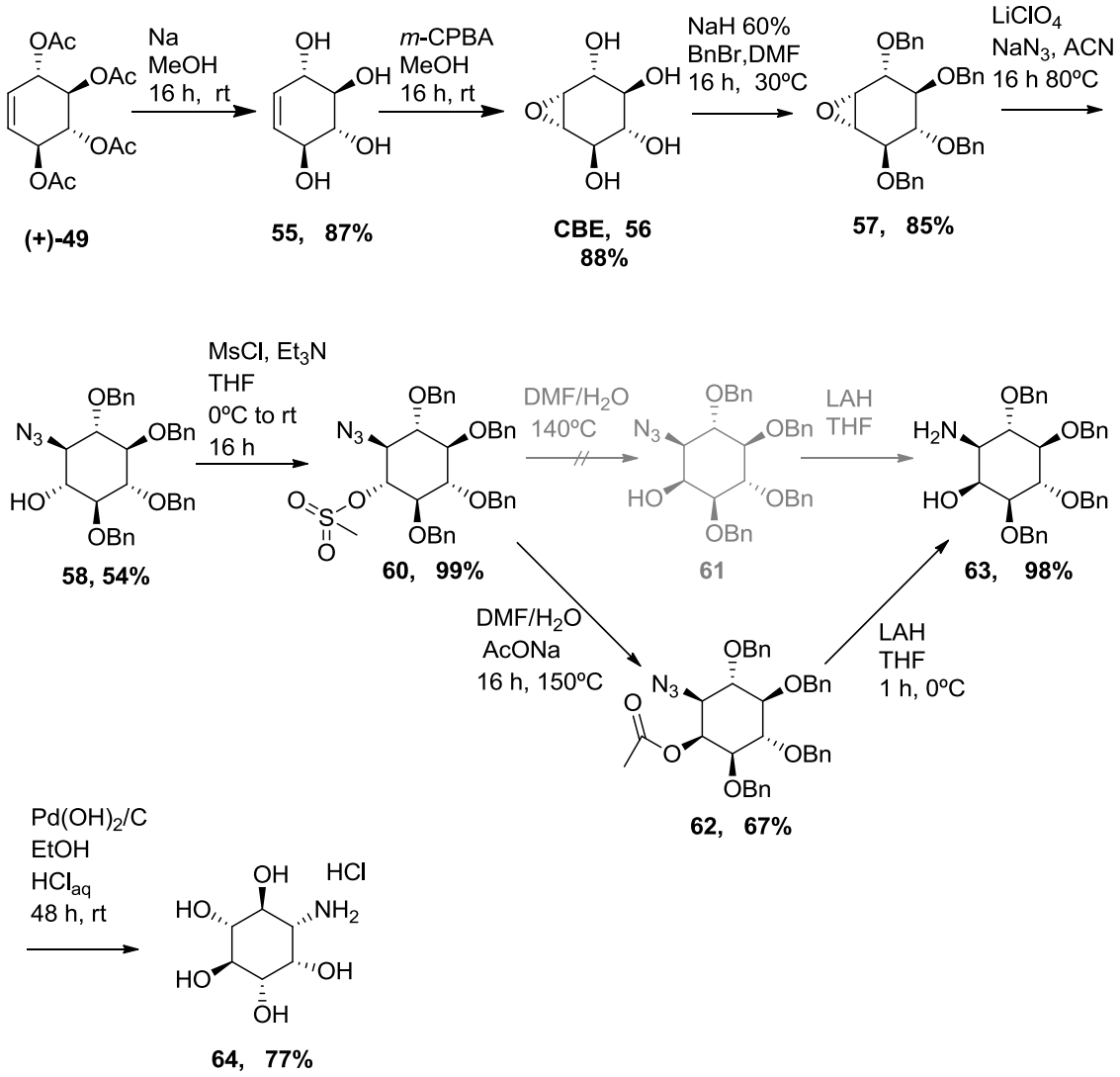

Esquema 8 Síntesi dels compostos **63** i **64**.

Per altra banda, es va procedir a la síntesi dels derivats de *myo*-inositol amb el fluor substituït en la posició 2 de l'anell, partint del derivat **58** descrit anteriorment, tal i com es detalla a l'Esquema 9. En primer lloc, es va introduir el fluor per activació del grup hidroxil en forma de triflat i substitució del mateix utilitzant TBAF. Un cop obtingut el derivat **66**, una part d'aquest compost es va hidrogenar per obtenir el derivat amina desbenzilat **69**. Paral·lelament es va procedir a la síntesi dels compostos **67x**, **67y**, **68x** i **68y** mitjançant reducció de la azida del compost **66**, seguida d'una aminació reductiva amb el corresponent aldehid i posterior desbenzilació en medi àcid.

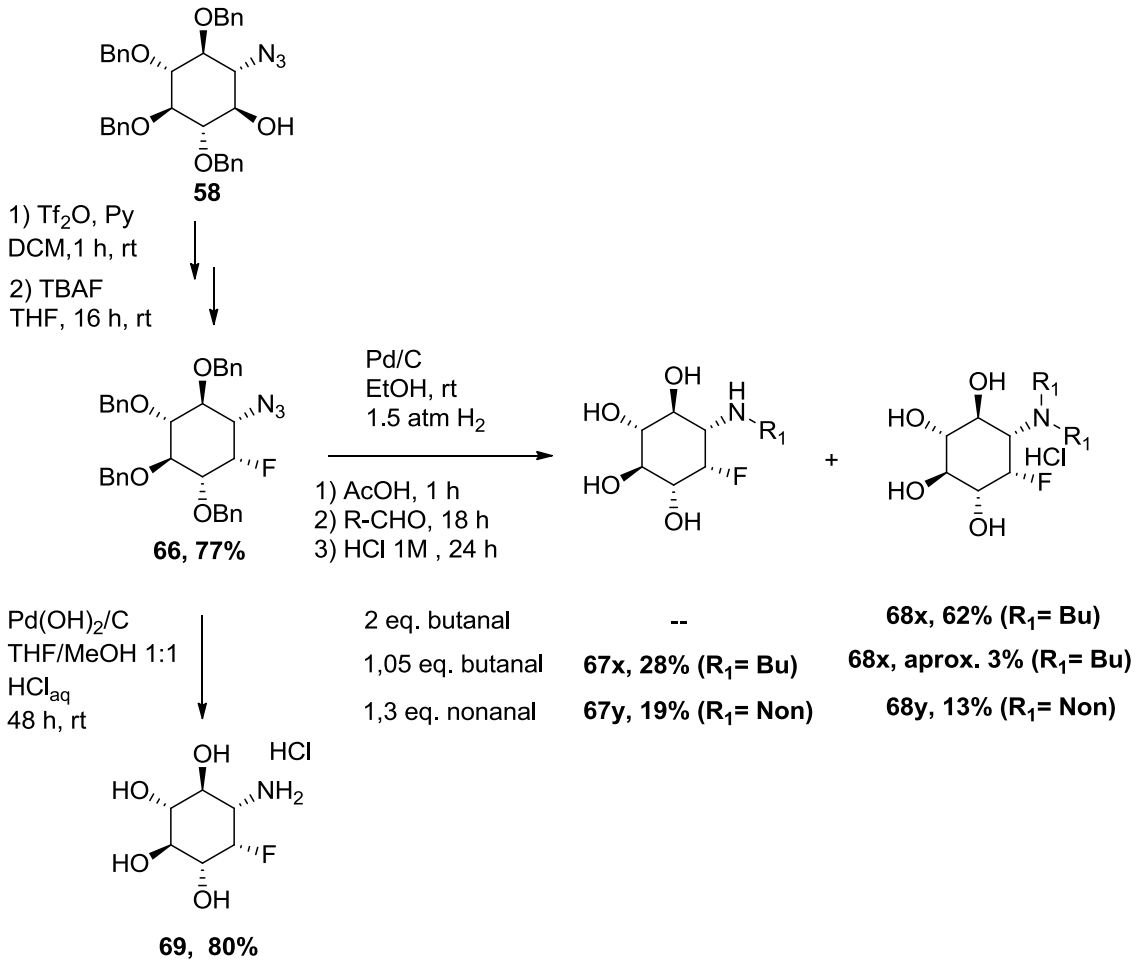

Esquema 9 Síntesi dels compostos **67x**, **68x**, **67y**, **68y** i **69**.

Per a la síntesi dels derivats *N*-butil inositol sense β-substitució o bé difluorats en aquesta posició, es va optar per fer la acilació de **63** amb el corresponent àcid seguit de la reducció de l'amida a amina amb borà i posterior desbenzilació per hidrogenació catalitzada amb $Pd(OH)_2/C$ en medi àcid (Esquema 10).

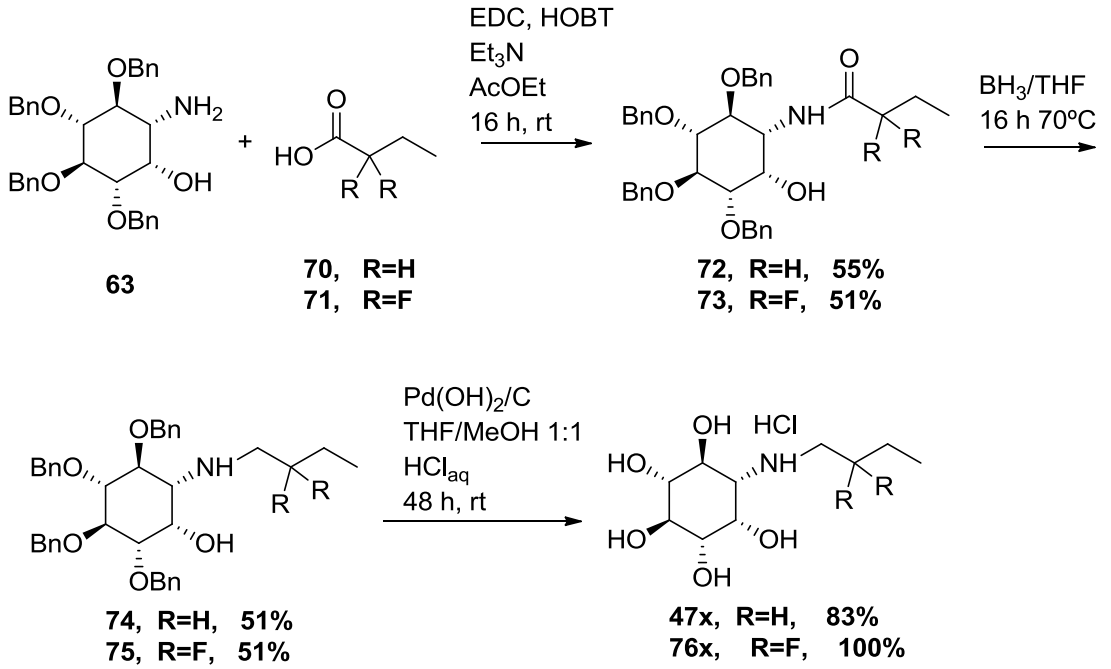

Esquema 10 Obtenció dels compostos **47x** i **76x**.

En canvi, aquesta estratègia no va funcionar per a sintetitzar el derivat de DNJ difluorat **82x** ja que l'acilació no va tenir lloc ni activant l'àcid amb EDC i HOBT, ni via el clorur d'àcid. Així doncs, la síntesi del derivat es va assolir mitjançant alquilació de **13** amb la bromocetona **79** i posterior fluoració de la cetona amb Deoxofluor®, per acabar amb la hidrogenació en medi àcid per desbenzilar el derivat **81** (Esquema 11).

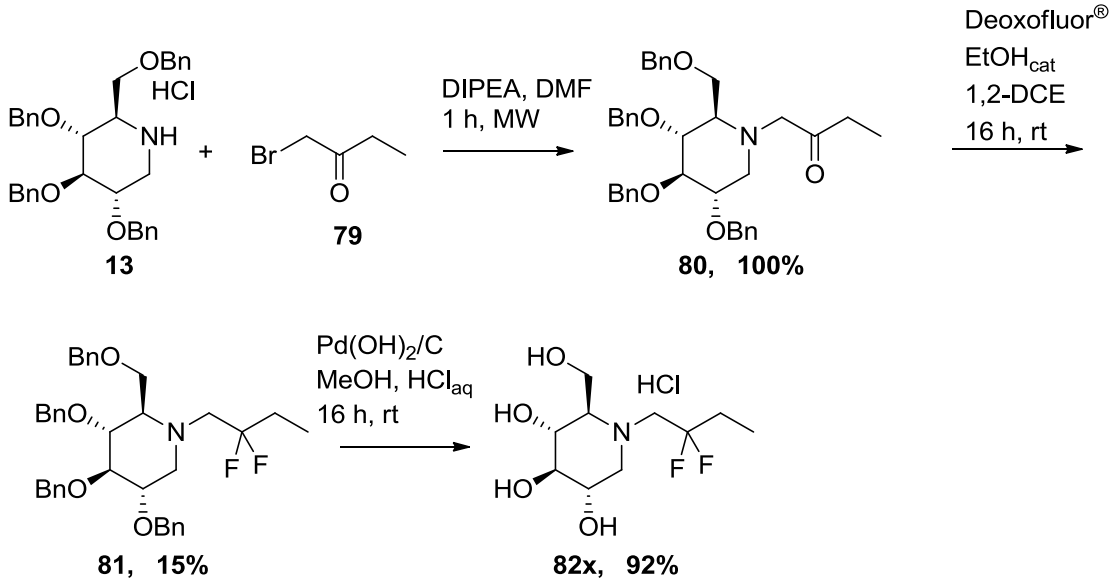

Esquema 11 Esquema sintètic per a l'obtenció del compost **82x**.

Pel que fa a la síntesi dels derivats amb un grup hidroxil o un fluor en la posició β de la cadena lateral, es va plantejar de manera equivalent en els derivats de DNJ que ens els de inositol.

Tal i com es pot veure a l'Esquema 12, els derivats de DNJ amb un hidroxil a la cadena es van sintetitzar tant per reducció del grup cetona del compost **80**, obtenint-se una mescla de diastereòmers que es van poder separar per cromatografia *flash*, com per apertura del corresponent epòxid amb el derivat amina **13**. Un cop es van obtenir els derivats 84, es va procedir a la seva desbenzilació per hidrogenació en les condicions anteriorment descrites.

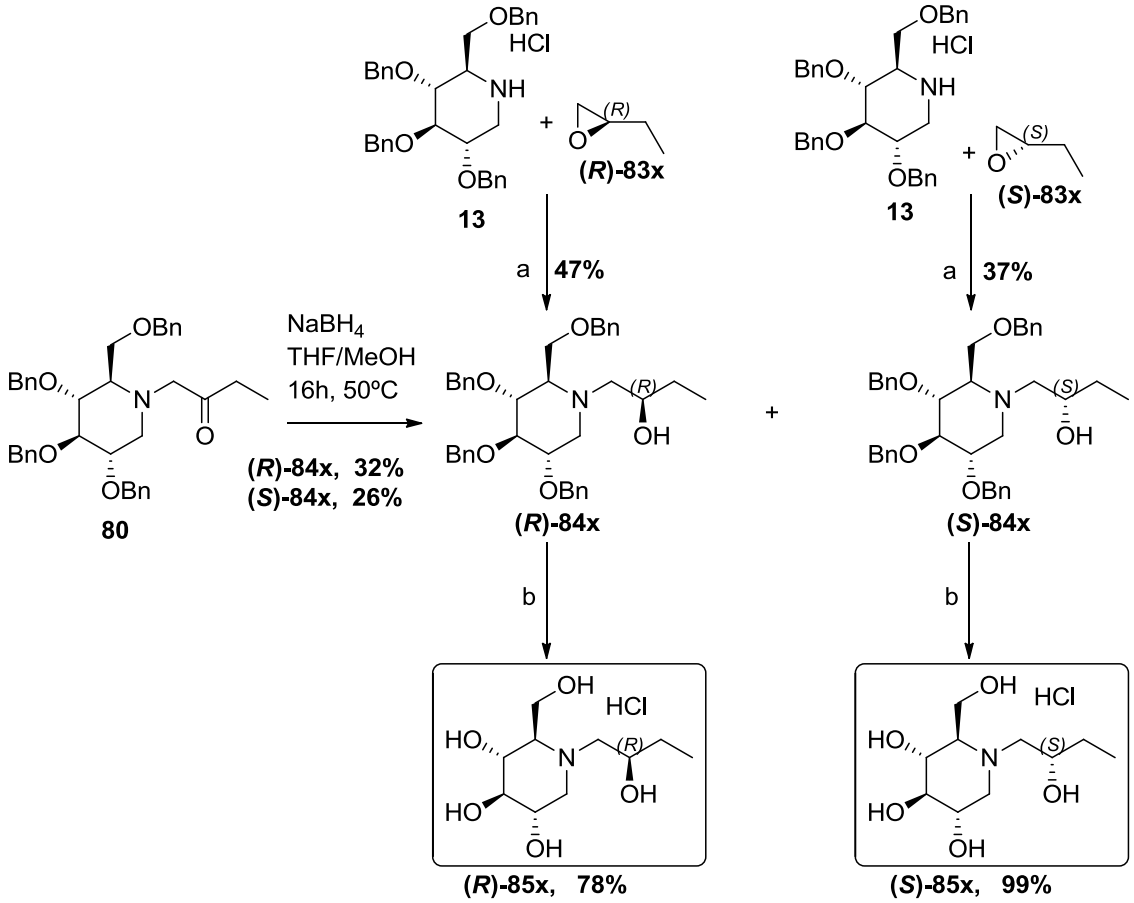

Esquema 12 Síntesi dels compostos **(*R*)-85x** i **(*S*)-85x**.

Els derivats de *myo*-inositol **(*R*)-85y** i **(*S*)-85y** es van sintetitzar similarment per apertura dels epòxids, partint de l'amino alcohol benzilat **63**.

Els derivats de DNJ β-fluorosubstituits, es van obtenir per substitució del grup hidroxil lliure dels derivats 84x utilitzant Deoxofluor® com a agent fluorant, i posterior desbenzilació per hidrogenació catalitzada en medi àcid (Esquema 13). En canvi, la síntesi dels derivats de

inositol β-fluorosubstituits no va ser possible en aquestes condicions, degut a la presència del hidroxil lliure en el propi nucli d'inositol.

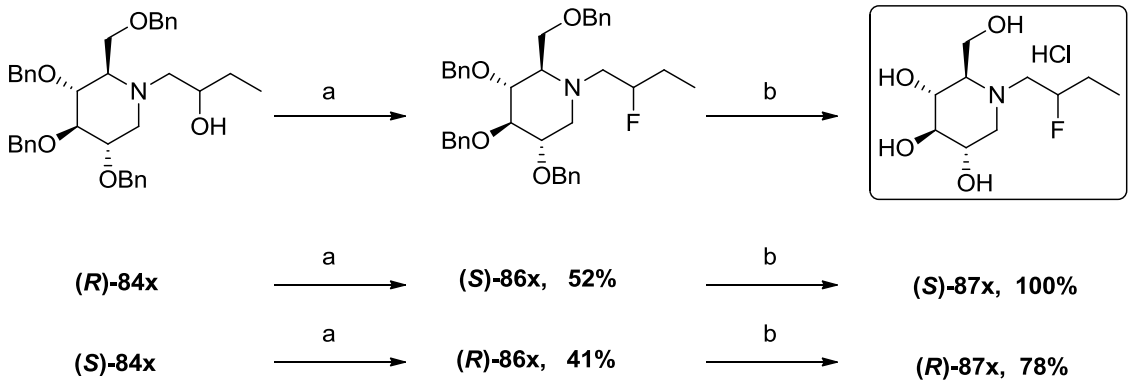

(*R*)-84x —a→ **(*S*)-86x, 52%** —b→ **(*S*)-87x, 100%**

(*S*)-84x —a→ **(*R*)-86x, 41%** —b→ **(*R*)-87x, 78%**

Esquema 13 Síntesi dels compostos **86x** i **87x**.[a] Deoxofluor®, DCM, 16 h, rt. [b] $Pd(OH)_2$/C, THF/MeOH 1:1, HCl_{aq}, 16 h, rt.

Després d'avaluar com a inhibidors de la imiglucerasa els compostos sintetitzats, es va decidir sintetitzar també els corresponents derivats *N*-nonil β-substituits per tal d'intentar obtenir compostos amb major potència inhibitòria. Aquests derivats van ser sintetitzats de manera anàloga als derivats *N*-butil, partint dels corresponents 2-heptiloxirans.

Els valors de IC_{50} en front de la imiglucerasa d'aquests compostos, així com els seus pK_as experimentals es troben detallats a la Taula 4. La majoria dels compostos estudiats en aquest capítol van mostrar major afinitat per imiglucerasa a pH 7,0 que a 5.2 en l'assaig amb detergents, tal i com desitjàvem. Un punt que mereix especial atenció és l'increment de potència inhibitòria dels derivats de DNJ quan s'introdueix un grup hidroxil amb configuració *R* en la posició β de la cadena lateral. Aquest augment d'afinitat per l'enzim es va observar tant en els derivats butil com nonil de la DNJ, però no en el cas dels derivats inositol. Cal remarcar que el compost **(*R*)-85y** és el derivat de DNJ més potent descrit fins el moment.

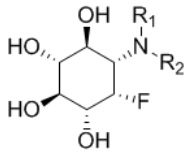

69: R_1=R_2=H
67x: R_1=H, R_2= Bu
67y: R_1=H, R_2=Non
68x: R_1=R_2=Bu
68y: R_1=R_2=Non

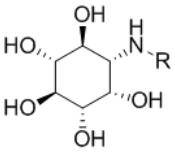

64: R=H
47x: R=Bu
47y: R=Non
89x: R=Bu-OH
89y: R=Non-OH
76x: R=Bu-F_2

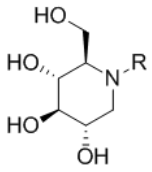

27: R=H
NB-DNJ R=Bu
NN-DNJ R=Non
85x: R=Bu-OH
85y: R=Non-OH
87x: R=Bu-F
87y: R=Non-F
82x: R=Bu-F_2

compost	pK_a	pH 5,2 IC_{50} (μM)	pH 7,0 IC_{50} (μM)	Δ
69	7,15 ± 0,06	326	225	1,4
67x	7,5[a]	70	12	5,8
67y	7,47 ± 0,19	0,24	0,024	10,0
68x	n.d.	4,6	7,6	0,6
68y	n.d.	0,93	0,25	3,7
64	7,93 ± 0,08	120	89	1,3
47x	8,67 ± 0,03	34	5,5	6,3
47y	8,95 ± 0,04	0,06	0,008	7,5
(*R*)-89x	7,2[a]	29	7,0	4,1
(*S*)-89x	7,19 ± 0,18	78	43	1,8
(*R*)-89y	7,22[b]	0,11[b]	0,017[b]	6,5
(*S*)-89y	7,17[b]	2,12[b]	0,244[b]	8,8
76x	5,50 ± 0,04	315	134	2,3
27	6,51 ± 0,09	425	136	3,1
NB-DNJ	6,84 ± 0,09	429	145	3,0
NN-DNJ	6,84 ± 0,08	1,03	0,25	4,1
(*R*)-85x	5,94 ± 0,38	38	27	1,4
(*S*)-85x	5,95 ± 0,40	>400	296	-
(*R*)-85y	5,98 ± 0,11	0,078	0,045	1,7
(*S*)-85y	5,94 ± 0,04	2,10	1,23	1,5
(*R*)-87x	5,39 ± 0,21	33	13	2,5
(*S*)-87x	5,21 ± 0,25	>400	>400	-
(*R*)-87y	5,2[a]	5,90	6,7[b]	0,9
(*S*)-87y	5,16 ± 0,10	2,94	4,94	0,6
82x	3,93 ± 0,17	>400	170	-

Taula 4 Inhibició de imiglucerasa i valors de pK_a experimental per a diversos compostos sintetitzats en aquesta secció. [a] valor predit. [b] única determinació.

És interesant remarcar que els compostos amb la mateixa substitució en la posició β tenen valors de pK_a similars, independentment de la configuració de l'enllaç (*R* o *S*) i la llargada de la cadena (butil o nonil).

Tal i com es pot observar a la Figura 9, la introducció d'un grup hidroxil en la posició β de la cadena en els derivats de DNJ redueix en 0.9 unitats el valor de pK_a tant per a derivats N-butil com N-nonil. En el cas que la unitat introduïda és un àtom de fluor, el valor de pK_a es va reduir en 1.6 unitats. La introducció d'un segon àtom de fluor va mostrar un efecte una mica menor que dos cops l'efecte de l'adició d'un fluor.

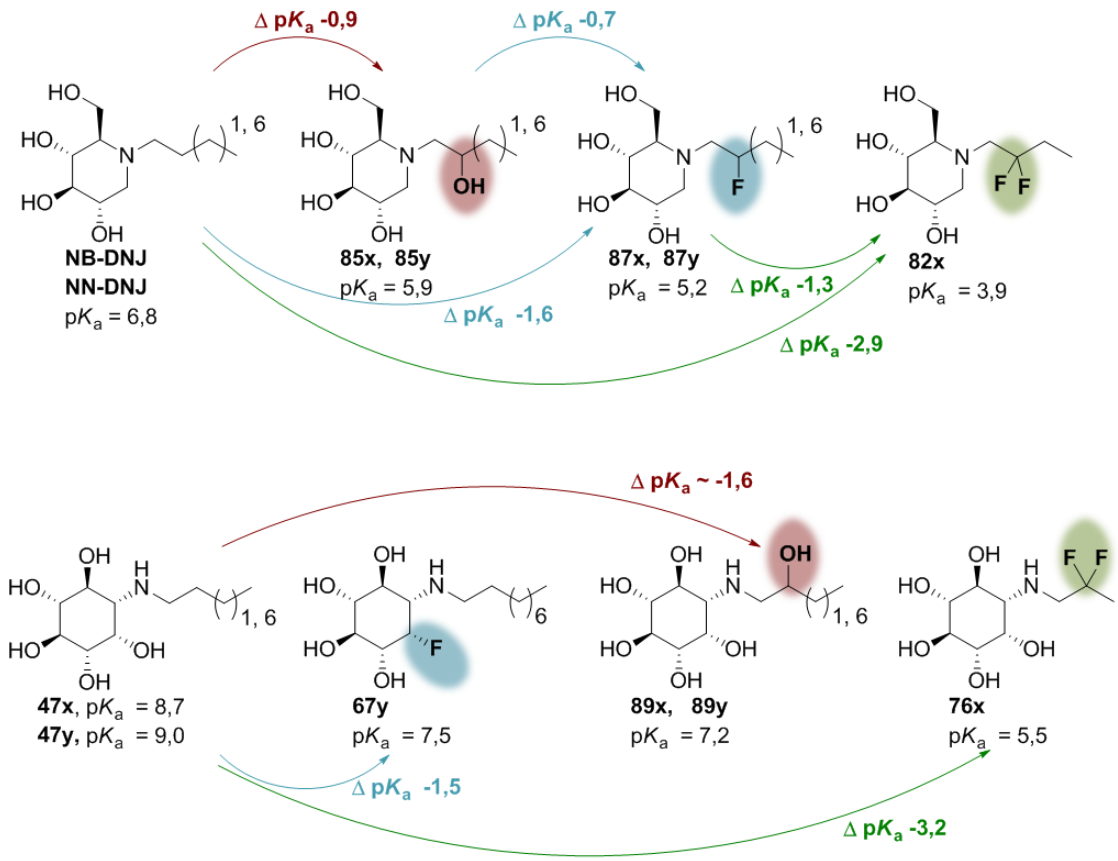

Figura 9 Influència dels β-substituents en el pK_a de l'amina en diferents famílies.

Pel que fa als derivats de inositol, la introducció d'un grup hidroxil en la posició β de la cadena, va fer decréixer en 1.6 unitats el pK_a , respecte el compost sense la β-substitució. En canvi, la introducció de dos àtoms de fluor va suposar una disminució de 3.2 unitats de pK_a. La substitució del grup hidroxil en la posició C-2 de l'anell per un àtom de fluor (compost **67y**), va mostrar un efecte en el pK_a similar a la introducció d'un grup hidroxil en la cadena lateral en els derivats inositol (compostos **(*R*)-89y** i **(*S*)-89y**). D'aquesta manera s'obtingueren tant compostos amb estructures similars i diferents valors de pK_a, com compostos amb nuclis diferents i valors de pK_a semblants.

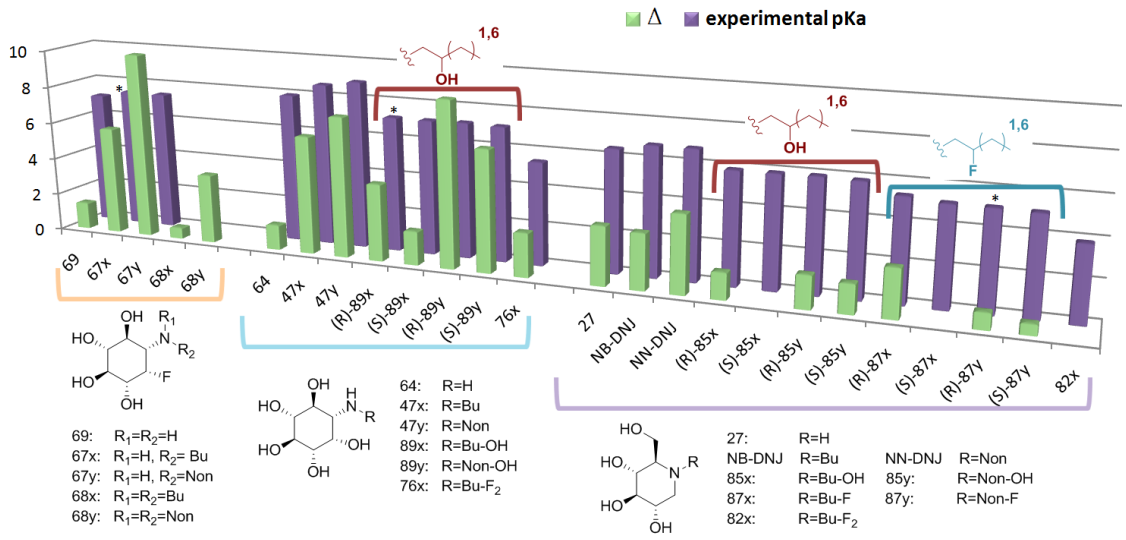

Gràfic 3 Comparativa dels valors Δ i els pK_as experimentals de diferents compostos. (Δ= IC_{50} (pH 5,2, µM) / IC_{50} (pH 7,0, µM)).(* valors extrapolats.)

Malgrat no va ser possible establir una correlació directa entre els valors de pK_a i els coeficients Δ (Gràfic 3), si que es pot intuir una certa tendència ja que els compostos amb major valor de Δ (compostos **(*R*)-89y**, **(*S*)-89y**, **67y**, **47y** i **47x**) tenen uns valors de pK_a entre 7.2 i 8.9. La major diferència de capacitat inhibitòria d'imiglucerasa en funció del pH de l'assaig es va observa amb el compost **67y**, presentant una IC_{50} 10 cops menor quan l'assaig es va realitzar a pH 7,0 que quan es va fer a pH 5,2.

També es va estudiar la capacitat inhibitòria de GCS d'aquests compostos. Només el compost **(*R*)-85y**, amb un 33% d'inhibició a 10 µM, va presentar major inhibició de GCS que NB-DNJ (26% inhibició a aquesta concentració). Tot i presentar una capacitat inhibitòria d'aquest enzim similar als derivats de DNJ amida i azida (**31d(I-III)** i **24d**), en aquest cas no parlaríem d'un compost dual inhibidor de GCS i chaperona farmacològica per GCase degut a la seva elevada afinitat per l'enzim imiglucerasa (valors d'IC_{50} de 0.078 µM a pH 5,2 i 0.045 µM a pH 7,0).

En general, tots els compostos d'interès com a inhibidors de imiglucerasa d'aquest apartat van presentar rangs de selectivitat acceptables en front d'altres glicosidases comercials. La excepció van ser els derivats **(*R*)-85x** i **(*S*)-85y**, que no van resultar selectius en front de la β-glucosidasa d'ametlla. Igualment, tots els compostos excepte el derivat dinonil inositol **68y**, van presentar bons marges de seguretat després d'analitzar la seva possible toxicitat amb l'assaig de MTT.

6.3.3 Assajos sense detergents

6.3.3.1 Assajos en homogenats cel·lulars

Donat que alguns estudis suggerien que l'ús de detergents en l'assaig per determinar la inhibició de GCase podien estar modificant l'afinitat dels diferents inhibidors per aquest enzim a diferents pHs, es va decidir provar la capacitat d'inhibició de GCase d'alguns compostos en un assaig sense detergents. Així doncs, es va estudiar la inhibició de GBA1 en homogenats cel·lulars de HAP1 (GBA2-KO), seguint els procediments descrits per Körchen *et al*[24].

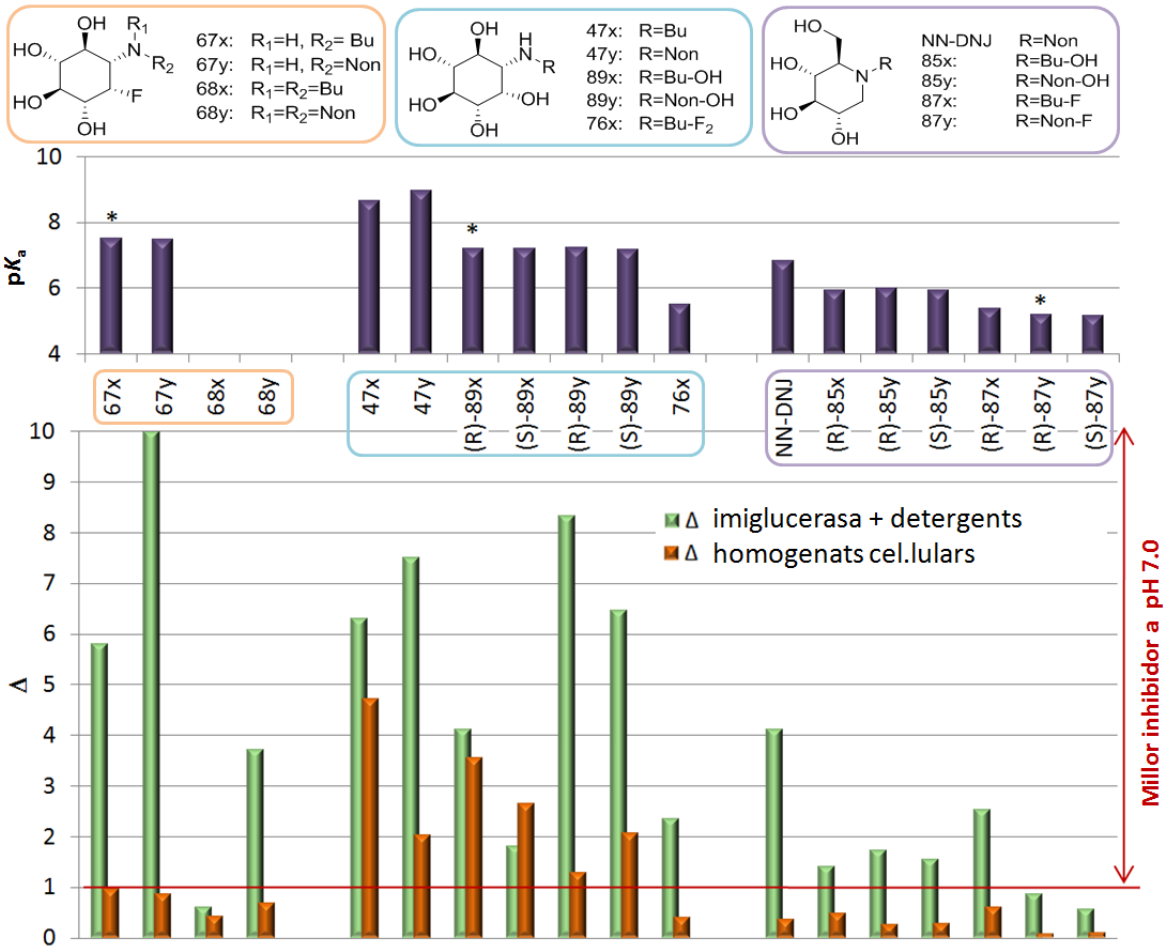

Gràfic 4 Comparativa dels coeficients Δ obtinguts amb els diferents assaigs, i representació gràfica dels valors de pK_a per a cada compost. Valors de Δ menors que 1, representa compostos amb millor inhibició de imiglucerasa a pH 5,2 que a pH 7,0. (Δ= IC_{50} (pH 5.2, µM) / IC_{50} (pH 7.0, µM); * valors de pK_a extrapolats).

Tal i com es por observar al Gràfic 4, els resultats de les diferències d'activitat segons el pH de l'assaig (Δ) obtinguts en l'assaig amb homogenats cel·lulars sense detergents condueixen a conclusions completament diferents. Així doncs, mentre amb l'assaig d'inhibició

d'imiglucerasa, amb presència de detergents, la majoria de compostos eren millor inhibidors a pH 7,0 que a pH 5,2, en l'assaig amb homogenats cel·lulars sense detergents els únics compostos que presentaven major inhibició a pH 7,0 que a pH 5,2 eren derivats d'inositol.

Així doncs, el compost **67y**, que tenia la major diferència d'activitat segons el pH de l'assaig en l'estudi d'inhibició d'imiglucerasa amb detergents, en l'assaig amb homogenats cel·lulars sense detergents gairebé no s'observa diferència d'activitat segons el pH de l'assaig. En el cas de l'assaig sense detergents, els compostos que van presentar uns valors del coeficient Δ majors van ser el *N*-butil (**47x**) i els *N*-hidroxibutil (**(*R*)-89x** i **(*S*)-89x**) derivats d'inositol.

Per altra banda, es va decidir estudiar també la capacitat d'inhibició de GBA2 dels compostos sintetitzats, mitjançant un assaig amb homogenats cel·lulars de CHO (GBA2 sobre expressat). Els derivats de DNJ van resultar una família d'inhibidors molt potents, d'ordre nanomolar (Figura 10).

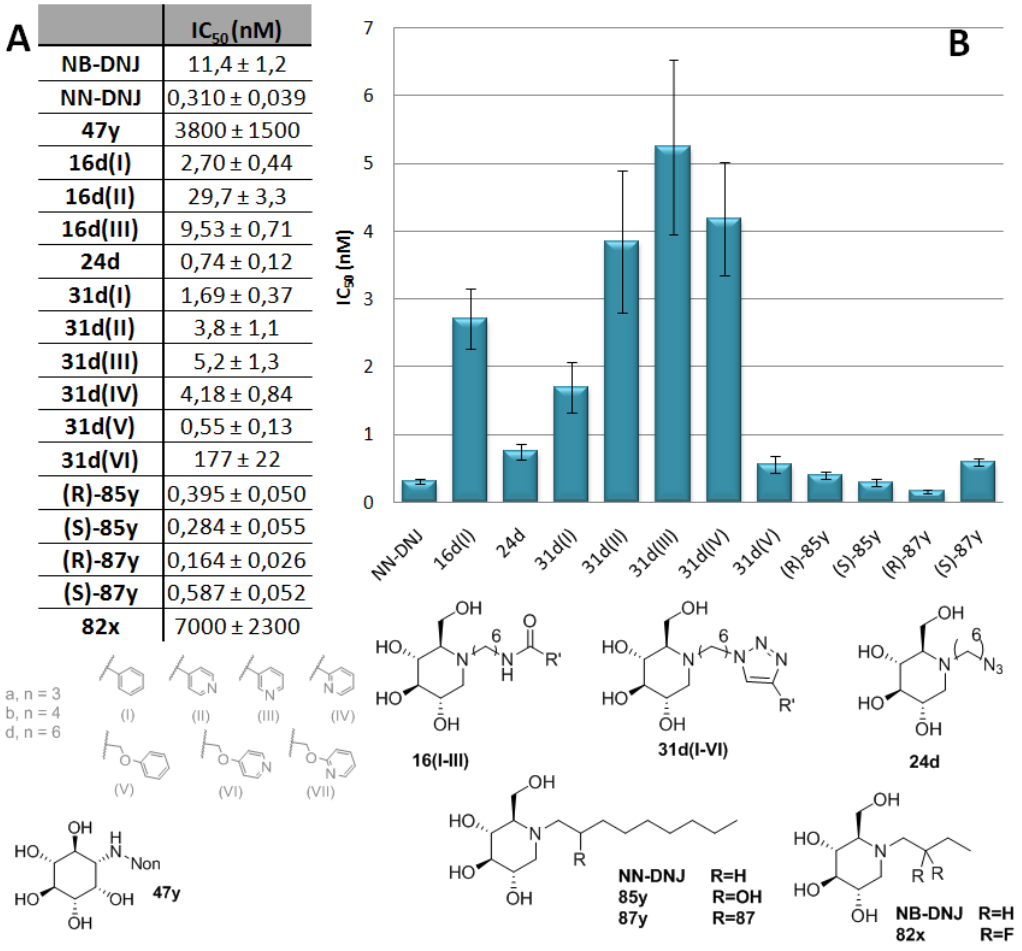

Figura 10 Inhibició de GBA2 en homogenats cel·lulars de CHO amb GBA2 sobre expressat. **(A)** valors de IC_{50}. **(B)** representació gràfica dels valors de IC_{50} dels compostos més potents.

6.3.3.2 Assajos en cèl·lula intacta

Després d'estudiar diferents condicions d'assaig, es va desenvolupar un nou assaig en cèl·lula intacta que permet l'estudi de la inhibició de GBA1 o GBA2 sense lisar les cèl·lules. Això suposa una avantatge respecte els assajos que es solien fer fins ara, on després de la incubació de les cèl·lules amb els inhibidors, s'acabaven lisant les cèl·lules per a determinar l'activitat GCase. A més a més, els estudis realitzats amb cèl·lula intacta han demostrat que un cop el substrat 4-MUG és hidrolitzat, la 4-metilumbeliferona és excretada de la cèl·lula i s'acumula en el medi de cultiu i no en l'interior cel·lular. Tot això obre la possibilitat de determinar la activitat GCase en un placa diferent d'on estan les cèl·lules, i per tant mantenir les cèl·lules en un ambient més controlat durant tot l'assaig, i ha permès l'estudi de la recuperació de l'activitat GCase després d'eliminar l'inhibidor del medi de cultiu.

Un cop posat a punt l'assaig, es va estudiar la inhibició de GBA2 en cèl·lula intacta per part d'alguns compostos representatius, mostrant la inhibició de l'activitat d'aquest enzim quan les cèl·lules van ser cultivades durant 26 h en un medi de cultiu que contenia concentracions d'inhibidor de 10 µM (Gràfic 5).

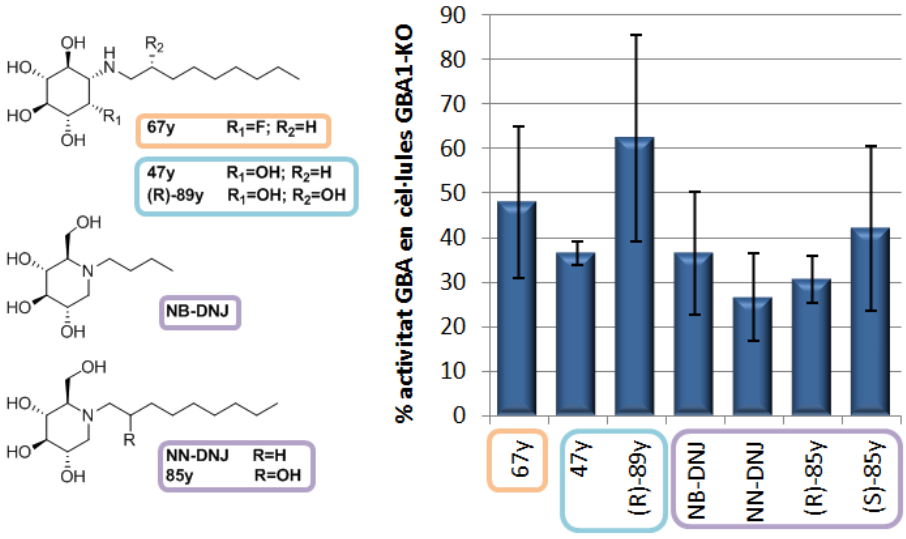

Gràfic 5 Activitat GCase en cèl·lules GBA1-KO.

Per altra banda, també es va estudiar la capacitat d'inhibició de GBA1 d'alguns compostos, juntament amb la capacitat de recuperació de l'activitat GCase després de retirar l'inhibidor present en el medi (Gràfic 6). En aquest assaig es va observar que els compostos estudiats

presentaven bons percentatges d'inhibició de GBA1 en cèl·lules cultivades amb concentracions d'inhibidor de 1 o 10 µM. En la majoria de casos, incloses les cèl·lules tractades amb CBE, es va observar una alta recuperació de l'activitat GBA 1,5 dies després de retirar l'inhibidor del medi. En canvi, les cèl·lules tractades amb *N*-nonil inositol (**47y**) van presentar una lenta recuperació de l'activitat GCase després de retirar aquest compost del medi, suggerint una certa retenció intracel·lular d'aquest compost.

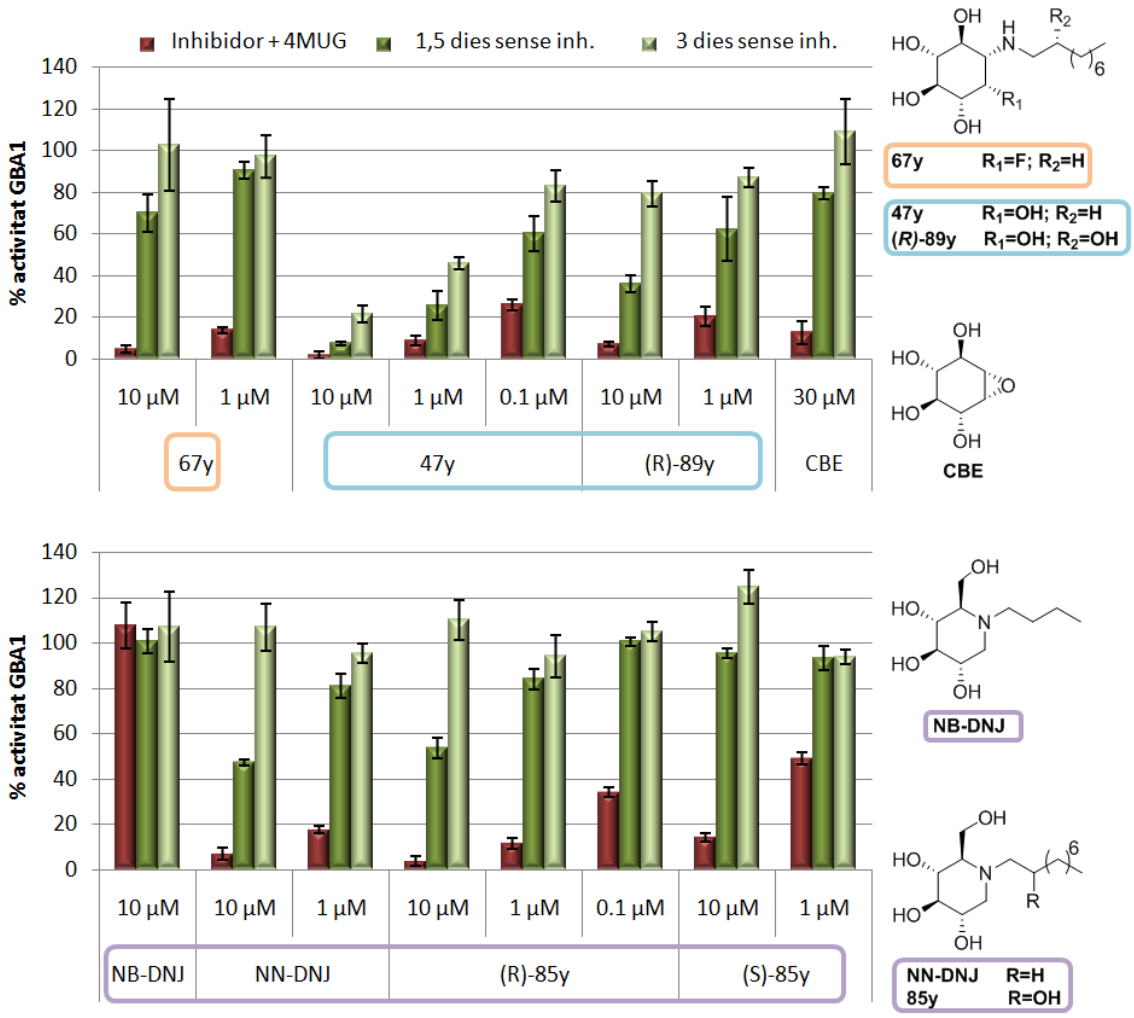

Gràfic 6 Activitat GCase en cèl·lules GBA2-KO cultivades en medi amb presencia d'inhibidors.

6.4 Conclusions

- S'ha sintetitzat una petita biblioteca de derivats de DNJ amb i sense substituents protonables al final de la cadena, per tal d'avaluar la influència del pK_a d'aquests grups terminals en l'afinitat en front imiglucerasa.

- Els compostos **16d(I-III), 24d, 31d(I-V)** i 43 han resultar ser millor inhibidors d'imiglucerasa que NB-DNJ, tot I que no són tant potents com NN-DNJ.

- Els triazols i derivats de tipus azida **31d(I-IV)** i **24d** han resultat millors inhibidors de imiglucerasa que els seus respectius homòlegs amb amida o amina (compostos **16(I-III)** i **25d**).

- El pK_a dels compostos **31b(VI)** i **31b(VII)** i altres homòlegs triazole o amida sense el nucli de DNJ (compostos **34(II-IV)** i **35(II-IV, VI-VII**) van ser experimentalment determinats, obtenint-se un rang de pK_a de les piridines terminals entre 2,6 i 4,9. Els derivats amb una piridina no van presentar valors Δ majors que els seus homòlegs sense aquest grup terminal.

- El derivat **44** va presentar uns valor de pK_a de 4,85 i 6,18. Tot i que s'esperaria que un compost diprotonable amb aquests pK_as romangués neutre a pH 7,0 i ionitzat a pH 5,2, aquest compost no va mostrar una diferència en l'afinitat respecte la imiglucerasa segons el pH de l'assaig major que el derivat **43**, amb una piperidina en lloc de la piridina terminal.

- Els compostos sintetitzats van ser avaluats com a potencials inhibidors de GCS. Les famílies de compostos **16d(I-III)**, **24d** i **31d(I-V)** van presentar una potència inhibitòria de GCS major que NB-DNJ, un compost que actualment s'administra com a inhibidor de GCS per al tractament de la malaltia de Gaucher.

- S'ha descobert una família de compostos amb possible interacció dual inhibidora de GCS i com a chaperona farmacològica per a GCase, amb bona selectivitat en front altres glicosidases comercials i baixa toxicitat.

- S'ha sintetitzat una llibreria de compostos per a l'estudi de la influència en la capacitat inhibitòria de GCase dels diferents nuclis centrals dels inhibidors i, especialment, el pK_a de les amines contingudes en aquests esquelets, modulat per la introducció de diferents substituents en la posició β respecte l'amina.

- Després d'estudiar la capacitat d'inhibició d'imiglucerasa dels assajos sintetitzats, el derivat hidroxinonil **(*R*)-85y** s'ha mostrat com l'inhibidor de imiglucerase de la família de la DNJ més potent descrit fins el moment.

- S'ha observat un increment de potència inhibitòria de imiglucerasa quan un grup hidroxil amb configuració *R* s'introdueix en la posició β de la cadena lateral dels derivats de DNJ **(*R*)-85x** i **(*R*)-85y**, però no en el cas dels derivats d'inositol **(*R*)-89x** o **(*R*)-89y**.

- La majoria dels compostos analitzats en l'assaig d'inhibició d'imiglucerasa en presència de detergents van presentar major afinitat per aquest enzim a pH 7,0 que a pH 5,2.

- S'ha determinat experimentalment el pK_a de la majoria de compostos amb β-substitució i s'ha estudiat la influència d'aquests substituents en el pK_a del nitrogen del nuclis centrals dels inhibidors. Els derivats amb la mateixa substitució van presentar valors de pK_a similars, independentment de la configuració de l'enllaç (*R* o *S*) i l'allargada de la cadena (butil o nonil).

- L'anàlisi dels valors de pK_a i del coeficient Δ no ha permès establir una correlació directa entre ambdós paràmetres. No obstant, es pot observar una certa tendència donat que els compostos amb major diferència d'activitat segons el pH de l'assaig van presentar valors de pK_a entre 7,2 i 8,9.

- El compost 67y va mostrar la major diferència de inhibició de imiglucerasa segons el pH de l'assaig d'entre tots els compostos estudiats, amb uns valors de IC_{50} 10 cops menor quan l'assaig d'inhibició d'aquest enzim en presència de detergents es va realitzar a pH 7,0 que quan es va fer a pH 5,2.

- S'ha estudiat la selectivitat en front GCS i altres glicosidases comercials dels compostos amb diferents β-substituents, així com la seva toxicitat. En general, els compostos que van

mostrar una inhibició de GCase acceptable van presentar també bona selectivitat en front d'aquests enzims i uns rangs de seguretat acceptables.

- S'ha posat de manifest la rellevància del les condicions d'assaig a l'hora d'analitzar la capacitat d'inhibició de GCase dels diferents compostos. En aquest sentit, hem demostrat que els valors de IC_{50} obtinguts a partir de l'assaig utilitzant un enzim recombinant amb detergents conduïen a unes conclusions diferents que quan l'assaig es va realitzar amb homogenats cel·lulars sense addició de taurocolat sòdic ni Triton X-100®.

- Alguns compostos representatius es van assajar com a inhibidors de GBA1 en un assaig sense detergents amb homogenats cel.lulars de HAP1 (GBA2-KO). En aquestes condicions d'assaig només alguns derivats d'inositol van resultar millor inhibidors a pH7,0 que a pH 5,2.

- Els derivats d'inositol *N*-butil (**47x**) i *N*-hidroxibutil (**(*R*)-89x** i **(*S*)-89x**) van presentar els valors de Δ més elevats d'entre tots els compostos estudiats en l'assaig sense detergents.

- Els derivats de DNJ *N*-nonil amb una substitució de hidroxil o fluor a la cadena **(85y** i **87y**) van presentar el mateix valor de Δ per als compostos amb l'enllaç amb configuració *R* que per als de configuració *S* (0,3 per als derivats hidroxil i 0,1 per als derivats amb fluor) a l'assaig amb homogenats cel·lulars, malgrat la seva diferència d'activitat. Tot i presentar valors de pK_a similars, els valors Δ dels derivats butil **(*R*)-85x** i **(*R*)-87x** no correlacionen amb els dels derivats nonil.

- No s'ha pogut establir cap interconnexió entre l'afinitat vers la GCase i la influència de les condicions de l'assaig, el pK_a del l'amina del nucli central, l'allargada de la cadena lateral o la configuració de la β-substitució.

- S'ha estudiat la capacitat d'inhibició de GBA2 dels compostos sintetitzats en homogenats cel·lulars, mostrant que els derivats de DNJ són una família d'inhibidors de GBA2 potents i selectius.

- S'ha desenvolupat un nou assaig per l'estudi de la inhibició de GBA en cèl·lula intacta, que permet l'estudi de l'activitat GBA1 o GBA2 directament a la placa de cultiu o transferint

els sobrenedants en una altra placa, sense necessitat de lisar les cèl·lules, en presència o després d'eliminar l'inhibidor. Aquest assaig permet l'estudi de l'efecte de l'inhibidor present en el medi i la posterior recuperació o no de l'activitat GCase de les cèl·lules un cop l'inhibidor és eliminat del medi.

- Les dades extretes del nou assaig en cèl·lula intacta suggereixen que 4-MUG penetra la cèl·lula però, un cop és hidrolitzat, el 4-MUG és excretat al medi i no s'acumula a l'interior cel·lular.

- S'ha estudiat la capacitat d'inhibició de GBA2 en cèl·lula intacta d'alguns compostos representatius, mostrant tots ells un bloqueig complet de l'activitat d'aquest enzim quan les cèl·lules van ser cultivades durant 26 h en presència d'una concentració de 10 μM d'aquests inhibidors.

- Tots els compostos provats com a inhibidors de GBA1 en l'assaig de cèl·lula intacta van mostrar bons percentatges d'inhibició d'aquest enzim tant en l'assaig realitzat a 10 μM com a 1 μM. La majoria d'ells, inclòs CBE, van mostrar una recuperació de l'activitat GBA moderada o alta 1,5 dies després d'eliminar l'inhibidor present en el medi de cultiu. Contràriament, les cèl·lules cultivades en presència del derivat d'inositol **47y** van mostrar una recuperació baixa de l'activitat GCase, suggerint una retenció intracel·lular d'aquest compost elevada.

BIBLIOGRAPHIC REFERENCES

It is what you read when you don't have to
that determines what you will be when you can't help it.
Oscar Wilde

(1) Trapero, A.; Llebaria, A.: Glucocerebrosidase inhibitors for the treatment of Gaucher disease. *Future medicinal chemistry* **2013**, *5*, 573-90.

(2) Pastores, G. M.; Patel, M. J.; Firooznia, H.: Bone and joint complications related to Gaucher disease. *Current rheumatology reports* **2000**, *2*, 175-80.

(3) Grabowski, G. A.; Leslie, N.; Wenstrup, R.: Enzyme therapy for Gaucher disease: the first 5 years. *Blood reviews* **1998**, *12*, 115-33.

(4) Brady, R. O.; Kanfer, J. N.; Shapiro, D.: Metabolism of Glucocerebrosides. Ii. Evidence of an Enzymatic Deficiency in Gaucher's Disease. *Biochemical and biophysical research communications* **1965**, *18*, 221-5.

(5) Brady, R. O.; Kanfer, J. N.; Bradley, R. M.; Shapiro, D.: Demonstration of a deficiency of glucocerebroside-cleaving enzyme in Gaucher's disease. *The Journal of clinical investigation* **1966**, *45*, 1112-5.

(6) Zeller, J. L.; Burke, A. E.; Glass, R. M.: JAMA patient page. Gaucher disease. *Jama* **2007**, *298*, 1358.

(7) Cherin, P.; Rose, C.; de Roux-Serratrice, C.; Tardy, D.; Dobbelaere, D.; Grosbois, B.; Hachulla, E.; Jaussaud, R.; Javier, R. M.; Noel, E.; Clerson, P.; Hartmann, A.: The neurological manifestations of Gaucher disease type 1: the French Observatoire on Gaucher disease (FROG). *Journal of inherited metabolic disease* **2010**, *33*, 331-8.

(8) Siebert, M.; Sidransky, E.; Westbroek, W.: Glucocerebrosidase is shaking up the synucleinopathies. *Brain : a journal of neurology* **2014**, *137*, 1304-22.

(9) Pastores, G. M.; Barnett, N. L.; Bathan, P.; Kolodny, E. H.: A neurological symptom survey of patients with type I Gaucher disease. *Journal of inherited metabolic disease* **2003**, *26*, 641-5.

(10) Goker-Alpan, O.; Hruska, K. S.; Orvisky, E.; Kishnani, P. S.; Stubblefield, B. K.; Schiffmann, R.; Sidransky, E.: Divergent phenotypes in Gaucher disease implicate the role of modifiers. *Journal of medical genetics* **2005**, *42*, e37.

(11) Sidransky, E.: Gaucher disease: complexity in a "simple" disorder. *Molecular genetics and metabolism* **2004**, *83*, 6-15.

(12) Goker-Alpan, O.; Schiffmann, R.; Park, J. K.; Stubblefield, B. K.; Tayebi, N.; Sidransky, E.: Phenotypic continuum in neuronopathic Gaucher disease: an intermediate phenotype between type 2 and type 3. *The Journal of pediatrics* **2003**, *143*, 273-6.

(13) Yu, R. K.; Tsai, Y. T.; Ariga, T.; Yanagisawa, M.: Structures, biosynthesis, and functions of gangliosides--an overview. *Journal of oleo science* **2011**, *60*, 537-44.

(14) van Meer, G.; Wolthoorn, J.; Degroote, S.: The fate and function of glycosphingolipid glucosylceramide. *Philosophical transactions of the Royal Society of London. Series B, Biological sciences* **2003**, *358*, 869-73.

(15) Ichikawa, S.; Hirabayashi, Y.: Glucosylceramide synthase and glycosphingolipid synthesis. *Trends in cell biology* **1998**, *8*, 198-202.

(16) Messner, M. C.; Cabot, M. C.: Glucosylceramide in humans. *Advances in experimental medicine and biology* **2010**, *688*, 156-64.

(17) Sillence, D. J.; Puri, V.; Marks, D. L.; Butters, T. D.; Dwek, R. A.; Pagano, R. E.; Platt, F. M.: Glucosylceramide modulates membrane traffic along the endocytic pathway. *Journal of lipid research* **2002**, *43*, 1837-45.

(18) Basu, S.; Kaufman, B.; Roseman, S.: Enzymatic synthesis of ceramide-glucose and ceramide-lactose by glycosyltransferases from embryonic chicken brain. *The Journal of biological chemistry* **1968**, *243*, 5802-4.

(19) Varki, A.: Biological roles of oligosaccharides: all of the theories are correct. *Glycobiology* **1993**, *3*, 97-130.

(20) Liu, Y. Y.; Hill, R. A.; Li, Y. T.: Ceramide glycosylation catalyzed by glucosylceramide synthase and cancer drug resistance. *Advances in cancer research* **2013**, *117*, 59-89.

(21) Ichikawa, S.; Ozawa, K.; Hirabayashi, Y.: Assignment of a UDP-glucose:ceramide glucosyltransferase gene (UGCG) to human chromosome band 9q31 by in situ hybridization. *Cytogenetics and cell genetics* **1997**, *79*, 233-4.

(22) Ichikawa, S.; Sakiyama, H.; Suzuki, G.; Hidari, K. I.; Hirabayashi, Y.: Expression cloning of a cDNA for human ceramide glucosyltransferase that catalyzes the first glycosylation step of glycosphingolipid synthesis. *Proceedings of the National Academy of Sciences of the United States of America* **1996**, *93*, 4638-43.

(23) Marks, D. L.; Dominguez, M.; Wu, K.; Pagano, R. E.: Identification of active site residues in glucosylceramide synthase. A nucleotide-binding catalytic motif conserved with processive beta-glycosyltransferases. *The Journal of biological chemistry* **2001**, *276*, 26492-8.

(24) Körschen, H. G.; Yildiz, Y.; Raju, D. N.; Schonauer, S.; Bönigk, W.; Jansen, V.; Kremmer, E.; Kaupp, U. B.; Wachten, D.: The Non-lysosomal β-Glucosidase GBA2 Is a Non-integral Membrane-associated Protein at the Endoplasmic Reticulum (ER) and Golgi. *Journal of Biological Chemistry* **2013**, *288*, 3381-3393.

(25) Lu, J.; Chiang, J.; Iyer, R. R.; Thompson, E.; Kaneski, C. R.; Xu, D. S.; Yang, C.; Chen, M.; Hodes, R. J.; Lonser, R. R.; Brady, R. O.; Zhuang, Z.: Decreased glucocerebrosidase activity in Gaucher disease parallels quantitative enzyme loss due to abnormal interaction with TCP1 and c-Cbl. *Proceedings of the National Academy of Sciences of the United States of America* **2010**, *107*, 21665-70.

(26) Dekker, N.; Voorn-Brouwer, T.; Verhoek, M.; Wennekes, T.; Narayan, R. S.; Speijer, D.; Hollak, C. E.; Overkleeft, H. S.; Boot, R. G.; Aerts, J. M.: The cytosolic beta-glucosidase GBA3 does not influence type 1 Gaucher disease manifestation. *Blood cells, molecules & diseases* **2011**, *46*, 19-26.

(27) Aureli, M.; Bassi, R.; Loberto, N.; Regis, S.; Prinetti, A.; Chigorno, V.; Aerts, J. M.; Boot, R. G.; Filocamo, M.; Sonnino, S.: Cell surface associated glycohydrolases in normal and Gaucher disease fibroblasts. *Journal of inherited metabolic disease* **2012**, *35*, 1081-91.

(28) Yildiz, Y.; Matern, H.; Thompson, B.; Allegood, J. C.; Warren, R. L.; Ramirez, D. M.; Hammer, R. E.; Hamra, F. K.; Matern, S.; Russell, D. W.: Mutation of beta-glucosidase 2

causes glycolipid storage disease and impaired male fertility. *The Journal of clinical investigation* **2006**, *116*, 2985-94.

(29) Grabowski, G. A.; Gatt, S.; Horowitz, M.: Acid beta-glucosidase: enzymology and molecular biology of Gaucher disease. *Critical reviews in biochemistry and molecular biology* **1990**, *25*, 385-414.

(30) Horowitz, M.; Wilder, S.; Horowitz, Z.; Reiner, O.; Gelbart, T.; Beutler, E.: The human glucocerebrosidase gene and pseudogene: structure and evolution. *Genomics* **1989**, *4*, 87-96.

(31) Winfield, S. L.; Tayebi, N.; Martin, B. M.; Ginns, E. I.; Sidransky, E.: Identification of three additional genes contiguous to the glucocerebrosidase locus on chromosome 1q21: implications for Gaucher disease. *Genome research* **1997**, *7*, 1020-6.

(32) Dvir, H.; Harel, M.; McCarthy, A. A.; Toker, L.; Silman, I.; Futerman, A. H.; Sussman, J. L.: X-ray structure of human acid-beta-glucosidase, the defective enzyme in Gaucher disease. *EMBO reports* **2003**, *4*, 704-9.

(33) Hruska, K. S.; LaMarca, M. E.; Scott, C. R.; Sidransky, E.: Gaucher disease: mutation and polymorphism spectrum in the glucocerebrosidase gene (GBA). *Human mutation* **2008**, *29*, 567-83.

(34) Lieberman, R. L.; Wustman, B. A.; Huertas, P.; Powe, A. C., Jr.; Pine, C. W.; Khanna, R.; Schlossmacher, M. G.; Ringe, D.; Petsko, G. A.: Structure of acid beta-glucosidase with pharmacological chaperone provides insight into Gaucher disease. *Nature chemical biology* **2007**, *3*, 101-7.

(35) Koprivica, V.; Stone, D. L.; Park, J. K.; Callahan, M.; Frisch, A.; Cohen, I. J.; Tayebi, N.; Sidransky, E.: Analysis and classification of 304 mutant alleles in patients with type 1 and type 3 Gaucher disease. *American journal of human genetics* **2000**, *66*, 1777-86.

(36) Gloster, T. M.; Meloncelli, P.; Stick, R. V.; Zechel, D.; Vasella, A.; Davies, G. J.: Glycosidase inhibition: an assessment of the binding of 18 putative transition-state mimics. *Journal of the American Chemical Society* **2007**, *129*, 2345-54.

(37) Miao, S.; McCarter, J. D.; Grace, M. E.; Grabowski, G. A.; Aebersold, R.; Withers, S. G.: Identification of Glu340 as the active-site nucleophile in human glucocerebrosidase by use of electrospray tandem mass spectrometry. *The Journal of biological chemistry* **1994**, *269*, 10975-8.

(38) Premkumar, L.; Sawkar, A. R.; Boldin-Adamsky, S.; Toker, L.; Silman, I.; Kelly, J. W.; Futerman, A. H.; Sussman, J. L.: X-ray structure of human acid-beta-glucosidase covalently bound to conduritol-B-epoxide. Implications for Gaucher disease. *The Journal of biological chemistry* **2005**, *280*, 23815-9.

(39) Liou, B.; Kazimierczuk, A.; Zhang, M.; Scott, C. R.; Hegde, R. S.; Grabowski, G. A.: Analyses of variant acid beta-glucosidases: effects of Gaucher disease mutations. *The Journal of biological chemistry* **2006**, *281*, 4242-53.

(40) Wilkening, G.; Linke, T.; Sandhoff, K.: Lysosomal degradation on vesicular membrane surfaces. Enhanced glucosylceramide degradation by lysosomal anionic lipids and activators. *The Journal of biological chemistry* **1998**, *273*, 30271-8.

(41) Vaccaro, A. M.; Ciaffoni, F.; Tatti, M.; Salvioli, R.; Barca, A.; Tognozzi, D.; Scerch, C.: pH-dependent conformational properties of saposins and their interactions with phospholipid membranes. *The Journal of biological chemistry* **1995**, *270*, 30576-80.

(42) de Alba, E.; Weiler, S.; Tjandra, N.: Solution structure of human saposin C: pH-dependent interaction with phospholipid vesicles. *Biochemistry* **2003**, *42*, 14729-40.

(43) Vaccaro, A. M.; Tatti, M.; Ciaffoni, F.; Salvioli, R.; Barca, A.; Scerch, C.: Effect of saposins A and C on the enzymatic hydrolysis of liposomal glucosylceramide. *The Journal of biological chemistry* **1997**, *272*, 16862-7.

(44) Sun, Y.; Qi, X.; Grabowski, G. A.: Saposin C is required for normal resistance of acid beta-glucosidase to proteolytic degradation. *The Journal of biological chemistry* **2003**, *278*, 31918-23.

(45) Tamargo, R. J.; Velayati, A.; Goldin, E.; Sidransky, E.: The role of saposin C in Gaucher disease. *Molecular genetics and metabolism* **2012**, *106*, 257-63.

(46) Tylki-Szymanska, A.; Czartoryska, B.; Vanier, M. T.; Poorthuis, B. J.; Groener, J. A.; Lugowska, A.; Millat, G.; Vaccaro, A. M.; Jurkiewicz, E.: Non-neuronopathic Gaucher disease due to saposin C deficiency. *Clinical genetics* **2007**, *72*, 538-42.

(47) Horowitz, M.; Zimran, A.: Mutations causing Gaucher disease. *Human mutation* **1994**, *3*, 1-11.

(48) Ahn, V. E.; Leyko, P.; Alattia, J. R.; Chen, L.; Prive, G. G.: Crystal structures of saposins A and C. *Protein science : a publication of the Protein Society* **2006**, *15*, 1849-57.

(49) Alattia, J. R.; Shaw, J. E.; Yip, C. M.; Prive, G. G.: Molecular imaging of membrane interfaces reveals mode of beta-glucosidase activation by saposin C. *Proceedings of the National Academy of Sciences of the United States of America* **2007**, *104*, 17394-9.

(50) Freud, E.; Cohen, I. J.; Mor, C.; Golinsky, D.; Blumenfeld, A.; Zer, M.: Splenic "regeneration" after partial splenectomy for Gaucher disease: histological features. *Blood cells, molecules & diseases* **1998**, *24*, 309-16.

(51) Karlsson, S.; Correll, P. H.; Xu, L.: Gene transfer and bone marrow transplantation with special reference to Gaucher's disease. *Bone marrow transplantation* **1993**, *11 Suppl 1*, 124-7.

(52) Ringden, O.; Groth, C. G.; Erikson, A.; Granqvist, S.; Mansson, J. E.; Sparrelid, E.: Ten years' experience of bone marrow transplantation for Gaucher disease. *Transplantation* **1995**, *59*, 864-70.

(53) Rappeport, J. M.; Ginns, E. I.: Bone-marrow transplantation in severe Gaucher's disease. *The New England journal of medicine* **1984**, *311*, 84-8.

(54) Nagral, A.: Gaucher disease. *Journal of clinical and experimental hepatology* **2014**, *4*, 37-50.

(55) Beck, M.: Therapy for lysosomal storage disorders. *IUBMB life* **2010**, *62*, 33-40.

(56) Fabrega, S.; Lehn, P.: [Gene therapy of Gaucher's and Fabry's diseases: current status and prospects]. *Journal de la Societe de biologie* **2002**, *196*, 175-81.

(57) Barranger, J. A.; Rice, E. O.; Dunigan, J.; Sansieri, C.; Takiyama, N.; Beeler, M.; Lancia, J.; Lucot, S.; Scheirer-Fochler, S.; Mohney, T.; Swaney, W.; Bahnson, A.; Ball, E.: Gaucher's disease: studies of gene transfer to haematopoietic cells. *Bailliere's clinical haematology* **1997**, *10*, 765-78.

(58) Nimgaonkar, M. T.; Bahnson, A. B.; Boggs, S. S.; Ball, E. D.; Barranger, J. A.: Transduction of mobilized peripheral blood CD34+ cells with the glucocerebrosidase cDNA. *Gene therapy* **1994**, *1*, 201-7.

(59) Dunbar, C.; Kohn, D.: Retroviral mediated transfer of the cDNA for human glucocerebrosidase into hematopoietic stem cells of patients with Gaucher disease. A phase I study. *Human gene therapy* **1996**, *7*, 231-53.

(60) Charrow, J.: Enzyme replacement therapy for Gaucher disease. *Expert opinion on biological therapy* **2009**, *9*, 121-31.

(61) Barton, N. W.; Furbish, F. S.; Murray, G. J.; Garfield, M.; Brady, R. O.: Therapeutic response to intravenous infusions of glucocerebrosidase in a patient with Gaucher disease. *Proceedings of the National Academy of Sciences of the United States of America* **1990**, *87*, 1913-6.

(62) Zimran, A.; Elstein, D.: Gaucher disease and the clinical experience with substrate reduction therapy. *Philosophical transactions of the Royal Society of London. Series B, Biological sciences* **2003**, *358*, 961-6.

(63) Barton, N. W.; Brady, R. O.; Dambrosia, J. M.; Di Bisceglie, A. M.; Doppelt, S. H.; Hill, S. C.; Mankin, H. J.; Murray, G. J.; Parker, R. I.; Argoff, C. E.; et al.: Replacement therapy for inherited enzyme deficiency--macrophage-targeted glucocerebrosidase for Gaucher's disease. *The New England journal of medicine* **1991**, *324*, 1464-70.

(64) Barton, N. W.; Brady, R. O.; Dambrosia, J. M.; Doppelt, S. H.; Hill, S. C.; Holder, C. A.; Mankin, H. J.; Murray, G. J.; Zirzow, G. C.; Parker, R. I.: Dose-dependent responses to macrophage-targeted glucocerebrosidase in a child with Gaucher disease. *The Journal of pediatrics* **1992**, *120*, 277-80.

(65) Deegan, P. B.; Cox, T. M.: Imiglucerase in the treatment of Gaucher disease: a history and perspective. *Drug design, development and therapy* **2012**, *6*, 81-106.

(66) Brumshtein, B.; Salinas, P.; Peterson, B.; Chan, V.; Silman, I.; Sussman, J. L.; Savickas, P. J.; Robinson, G. S.; Futerman, A. H.: Characterization of gene-activated human acid-beta-glucosidase: crystal structure, glycan composition, and internalization into macrophages. *Glycobiology* **2010**, *20*, 24-32.

(67) Zimran, A.; Pastores, G. M.; Tylki-Szymanska, A.; Hughes, D. A.; Elstein, D.; Mardach, R.; Eng, C.; Smith, L.; Heisel-Kurth, M.; Charrow, J.; Harmatz, P.; Fernhoff, P.; Rhead, W.; Longo, N.; Giraldo, P.; Ruiz, J. A.; Zahrieh, D.; Crombez, E.; Grabowski, G. A.: Safety and efficacy of velaglucerase alfa in Gaucher disease type 1 patients previously treated with imiglucerase. *American journal of hematology* **2013**, *88*, 172-8.

(68) Zimran, A.; Gonzalez-Rodriguez, D. E.; Abrahamov, A.; Elstein, D.; Paz, A.; Brill-Almon, E.; Chertkoff, R.: Safety and efficacy of two dose levels of taliglucerase alfa in pediatric patients with Gaucher disease. *Blood cells, molecules & diseases* **2015**, *54*, 9-16.

(69) Hollak, C. E.: An evidence-based review of the potential benefits of taliglucerase alfa in the treatment of patients with Gaucher disease. *Core evidence* **2012**, *7*, 15-20.

(70) Radin, N. S.; Arora, R. C.; Ullman, M. D.; Brenkert, A. L.; Austin, J.: A possible therapeutic approach to Krabbe's globoid leukodystrophy and the status of cerebroside synthesis in the disorder. *Research communications in chemical pathology and pharmacology* **1972**, *3*, 637-44.

(71) Radin, N. S.: Treatment of Gaucher disease with an enzyme inhibitor. *Glycoconjugate journal* **1996**, *13*, 153-7.

(72) Aerts, J. M.; Hollak, C. E.; Boot, R. G.; Groener, J. E.; Maas, M.: Substrate reduction therapy of glycosphingolipid storage disorders. *Journal of inherited metabolic disease* **2006**, *29*, 449-56.

(73) Cox, T.; Lachmann, R.; Hollak, C.; Aerts, J.; van Weely, S.; Hrebicek, M.; Platt, F.; Butters, T.; Dwek, R.; Moyses, C.; Gow, I.; Elstein, D.; Zimran, A.: Novel oral treatment of Gaucher's disease with N-butyldeoxynojirimycin (OGT 918) to decrease substrate biosynthesis. *Lancet* **2000**, *355*, 1481-5.

(74) Elstein, D.; Hollak, C.; Aerts, J. M.; van Weely, S.; Maas, M.; Cox, T. M.; Lachmann, R. H.; Hrebicek, M.; Platt, F. M.; Butters, T. D.; Dwek, R. A.; Zimran, A.: Sustained therapeutic effects of oral miglustat (Zavesca, N-butyldeoxynojirimycin, OGT 918) in type I Gaucher disease. *Journal of inherited metabolic disease* **2004**, *27*, 757-66.

(75) Ficicioglu, C.: Review of miglustat for clinical management in Gaucher disease type 1. *Therapeutics and clinical risk management* **2008**, *4*, 425-31.

(76) Poole, R. M.: Eliglustat: first global approval. *Drugs* **2014**, *74*, 1829-36.

(77) Shayman, J. A.: ELIGLUSTAT TARTRATE: Glucosylceramide Synthase Inhibitor Treatment of Type 1 Gaucher Disease. *Drugs of the future* **2010**, *35*, 613-620.

(78) Schiffmann, R.; Fitzgibbon, E. J.; Harris, C.; DeVile, C.; Davies, E. H.; Abel, L.; van Schaik, I. N.; Benko, W.; Timmons, M.; Ries, M.; Vellodi, A.: Randomized, controlled trial of miglustat in Gaucher's disease type 3. *Annals of neurology* **2008**, *64*, 514-22.

(79) Sawkar, A. R.; D'Haeze, W.; Kelly, J. W.: Therapeutic strategies to ameliorate lysosomal storage disorders--a focus on Gaucher disease. *Cellular and molecular life sciences : CMLS* **2006**, *63*, 1179-92.

(80) Parenti, G.: Treating lysosomal storage diseases with pharmacological chaperones: from concept to clinics. *EMBO molecular medicine* **2009**, *1*, 268-79.

(81) Fan, J. Q.; Ishii, S.; Asano, N.; Suzuki, Y.: Accelerated transport and maturation of lysosomal alpha-galactosidase A in Fabry lymphoblasts by an enzyme inhibitor. *Nature medicine* **1999**, *5*, 112-5.

(82) Yu, Z.; Sawkar, A. R.; Kelly, J. W.: Pharmacologic chaperoning as a strategy to treat Gaucher disease. *The FEBS journal* **2007**, *274*, 4944-50.

(83) Tropak, M. B.; Kornhaber, G. J.; Rigat, B. A.; Maegawa, G. H.; Buttner, J. D.; Blanchard, J. E.; Murphy, C.; Tuske, S. J.; Coales, S. J.; Hamuro, Y.; Brown, E. D.; Mahuran, D. J.: Identification of pharmacological chaperones for Gaucher disease and characterization of their effects on beta-glucocerebrosidase by hydrogen/deuterium exchange mass spectrometry. *Chembiochem : a European journal of chemical biology* **2008**, *9*, 2650-62.

(84) Porto, C.; Cardone, M.; Fontana, F.; Rossi, B.; Tuzzi, M. R.; Tarallo, A.; Barone, M. V.; Andria, G.; Parenti, G.: The pharmacological chaperone N-butyldeoxynojirimycin enhances enzyme replacement therapy in Pompe disease fibroblasts. *Molecular therapy : the journal of the American Society of Gene Therapy* **2009**, *17*, 964-71.

(85) Porto, C.; Pisani, A.; Rosa, M.; Acampora, E.; Avolio, V.; Tuzzi, M. R.; Visciano, B.; Gagliardo, C.; Materazzi, S.; la Marca, G.; Andria, G.; Parenti, G.: Synergy between the pharmacological chaperone 1-deoxygalactonojirimycin and the human recombinant alpha-galactosidase A in cultured fibroblasts from patients with Fabry disease. *Journal of inherited metabolic disease* **2012**, *35*, 513-20.

(86) Benjamin, E. R.; Khanna, R.; Schilling, A.; Flanagan, J. J.; Pellegrino, L. J.; Brignol, N.; Lun, Y.; Guillen, D.; Ranes, B. E.; Frascella, M.; Soska, R.; Feng, J.; Dungan, L.; Young, B.; Lockhart, D. J.; Valenzano, K. J.: Co-administration with the pharmacological chaperone AT1001 increases recombinant human alpha-galactosidase A tissue uptake and improves substrate reduction in Fabry mice. *Molecular therapy : the journal of the American Society of Gene Therapy* **2012**, *20*, 717-26.

(87) Khanna, R.; Flanagan, J. J.; Feng, J.; Soska, R.; Frascella, M.; Pellegrino, L. J.; Lun, Y.; Guillen, D.; Lockhart, D. J.; Valenzano, K. J.: The pharmacological chaperone AT2220 increases recombinant human acid alpha-glucosidase uptake and glycogen reduction in a mouse model of Pompe disease. *PloS one* **2012**, *7*, e40776.

(88) Xu, S.; Lun, Y.; Brignol, N.; Hamler, R.; Schilling, A.; Frascella, M.; Sullivan, S.; Boyd, R. E.; Chang, K.; Soska, R.; Garcia, A.; Feng, J.; Yasukawa, H.; Shardlow, C.; Churchill, A.; Ketkar, A.; Robertson, N.; Miyamoto, M.; Mihara, K.; Benjamin, E. R.; Lockhart, D. J.; Hirato, T.; Fowles, S.; Valenzano, K. J.; Khanna, R.: Coformulation of a Novel Human alpha-Galactosidase A With the Pharmacological Chaperone AT1001 Leads to Improved Substrate Reduction in Fabry Mice. *Molecular therapy : the journal of the American Society of Gene Therapy* **2015**, *23*, 1169-81.

(89) Lieberman, R. L.; D'Aquino J, A.; Ringe, D.; Petsko, G. A.: Effects of pH and iminosugar pharmacological chaperones on lysosomal glycosidase structure and stability. *Biochemistry* **2009**, *48*, 4816-27.

(90) Futerman, A. H.; Sussman, J. L.; Horowitz, M.; Silman, I.; Zimran, A.: New directions in the treatment of Gaucher disease. *Trends in pharmacological sciences* **2004**, *25*, 147-51.

(91) Parenti, G.; Pignata, C.; Vajro, P.; Salerno, M.: New strategies for the treatment of lysosomal storage diseases (review). *International journal of molecular medicine* **2013**, *31*, 11-20.

(92) Abian, O.; Alfonso, P.; Velazquez-Campoy, A.; Giraldo, P.; Pocovi, M.; Sancho, J.: Therapeutic strategies for Gaucher disease: miglustat (NB-DNJ) as a pharmacological chaperone for glucocerebrosidase and the different thermostability of velaglucerase alfa and imiglucerase. *Molecular pharmaceutics* **2011**, *8*, 2390-7.

(93) Sun, Y.; Liou, B.; Xu, Y. H.; Quinn, B.; Zhang, W.; Hamler, R.; Setchell, K. D.; Grabowski, G. A.: Ex vivo and in vivo effects of isofagomine on acid beta-glucosidase variants and substrate levels in Gaucher disease. *The Journal of biological chemistry* **2012**, *287*, 4275-87.

(94) Kornhaber, G. J.; Tropak, M. B.; Maegawa, G. H.; Tuske, S. J.; Coales, S. J.; Mahuran, D. J.; Hamuro, Y.: Isofagomine induced stabilization of glucocerebrosidase. *Chembiochem : a European journal of chemical biology* **2008**, *9*, 2643-9.

(95) Ishii, S.: Pharmacological chaperone therapy for Fabry disease. *Proceedings of the Japan Academy. Series B, Physical and biological sciences* **2012**, *88*, 18-30.

(96) Flanagan, J. J.; Rossi, B.; Tang, K.; Wu, X.; Mascioli, K.; Donaudy, F.; Tuzzi, M. R.; Fontana, F.; Cubellis, M. V.; Porto, C.; Benjamin, E.; Lockhart, D. J.; Valenzano, K. J.; Andria, G.; Parenti, G.; Do, H. V.: The pharmacological chaperone 1-deoxynojirimycin increases the activity and lysosomal trafficking of multiple mutant forms of acid alpha-glucosidase. *Human mutation* **2009**, *30*, 1683-92.

(97) Trapero, A.; Egido-Gabas, M.; Bujons, J.; Llebaria, A.: Synthesis and evaluation of hydroxymethylaminocyclitols as glycosidase inhibitors. *The Journal of organic chemistry* **2015**, *80*, 3512-29.

(98) Trapero, A.; Llebaria, A.: A prospect for pyrrolidine iminosugars as antidiabetic alpha-glucosidase inhibitors. *Journal of medicinal chemistry* **2012**, *55*, 10345-6.

(99) van den Berg, R. J.; Wennekes, T.; Ghisaidoobe, A.; Donker-Koopman, W. E.; Strijland, A.; Boot, R. G.; van der Marel, G. A.; Aerts, J. M.; Overkleeft, H. S.: Assessment of partially deoxygenated deoxynojirimycin derivatives as glucosylceramide synthase inhibitors. *ACS medicinal chemistry letters* **2011**, *2*, 519-22.

(100) Ghisaidoobe, A.; Bikker, P.; de Bruijn, A. C.; Godschalk, F. D.; Rogaar, E.; Guijt, M. C.; Hagens, P.; Halma, J. M.; Van't Hart, S. M.; Luitjens, S. B.; van Rixel, V. H.; Wijzenbroek, M.; Zweegers, T.; Donker-Koopman, W. E.; Strijland, A.; Boot, R.; van der Marel, G.; Overkleeft, H. S.; Aerts, J. M.; van den Berg, R. J.: Identification of potent and selective glucosylceramide synthase inhibitors from a library of N-alkylated iminosugars. *ACS medicinal chemistry letters* **2011**, *2*, 119-23.

(101) Cheng, W. C.; Weng, C. Y.; Yun, W. Y.; Chang, S. Y.; Lin, Y. C.; Tsai, F. J.; Huang, F. Y.; Chen, Y. R.: Rapid modifications of N-substitution in iminosugars: development of new beta-glucocerebrosidase inhibitors and pharmacological chaperones for Gaucher disease. *Bioorganic & medicinal chemistry* **2013**, *21*, 5021-8.

(102) Alfonso, P.; Pampin, S.; Estrada, J.; Rodriguez-Rey, J. C.; Giraldo, P.; Sancho, J.; Pocovi, M.: Miglustat (NB-DNJ) works as a chaperone for mutated acid beta-glucosidase in cells transfected with several Gaucher disease mutations. *Blood cells, molecules & diseases* **2005**, *35*, 268-76.

(103) Sawkar, A. R.; Cheng, W. C.; Beutler, E.; Wong, C. H.; Balch, W. E.; Kelly, J. W.: Chemical chaperones increase the cellular activity of N370S beta -glucosidase: a therapeutic strategy for Gaucher disease. *Proceedings of the National Academy of Sciences of the United States of America* **2002**, *99*, 15428-33.

(104) Serrano, P.; Casas, J.; Zucco, M.; Emeric, G.; Egido-Gabas, M.; Llebaria, A.; Delgado, A.: Combinatorial approach to N-substituted aminocyclitol libraries by solution-phase parallel synthesis and preliminary evaluation as glucocerebrosidase inhibitors. *Journal of combinatorial chemistry* **2007**, *9*, 43-52.

(105) Egido-Gabas, M.; Serrano, P.; Casas, J.; Llebaria, A.; Delgado, A.: New aminocyclitols as modulators of glucosylceramide metabolism. *Organic & biomolecular chemistry* **2005**, *3*, 1195-201.

(106) Diaz, L.; Bujons, J.; Casas, J.; Llebaria, A.; Delgado, A.: Click chemistry approach to new N-substituted aminocyclitols as potential pharmacological chaperones for Gaucher disease. *Journal of medicinal chemistry* **2010**, *53*, 5248-55.

(107) Diaz, L.; Casas, J.; Bujons, J.; Llebaria, A.; Delgado, A.: New glucocerebrosidase inhibitors by exploration of chemical diversity of N-substituted aminocyclitols using click chemistry and in situ screening. *Journal of medicinal chemistry* **2011**, *54*, 2069-79.

(108) Egido-Gabas, M.; Canals, D.; Casas, J.; Llebaria, A.; Delgado, A.: Aminocyclitols as pharmacological chaperones for glucocerebrosidase, a defective enzyme in Gaucher disease. *ChemMedChem* **2007**, *2*, 992-4.

(109) Trapero, A.; Alfonso, I.; Butters, T. D.; Llebaria, A.: Polyhydroxylated bicyclic isoureas and guanidines are potent glucocerebrosidase inhibitors and nanomolar enzyme activity enhancers in Gaucher cells. *Journal of the American Chemical Society* **2011**, *133*, 5474-84.

(110) Trapero, A.; Llebaria, A.: The myo-1,2-Diaminocyclitol Scaffold Defines Potent Glucocerebrosidase Activators and Promising Pharmacological Chaperones for Gaucher Disease. *ACS medicinal chemistry letters* **2011**, *2*, 614-9.

(111) Trapero, A.: Nous ciclitols com a inhibidors de la Glucocerebrosidasa. Aplicació al disseny de xaperones farmacològiques per al tractament de la malaltia de Gaucher., Doctoral Thesis. Universitat de Barcelona, 2011.

(112) Brumshtein, B.; Greenblatt, H. M.; Butters, T. D.; Shaaltiel, Y.; Aviezer, D.; Silman, I.; Futerman, A. H.; Sussman, J. L.: Crystal structures of complexes of N-butyl- and N-nonyl-deoxynojirimycin bound to acid beta-glucosidase: insights into the mechanism of chemical chaperone action in Gaucher disease. *The Journal of biological chemistry* **2007**, *282*, 29052-8.

(113) Alfonso, P.; Pampín, S.; Estrada, J.; Rodríguez-Rey, J. C.; Giraldo, P.; Sancho, J.; Pocoví, M.: Miglustat (NB-DNJ) works as a chaperone for mutated acid β-glucosidase in cells transfected with several Gaucher disease mutations. *Blood Cells, Molecules, and Diseases* **2005**, *35*, 268-276.

(114) Gloster, T. M.; Roberts, S.; Perugino, G.; Rossi, M.; Moracci, M.; Panday, N.; Terinek, M.; Vasella, A.; Davies, G. J.: Structural, kinetic, and thermodynamic analysis of glucoimidazole-derived glycosidase inhibitors. *Biochemistry* **2006**, *45*, 11879-84.

(115) Fan, J. Q.; Sheth, K.; Zhu, X.: Glucoimidazole and polyhydroxycyclohexenyl amine derivatives to treat gaucher disease. Google Patents, 2005.

(116) Joosten, A.; Decroocq, C.; de Sousa, J.; Schneider, J. P.; Etame, E.; Bodlenner, A.; Butters, T. D.; Compain, P.: A systematic investigation of iminosugar click clusters as pharmacological chaperones for the treatment of Gaucher disease. *Chembiochem : a European journal of chemical biology* **2014**, *15*, 309-19.

(117) Diot, J. D.; Garcia Moreno, I.; Twigg, G.; Ortiz Mellet, C.; Haupt, K.; Butters, T. D.; Kovensky, J.; Gouin, S. G.: Amphiphilic 1-deoxynojirimycin derivatives through click strategies for chemical chaperoning in N370S Gaucher cells. *The Journal of organic chemistry* **2011**, *76*, 7757-68.

(118) Ardes-Guisot, N.; Alonzi, D. S.; Reinkensmeier, G.; Butters, T. D.; Norez, C.; Becq, F.; Shimada, Y.; Nakagawa, S.; Kato, A.; Bleriot, Y.; Sollogoub, M.; Vauzeilles, B.: Selection of the biological activity of DNJ neoglycoconjugates through click length variation of the side chain. *Organic & biomolecular chemistry* **2011**, *9*, 5373-88.

(119) Kolb, H. C.; Finn, M. G.; Sharpless, K. B.: Click Chemistry: Diverse Chemical Function from a Few Good Reactions. *Angewandte Chemie* **2001**, *40*, 2004-2021.

(120) Shaaltiel, Y.; Bartfeld, D.; Hashmueli, S.; Baum, G.; Brill-Almon, E.; Galili, G.; Dym, O.; Boldin-Adamsky, S. A.; Silman, I.; Sussman, J. L.; Futerman, A. H.; Aviezer, D.: Production of glucocerebrosidase with terminal mannose glycans for enzyme replacement therapy of Gaucher's disease using a plant cell system. *Plant biotechnology journal* **2007**, *5*, 579-90.

(121) Babić, S.; Horvat, A. J. M.; Mutavdžić Pavlović, D.; Kaštelan-Macan, M.: Determination of pKa values of active pharmaceutical ingredients. *TrAC Trends in Analytical Chemistry* **2007**, *26*, 1043-1061.

(122) Güven, A.: Acidity Study on 3-Substituted Pyridines. *International Journal of Molecular Sciences* **2005**, *6*, 257.

(123) Schofield, K.: *Hetero-Aromatic Nitrogen Compounds: Pyrroles and Pyridines*; 4th ed.; Springer US, 2013.

(124) Ardes-Guisot, N.; Alonzi, D. S.; Reinkensmeier, G.; Butters, T. D.; Norez, C.; Becq, F.; Shimada, Y.; Nakagawa, S.; Kato, A.; Bleriot, Y.; Sollogoub, M.; Vauzeilles, B.: Selection of the biological activity of DNJ neoglycoconjugates through click length variation of the side chain. *Organic & biomolecular chemistry* **2011**, *9*, 5373-5388.

(125) Gracias, V.; Frank, K. E.; Milligan, G. L.; Aubé, J.: Ring expansion by in situ tethering of hydroxy azides to ketones: The boyer reaction. *Tetrahedron* **1997**, *53*, 16241-16252.

(126) Zundel, M.; Peschke, B.: C-terminally pegylated growth hormones. Google Patents, 2006.

(127) Diot, J. D.; Moreno, I. G.; Twigg, G.; Mellet, C. O.; Haupt, K.; Butters, T. D.; Kovensky, J.; Gouin, S. G.: Amphiphilic 1-Deoxynojirimycin Derivatives through Click Strategies for Chemical Chaperoning in N370S Gaucher Cells. *The Journal of Organic Chemistry* **2011**, *76*, 7757-7768.

(128) Sarin, V. K.; Kent, S. B. H.; Merrifield, R. B.: Properties of swollen polymer networks. Solvation and swelling of peptide-containing resins in solid-phase peptide synthesis. *Journal of the American Chemical Society* **1980**, *102*, 5463-5470.

(129) McDonald, C. E.; Ramsey, J. D.; Sampsell, D. G.; Butler, J. A.; Cecchini, M. R.: Tripyrrolidinophosphoric Acid Triamide as an Activator in Samarium Diiodide Reductions. *Organic Letters* **2010**, *12*, 5178-5181.

(130) Coste, J.; Frerot, E.; Jouin, P.: Coupling N-Methylated Amino Acids Using PyBroP and PyCloP Halogenophosphonium Salts: Mechanism and Fields of Application. *The Journal of Organic Chemistry* **1994**, *59*, 2437-2446.

(131) Büsch, F.; Pieck, J. C.; Ober, M.; Gierlich, J.; Hsu, G. W.; Beese, L. S.; Carell, T.: Dissecting the Differences between the α and β Anomers of the Oxidative DNA Lesion FaPydG. *Chemistry – A European Journal* **2008**, *14*, 2125-2132.

(132) Compain, P.; Decroocq, C.; Iehl, J.; Holler, M.; Hazelard, D.; Mena Barragán, T.; Ortiz Mellet, C.; Nierengarten, J.-F.: Glycosidase Inhibition with Fullerene Iminosugar Balls: A Dramatic Multivalent Effect. *Angewandte Chemie International Edition* **2010**, *49*, 5753-5756.

(133) Wennekes, T.; Lang, B.; Leeman, M.; Marel, G. A. v. d.; Smits, E.; Weber, M.; Wiltenburg, J. v.; Wolberg, M.; Aerts, J. M. F. G.; Overkleeft, H. S.: Large-Scale Synthesis of the Glucosylceramide Synthase Inhibitor N-[5-(Adamantan-1-yl-methoxy)-pentyl]-1-deoxynojirimycin. *Organic Process Research & Development* **2008**, *12*, 414-423.

(134) Abdel-Magid, A. F.; Mehrman, S. J.: A Review on the Use of Sodium Triacetoxyborohydride in the Reductive Amination of Ketones and Aldehydes. *Organic Process Research & Development* **2006**, *10*, 971-1031.

(135) Ma, Y.: A tandem reaction of 4-bromoalkyl aldehydes with sodium azide: Synthesis of 5,6,7,7a-tetrahydro-pyrrolo[1,2-d]-[1.2.3.4]oxatriazole. *Heteroatom Chemistry* **2002**, *13*, 307-309.

(136) Díaz, L.; Bujons, J.; Casas, J.; Llebaria, A.; Delgado, A.: Click Chemistry Approach to New N-Substituted Aminocyclitols as Potential Pharmacological Chaperones for Gaucher Disease. *Journal of Medicinal Chemistry* **2010**, *53*, 5248-5255.

(137) Spiteri, C.; Moses, J. E.: Copper-Catalyzed Azide–Alkyne Cycloaddition: Regioselective Synthesis of 1,4,5-Trisubstituted 1,2,3-Triazoles. *Angewandte Chemie International Edition* **2010**, *49*, 31-33.

(138) Egido-Gabas, M.; Serrano, P.; Casas, J.; Llebaria, A.; Delgado, A.: New aminocyclitols as modulators of glucosylceramide metabolism. *Organic & biomolecular chemistry* **2005**, *3*, 1195-1201.

(139) Butters, T. D.; Dwek, R. A.; Platt, F. M.: Imino sugar inhibitors for treating the lysosomal glycosphingolipidoses. *Glycobiology* **2005**, *15*, 43R-52R.

(140) Trapero, A.; Egido-Gabás, M.; Bujons, J.; Llebaria, A.: Synthesis and Evaluation of Hydroxymethylaminocyclitols as Glycosidase Inhibitors. *The Journal of Organic Chemistry* **2015**, *80*, 3512-3529.

(141) Ghisaidoobe, A. T.; van den Berg, R. J.; Butt, S. S.; Strijland, A.; Donker-Koopman, W. E.; Scheij, S.; van den Nieuwendijk, A. M.; Koomen, G. J.; van Loevezijn, A.; Leemhuis, M.; Wennekes, T.; van der Stelt, M.; van der Marel, G. A.; van Boeckel, C. A.; Aerts, J. M.; Overkleeft, H. S.: Identification and development of biphenyl substituted iminosugars as improved dual glucosylceramide synthase/neutral glucosylceramidase inhibitors. *J Med Chem* **2014**, *57*, 9096-104.

(142) Mosmann, T.: Rapid colorimetric assay for cellular growth and survival: application to proliferation and cytotoxicity assays. *Journal of immunological methods* **1983**, *65*, 55-63.

(143) Lieberman, R. L.: A Guided Tour of the Structural Biology of Gaucher Disease: Acid-β-Glucosidase and Saposin C. *Enzyme Research* **2011**, *2011*, 15.

(144) Morgenthaler, M.; Schweizer, E.; Hoffmann-Röder, A.; Benini, F.; Martin, R. E.; Jaeschke, G.; Wagner, B.; Fischer, H.; Bendels, S.; Zimmerli, D.; Schneider, J.; Diederich, F.; Kansy, M.; Müller, K.: Predicting and Tuning Physicochemical Properties in Lead Optimization: Amine Basicities. *ChemMedChem* **2007**, *2*, 1100-1115.

(145) Trapero, A.; González-Bulnes, P.; Butters, T. D.; Llebaria, A.: Potent Aminocyclitol Glucocerebrosidase Inhibitors are Subnanomolar Pharmacological Chaperones for Treating Gaucher Disease. *Journal of Medicinal Chemistry* **2012**, *55*, 4479-4488.

(146) Trapero, A.; Egido-Gabas, M.; Llebaria, A.: Adamantane substituted aminocyclitols as pharmacological chaperones for Gaucher disease. *MedChemComm* **2013**, *4*, 1584-1589.

(147) Gonzalez-Bulnes, P.; Casas, J.; Delgado, A.; Llebaria, A.: Practical synthesis of (−)-1-amino-1-deoxy-myo-inositol from achiral precursors. *Carbohydrate Research* **2007**, *342*, 1947-1952.

(148) Trost, B. M.; Hembre, E. J.: Pd catalyzed kinetic resolution of conduritol B. Asymmetric synthesis of (+)-cyclophellitol. *Tetrahedron Letters* **1999**, *40*, 219-222.

(149) Sanfilippo, C.; Patti, A.; Nicolosi, G.: Enzymatic resolution of (±)-conduritol-B, a key intermediate for the synthesis of glycosidase inhibitors. *Tetrahedron: Asymmetry* **1999**, *10*, 3273-3276.

(150) Trost, B. M.; Dudash, J. J.; Hembre, E. J.: Asymmetric Induction of Conduritols via AAA Reactions: Synthesis of the Aminocyclohexitol of Hygromycin A. *Chemistry – A European Journal* **2001**, *7*, 1619-1629.

(151) Rempel, B. P.; Withers, S. G.: Covalent inhibitors of glycosidases and their applications in biochemistry and biology. *Glycobiology* **2008**, *18*, 570-586.

(152) Premkumar, L.; Sawkar, A. R.; Boldin-Adamsky, S.; Toker, L.; Silman, I.; Kelly, J. W.; Futerman, A. H.; Sussman, J. L.: X-ray Structure of Human Acid-β-Glucosidase Covalently Bound to Conduritol-B-Epoxide: IMPLICATIONS FOR GAUCHER DISEASE. *Journal of Biological Chemistry* **2005**, *280*, 23815-23819.

(153) Grethe, G.; Mitt, T.; Williams, T. H.; Uskokovic, M. R.: Synthesis of daunosamine. *The Journal of Organic Chemistry* **1983**, *48*, 5309-5315.

(154) Stevens, C. L.; Schultze, K. W.; Smith, D. J.; Pillai, P. M.: Synthesis of 3,6-dideoxy-D-erythro-hexos-4-ulose (3,6-dideoxy-4-keto-D-glucose). *The Journal of Organic Chemistry* **1975**, *40*, 3704-3708.

(155) Singh, R. P.; Shreeve, J. n. M.: Recent Advances in Nucleophilic Fluorination Reactions of Organic Compounds- Using Deoxofluor and DAST. *Synthesis* **2002**, *2002*, 2561-2578.

(156) Lopez, O.; Qing, F. L.; Pedersen, C. M.; Bols, M.: Enzyme inhibition by iminosugars: analysis and insight into the glycosidase-iminosugar dependency of pH. *Bioorg Med Chem* **2013**, *21*, 4755-61.

(157) Daniels, L. B.; Glew, R. H.; Radin, N. S.; Vunnam, R. R.: A revised fluorometric assay for Gaucher's disease using conduritol-β-epoxide with liver as the source of β-glucosidase. *Clinica Chimica Acta* **1980**, *106*, 155-163.

(158) Adams, B. T.; Niccoli, S.; Chowdhury, M. A.; Esarik, A. N. K.; Lees, S. J.; Rempel, B. P.; Phenix, C. P.: N-Alkylated aziridines are easily-prepared, potent, specific and cell-permeable covalent inhibitors of human [small beta]-glucocerebrosidase. *Chemical Communications* **2015**, *51*, 11390-11393.

(159) Ridley, C. M.; Thur, K. E.; Shanahan, J.; Thillaiappan, N. B.; Shen, A.; Uhl, K.; Walden, C. M.; Rahim, A. A.; Waddington, S. N.; Platt, F. M.; van der Spoel, A. C.: beta-Glucosidase 2 (GBA2) activity and imino sugar pharmacology. *The Journal of biological chemistry* **2013**, *288*, 26052-66.

(160) Prelich, G.: Gene Overexpression: Uses, Mechanisms, and Interpretation. *Genetics* **2012**, *190*, 841-854.

(161) Newburg, D. S.; Yatziv, S.; McCluer, R. H.; Raghavan, S.: beta-Glucosidase inhibition in murine peritoneal macrophages by conduritol-B-epoxide: an in vitro model of the Gaucher cell. *Biochimica et biophysica acta* **1986**, *877*, 121-6.

(162) Li, F.; Pham, H.; Anderson, D. J.: Methods to produce polymer nanoparticles and formulations of active ingredients. Google Patents, 2010.

(163) Shi, W.; Nacev, B. A.; Aftab, B. T.; Head, S.; Rudin, C. M.; Liu, J. O.: Itraconazole Side Chain Analogues: Structure–Activity Relationship Studies for Inhibition of Endothelial Cell Proliferation, Vascular Endothelial Growth Factor Receptor 2 (VEGFR2) Glycosylation, and Hedgehog Signaling. *Journal of Medicinal Chemistry* **2011**, *54*, 7363-7374.

(164) Pop, I. E.; Deprez, B. P.; Tartar, A. L.: Versatile Acylation of N-Nucleophiles Using a New Polymer-Supported 1-Hydroxybenzotriazole Derivative. *J Org Chem* **1997**, *62*, 2594-2603.

(165) Sisa, M.; Trapero, A.; Llebaria, A.; Delgado, A.: Small-Scale One-Pot Reductive Alkylation of Unprotected Aminocyclitols with Supported Reagents. *Synthesis* **2008**, *2008*, 3167-3170.

(166) Rubinshtein, M.; James, C. R.; Young, J. L.; Ma, Y. J.; Kobayashi, Y.; Gianneschi, N. C.; Yang, J.: Facile Procedure for Generating Side Chain Functionalized Poly(α-hydroxy acid) Copolymers from Aldehydes via a Versatile Passerini-Type Condensation. *Organic Letters* **2010**, *12*, 3560-3563.

(167) Song, X.; Hollingsworth, R. I.: Facile syntheses of 1-deoxynojirimycin (DNJ) and 1-deoxymannojirimycin (DMJ). *Tetrahedron Letters* **2007**, *48*, 3115-3118.

(168) Lahmann, M.; Garegg, P. J.; Konradsson, P.; Oscarson, S.: Synthesis of a polyphosphorylated GPI-anchor core structure. *Canadian Journal of Chemistry* **2002**, *80*, 1105-1111.

(169) Li, H.; Yao, Y.; Han, C.; Zhan, J.: Triazole-ester modified silver nanoparticles: click synthesis and Cd2+ colorimetric sensing. *Chemical Communications* **2009**, 4812-4814.

(170) Poirot, E.; Chang, A. H. C.; Horton, D.; Kováč, P.: Synthetic explorations towards 3-deoxy-3-fluoro derivatives of d-perosamine. *Carbohydrate Research* **2001**, *334*, 195-205.

(171) Suntornchashwej, S.; Suwanborirux, K.; Isobe, M.: Total synthesis of malyngamide X and its 7'S-epi isomer. *Tetrahedron* **2007**, *63*, 3217-3226.

(172) Frost, C. G.; Penrose, S. D.; Gleave, R.: Rhodium catalysed conjugate addition of a chiral alkenyltrifluoroborate salt: the enantioselective synthesis of hermitamides A and B. *Organic & biomolecular chemistry* **2008**, *6*, 4340-4347.

(173) Trapero, A.; Alfonso, I.; Butters, T. D.; Llebaria, A.: Polyhydroxylated Bicyclic Isoureas and Guanidines Are Potent Glucocerebrosidase Inhibitors and Nanomolar Enzyme Activity Enhancers in Gaucher Cells. *Journal of the American Chemical Society* **2011**, *133*, 5474-5484.

(174) Korschen, H. G.; Yildiz, Y.; Raju, D. N.; Schonauer, S.; Bonigk, W.; Jansen, V.; Kremmer, E.; Kaupp, U. B.; Wachten, D.: The non-lysosomal beta-glucosidase GBA2 is a non-integral membrane-associated protein at the endoplasmic reticulum (ER) and Golgi. *The Journal of biological chemistry* **2013**, *288*, 3381-93.

INDEX OF COMPOUNDS

It's not about the end goal, its about who you become
by consistently pushing to the edge of your limits.
Robin Sharma

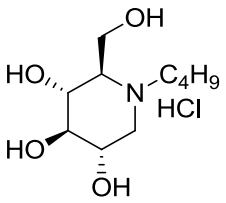

(1) NB-DNJ

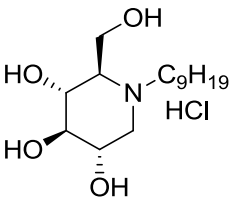

(2) NN-DNJ

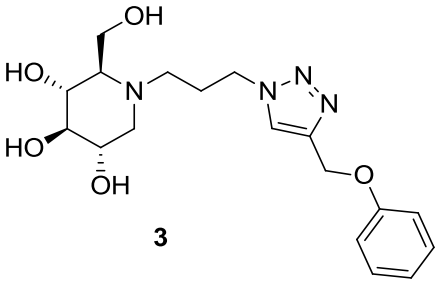

3

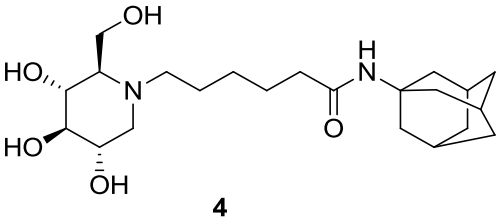

4

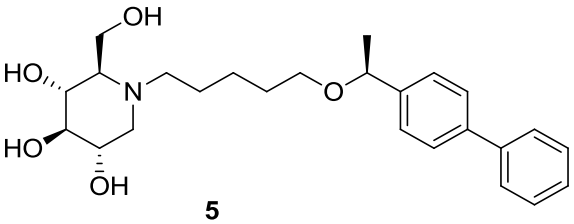

5

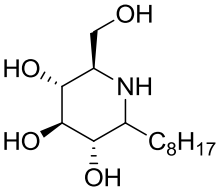

6

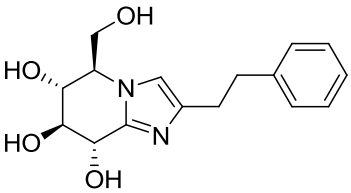

7

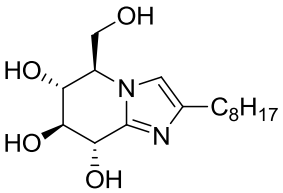

8

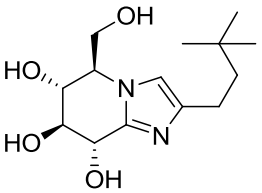

9

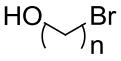

10a, n=3
10b, n=4
10c, n=5
10d, n=6

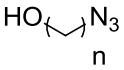

11a, n=3
11b, n=4
11c, n=5
11d, n=6

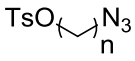

12a, n=3
12b, n=4
12c, n=5
12d, n=6

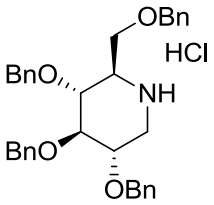

13

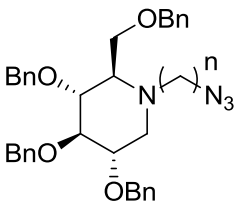

14a, n=3
14b, n=4
14c, n=5
14d, n=6

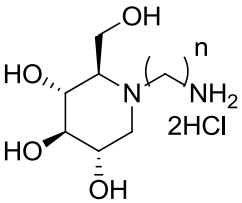

15a, n=3
15b, n=4
15c, n=5
15d, n=6

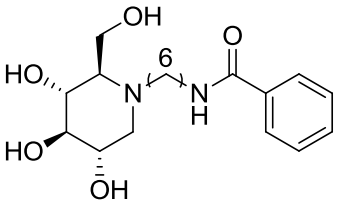

16d(I)

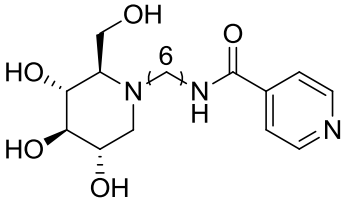

16d(II)

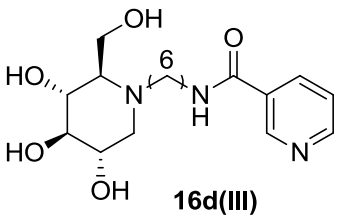

16d(III)

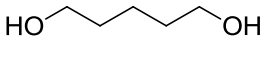

17

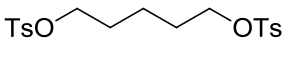

18

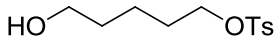

19

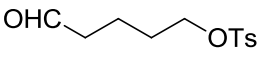

20

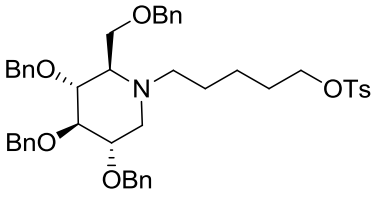

21

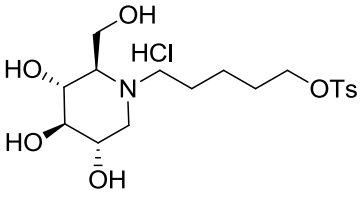

22

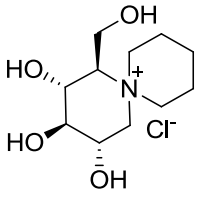

23

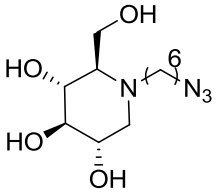

24c, n=5, free base
24d, n=6, HCOOH

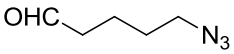

25

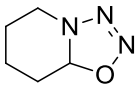

26

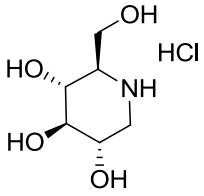

27

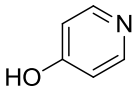

28(VI)

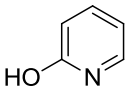

28(VII)

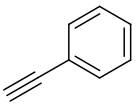

30(I)

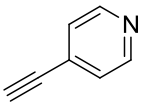

30(II)

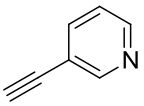

30(III)

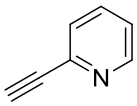

30(IV)

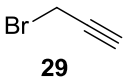

29

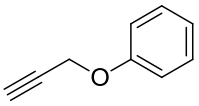

30(V)

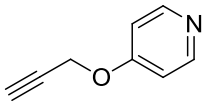

30(VI)

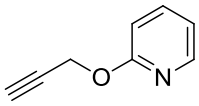

30(VII)

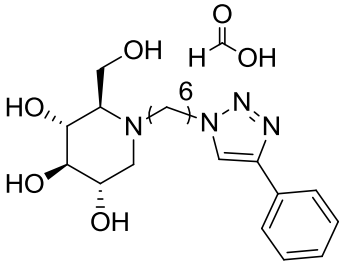

31d(I)

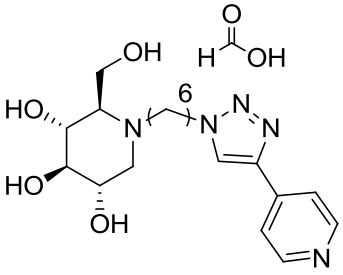

31d(II)

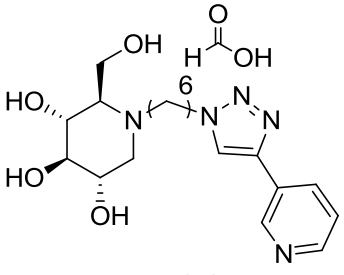

31d(III)

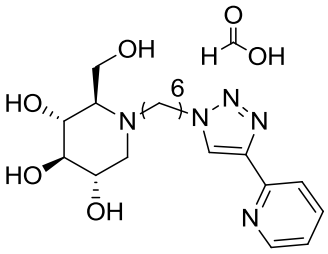

31d(IV)

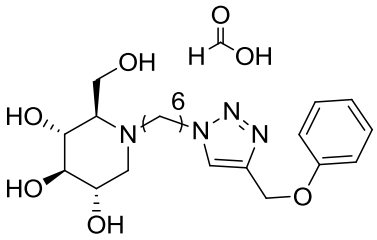

31d(V)

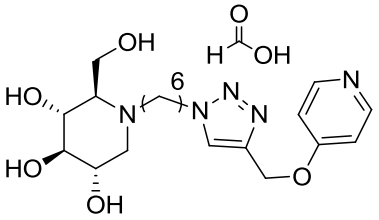

31d(VI)

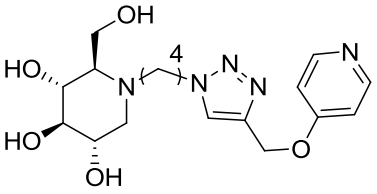

31b(VI)

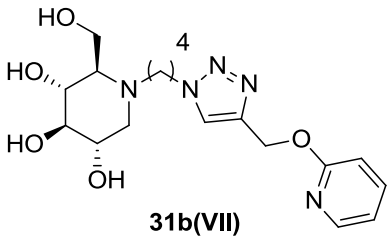

31b(VII)

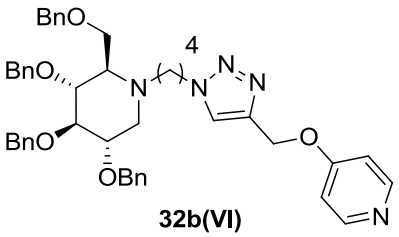

32b(VI)

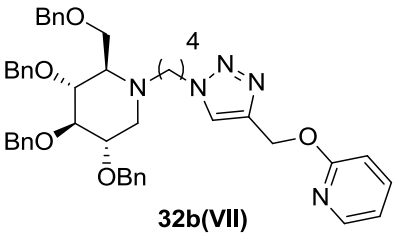

32b(VII)

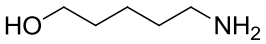

33

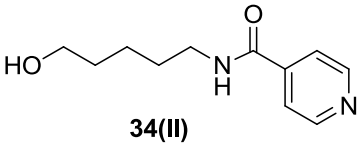

34(II)

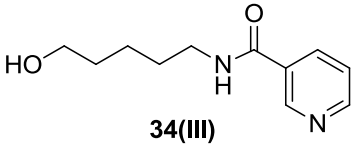

34(III)

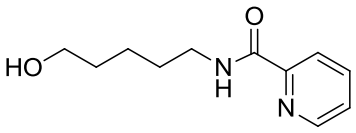

34(IV)

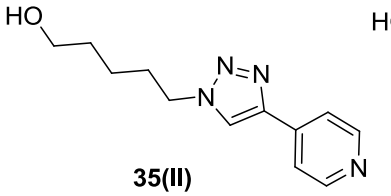

35(II)

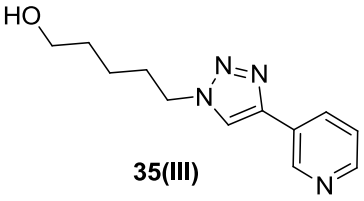

35(III)

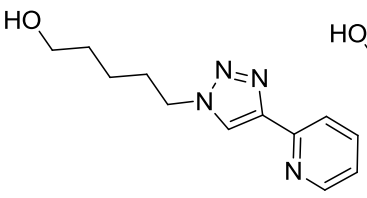

35(IV)

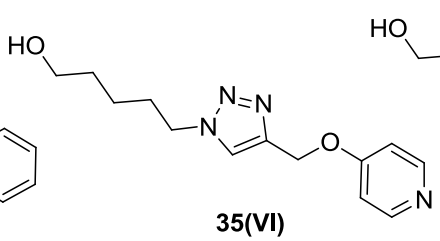

35(VI)

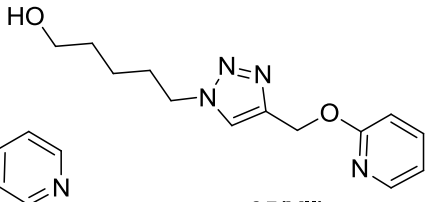

35(VII)

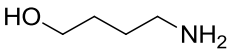

36

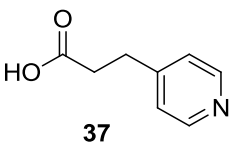

37

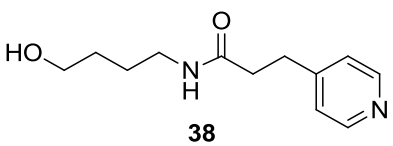

38

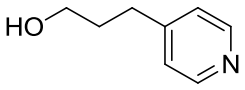

39

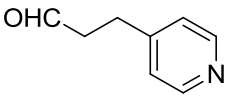

40

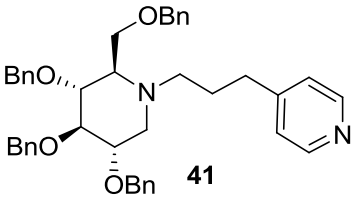

41

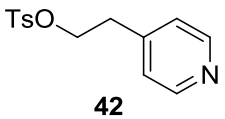

42

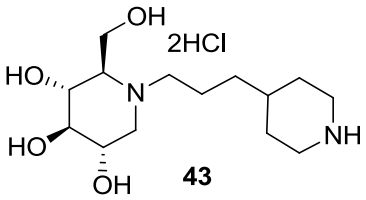

43

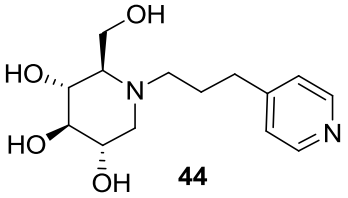

44

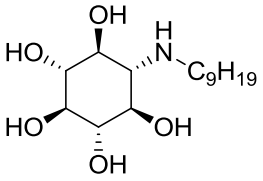

45

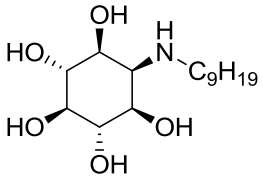

46

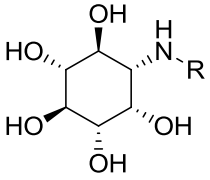

47x, R=Bu (HCl)
47y, R=Non (free base)

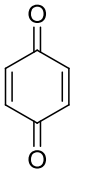

48

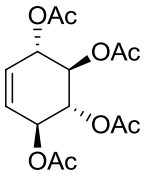

(+)-49

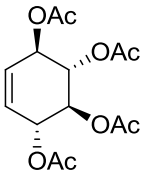

(-)-49

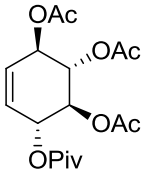

(-)-50

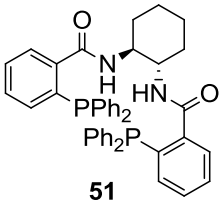

51

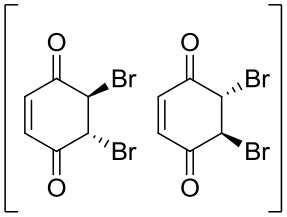

(±)-52

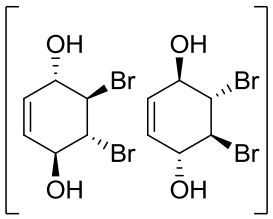

(±)-53

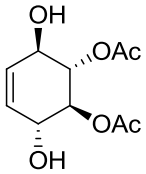

(-)-54

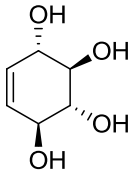

55

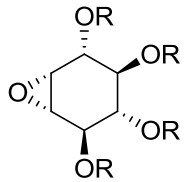

56 (CBE) R = H
57 R = Bn

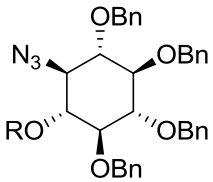

58, R = H
60, R = Ms

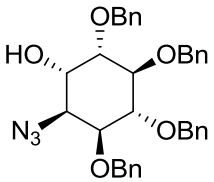

59

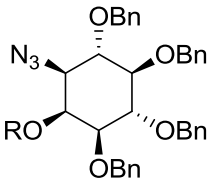

61, R = H
62, R = Ac

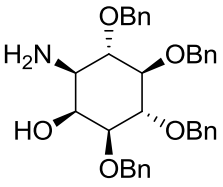

63

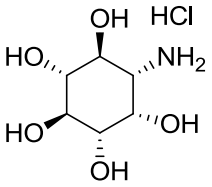

64

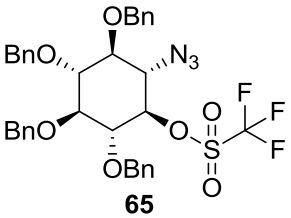

65

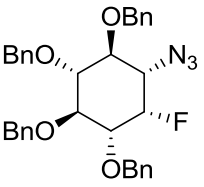

66

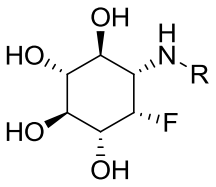

67x, R=Bu
67y, R=Non

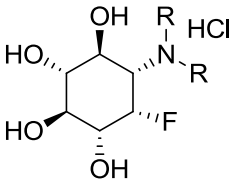

68x, R=Bu
68y, R=Non

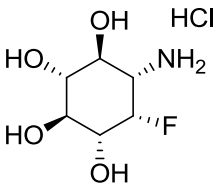

69

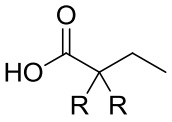

70, R=H
71, R=F

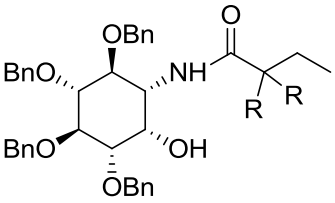

72, R=H
73, R=F

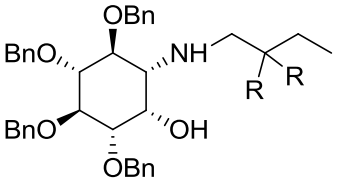

74, R=H
75, R=F

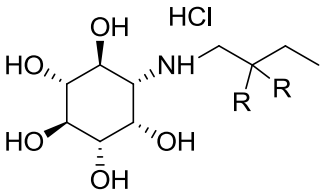

47x, R=H
76x, R=F

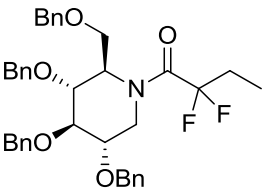

77

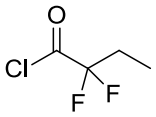

78

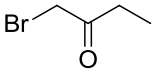

79

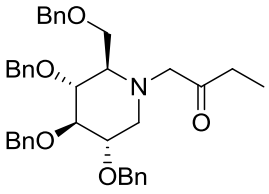

80

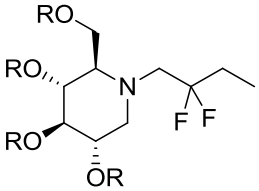

81, R=Bn (free base)
82x, R=H (HCl)

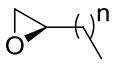

(R)-83x, n=1
(R)-83y, n=6

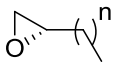

(S)-83x, n=1
(S)-83y, n=6

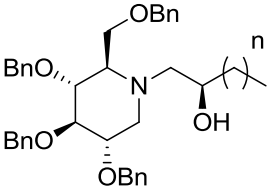

(R)-84x, n=1
(R)-84y, n=6

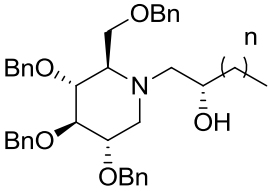

(S)-84x, n=1
(S)-84y, n=6

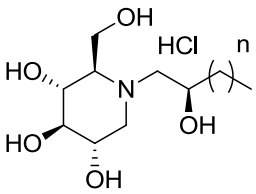

(R)-85x, n=1
(R)-85y, n=6

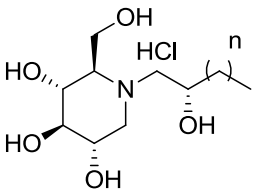

(S)-85x, n=1
(S)-85y, n=6

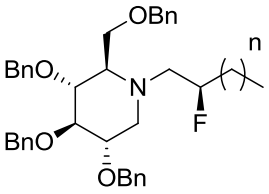

(R)-86x, n=1
(R)-86y, n=6

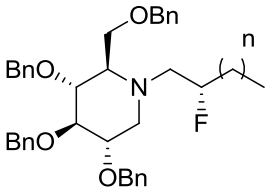

(S)-86x, n=1
(S)-86y, n=6

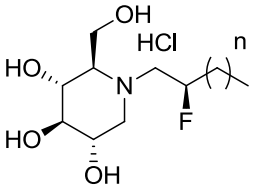

(R)-87x, n=1
(R)-87y, n=6

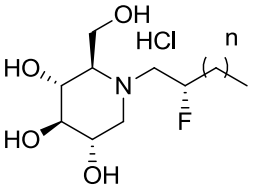

(S)-87x, n=1
(S)-87y, n=6

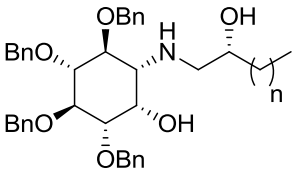

(R)-88x, n=1
(R)-88y, n=6

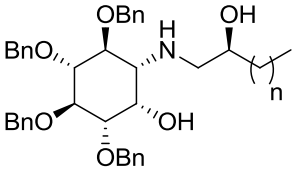

(S)-88x, n=1
(S)-88y, n=6

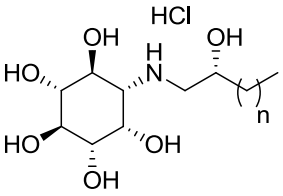

(R)-89x, n=1
(R)-89y, n=6

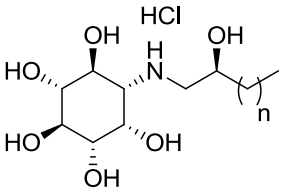

(S)-89x, n=1
(S)-89y, n=6

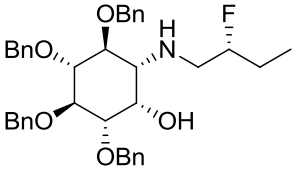

(R)-90x

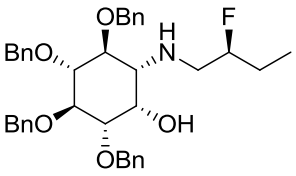

(S)-90x

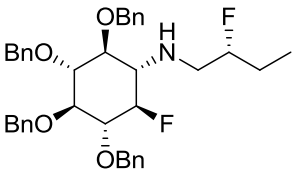

(R)-91x

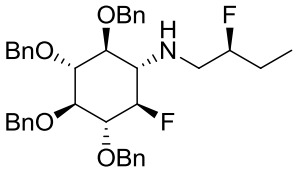

(S)-91x

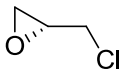

(R)-92

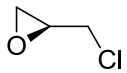

(S)-92

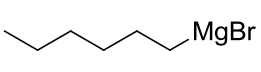

93

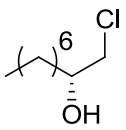

(R)-94

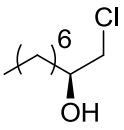

(S)-94